UNIVERSITY OF MICHIGAN
RADIATION LABORATORY

EECS 633 COURSEPACK

NUMERICAL METHODS IN ELECTROMAGNETICS

FALL 1993

These notes were written by John L. Volakis for the benefit of the University of Michigan(U-M) Radiation Laboratory students. Selected portions of these notes are used for the U-M Numerical Electromagnetics Course EECS 633. The preparation of the manuscript was inspired by the need to provide the Radiation Laboratory students with an understanding of numerical (integral and differential) methods. The proliferation of numerical methods and their application in electromagnetics will be continued at an even greater pace, and it is thus important that all contemporary EM students have an introductory or, if possible, a working knowledge of these techniques. In EECS 633 we will cover certain sections of these notes on the assumption that the student has little or no knowledge of numerical solution techniques in electromagnetics. Basic understanding of electromagnetics (EECS 530), integral calculus, matrix algebra, numerical integration and parametric equations is required. Students who are interested in some specific application may read additional sections of the notes, not covered in class.

I am indebted to many of my students for their help and whose encouragement was important in pursuing this project. Special acknowledgement goes to Leo C. Kempel who provided most of the computations in Chapter 5 (2D scattering) using our computer programs RUFCODE and RESTE/H. John Natzke wrote the sample wire analysis program and provided many of the computed results included in Chapter 4.

This manuscript has not been proofread thoroughly, and I apologize for any errors you may find in the text. Please bring them to my attention along with any other comments. I will keep you updated on any corrections during the course.

Fall 1993

Contents

Chapter 1

Fundamental Concepts and Theorems

It is assumed that the reader is already familiar with basic electromagnetic theory usually covered in courses on general electromagnetics and antennas beyond the required undergraduate material. Below we simply provide a review of Maxwell's equations and related theorems which are of importance in this course. This chapter also provides the required notational definitions for the various field quantities.

1.1 Maxwell's equation in Differential Time Domain Form

In 1861 Maxwell presented the electromagnetic field equations in the form that is known today. Maxwell formulated these equations on the basis of the electromagnetic laws that were developed already by Gauss, Ampere, Faraday, Henry, and so on. Other than the compact form of the field relations that he provided, his only new contribution in this respect was the introduction of the displacement current to supplement Ampere's law. This was essentially postulated in order to make the equations compatible with Gauss' law and the equation of continuity.

Maxwell's equations in differential time domain form are

$$\nabla \times \mathcal{H} = \mathcal{J} + \frac{\partial \mathcal{D}}{\partial t} \quad \text{(Ampere-Maxwell law)} \tag{1.1}$$

$$\nabla \times \mathcal{E} = -\mathcal{M} - \frac{\partial \mathcal{B}}{\partial t} \quad \text{(Faraday's law)} \tag{1.2}$$

$$\nabla \cdot \mathcal{B} = +\varrho_m \quad \text{(Gauss' law-magnetic)} \tag{1.3}$$

$$\nabla \cdot \mathcal{D} = \varrho \quad \text{(Gauss' law)} \tag{1.4}$$

where t denotes time and

$\mathcal{E}$ = electric field intensities in Volts/meter (V/m)
$\mathcal{D}$ = electric flux densities in Coulombs/meter^2 (C/m^2)
$\mathcal{H}$ = magnetic field intensity in Amperes/meter (A/m)
$\mathcal{B}$ = magnetic field density in Webers/meter^2 (Wb/m^2)
$\mathcal{J}$ = electric current density in Amperes/meter^2 (A/m^2)
$\mathcal{M}$ = magnetic current density in Volts/meter^2 (V/m^2)
ϱ = electric charge density in Coulombs/meter^3 (C/m^3)
ϱ_m = magnetic charge density in Webers/m^3 (Wb/m^3)

Each of the field current or charge quantities is, of course, assumed to be a function of position and time, and will be measured in the rationalized MKSC system of units as noted above. The introduction of the magnetic currents and charges in (1.1)-(1.4) is purely arbitrary since to date there is no evidence of their existance. However, they have been found very useful for constructing mathematical models of electromagnetic problems, where they are often employed as equivalent fictitious sources and this is the primary reason for including them in the definition of Maxwell's equations.

By taking the divergence of (1.1) and making use of (1.4) we obtain

$$\nabla \cdot \mathcal{J} + \frac{\partial \varrho}{\partial t} = 0 \tag{1.5}$$

where we have also invoked the identity $\nabla \cdot (\nabla \times \mathbf{A}) = 0$ which holds for any vector $\mathbf{A}$. Expression (1.5) is known as the continuity equation and implies conservation of charge. Similarly, from (1.2) and (1.3) we obtain the continuity equation for magnetic changes given by

$$\nabla \cdot \mathcal{M} + \frac{\partial \varrho_m}{\partial t} = 0 \tag{1.6}$$

Conversely, one can derive (1.4) by taking the divergence of (1.1) and making use of (1.5). Equation (1.4) then follows by setting the integration constant

with respect to time equal to zero. Likewise, (1.3) can be obtained from (1.2) and (1.6). Consequently, we may take (1.1)-(1.4) as the fundamental equations of electromagnetism or alternatively (1.1), (1.2), (1.5) and (1.6) could be used to form an independent set of equations for the solution of the fields. We will choose here (1.1) - (1.4) as the fundamental set of equation.

The four independent equations (1.1)-(1.4) actually consist of eight scalar ones since (1.1) and (1.2) are vector equations. Noting then that each vector field has three components, we have 20 scalar unknown functions appearing in (1.1)-(1.4) and it is obvious that additional field relations are required for a unique solution of the field quantities. These are provided from the constitutive relations given by

$$\mathcal{D} = \epsilon\mathcal{E} = \epsilon_o\epsilon_r\mathcal{E} \tag{1.7}$$

$$\mathcal{B} = \mu\mathcal{H} = \mu_o\mu_r\mathcal{H} \tag{1.8}$$

$$\mathcal{J} = \sigma\mathcal{E} \tag{1.9}$$

$$\mathcal{M} = \sigma_m\mathcal{H}. \tag{1.10}$$

In (1.7)-(1.10),

ϵ_o = free space permittivity = 8.854×10^{-12} Farads/meter (F/m)

μ_o = free space permeability = $4\pi \times 10^{-7}$ Henrys/meter (H/m)

ϵ_r = medium's relative permittivity constant

μ_r = medium's relative permeability constant

σ = electric current conductivity in Mhos/m ($\mho$/m)

σ_m = magnetic current conductivity in Ohms/m (Ω/m)

which characterize the electrical properties of the medium. They are referred to as the constitutive parameters of that medium and based on their spatial or frequency dependence, the medium can be characterized as linear or non-linear, homogeneous or inhomogeneous, dispersive or non-dispersive, and isotropic or anisotropic.

- If the constitutive parameters are independent of the field intensities, the material is said to be linear
- If the constitutive parameters are constant or uniform throughout a material section, that section of the medium is said to be homogeneous

- If the constitutive parameters are dependent on the oscillating frequency of the fields, that medium is said to be dispersive
- If the constitutive parameters are independent of the field polarity, that medium is referred to as isotropic.

In the case of anisotropic media, the constitutive relations (1.7) and (1.8) take the form

$$\mathcal{D} = \bar{\bar{\epsilon}} \cdot \mathcal{E} \tag{1.11}$$

$$\mathcal{B} = \bar{\bar{\mu}} \cdot \mathcal{H} \tag{1.12}$$

where $\bar{\bar{\epsilon}}$ and $\bar{\bar{\mu}}$ are 3x3 matricies or tensors and can be more explicitly written as

$$\bar{\bar{\epsilon}} = \begin{pmatrix} \epsilon_{xx} & \epsilon_{xy} & \epsilon_{xz} \\ \epsilon_{yx} & \epsilon_{yy} & \epsilon_{yz} \\ \epsilon_{zx} & \epsilon_{zy} & \epsilon_{zz} \end{pmatrix} \tag{1.13}$$

$$\bar{\bar{\mu}} = \begin{pmatrix} \mu_{xx} & \mu_{xy} & \mu_{xz} \\ \mu_{yx} & \mu_{yy} & \mu_{yz} \\ \mu_{zx} & \mu_{zy} & \mu_{zz} \end{pmatrix}. \tag{1.14}$$

We remark that for physically realizable material

$$\epsilon_{ij} = \epsilon_{ji}^{*}, \qquad \mu_{ij} = \mu_{ij}^{*} \tag{1.15}$$

implying that the permittivity and permeability matricies are Hermitian. The * in (1.15) denotes complex conjugation and in the case of real ϵ or μ the corresponding Hermitian matricies are also symmetric. Depending on the specific value and/or relation of the permittivity or permeability matrix components, the material can be classified as uniaxial, biaxial, gyrotropic, etc. In particular, for biaxial material $\bar{\bar{\epsilon}}$ and $\bar{\bar{\mu}}$ take the form,

$$\bar{\bar{\epsilon}} = \begin{pmatrix} \epsilon_x & 0 & 0 \\ 0 & \epsilon_y & 0 \\ 0 & 0 & \epsilon_z \end{pmatrix} \qquad \bar{\bar{\mu}} = \mu\bar{\bar{\mathrm{I}}} = \begin{pmatrix} \mu & 0 & 0 \\ 0 & \mu & 0 \\ 0 & 0 & \mu \end{pmatrix} \tag{1.16}$$

where $\bar{\bar{I}}$ denotes the unit dyad and can be alternatively written as $\bar{\bar{I}} = \hat{x}\hat{x} + \hat{y}\hat{y} + \hat{z}\hat{z}$. When $\epsilon_x = \epsilon_y = \epsilon$ in (1.16), the material is referred to as uniaxial with the z axis being the optics axis. Gyrotropic media are encountered in various plasma studies, and in this case

$$\bar{\bar{\epsilon}} = \begin{pmatrix} \epsilon & -j\epsilon_g & 0 \\ j\epsilon_g & \epsilon & 0 \\ 0 & 0 & \epsilon_z \end{pmatrix} \qquad \bar{\bar{\mu}} = \mu\bar{\bar{I}} \tag{1.17}$$

Generally, biological media such as human tissues, are anisotropic. For example, retina fibers are thought to be uniaxial whereas the cornea appears to be similar to biaxial crystals.

Finally, when the constitutive relations are of the form

$$c\mathcal{D} = \bar{\bar{\epsilon}} \cdot \mathcal{E} + c\bar{\bar{\zeta}} \cdot \mathcal{B} \tag{1.18}$$

$$\mathcal{B} = \bar{\bar{\mu}} \cdot \mathcal{H} + c\bar{\bar{\xi}} \cdot \mathcal{E} \tag{1.19}$$

where $\bar{\bar{\xi}}$ and $\bar{\bar{\zeta}}$ denote tensors, the corresponding medium is referred to as bianisotropic. The representations (1.18) and (1.19) are encountered in the theory of relativity (moving media). However, special forms of these have also been found to hold for stationary magnetoelectric material (Astrov, 1960). For example, Dzyaloshinskie proposed that $\bar{\bar{\epsilon}} = \hat{x}\hat{x}\epsilon + \hat{y}\hat{y}\epsilon + \hat{z}\hat{z}\epsilon_z, \bar{\bar{\zeta}} = \bar{\bar{\xi}} = \hat{x}\hat{x}\xi + \hat{y}\hat{y}\xi + \hat{z}\hat{z}\xi_z$ and $\bar{\bar{\mu}} = \hat{x}\hat{x}\mu + \hat{y}\hat{y}\mu + \hat{z}\hat{z}\mu_z$ for chromium oxide. When $\bar{\bar{\epsilon}} = \epsilon\bar{\bar{I}}$, $\bar{\bar{\mu}} = \mu\bar{\bar{I}}$ and $\bar{\bar{\zeta}} = -j\bar{\bar{\xi}}/\mu = -j\chi\bar{\bar{I}}$ the material is referred to as chiral anisotropic or riisotropic (Engheta, Laktakia (see Post 1962)) with χ being the charality parameter. Chiral material have the characteristic property of not supporting linearly polarized waves. This has been experimentally demonstrated at optical frequencies, but to date we have not found natural material with this behavior at microwave frequencies.

1.2 Maxwell's Equations in Integral Form

The integral form of Maxwell's equations can be directly obtained from their differential counterpoint. By integrating (1.1) and (1.2) over a surface S we

obtain

$$\int\int_S (\nabla \times \mathcal{H}) \cdot d\mathbf{s} = \int\int_S \mathcal{J} \cdot d\mathbf{s} + \int\int_S \frac{\partial \mathcal{D}}{\partial t} \cdot d\mathbf{s} \tag{1.20}$$

$$\int\int_S (\nabla \times \mathcal{E}) \cdot d\mathbf{s} = -\int\int_S \mathcal{M} \cdot d\mathbf{s} - \int\int_S \frac{\partial \mathcal{B}}{\partial t} \cdot d\mathbf{s} \tag{1.21}$$

where $d\mathbf{s} = \hat{n} ds$, in which $\hat{n}$ is the outward unit normal and $d\mathbf{s}$ denotes the differential surface element. Similarly, by integrating (1.3) and (1.4) over a volume V we have

$$\int\int\int_V (\nabla \cdot \mathcal{D}) dv = \int\int\int \varrho dv \tag{1.22}$$

$$\int\int\int (\nabla \cdot \mathcal{B}) dv = \int\int\int \varrho_m dv \tag{1.23}$$

Employing now Stokes theorem in (1.20) and (1.21) and the divergence theorem in (1.22) and (1.23) yields the customary integral form of Maxwell's equations given by

$$\oint_C \mathcal{H} \cdot d\ell = \int\int_S \left(\mathcal{J} + \frac{\partial \mathcal{D}}{\partial t} \right) \cdot d\mathbf{s} \tag{1.24}$$

$$\oint_C \mathcal{E} \cdot d\bar{\ell} = -\int\int_S \left(\mathcal{M} + \frac{\partial \mathcal{B}}{\partial t} \right) \cdot d\mathbf{s} \tag{1.25}$$

$$\oiint_{S_c} \mathcal{D} \cdot d\mathbf{s} = \int\int\int_V \varrho dv \tag{1.26}$$

$$\oiint_{S_c} \mathcal{B} \cdot d\mathbf{s} = +\int\int\int_V \varrho_m dv \tag{1.27}$$

where C is the contour bounding the open surface S illustrated in Fig. 1. As usual, the circle through the single integral implies integration over a closed contour whereas the same symbol through the surface integral implies integration over the surface S_c enclosing the corresponding volume V. We remark that the surface S associated with the integral (1.24) and (1.25) is completely unrelated to that enclosing the volume V.

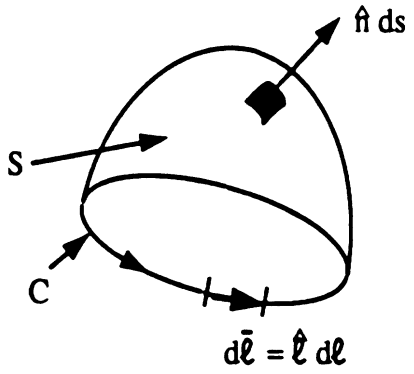

Figure 1.1: Illustration of the differential element ds and the contour C.

1.3 Maxwell's equations in phasor form

Of primary interest in this course is the study of harmonically varying fields with an oscillating angular frequency $\omega = 2\pi f$ rad/sec. The electric field then takes the form ($j = \sqrt{-1}$)

$$\begin{aligned} \mathcal{E}(x,y,z;t) &= Re\left[\mathbf{E}(x,y,z)e^{j\omega t}\right] \\ &= \hat{x}E_{xo}\cos(\omega t + \phi_x) + \hat{y}E_{yo}\cos(\omega t + \phi_y) + \hat{z}E_{zo}\cos(\omega t + \phi_z) \end{aligned} \tag{1.28}$$

where the complex vector

$$\mathbf{E}(x,y,z) = \hat{x}E_{xo}e^{j\phi_x} + \hat{y}E_{yo}e^{j\phi_y} + \hat{z}E_{zo}e^{j\phi_z} \tag{1.29}$$

is referred to as the field phasor, and similar representations can be employed for the other field quantities $\mathcal{D}, \mathcal{H}, \mathcal{B}, \mathcal{J}, \mathcal{M}, \varrho$ and ϱ_m. Introducing these into (1.1)-(1.4) we obtain the simplified set of Maxwell's equations

$$\nabla \times \mathbf{H} = \mathbf{J} + j\omega\epsilon\mathbf{E} \tag{1.30}$$

$$\nabla \times \mathbf{E} = -\mathbf{M} - j\omega\mu\mathbf{H} \tag{1.31}$$

$$\nabla \cdot (\mu\mathbf{H}) = \rho_m \tag{1.32}$$

$$\nabla \cdot (\epsilon\mathbf{E}) = \rho \tag{1.33}$$

where $\mathbf{E}, \mathbf{H}, \mathbf{J}, \mathbf{M}, \rho$ and ρ_m are the corresponding field phasors. In terms of these, the constitutive relations become

$$\mathbf{D} = \epsilon \mathbf{E} \tag{1.34}$$

$$\mathbf{B} = \mu \mathbf{H} \tag{1.35}$$

$$\mathbf{J} = \sigma \mathbf{E} \tag{1.36}$$

$$\mathbf{M} = \sigma_m \mathbf{H} \tag{1.37}$$

where the first two were combined with (1.3) and (1.4) to yield (1.32) and (1.33) above. Similarly, the phasor forms of the continuity equations are

$$\nabla \cdot \mathbf{J} + j\omega\rho = 0 \tag{1.38}$$

$$\nabla \cdot \mathbf{M} + j\omega\rho_m = 0. \tag{1.39}$$

Once (1.30) and (1.31) are solved in conjunction with (1.36) and (1.37) for the phasor quantities, the associated instantaneous fields can be obntained from (1.28).

In general, the current densities $\mathbf{J}$ and $\mathbf{M}$ appearing in (1.30) and (1.31) can be written as a sum of impressed (or excitation) and induced (or conduction) currents. That is, we may write

$$\mathbf{J} = \mathbf{J}_i + \mathbf{J}_c = \mathbf{J}_i + \sigma \mathbf{E} \tag{1.40}$$

$$\mathbf{M} = \mathbf{M}_i + \mathbf{M}_c = \mathbf{M}_i + \sigma_m \mathbf{H} \tag{1.41}$$

where the subscript i denotes impressed currents and the subscript c implies conduction currents. When these are substituted into (1.30) and (1.31), we obtain

$$\nabla \times \mathbf{H} = \mathbf{J}_i + j\omega\epsilon_o\dot{\epsilon}_r\mathbf{E} \tag{1.42}$$

$$\nabla \times \mathbf{E} = -\mathbf{M}_i - j\omega\mu_o\dot{\mu}_r\mathbf{H} \tag{1.43}$$

where

$$\dot{\epsilon}_r = \epsilon_r - j\frac{\sigma}{\omega\epsilon_o} = \epsilon' - j\epsilon'' = \epsilon'(1 - j\tan\delta) \tag{1.44}$$

and

$$\dot{\mu}_r = \mu_r - j\frac{\sigma_m}{\omega\mu_o} = \mu' - j\mu'' = \mu'(1 - j\tan\delta_m) \tag{1.45}$$

represent equivalent relative complex permittivity and permeability constants. Anyone of the representations given in (1.44) and (1.45) is likely to be found in the literature with the quantities

$$\tan\delta = \frac{\epsilon''}{\epsilon'} \tag{1.46}$$

$$\tan\delta_m = \frac{\mu''}{\mu'} \tag{1.47}$$

referred to as the electric and magnetic loss tangents, respectively, of the material.

To summarize, in phasor form Maxwell's equations for isotropic media are

$$\nabla \times \mathbf{H} = \mathbf{J}_i + j\omega\epsilon\mathbf{E} \tag{1.48}$$

$$\nabla \times \mathbf{E} = -\mathbf{M}_i - j\omega\mu\mathbf{H} \tag{1.49}$$

$$\nabla \cdot (\mu\mathbf{H}) = -(\nabla \cdot \mathbf{M}_i)/j\omega \tag{1.50}$$

$$\nabla \cdot (\epsilon\mathbf{E}) = -(\nabla \cdot \mathbf{J}_i)/j\omega \tag{1.51}$$

where we employed the phasor form of (1.38) and (1.39) to rewrite (1.32) and (1.33) as given above. The corresponding integral representations of (1.48) - (1.51) are (see (1.20)-(1.23))

$$\oint \mathbf{H} \cdot d\bar{\ell} = \int\int_S (\mathbf{J}_i + j\omega\epsilon\mathbf{E}) \cdot d\mathbf{s} \tag{1.52}$$

$$\oint \mathbf{E} \cdot d\bar{\ell} = -\int\int_S (\mathbf{M}_i + j\omega\mu\mathbf{H})\, d\mathbf{s} \tag{1.53}$$

$$\oiint_{S_c} \dot{\mu}\mathbf{H} \cdot d\mathbf{s} = -\int\int\int_V \frac{\nabla \cdot \mathbf{M}_i}{j\omega} dv = \int\int\int_V \rho_m dv \tag{1.54}$$

$$\oiint_{S_c} \dot{\epsilon}\mathbf{E} \cdot d\mathbf{s} = -\int\int\int_V \frac{\nabla \cdot \mathbf{J}_i}{j\omega} dv = \int\int\int_V \rho dv \tag{1.55}$$

The parameters ϵ and μ in (1.48)-(1.55) are assumed to be given in terms of the equivalent complex constants (1.44) and (1.45), i.e. $\dot{\epsilon} = \epsilon_o\epsilon_r$ and $\dot{\mu} = \mu_o\mu_r$. For notational convenience, hereon we will drop the dot over the relative constitutive parameters with the understanding that these will still represent all possible material losses.

We observe that given $\mathbf{J}_i$ and $\mathbf{M}_i$, (1.48) and (1.49) imply six scalar equations for the solution of the six components associated with $\mathbf{E}$ and $\mathbf{H}$. Thus, for time harmonic fields, (1.48) and (1.49) or (1.52) and (1.53) are sufficient for a solution of the electric and magnetic fields, and (1.50) and (1.51), or their integral counterparts, are superflous. In fact, the last two equations follow directly from the first two upon taking their divergence and noting again that $\nabla \cdot (\nabla \times \mathbf{A}) = 0$ for any vector $\mathbf{A}$.

Equations (1.48)-(1.55) can be easily modified to apply for anisotropic material as well. This requires that $\epsilon\mathbf{E}$ and $\mu\mathbf{H}$ be replaced by $\overline{\overline{\epsilon}} \cdot \mathbf{E}$ and $\overline{\overline{\mu}} \cdot \mathbf{H}$, respectively. In the case of bianisotropic media the same quantities should be replaced by $\overline{\overline{\epsilon}} \cdot \mathbf{E} + \overline{\overline{\zeta}} \cdot \mathbf{H}$ and $\overline{\overline{\mu}} \cdot \mathbf{H} + \overline{\overline{\xi}} \cdot \mathbf{E}$, respectively, as dictated by the constitutive relations (1.18) and (1.19).

1.4 Natural Boundary Conditions

Maxwell's equations either in their differential or integral form cannot be solved without the specification of the required boundary conditions at material interfaces. The pertinent boundary conditions can be derived directly from the integral form of Maxwell's equations. Instead of (1.52) and (1.53), it is however more convenient to employ the integral equations

$$\int\int\int_V (\nabla \times \mathbf{H}) dv = \int\int\int_V (\mathbf{J}_i + j\omega\epsilon\mathbf{E}) dv \tag{1.56}$$

and

$$\int\int\int_V (\nabla \times \mathbf{E}) dv = -\int\int\int_V (\mathbf{M}_i + j\omega\mu\mathbf{H}) dv \tag{1.57}$$

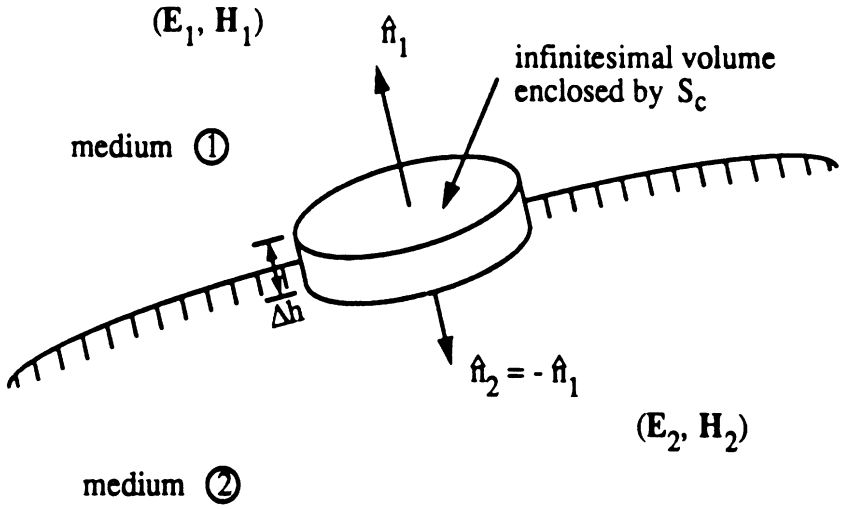

Figure 1.2: Geometry for deriving the boundary conditions.

or equivalently

$$\oiint_{S_c}(\hat{n} \times \mathbf{H})ds = \int\int\int(\mathbf{J}_i + j\omega\epsilon\mathbf{E})dv \tag{1.58}$$

$$\oiint_{S_c}(\hat{n} \times \mathbf{E})ds = -\int\int\int(\mathbf{M}_i + j\omega\mu\mathbf{H})dv \tag{1.59}$$

obtained via application of Stoke's vector identity (Tai, 1971). The boundary conditions for the first two of Maxwell's equation can now be readily derived by selecting S_c to be the surface of a small pillbox (see Fig. 2) enclosing the volume V. The pillbox is positioned at the interface so that half of it is in medium 1 and the other half is in medium 2. It is assumed that $\Delta h \to 0$ so that only its flat faces need be considered in performing the integrations called for in (1.58) and (1.59). Noting that $\hat{n} = \hat{n}_1$ for integration over the top face and $\hat{n} = \hat{n}_2 = -\hat{n}_1$ for the bottom face, by taking the fields to be constant over each face of the pillbox we deduce the boundary conditions (valid at each point on the interface)

$$\hat{n}_1 \times (\mathbf{H}_1 - \mathbf{H}_2) = \mathbf{J}_{is}, \tag{1.60}$$

$$\hat{n}_1 \times (\mathbf{E}_1 - \mathbf{E}_2) = -\mathbf{M}_{is}, \tag{1.61}$$

In these, $\mathbf{J}_{is}$ and $\mathbf{M}_{is}$ denote the impressed electric and (equivalent) magnetic current densities in A/m and Wb/m, respectively, at the interface. In deriving (1.60) and (1.61) we assumed that

$$\lim_{\Delta h \to 0} \frac{1}{2} \Delta h \left[\epsilon_1 \mathbf{E}_1 + \epsilon_2 \mathbf{E}_2\right] = 0$$

and

$$\lim_{\Delta h \to 0} \frac{1}{2} \Delta h \left[\mu_1 \mathbf{H}_1 + \mu_2 \mathbf{H}_2\right] = 0$$

implying the $\epsilon\mathbf{E}$ and $\mu\mathbf{H}$ are finite at the interface.

To generate the boundary condition corresponding to (1.54) and (1.55), we again select the same S_c and V. Through direct integration we readily obtain

$$\hat{n}_1 \cdot (\mu_1 \mathbf{H}_1 - \mu_2 \mathbf{H}_2) = \rho_{ms} \tag{1.62}$$

$$\hat{n}_1 \cdot (\epsilon_1 \mathbf{E}_1 - \epsilon_2 \mathbf{E}_2) = \rho_s \tag{1.63}$$

where ρ_s denotes the unbounded electric surface charge density in C/m^2 at the interface and ρ_{ms} is the corresponding fictitious surface magnetic charge density in Wb/m^2.

The boundary conditions (1.60)-(1.63) although derived for time harmonic fields they are applicable for instantaneous fields as well. As noted earlier, in the time harmonic case, only (1.60) and (1.61) are required in conjunction with (1.48) and (1.49) for a unique solution of the fields.

If we ignore the fictitious magnetic currents and charges appearing in (1.60)-(1.63) we have

$$\hat{n}_1 \times (\mathbf{H}_1 - \mathbf{H}_2) = \mathbf{J}_{is} \tag{1.64}$$

$$\hat{n}_1 \times (\mathbf{E}_1 - \mathbf{E}_2) = 0 \tag{1.65}$$

$$\hat{n}_1 \cdot (\mu_1 \mathbf{H}_1 - \mu_2 \mathbf{H}_2) = 0 \tag{1.66}$$

$$\hat{n}_1 \cdot (\epsilon_1 \mathbf{E}_1 - \epsilon_2 \mathbf{E}_2) = \rho_s \tag{1.67}$$

The first two of these state that the tangential electric fields are continuous across the interface whereas the tangential magnetic fields are discontinuous at the same location by an amount equal to the impressed electric current. Unless a source (i.e. free charge) is actually placed at the interface, $\mathbf{J}_{is}$ is also zero and in that case, the tangential magnetic fields will be continuous across the media as well.

When medium 2 is a perfect electric conductor then $\mathbf{E}_2 = \mathbf{H}_2 = 0$. In addition, M_{is} and ρ_{ms} vanish and (1.60)-(1.63) reduce to

$$\hat{n}_1 \times \mathbf{H}_1 = \mathbf{J}_{is} \tag{1.68}$$

$$\hat{n}_1 \times \mathbf{E}_1 = 0 \tag{1.69}$$

$$\hat{n}_1 \cdot (\mu_1 \mathbf{H}_1) = 0 \tag{1.70}$$

$$\hat{n}_1 \cdot (\epsilon_1 \mathbf{E}_1) = \rho_s. \tag{1.71}$$

The first two of these now imply that the tangential electric field vanishes on the surface of the perfect electric conductor whereas the tangential magnetic field is equal to the impressed electric surface current on the conductor.

1.5 Poynting's Theorem

We observe that the quantity

$$\mathcal{S} = \mathcal{E} \times \mathcal{H} \tag{1.72}$$

has units of power (i.e. Watts/m^2) and can therefore be associated with the energy carried by the instantaneous wave per square unit. This is in the direction coincident with that of the vector $\mathcal{S}$. As stated above, $\mathcal{S}$ denotes instantaneous power, but generally of interest is the time-averaged power. We therefore consider the quantity

$$\langle \mathcal{S} \rangle = \frac{1}{T} \int_0^T (\mathcal{E} \times \mathcal{H})\, dt \tag{1.73}$$

where T is the period of the oscillation, i.e. $\omega = 2\pi/T$. Assuming time harmonic fields, we set

$$\mathcal{E} = Re\left(\mathbf{E}e^{j\omega t}\right) = \hat{e}|E|\cos(\omega t + \alpha) \tag{1.74}$$

$$\mathcal{H} = Re\left(\mathbf{H}e^{j\omega t}\right) = \hat{h}|H|\cos(\omega t + \beta) \tag{1.75}$$

with $\mathbf{E} = \hat{e}|E| = \hat{e}Ee^{j\alpha}$ and $\mathbf{H} = \hat{h}H = \hat{h}|H|e^{j\beta}$. We then have

$$\mathcal{E} \times \mathcal{H} = \frac{1}{2}\hat{e} \times \hat{h}|E||H|\left[\cos(\alpha - \beta) + \cos(2\omega t + \alpha + \beta)\right] \tag{1.76}$$

and by substituting this into (1.73) and integrating, we obtain

$$\langle \mathcal{S} \rangle = \frac{1}{2}\hat{e} \times \hat{h}|E||H|\cos(\alpha - \beta) = \frac{1}{2}Re\left(\mathbf{E} \times \mathbf{H}^*\right) \tag{1.77}$$

where the superscript star implies the complex conjugate of the vector.

The quantity

$$\mathbf{S} = \frac{1}{2}\mathbf{E} \times \mathbf{H}^* \tag{1.78}$$

is known as the complex Poynting vector. Since it is equal to the complex power density of the wave, it is important that we qualify the source and nature of this power. To do this we refer to (1.48) and (1.49), where by dotting each equation with $\mathbf{E}$ or $\mathbf{H}^*$, we have

$$\mathbf{E} \cdot \nabla \times \mathbf{H}^* = \mathbf{J}_i^* \cdot \mathbf{E} - j\omega\epsilon^*\mathbf{E}^* \cdot \mathbf{E} = \mathbf{J}_i^* \cdot \mathbf{E} - j\omega\epsilon^*|\mathbf{E}|^2 \tag{1.79}$$

$$\mathbf{H}^* \cdot \nabla \times \mathbf{E} = -\mathbf{M}_i \cdot \mathbf{H}^* - j\omega\mu\mathbf{H} \cdot \mathbf{H}^* = -\mathbf{M}^i \cdot \mathbf{H}^* - j\omega\mu|\mathbf{H}|^2 \tag{1.80}$$

From the vector identity

$$\nabla \cdot (\mathbf{E} \times \mathbf{H}^*) = \mathbf{H}^* \cdot \nabla \times \mathbf{E} - \mathbf{E} \cdot \nabla \times \mathbf{H}^* \tag{1.81}$$

we then obtain

$$\nabla \cdot (\mathbf{E} \times \mathbf{H}^*) = j\omega\epsilon^*|\mathbf{E}|^2 - j\omega\mu|\mathbf{H}|^2 - \mathbf{J}_i^* \cdot \mathbf{E} - \mathbf{M}_i \cdot \mathbf{H}^* \tag{1.82}$$

which is an identity valid everywhere in space. Integrating both sides of this over a volume V containing all sources, and invoking the divergence theorem yields

$$\frac{1}{2}\oiint_{S_c}(\mathbf{E}\times\mathbf{H}^*)\cdot d\mathbf{s}=\frac{1}{2}\int\int\int_V\left[j\omega\epsilon^*|\mathbf{E}|^2+j\omega\mu|\mathbf{H}|^2-\mathbf{J}_i^*\cdot\mathbf{E}-\mathbf{M}_i\cdot\mathbf{H}^*\right]dv \tag{1.83}$$

which is commonly referred to as Poynting's theorem. Since S_c is closed, based on energy conservation one deduces that the right hand side of (1.83) must represent the sum of the power stored or radiated, i.e. escaping, out of the volume V. Each term of the volume integral of (1.83) is associated with a specific type of power but before proceeding with their identification, it is instructive that ϵ^* be first replaced by $\epsilon_o\epsilon_r+j\frac{\sigma}{w}$. Equation (1.85) can then be rewritten as

$$\frac{1}{2}Re\oiint_{S_c}(\mathbf{E}\times\mathbf{H})\cdot d\mathbf{s}=P_{ei}+P_{mi}-P_d \tag{1.84}$$

$$\frac{1}{2}Im\oiint_{S_c}(\mathbf{E}\times\mathbf{H})\cdot d\mathbf{s}=2\omega[W_e-W_m]-\frac{1}{2}Im\int\int\int[\mathbf{J}_i^*\cdot\mathbf{E}+\mathbf{M}_i\cdot\mathbf{H}^*]\,dv \tag{1.85}$$

where

$$P_{ei} = -\frac{1}{2}\int\int\int_V Re(\mathbf{J}_i^*\cdot\mathbf{E})dv = \text{average outgoing power due to the source } \mathbf{J}_i \tag{1.86}$$

$$P_{mi} = -\frac{1}{2}\int\int\int_V Re(\mathbf{M}_i\cdot\mathbf{H}^*)dv = \text{average outgoing power due to the source } \mathbf{M}_i \tag{1.87}$$

$$P_d = \frac{1}{2}\int\int\int_V \sigma|\mathbf{E}|^2dv = \text{average power dissipated in } V \tag{1.88}$$

$$W_e = \frac{1}{4}\int\int\int_V \epsilon_o\epsilon_r|\mathbf{E}|^2dv = \text{average electric energy in } V \tag{1.89}$$

$$W_m = \frac{1}{4}\int\int\int_V \mu_o\mu_r|\mathbf{H}|^2dv = \text{average magnetic energy in } V \tag{1.90}$$

The time-averaged power delivered to the electromagnetic field outside V is clearly the sum of P_{ei} and P_{mi} whereas P_d is that dissipated in V due to conductor losses. Thus we may consider

$$P_{av} = \frac{1}{2} Re \oiint_{S_c} (\mathbf{E} \times \mathbf{H}^*) \cdot d\mathbf{s} \tag{1.91}$$

to be the average radiated power outside V if σ is zero in V. Expression (1.85) gives the reactive power, i.e. that which is stored within V and is not allowed to escape outside the boundary of S_c.

1.6 Uniqueness Theorem

Whenever one pursues a solution to a set of equations it is important to know a priori whether this solution is unique and if not, what are the required conditions for a unique solution. This is important because depending on the application, different analytical or numerical methods will likely be used for the solution of Maxwell's equations. Given that Maxwell's equation (subject to the appropriate boundary conditions) yield a unique solution, one is then comforted to know that any convenient method of analysis will yield the correct solution to the problem.

The most common form of the uniqueness theorem is: *In a region V completely occupied with dissipative media, a harmonic field $(\mathbf{E}, \mathbf{H})$ is uniquely determined by the impressed currents in that region plus the tangential components of the electric and magnetic fields on the closed surface S_c bounding V.* This theorem may be proved by assuming for the moment that two solutions exist, denoted by $(\mathbf{E}_1, \mathbf{H}_1)$ and $(\mathbf{E}_2, \mathbf{H}_2)$. Both fields must, of course, satisfy Maxwell's equations (1.48) and (1.49) with the same impressed currents $(\mathbf{J}_i, \mathbf{M}_i)$. We have

$$\nabla \times \mathbf{H}_1 = \mathbf{J}_i + j\omega\epsilon\mathbf{E}_1 , \quad \nabla \times \mathbf{H}_2 = \mathbf{J}_i + j\omega\epsilon\mathbf{E}_2$$

$$\nabla \times \mathbf{E}_1 = -\mathbf{M}_i - j\omega\mu\mathbf{H}_1 , \quad \nabla \times \mathbf{E}_2 = -\mathbf{M}_i - j\omega\mu\mathbf{H}_2$$

and when these are subtracted we obtain

$$\nabla \times \mathbf{H}' = j\omega\epsilon\mathbf{E}' \tag{1.92}$$

$$\nabla \times \mathbf{E}' = -j\omega\mu\mathbf{H}' \tag{1.93}$$

where $\mathbf{E}' = \mathbf{E}_1 - \mathbf{E}_2$ and $\mathbf{H}' = \mathbf{H}_1 - \mathbf{H}_2$. To prove the theorem it is then necessary to show that $(\mathbf{E}', \mathbf{H}')$ are zero or equivalently, if no sources are enclosed by a volume V, the fields in that volume are zero for a given set of tangential electric and magnetic fields on S_c. Recalling Poynting's theorem for a source-free region, from (1.84)-(1.90) (with $\mathbf{J}_i = \mathbf{M}_i = 0$) we have

$$Re \oiint_{S_c} (\mathbf{E}' \times \mathbf{H}'^*) \cdot d\mathbf{s} = -\int\int\int_V \sigma |\mathbf{E}'|^2 dv \tag{1.94}$$

$$Im \oiint_{S_c} (\mathbf{E}' \times \mathbf{H}'^*) \cdot d\mathbf{s} = \int\int\int_V \omega \left(\epsilon_o \epsilon_r |\mathbf{E}'|^2 - \mu_o \mu_r |\mathbf{H}'|^2 \right) dv \tag{1.95}$$

Since we assumed that the tangential $\mathbf{E}$ and $\mathbf{H}$ are also given on S_c, it follows that $(\mathbf{E}' \times \mathbf{H}'^*) \cdot d\mathbf{s}$ vanishes everywhere on S_c. Thus, the right hand side of (1.94) must be zero and since $|\mathbf{E}'|^2$ is always greater than zero we deduce that $\mathbf{E}'$ must vanish everywhere in V. Consequently, $\mathbf{H}'$ must also vanish in V proving the uniqueness theorem stated above.

As a corolary to the uniqueness theorem, it can be shown from (1.94) that *if a harmonic field has zero tangential* $\mathbf{E}$ *or zero tangential* $\mathbf{H}$ *field on a surface enclosing a source-free region* V *occupied by dissipative media, the field vanishes everywhere within* V.

In the case of lossless media, (1.94) can no longer be used to show that $\mathbf{E}$ vanishes in V if no sources are enclosed. We must then resort to (1.95) which states that no time-averaged power enters or leaves the region. It is consequently possible that the fields be nonzero in the volume V even when the tangential $\mathbf{E}$ and $\mathbf{H}$ are zero on different parts of the surface S_c. This implies the existance of resonant-mode fields within V for which the time-averaged energy stored in the electric field is equal to the time-averaged energy stored in the magnetic field within that region. By definition the volume integral vanishes in (1.95) for such a field. This nonuniqueness for lossless media will be discussed in later chapters when we consider numerical solutions for the scattered field from specific structures. In general, it will be seen that the numerical solution fails when resonant modes are excited unless some remedies are taken to suppress these nonphysical modes.

1.7 Superposition Theorem

The superposition theorem states that for a linear medium, the total field intensity due to two or more sources is equal to the sum of the field intensities attributed to each individual source radiating independent of the others. In particular, let us consider two electric sources $\mathbf{J}_1$ and $\mathbf{J}_2$. On the basis of the superposition theorem, to find the total field caused by the simultaneous presence of both sources we can consider the field due each individual source in isolation. The fields $(\mathbf{E}_1, \mathbf{H}_1)$ due to $\mathbf{J}_1$ satisfy the equation

$$\nabla \times \mathbf{H}_1 = \mathbf{J}_1 + j\omega\epsilon\mathbf{E}_1 \tag{1.96}$$

$$\nabla \times \mathbf{E}_1 = -j\omega\mu\mathbf{H}_1 \tag{1.97}$$

and the fields corresponding to $\mathbf{J}_2$ satisfy

$$\nabla \times \mathbf{H}_2 = \mathbf{J}_2 + j\omega\epsilon\mathbf{E}_2 \tag{1.98}$$

$$\nabla \times \mathbf{E}_2 = -j\omega\mu\mathbf{H}_2 \tag{1.99}$$

By adding these two sets of equations, it is clear that the total field due to both sources combined is given by

$$\mathbf{E} = \mathbf{E}_1 + \mathbf{E}_2 \qquad \mathbf{H} = \mathbf{H}_1 + \mathbf{H}_2 \tag{1.100}$$

where $(\mathbf{E}_1, \mathbf{H}_1)$ and $(\mathbf{E}_2, \mathbf{H}_2)$ are obtained by solving seperately (1.96)-(1.97) and (1.98)-(1.99), respectively.

1.8 Duality Theorem

The duality theorem relates to the interchangability of the electric and magnetic fields, currents, charges or material properties. We observe from (1.30) and (1.31) that the first can be obtained from the second via the interchanges

$$\begin{aligned} &\mathbf{M} \rightarrow -\mathbf{J} \\ &\mathbf{E} \rightarrow \mathbf{H} \\ &\mathbf{H} \rightarrow -\mathbf{E} \\ &\mu \rightarrow \epsilon \end{aligned} \tag{1.101a}$$

Similarly, (1.31) can be obtained from (1.30) via the interchanges

$$\begin{aligned} \mathbf{J} &\rightarrow \mathbf{M} \\ \mathbf{E} &\rightarrow \mathbf{H} \\ \mathbf{H} &\rightarrow -\mathbf{E} \\ \epsilon &\rightarrow \mu \end{aligned} \tag{1.101b}$$

Based on these observations we can state that if $(\mathbf{E}_1, \mathbf{H}_1)$ represent the fields due to the harmonic sources $(\mathbf{J}_1, \mathbf{M}_1)$ in a linear medium (μ_1, ϵ_1), then the sources $(\mathbf{J}_2 = -\mathbf{M}_1,\ \mathbf{M}_2 = \mathbf{J}_1)$ will generate the fields $(\mathbf{E}_2 = -\mathbf{H}_1,\ \mathbf{H}_2 = \mathbf{E}_1)$ if radiating in a linear medium having $(\mu_2 = \epsilon_1,\ \epsilon_2 = \mu_1)$. This is a statement of the duality theorem. If we assume $\mathbf{M}_1 = 0$, it simply states that the fields due to a magnetic source of equal strength, i.e. $\mathbf{M}_2 = \mathbf{J}_1$, radiating in the dual medium are $(\mathbf{E}_2 = -\mathbf{H}_1,\ \mathbf{H}_2 = \mathbf{E}_1)$. The material parameters dual to (ϵ_1, μ_1) are $(\epsilon_2 = \mu_1,\ \mu_2 = \epsilon_1)$ and the fields dual to $(\mathbf{E}_1, \mathbf{H}_1)$ are $(\mathbf{E}_2 = -\mathbf{H}_1, \mathbf{H}_2 = \mathbf{E}_2)$. Alternatively, if $\mathbf{J}_1 = 0$, the dual fields to $(\mathbf{E}_1, \mathbf{H}_1)$ are generated by the electric source $\mathbf{J}_2 = -\mathbf{M}_1$ radiating in the dual medium.

It is seen that the duality theorem can reduce computational time and effort when one is able to invoke it for a particular application.

1.9 Volume equivalence theorem

The volume equivalence theorem shows how one can replace field disturbances caused by the presence of a material body with some prescribed equivalent currents.

Let us consider the harmonic sources $(\mathbf{J}_i, \mathbf{M}_i)$ radiating in the presence of a material structure as dipicted in Fig. 3. When the source fields $(\mathbf{E}^i, \mathbf{H}^i)$ reach the inhomogeneous (linear) body there will be additional fields $(\mathbf{E}^s, \mathbf{H}^s)$ generated as dictated by the continuity boundary conditions. That is, because the fields penetrating the material will not be equal to the external excitation fields $(\mathbf{E}^i, \mathbf{H}^i)$, it will be necessary that new external fields be generated to ensure satisfaction of the tangential field continuity conditions. These new fields $(\mathbf{E}^s, \mathbf{H}^s)$ are commonly referred to as the *scattered fields* and the total field internal and external to the material body can be written as

$$\mathbf{E} = \mathbf{E}^i + \mathbf{E}^s \qquad \mathbf{H} = \mathbf{H}^i + \mathbf{H}^s \tag{1.102}$$

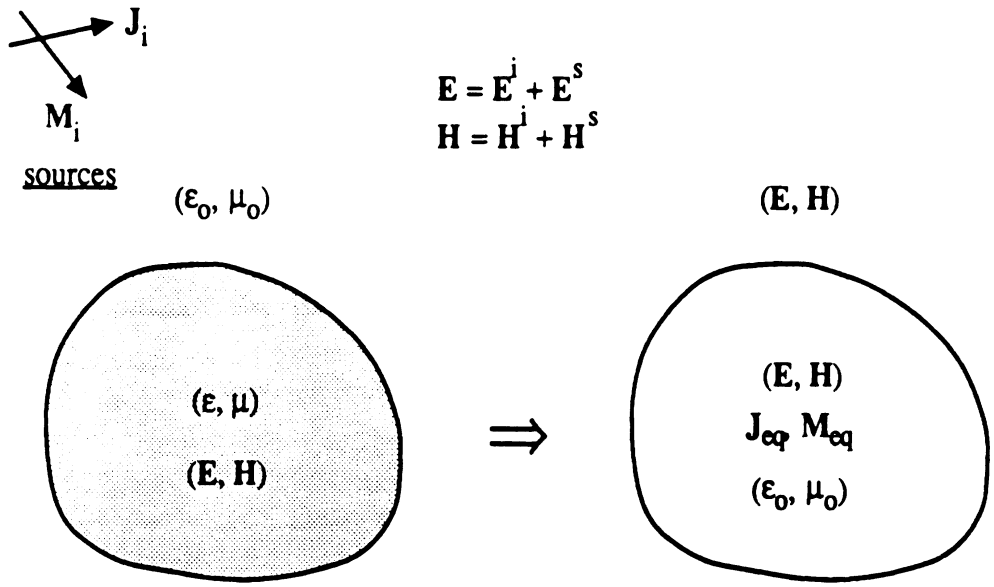

Figure 1.3: Volume Equivalence Theorem

The incident field is, of course, expected to satisfy the equations

$$\nabla \times \mathbf{H}^i = \mathbf{J}_i + j\omega\epsilon_o\mathbf{E}^i, \quad \nabla \times \mathbf{E}^i = -j\omega\mu_o\mathbf{H}^i \tag{1.103}$$

whereas the total field satisfies

$$\nabla \times \mathbf{H} = \mathbf{J}_i + j\omega\epsilon\mathbf{E}, \quad \nabla \times \mathbf{E} = -j\omega\mu\mathbf{H} \tag{1.104}$$

when measured within the material body having the material, parameters (ϵ, μ). Subtracting (1.103) from (1.104) and making use of (1.102) we obtain

$$\nabla \times \mathbf{H}^s = j\omega(\epsilon - \epsilon_o)\mathbf{E} + j\omega\epsilon_o\mathbf{E}^s \tag{1.105}$$

$$\nabla \times \mathbf{E}^s = -j\omega(\mu - \mu_o)\mathbf{H} - j\omega\mu_o\mathbf{H}^s \tag{1.106}$$

When these are compared to (1.30) and (1.31) we conclude that the scattered fields $(\mathbf{E}^s, \mathbf{H}^s)$ can be thought as generated by the equivalent harmonic sources

$$\mathbf{J}_{eq} = j\omega(\epsilon - \epsilon_o)\mathbf{E} = j\omega\epsilon_o(\epsilon_r - 1)\mathbf{E} \tag{1.107}$$

$$\mathbf{M}_{eq} = j\omega(\mu - \mu_o)\mathbf{H} = j\omega\mu_o(\mu_r - 1)\mathbf{H} \tag{1.108}$$

which occupy the original volume of the material body and radiate in free space. That is, the material body can be removed and instead be replaced by the equivalent volume currents defined by (1.107) and (1.108).

It would appear from (1.107) and (1.108) that six independent current components are required to model a ferrite material scatterer. However, a closer examination reveals otherwise and this is important in numerical simulations of material scatterers. By taking the curl of equations (1.104) and replacing $(\mathbf{J}_i, \mathbf{M}_i)$ with $(\mathbf{J}_{eq}, \mathbf{M}_{eq})$ we have

$$\nabla \times (\nabla \times \mathbf{E}) - k_o^2 \mathbf{E} = -j\omega\mu_o \mathbf{J}_{eq} - \nabla \times \mathbf{M}_{eq} \tag{1.109}$$

$$\nabla \times (\nabla \times \mathbf{H}) - k_o^2 \mathbf{H} = -j\omega\epsilon_o \mathbf{M}_{eq} + \nabla \times \mathbf{J}_{eq} \tag{1.110}$$

where $k_o = \omega\sqrt{\mu_o\epsilon_o} = 2\pi/\lambda_o$ is the free space propagation constant and λ_o is the wavelength. Also we have set $\epsilon_r = \mu_r = 1$ since $\mathbf{J}_{eq}$ and $\mathbf{M}_{eq}$ are assumed to radiate in free space. Clearly (1.109) can be solved independent of (1.110) and implies that the curl of the magnetic current appears as another electric current given by

$$\tilde{\mathbf{J}}_{eq} = \nabla \times \mathbf{M}_{eq}/j\omega\mu_o \tag{1.111}$$

Thus, instead of the equivalent currents (1.107) and (1.108), one could replace the presence of a material body by the radiation of the equivalent electric current density

$$\begin{aligned} \mathbf{J}_{eq} &= j\omega\epsilon_o(\epsilon_r - 1)\mathbf{E} + \nabla \times [(\mu_r - 1)\mathbf{H}] \\ &= \frac{(\epsilon_r - 1)}{\epsilon_r}\nabla \times \mathbf{H} + \nabla \times [(\mu_r - 1)\mathbf{H}] \end{aligned} \tag{1.112}$$

again occupying the original volume of the body. Similarly, we could replace the presence of the material body by the radiation of the equivalent magnetic current density

$$\begin{aligned} \mathbf{M}_{eq} &= j\omega\mu_o(\mu_r - 1)\mathbf{H} - \nabla \times [(\epsilon_r - 1)\mathbf{E}] \\ &= -\frac{(\mu_r - 1)}{\mu_r}\nabla \times \mathbf{E} - \nabla \times [(\epsilon_r - 1)\mathbf{E}] \end{aligned} \tag{1.113}$$

which is obviously the dual of (1.112). Thus, we observe that a material body can be modelled with only electric or magnetic currents, implying that three independent current components are required in either case. The aforementioned equivalence between electric and magnetic currents was originally presented by Mayes [], although in a different context. It should be noted, however, that in (1.109) - (1.113), $(\mathbf{J}_{eq}, \mathbf{M}_{eq})$ are defined over a finite domain, and this needs to be considered when taking the indicated curls. In other words, the fact that μ_r and ϵ_r are discontinuities at the outer boundary of the scatterer or perhaps at other boundaries internal to the scatterer must be accounted for when taking curl. We will discuss this in more detail when we later make use of these equivalences.

1.10 Surface equivalence theorem

The surface equivalence theorem follows directly from the uniqueness theorem stating that a harmonic field $(\mathbf{E}, \mathbf{H})$ in a source free region V can be uniquely determined by a knowledge of the tangential fields on an imaginary surface S_c bounding V. This implies that it is not necessary to explicitly know the sources of $(\mathbf{E}, \mathbf{H})$ in order that this field be determined in regions outside those sources. Instead, one could specify equivalent currents on the surface S bounding the source free region V by invoking Ampere's law (see (1.60) and (1.61)). This, of course, provides an alternative formulation which is often useful since it could lead to simplifications in the analysis.

To illustrate the surface equivalence theorem, let us consider a material region enclosed by the surface as shown in figure 4. We are interested in computing the field outside the material region and thus V is the volume between S and a surface at infinity. For the region interior to S we may arbitrarily assume that the fields are zero as illustrated in Fig. 4b. In accordance with the boundary conditions given by (1.60) and (1.61), the fields $(\mathbf{E}, \mathbf{H})$ outside S can then be thought as generated by the equivalent surface currents

$$\mathbf{J}_s = \hat{n} \times \mathbf{H} \tag{1.114}$$

$$\mathbf{M}_s = \mathbf{E} \times \hat{n} \tag{1.115}$$

where $\hat{n}$ is the unit normal to S_c pointing toward V. This form of the surface equivalence theorem is known as Love's equivalence principle. It assumes zero

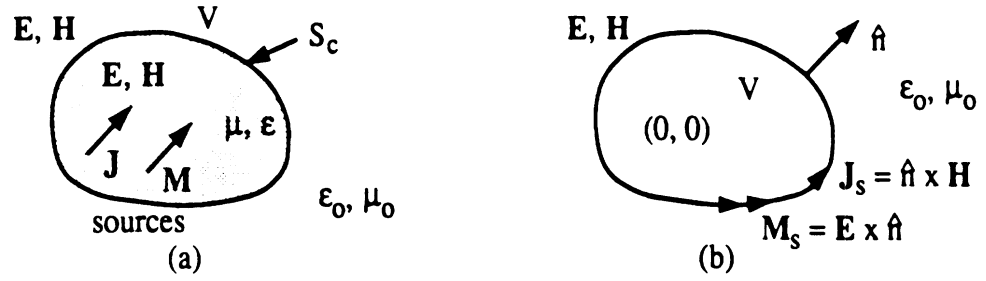

Figure 1.4: Love's equivalence principle (a) original problem (b) equivalent problem.

field within S_c, a condition which can be satisfied when this region is occupied by a perfect electric or magnetic conductor. For a planar electric conductor, image theory dictates that the net electric current on S_c will be zero whereas M_s is doubled (see Fig. 5). Thus, the field outside S_c can be also represented

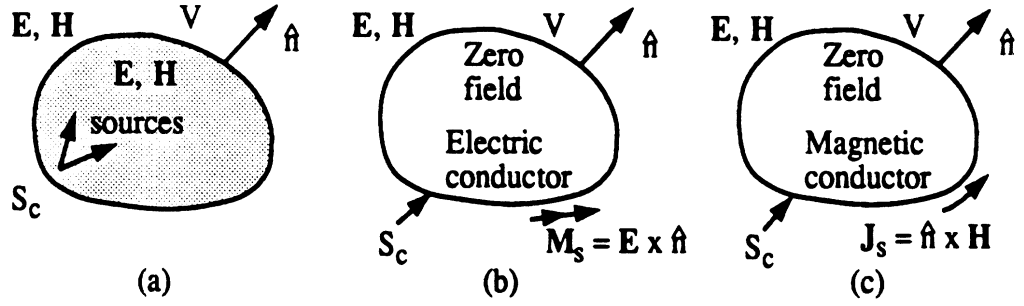

Figure 1.5: Other forms of Love's equivalence principle (a) original problem (b) equivalent problem with a magnetic current on an electric conductor (c) equivalent problem with an electric current on a magnetic conductor.

by the radiation of the equivalent surface magnetic current

$$\mathbf{M}_s = 2\mathbf{E} \times \hat{n} \tag{1.116}$$

where $\mathbf{E}$ is the value of the electric field on the planar surface S_c. Alternatively, the null field condition can be satisfied when S_c is the surface of a planar perfect magnetic conductor and in this case $\mathbf{M}_s$ vanishes whereas $\mathbf{J}_s = 2\hat{n} \times \mathbf{H}$.

When setting up the equivalent surface currents one can also select the field within S_c to be other than zero. For example, referring to Fig. 6, if these are set to $(\mathbf{E}^c, \mathbf{H}^c)$, the corresponding surface equivalent currents are

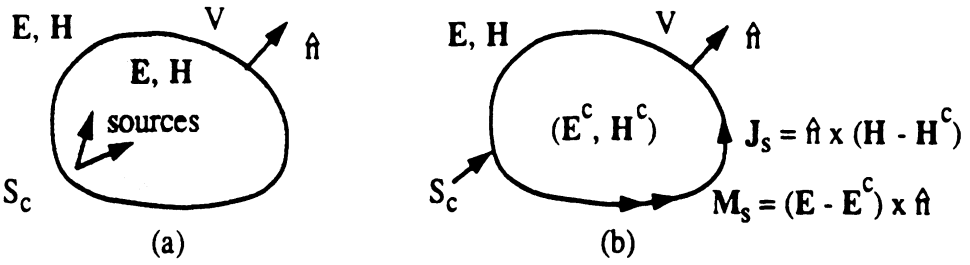

Figure 1.6: General form of the equivalence theorem (a) original problem (b) equivalence problem.

$$\mathbf{J}_s = \hat{n} \times (\mathbf{H} - \mathbf{H}^c) \tag{1.117a}$$

$$\mathbf{M}_s = (\mathbf{E} - \mathbf{E}^c) \times \hat{n}\,. \tag{1.117b}$$

These will now generate the field $(\mathbf{E}, \mathbf{H})$ exterior to S_c and the field $(\mathbf{E}^c, \mathbf{H}^c)$ interior to S_c.

1.11 Reciprocity and Reaction Theorems

The reciprocity theorem for electromagnetics parallels the familiar theorem in circuit theory. It simply states that the fields and sources can be interchanged in a given problem or set-up without effecting the system's response. This implies that the transmitting and receiving antenna patterns are the same even though in the first case the source was at the feed whereas for the receiving antenna the source is at infinity. Another example refers to the case of plane wave scattering illustrated in figure 7. Let us assume that the far zone scattered field $\mathbf{E}^s$ is measured along $\hat{r}$ and is caused by a plane wave excitation $\mathbf{E}^i$ incident along $\hat{r}^i$. Based on the reciprocity theorem, one can then state that the scattered field is unchanged when we let $\hat{r}^i \rightarrow -\hat{r}$ and $\hat{r} \rightarrow -\hat{r}^i$.

To derive a mathematical statement of the reciprocity theorem, we assume the existance of two sets of fields caused by two different sets of sources radiating in the same environment. In particular, suppose that the field $(\mathbf{E}_1, \mathbf{H}_1)$ are associated with the sources $(\mathbf{J}_1, \mathbf{M}_1)$, whereas the fields $(\mathbf{E}_2, \mathbf{H}_2)$ are due to the sources $(\mathbf{J}_2, \mathbf{M}_2)$. Each set of these fields and sources will then satisfy

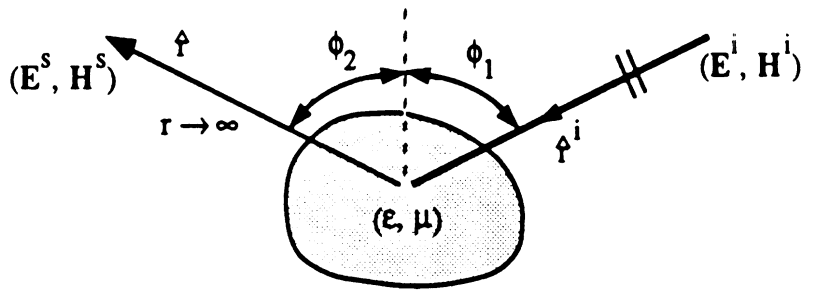

Figure 1.7: Illustration of reciprocity for plane wave incidence and far zone observation.

the equations

$$\nabla \times \mathbf{E}_{\substack{1\\2}} = -j\omega\mu \mathbf{H}_{\substack{1\\2}} - \mathbf{M}_{\substack{1\\2}} \tag{1.118a}$$

and

$$\nabla \times \mathbf{H}_{\substack{1\\2}} = j\omega\epsilon \mathbf{E}_{\substack{1\\2}} - \mathbf{J}_{\substack{1\\2}} . \tag{1.118b}$$

By invoking the identity

$$\nabla \cdot (\mathbf{A} \times \mathbf{B}) = \mathbf{B} \cdot \nabla \times \mathbf{A} - \mathbf{A} \cdot \nabla \times \mathbf{B} \tag{1.119}$$

we then have

$$\nabla \cdot (\mathbf{E}_1 \times \mathbf{H}_2 - \mathbf{E}_2 \times \mathbf{H}_1) = \mathbf{H}_2 \cdot \nabla \times \mathbf{E}_1 - \mathbf{E}_1 \cdot \nabla \times \mathbf{H}_2 - \mathbf{H}_1 \cdot \nabla \times \mathbf{E}_2 + \mathbf{E}_2 \cdot \nabla \times \mathbf{H}_1 . \tag{1.120}$$

This can be simplified by introducing (1.118) giving

$$\mathbf{H}_2 \cdot \nabla \times \mathbf{E}_1 = \mathbf{H}_2 \cdot (-j\omega\mu\mathbf{H}_1 - \mathbf{M}1) = -j\omega\mu\mathbf{H}_1 \cdot \mathbf{H}_2 - \mathbf{M}_1 \cdot \mathbf{H}_2$$

$$-\mathbf{H}_1 \cdot \nabla \times \mathbf{E}_2 = -\mathbf{H}_1 \cdot (-j\omega\mu\mathbf{H}_2 - \mathbf{M}_1) = j\omega\mu\mathbf{H}_1 \cdot \mathbf{H}_2 + \mathbf{M}_1 \cdot \mathbf{H}_2$$

etc., which upon substitution into (1.120) yield

$$-\nabla \cdot (\mathbf{E}_1 \times \mathbf{H}_2 - \mathbf{E}_2 \times \mathbf{H}_1) = \mathbf{E}_1 \cdot \mathbf{J}_2 + \mathbf{H}_2 \cdot \mathbf{M}_1 - \mathbf{E}_2 \cdot \mathbf{J}_1 - \mathbf{H}_1 \cdot \mathbf{M}_2 \tag{1.121}$$

Integrating both sides of this equation over a volume V enclosed by the surface S_c, and applying the divergence theorem it is further deduced that

$$-\oiint_{S_c}(\mathbf{E}_1 \times \mathbf{H}_2 - \mathbf{E}_2 \times \mathbf{H}_1)\cdot \hat{n} ds = \int\int\int_V (\mathbf{E}_1 \cdot \mathbf{J}_2 + \mathbf{H}_2 \cdot \mathbf{M}_1 - \mathbf{E}_2 \cdot \mathbf{J}_1 - \mathbf{H}_1 \cdot \mathbf{M}_2) dv \qquad (1.122)$$

It will be shown in the next chapter that in the far field (let S_c become an infinite circle),

$$\mathbf{E} = -Z_o \hat{r} \times \mathbf{H} \quad \textit{and} \quad \mathbf{H} = \frac{1}{Z_o}\hat{r} \times \mathbf{E}\,.$$

where $Z_o = \sqrt{\mu_o/\epsilon_o}$ is the free space intrinsic impedance, and thus

$$\mathbf{E}_1 \times \mathbf{H}_2 = \mathbf{E}_1 \times \frac{(\hat{r} \times \mathbf{E}_2)}{Z_o} = \frac{1}{Z_o}[(\mathbf{E}_1 \cdot \mathbf{E}_2)\hat{r} - (\mathbf{E}_1 \cdot \hat{r})\mathbf{E}_2] = \frac{1}{Z_o}(\mathbf{E}_1 \cdot \mathbf{E}_2)\hat{r}$$

$$\mathbf{E}_2 \times \mathbf{H}_1 = \frac{\mathbf{E}_2 \times (\hat{r} \times \mathbf{E}_1)}{Z_o} = \frac{1}{Z_o}[(\mathbf{E}_2 \cdot \mathbf{E}_1)\hat{r} - (\mathbf{E}_1 \cdot \hat{r})\mathbf{E}_1] = \frac{1}{Z_o}(\mathbf{E}_2 \cdot \mathbf{E}_1)\hat{r}$$

implying that the surface integral in (1.122) vanishes when S_c is a sphere of infinite radius. Consequently, we conclude that

$$\int\int\int_V (\mathbf{E}_1 \cdot \mathbf{J}_2 - \mathbf{H}_1 \cdot \mathbf{M}_2) dv = \int\int\int_V (\mathbf{E}_2 \cdot \mathbf{J}_1 - \mathbf{H}_2 \cdot \mathbf{M}_1) dv \qquad (1.123)$$

which is a mathematical statement of the reciprocity theorem (special case of the Lorentz reciprocity theorem given by (1.122)). It states that the fields and source can be interchanged without altering the outcome of (1.123). Integrals of the type in (1.123) are also referred to as reactions of one set of sources with the fields caused by another set of sources. Based on this reasoning, (1.123) is often written as

$$\langle 1,2\rangle = \langle 2,1\rangle \qquad (1.124)$$

where

$$\langle 1,2\rangle = \int\int\int_V (\mathbf{E}_1 \cdot \mathbf{J}_2 - \mathbf{H}_1 \cdot \mathbf{M}_2) dv. \qquad (1.125)$$

The symbolism $\langle 1,2\rangle$ denotes the reaction of fields $(\mathbf{E}_1, \mathbf{H}_1)$ with the sources $(\mathbf{J}_2, \mathbf{M}_2)$ and (1.125) is often referred to as the reaction theorem. If $\mathbf{J}_2$ represents a linear source of strength I_2 (i.e. $\mathbf{J}_2 = I_2\hat{\ell}$) and $\mathbf{M}_2 = 0$, (1.125) reduces to

$$\langle 1,2\rangle = \int\int\int_V \mathbf{E}_1 \cdot \mathbf{J}_2 dv = I_2 \int \mathbf{E}_1 \cdot \hat{\ell} d\ell = -V_2^{(1)} I_2 \tag{1.126}$$

where $V_2^{(1)}$ is the voltage across the terminals of source 2 due to some unspecified source 1. Similarly, across the terminals of a magnetic source $\mathbf{M} = K\hat{\ell}$

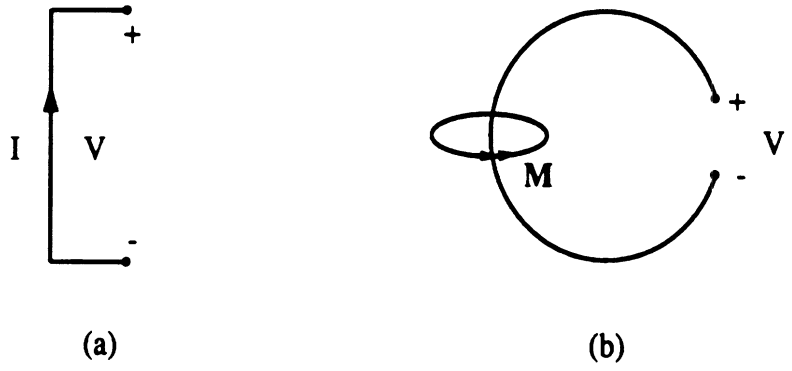

Figure 1.8: Illustration of circuit source (a) current source (b) voltage source.

(current loop), shown in Fig. 8, $V = -K$, and if we set $\mathbf{M}_2 = K_2\hat{\ell}$ and $\mathbf{J}_2 = 0$, (1.125) gives

$$\langle 1,2\rangle = -\int\int\int \mathbf{H}_1 \cdot \mathbf{M}_2 dv = -K_2 \int \mathbf{H}_1 \cdot \hat{\ell} d\ell = +V_2 I_2^{(1)} \tag{1.127}$$

where $I_2^{(1)}$ is now the current flowing to the terminal of source 2 due to the field excitation $\mathbf{H}_1$ from some unspecified source 1.

To illustrate the application of the reciprocity theorem in electromagnetics we consider the radiation of two antenna elements in free space as illustrated in fig. 9. Each of these radiate the fields $(\mathbf{E}_1, \mathbf{H}_1)$ and $(\mathbf{E}_2, \mathbf{H}_2)$, respectively, and their equivalent circuit parameters can be characterized by the usual system

$$\begin{bmatrix} V_1 \\ V_2 \end{bmatrix} = \begin{bmatrix} Z_{11} & Z_{12} \\ Z_{21} & Z_{22} \end{bmatrix} \begin{bmatrix} I_1 \\ I_2 \end{bmatrix} \tag{1.128}$$

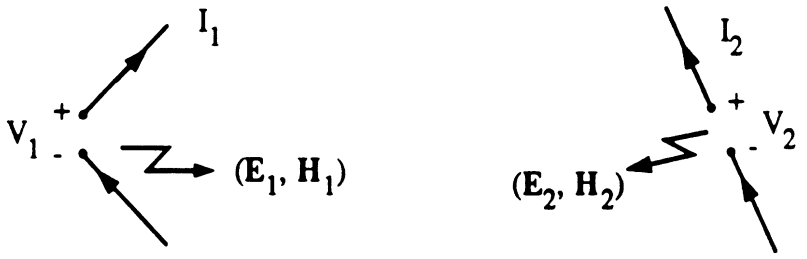

Figure 1.9: Reaction between two antennas.

which is identical to that for a two-part network in circuit theory. Reciprocity and the reaction theorem will now prove useful in determining the elements Z_{ij} of the impedance matrix. They can be easily determined by shorting or open-circuiting the antennas one at a time. Setting $I_2 = 0$, gives

$$Z_{21} = \frac{V_2^{(1)}}{I_1}$$

and by referring to (1.126) we may express Z_{21} as

$$Z_{21} = -\frac{\langle 1,2 \rangle}{I_1 I_2} \tag{1.129}$$

By invoking the reciprocity theorem (1.123), we also have $Z_{12} = Z_{21}$ and in general

$$Z_{ij} = -\frac{\langle j,i \rangle}{I_i I_j}. \tag{1.130}$$

This expression is valid for computing the self impedance elements Z_{ii} as well, and will be later found useful in numerical simulations of antenna and scattering problems.

1.12 Approximate Boundary Conditions

In section 1.4, we discussed the boundary conditions that must be imposed at dielectric interfaces. These are the usual natural or exact boundary conditions. However, in many cases, it is possible to employ approximate boundary conditions that effectively account for the presence of some inhomogeneous interface, a material coating on a conductor, or a dielectric layer without actually having to include their geometry explicitly in the analysis.

Impedance boundary conditions

The most common approximate boundary condition (abc) is the impedance boundary condition attributed to Leontovich [ ] which often carries his name in the literature. It can be derived by considering the simple problem of a plane wave incidence on a material half space. Choosing the interface to be the plane $y = 0$ with the y axis directed out of the half space, the Leontovich impedance boundary condition takes the form

$$E_z = -\eta Z_o H_x \qquad E_x = \eta Z_o H_z \tag{1.131}$$

where $Z_o = \sqrt{\frac{\mu_o}{\epsilon_o}}$ and η is a function of the material properties of the half space. These conditions are applied at $y = 0^+$ (just above the interface) and can be combined to yield the vector form

$$\hat{n} \times (\hat{n} \times \mathbf{E}) = -\eta Z_o \hat{n} \times \mathbf{H} \tag{1.132}$$

where $\hat{n}$ is the unit vector normal in the outward direction (see Fig. 10). As can be seen, the form of the impedance boundary condition is independent of the geometry of the interface or the boundary where it is enforced and is thus applicable to planar as well as curved surfaces. Further, it can be generalized to the case where there may be some anisotropy by writing it as

$$\hat{n} \times (\hat{n} \times \mathbf{E}) = -Z_o \overline{\overline{\eta}} \cdot \hat{n} \times \mathbf{H} \tag{1.133}$$

where $\overline{\overline{\eta}}$ is a tensor.

One way to derive the appropriate normalized impedance parameter η is to demand that the equivalent impedance surface satisfying the condition (1.132) reproduce the same reflected field. In doing so, for the planar dielectric interface we readily find that

$$\eta = \sqrt{\frac{\mu_r}{\epsilon_r}} \tag{1.134}$$

and for this choice of η the condition (1.132) becomes an approximation for simulating curved dielectric boundaries (see fig. 10b) provided

$$|Im(\sqrt{\epsilon_r \mu_r})|\, k_o \rho_i \gg 1, \tag{1.135}$$

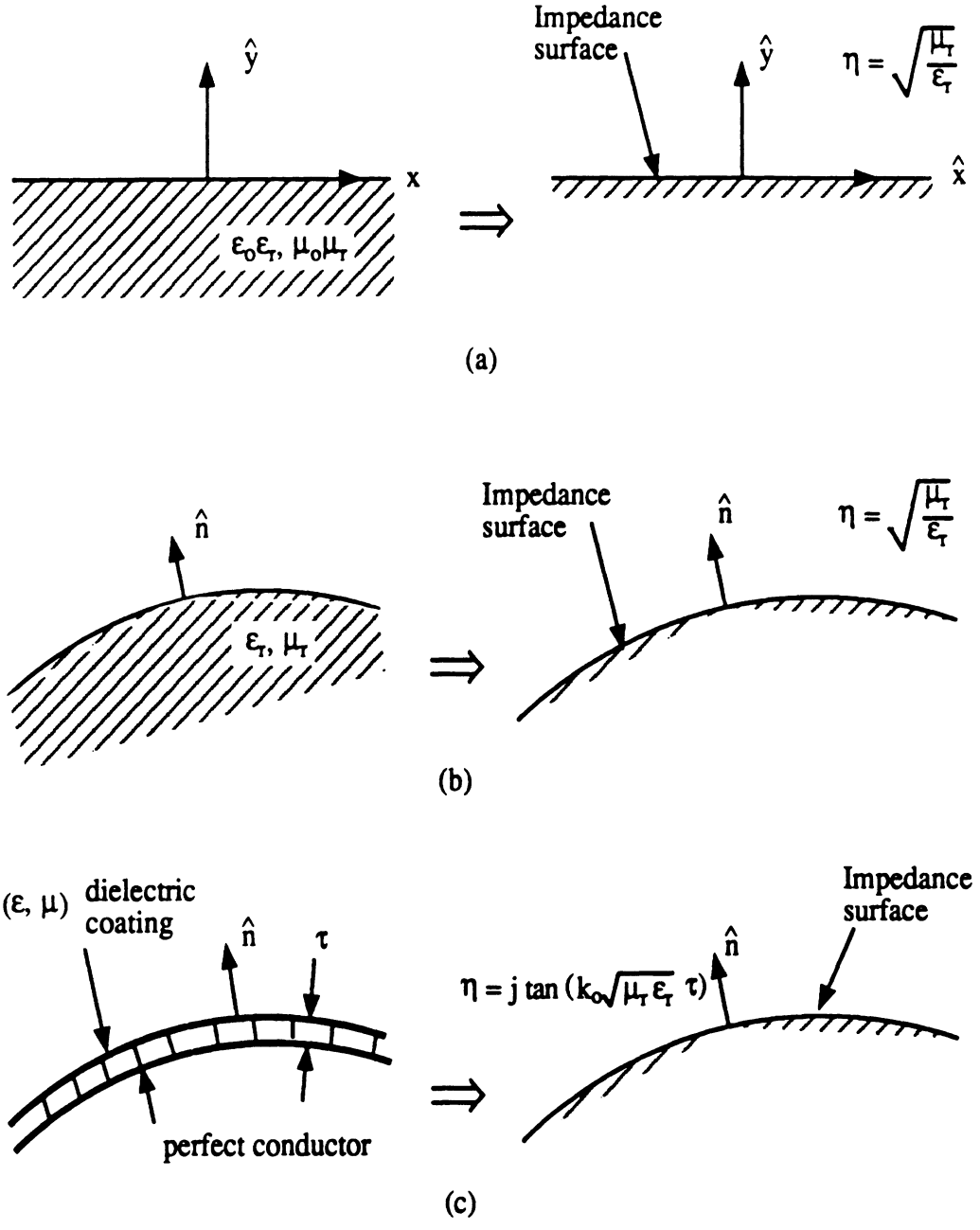

Figure 1.10: Simulation of dielectric boundaries and coatings with equivalent impenetrable impedance surfaces.

where ρ_i are the principal radii of curvature associated with the surface. This ensures that the material is sufficiently lossy so that the fields penetrating the surface do not re-emerge at some other point.

For the coated conductor in fig. 10(c), the value of η is generally chosen to be the actual impedance of the corresponding planar structure illuminated by a plane wave, typically at normal incidence. Accordingly, for an homogeneous coating of thickness τ [Harrington & Senior]

$$\eta = j\sqrt{\frac{\mu_r}{\epsilon_r}}\tan(k_o\sqrt{\epsilon_r\mu_r}\tau) \tag{1.136}$$

and we can readily compute the corresponding impedance for multilayer coatings. However, as can be expected, the accuracy of the proposed impedance boundary condition deteriorates for oblique angles of incidences, requiring that τ be kept small with respect to the wavelength to achieve resonable accuracies.

Provided the material parameters change slowly from one point of the simulated surface to another, the impedance boundary condition (1.132) still be applicable. In this case, the normalized surface impedance for the coating is computed from (1.136) with the material parameters now being functions of the location on the surface. For a planar interface, if ϵ_r and μ_r vary with respect to y, Rytov [ ] has shown that

$$\eta = \sqrt{\frac{\mu_r}{\epsilon_r}}\left\{1 + \frac{1}{2jk_oN}\frac{\partial}{\partial y}\ln(Z_oN) + O(N^{-2})\right\} \tag{1.137}$$

where $N = \sqrt{\mu_r\epsilon_r}$ is the refractive index and the derivative is evaluated at the surface.

Resistive and conductive sheet transition conditions

For certain applications, it is desirable to replace a thin dielectric layer with an equivalent model in an effort to simplify the analysis. To illustrate this idea, let us consider a thin dielectric slab of thickness τ as shown in fig. 11. The slab has a conductivity σ, and it will thus support a current density given by (see (1.36))

$$\mathbf{J} = \sigma\mathbf{E} \tag{1.138}$$

where $\mathbf{E}$ denotes the field within the slab. However, since $\tau \ll \lambda$, we may replace $\mathbf{J}$ by an equivalent sheet current (having units in A/m)

$$\mathbf{J}_s = \tau \mathbf{J} \tag{1.139}$$

and thus from (1.138)

$$\mathbf{E} = \mathbf{J}_s/\sigma\tau = Z_o R_e \mathbf{J}_s \tag{1.140}$$

This condition is a mathematical definition for a *resistive* sheet supporting a sheet current $\mathbf{J}_s$. The parameter $Z_o R_e$ is referred to as the *resistivity* of the sheet and is measured in Ohms/square.

In deriving (1.140) it has been assumed that $\mathbf{E}$ is tangential to the layer or sheet and therefore a more precise definition of the condition is

$$\hat{n} \times (\hat{n} \times \mathbf{E}) = -Z_o R_e \mathbf{J}_s \tag{1.141}$$

where $\hat{n}$ denotes the upper unit normal to the sheet. Further, it is desirable to work with field quantities that are measured outside the layer or sheet and since $\hat{n} \times \mathbf{E}$ is continuous across the layer we may rewrite (1.141) as

$$\hat{n} \times \left[\hat{n} \times (\mathbf{E}^+ + \mathbf{E}^-)\right] = -2Z_o R_e \mathbf{J}_s \tag{1.142a}$$

$$\hat{n} \times (\mathbf{E}^+ - \mathbf{E}^-) = 0 \tag{1.142b}$$

The superscripts $\pm$ denote the fields above and below the sheet or layer and it was necessary to introduce (1.142b) to maintain the equivalence of (1.142) with (1.141). Alternatively, by employing the natural boundary condition (1.60), (1.142) can be rewritten as

$$\hat{n} \times \left[\hat{n} \times (\mathbf{E}^+ + \mathbf{E}^-)\right] = -2Z_o R_e \, \hat{n} \times (\mathbf{H}^+ - \mathbf{H}^-) \tag{1.143a}$$

$$\hat{n} \times (\mathbf{E}^+ - \mathbf{E}^-) = 0 \tag{1.143b}$$

By allowing $\hat{n}$ to be other than constant, these can be employed for the simulation of curved layers, provided again there is sufficient loss in the layer to suppress multiple field penetrations.

The dual to (1.143) are

$$\begin{aligned} \hat{n} \times \left[\hat{n} \times (\mathbf{H}^+ + \mathbf{H}^-)\right] &= 2Y_o R_m \, \hat{n} \times (\mathbf{E}^+ - \mathbf{E}^-) \\ \hat{n} \times (\mathbf{H}^+ - \mathbf{H}^-) &= 0 \end{aligned} \tag{1.144}$$

and these define a *conductive* sheet capable of supporting a magnetic current $\mathbf{M}_s = -\hat{n} \times (\mathbf{E}^+ - \mathbf{E}^-)$. The parameter $Y_o R_m$ is now referred to as the *conductivity* of the magnetic sheet measured in Mhos/square. The utility of this sheet is not yet apparent but it will be shown below to be essential for a sheet simulation of dielectric layers with nontrivial permeability. Also, it has been shown [ ] that a special combination of coincident electric and magnetic current sheets is equivalent to an impenetrable impedance sheet. This equivalence holds when we set

$$R_e = \frac{\eta}{2}, \quad R_m = \frac{1}{2\eta} \tag{1.145}$$

implying $4R_e R_m = 1$, where η is the normalized impedance of the sheet. Because co-planar electric and magnetic currents are independent of each other, (1.145) is important in simplifing the analysis with flat impedance surfaces.

Let us now consider a dielectric layer having a relative permittivity ϵ_r and thickness τ such that $k_o\tau \ll 1$. Based on the volume equivalence theorem, this

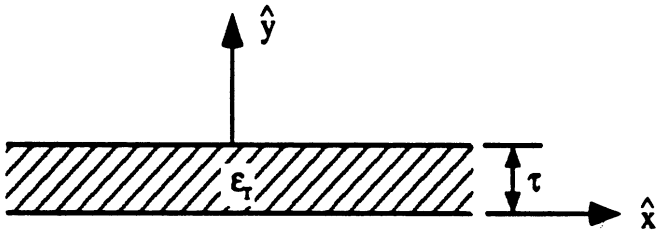

Figure 1.11:

layer can be replaced by the equivalent polarization currents

$$\begin{aligned} J_x &= jk_o Y_o(\epsilon_r - 1)E_x \\ J_y &= jk_o Y_o(\epsilon_r - 1)E_y \end{aligned} \tag{1.146}$$

$$J_z = jk_oY_o(\epsilon_r - 1)E_z.$$

On the assumption of $k_o\tau \ll 1$, the J_y component may be neglected and the current densities $J_{x,z}$ can then be replaced by the equivalent sheet currents

$$J_{sx} = \tau J_x, \quad J_{sz} = \tau J_z. \tag{1.147}$$

From (1.19), it now follows that

$$E_x = Z_oR_eJ_{sx}, \quad E_z = Z_oR_eJ_{sz} \tag{1.148}$$

with

$$R_e = \frac{-j}{k_o\tau(\epsilon_r - 1)} \tag{1.149}$$

Equation (1.148) are clearly identical to (1.140) except that R_e is now complex. Coordinate independent transition conditions for the dielectric layer are thus given by (1.141), (1.142) or (1.143) with the new definition for R_e.

When the dielectric slab is associated with non-unity μ_r, (1.143) must be complemented with a conductive sheet defined by (1.144) and in accordance with the volume equivalence theorem the normalized conductivity R_m is given by

$$R_m = \frac{-j}{k_o\tau(\mu_r - 1)} \tag{1.150}$$

Thus, the sheet transition conditions for a thin ferrite layer are

$$\begin{aligned} \hat{n} \times \left[\hat{n} \times (\mathbf{E}^+ + \mathbf{E}^-)\right] &= -2Z_oR_e\hat{n} \times (\mathbf{H}^+ - \mathbf{H}^-) \\ \hat{n} \times \left[\hat{n} \times (\mathbf{H}^+ + \mathbf{H}^-)\right] &= +2Y_oR_m\hat{n} \times (\mathbf{E}^+ - \mathbf{E}^-) \end{aligned} \tag{1.151}$$

with R_e and R_m as defined in (1.149) and (1.150), and $\hat{n}$ denoting the upward unit normal to the layer.

1.P1/p

Problems

1. A chiral medium has the constitutive relations

$$\mathbf{D} = \epsilon\mathbf{E} - j\chi\mathbf{B}, \quad \mathbf{H} = -j\chi\mathbf{E} + \frac{\mathbf{B}}{\mu}$$

where χ is the charality parameter.
(a) Show that the vector wave equation for this medium takes the form (see equations 1.109 and 1.110)

$$\nabla \times \nabla \times \mathbf{F} - k^2\mathbf{F} + \mathbf{V} = 0$$

where $\mathbf{F} = \mathbf{E}, \mathbf{H}, \mathbf{D}$ or $\mathbf{B}$, and $\mathbf{V}$ is a vector to be found from your solution.
(b) Assume now a circularly polarized plane wave (RCP or LCP) propagating along the z-direction. Find the propagation constants k_{RCP} and k_{LCP} so that the wave equation found in (a) is satisfied.
(c) If a linearly polarized plane wave is incident upon a chiral interface as shown, find the reflected and transmitted fields (by enforcing tangential field continuity at the interface).

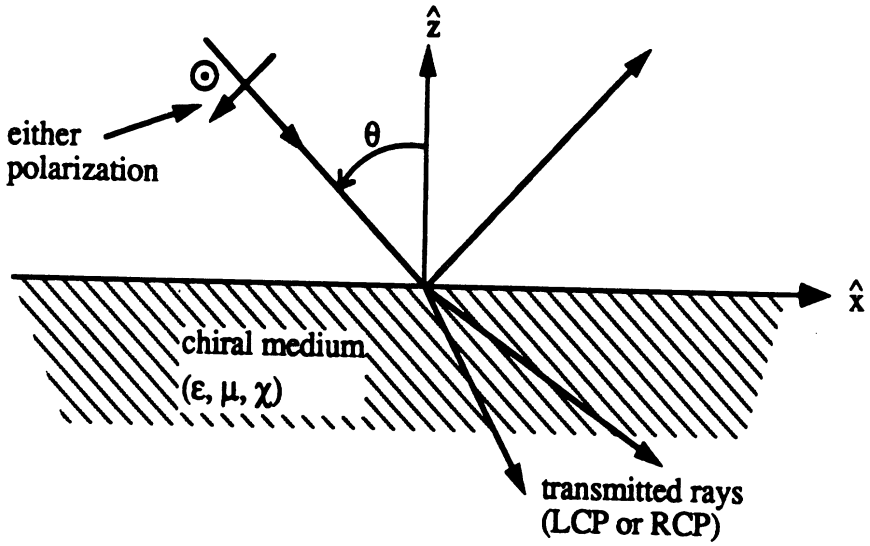

Figure 1.P1. Plane wave incidence on a chiral interface.

2. Use the divergence theorem

$$\int\int\int_V \nabla \cdot \mathbf{A} dv = \oiint_{S_c} \mathbf{A} \cdot d\mathbf{s} \tag{1}$$

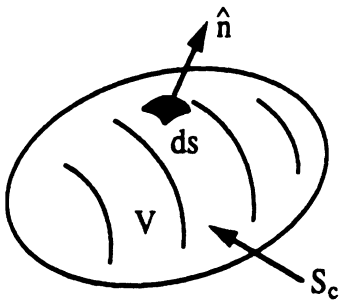

Figure 1.P2. Geometry for problem 2.

to (a) prove that

$$\int\int\int_V \nabla \times \mathbf{B} dv = \oiint_{S_c} \hat{n} \times \mathbf{B} d\mathbf{s} \quad \text{(vector Stokes theorem)}$$

where $d\mathbf{s} = \hat{n} ds$. hint: Set $\mathbf{A} = \hat{u} \times \mathbf{B}$ and make use of the identity $\nabla \cdot (\mathbf{a} \times \mathbf{b}) = -\mathbf{a} \cdot \nabla \times \mathbf{b}$, where $\hat{u}$ is an arbitrary unit vector.
and that
(b)

$$\int\int\int_V \nabla f dv = \oiint_{S_c} f \hat{n} ds$$

hint: set $\mathbf{A} = \hat{u} f$ and note that $\nabla \cdot (\hat{u} f) = \hat{u} \cdot \nabla f$.

3. Consider a surface whose unit normal is $\hat{n} = \hat{u}_3$ and $\hat{u}_{1,2}$ denote the principal directions of that surface. The directions $\hat{u}_{1,2,3}$ form an orthonormal set and are associated with the metric coefficients h_1, h_2, h_3. We are interested in obtaining the surface gradient, divergence and curl and these are defined by taking the pertinent vector or scalar function to be independent of v_3 (i.e. invarient along $\hat{u}_3 = \hat{n}$) and setting $h_3 = 1$.

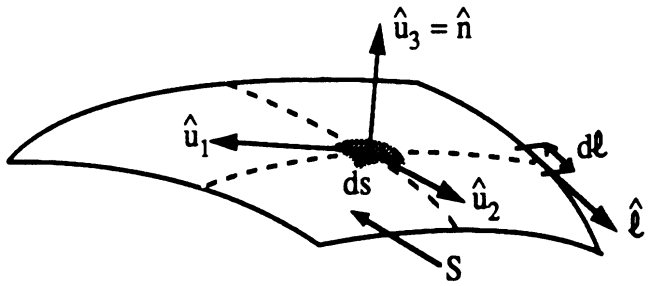

Figure 1.P3. Parameters and geometry for problem 3.

For example, in the case of the gradient we have

$$\nabla_s f = \frac{1}{h_1}\frac{\partial f}{\partial v_1}\hat{u}_1 + \frac{1}{h_2}\frac{\partial f}{\partial v_2}\hat{u}_2 + \frac{1}{h_3}\frac{\partial f}{\partial v_3}\hat{u}_3 = \frac{1}{h_1}\frac{\partial f}{\partial v_1}\hat{u}_1 + \frac{1}{h_2}\frac{\partial f}{\partial v_2}\hat{u}_2$$

since $f = f(v_1, v_2)$ on S. Similarly, for the divergence we have ($h_3 = 1$)

$$\nabla \cdot \mathbf{A} = \frac{1}{h_1 h_2}\left[\frac{\partial}{\partial v_1}(h_2 A_1) + \frac{\partial}{\partial v_2}(h_1 A_2)\right] + \frac{1}{h_1 h_2}\frac{\partial (h_1 h_2 A_3)}{\partial v_3}$$

But

$$\begin{aligned}\frac{1}{h_1 h_2}\frac{\partial (h_1 h_2 A_3)}{\partial v_3} &= \frac{1}{h_1 h_2}\left[\frac{\partial (h_1 h_2)}{\partial v_3}A_3 + h_1 h_2 \frac{\partial A_3}{\partial v_3}\right] \\ &= \left[\frac{1}{h_1}\frac{\partial h_1}{\partial v_3}A_3 + \frac{1}{h_2}\frac{\partial h_2}{\partial v_3}A_3 + \frac{\partial A_3}{\partial v_3}\right]\end{aligned}$$

where $\mathbf{A}_i = \mathbf{A} \cdot \hat{u}_i$, and if we set $\frac{\partial A_3}{\partial v_3} = 0$ as noted above, we obtain the surface divergence of $\mathbf{A}$ as

$$\nabla_s \cdot \mathbf{A} = \frac{1}{h_1 h_2}\left[\frac{\partial}{\partial v_1}(h_2 A_1) + \frac{\partial}{\partial v_2}(h_1 A_2)\right] - JA_3 = \nabla_s \cdot \mathbf{A}_t - JA_n$$

where $A_3 = \hat{n} \cdot \mathbf{A} = A_n$, $\mathbf{A}_t = \mathbf{A} - \hat{n}A_n$ and

$$J = \left(\frac{1}{R_1} + \frac{1}{R_2}\right) = -\left[\frac{1}{h_1}\frac{\partial h_1}{\partial v_3} + \frac{1}{h_2}\frac{\partial h_2}{\partial v_3}\right]$$

is the curvature of the surface with R_1 and R_2 being the principal radii of S (max and min radii at each point on S). More specifically, R_1 is the radius of curvature of the curve on S associated with $\hat{u}_1$ and R_2 is the same for the curve whose tangent is $\hat{u}_2$.

(a) Using a similar procedure, derive the surface curl $\nabla_s \times \mathbf{A}$ from $\nabla \times \mathbf{A}$.

(b) A generalization of Gauss' theorem for the surface divergence is ($\hat{b} = \hat{n} \times \hat{l}$)

$$\int\int_S \nabla_s \cdot \mathbf{A}_t ds = \oint_C \hat{b} \cdot \mathbf{A}_t d\ell$$

or

$$\int\int_S \nabla_s \cdot \mathbf{A} ds = \oint_C \hat{b} \cdot \mathbf{A} d\ell - \int\int_S J(\mathbf{A} \cdot \hat{n}) ds$$

Starting with this result, show that

$$\int\int_S \nabla_s f \, ds = \oint_C \hat{b} f d\ell - \int\int_S J f \hat{n} \, ds$$

and that

$$\int\int_S \nabla_s \times \mathbf{A} \, ds = \oint_C \hat{b} \times \mathbf{A} \, d\ell - \int\int_S J(\hat{n} \times \mathbf{A}) ds$$

(c) If the surface S in (b) coincides with a curved metal plate and $\mathbf{A}$ represents the current on the plate, what can you say about the value of the surface integral

$$\int\int_S \nabla_s \cdot \mathbf{A} \, ds = ?$$

4. Consider a finite length electric current sheet of the form

$$\mathbf{J}(x) = \hat{y} J_o P_{2\Delta}(x - x_o)$$

where

$$P_{2\Delta}(x) = \begin{cases} 1 & -\Delta < x < \Delta \\ 0 & \text{elsewhere} \end{cases}$$

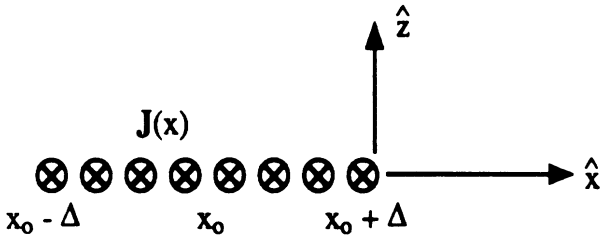

Figure 1.P4. Figure for problem 4. Finite width current sheet.

Find an equivalent magnetic current distribution whose radiation will be the same as that of the given electric current sheet.
(b) Repeat part (a) for $\mathbf{J}(x) = \hat{y} J_o f(x) P(x - x_o)$.

5. Give expressions for the equivalent surface currents on $S_{diel.}$ and $S_{cond.}$ for the structure shown in Figure 1.P5 under the following assumptions:

(a) $(\mathbf{E}_i, \mathbf{H}_i) \neq (0, 0)$

(b) $\mathbf{E}_i = 0$, but $\mathbf{H}_i \neq 0$

(c) $\mathbf{E}_i \neq 0$, but $\mathbf{H}_i = 0$,

6. The electric field generated by an infinitesimal dipole $\mathbf{J}_a = \hat{x} I\ell$ $(\ell \to 0)$ in the presence of a dielectric scatterer is found to be $\mathbf{E}_a(x, y, z)$. Give an expression of the x-component of the corresponding field generated by the source $\mathbf{J}_b(x, y, z)$.

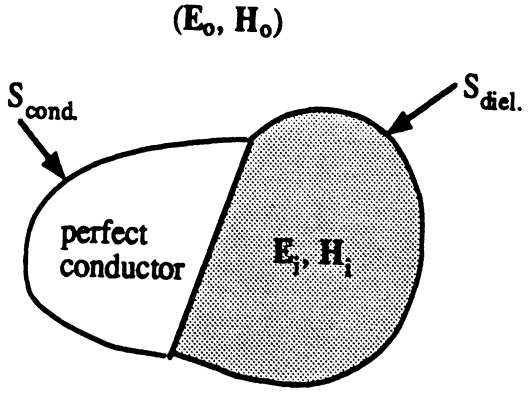

Figure 1.P5. Geometry for problem 5.

7. Assume the plane wave

$$\mathbf{E}^i = \hat{\theta} e^{j\mathbf{k}_i \cdot \mathbf{r}} = \hat{\theta} e^{jk_o(x \sin\theta \cos\phi + y \sin\theta \sin\phi + z \cos\theta)}$$

is incident upon the planar resistive sheet of (normalized) resistivity R_e as shown in figure 1.P7.

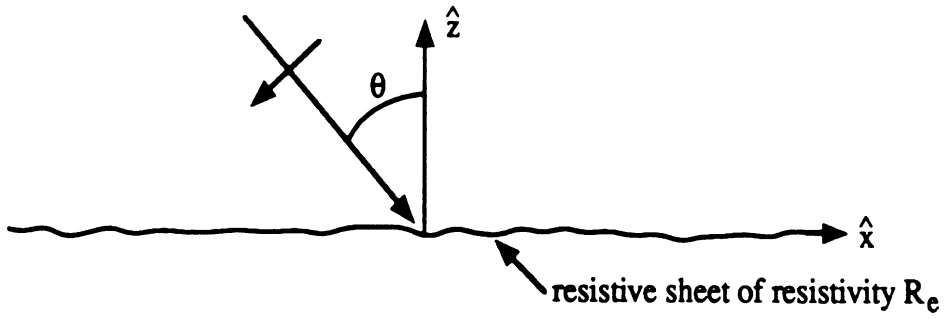

Figure 1.P7 Geometry for problem 7

(a) Determine the reflected and transmitted fields
(b) Repeat (a) for a conductive sheet of (normalized) conductivity R_m
(c) Combine the results of (a) and (b) to find the reflected field from a planar surface having a (normalized) impedance η.

8. Consider the material slab shown in figure 1.P8 having relative permittivity ϵ_r and relative permeability μ_r.

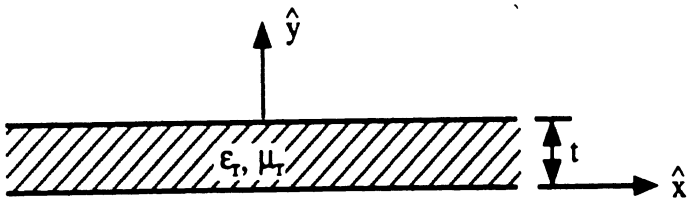

Figure 1.P8. Geometry for problem 8.

On the assumption $kt \ll 1$, where $k = \omega\sqrt{\mu_o\epsilon_o}\sqrt{\mu_r\epsilon_r} = k_o\sqrt{\mu_r\epsilon_r}$, introduce the approximations

$$\frac{\partial E_x}{\partial y} \approx \frac{\Delta E_x}{\Delta y} \approx \frac{E_x(t^-) - E_x(0^+)}{t}$$

$$\frac{\partial E_y}{\partial y} = \frac{\Delta E_y}{\Delta y} \approx \frac{E_y(t^-) - E_y(0^+)}{t}$$

$$H_{x,z} \approx \left[H_{x,z}(t^-) + H_{x,z}(0^+)\right]/2$$

and

$$E_y \approx \left[E_y(t^-) + E_y(0^+)\right]/2$$

where $F(t^-)$ denotes the field component F at $y = t - 0$ (i.e. just inside the layer) and similarly $F(0^+)$ denotes the field component at $y = 0^+$, just inside the layer.

(a) Using the boundary conditions

$$\epsilon_r E_y(t^-) = E_y(t^+),$$

$$\epsilon_r E_y(0^+) = E_y(0^-)$$

along with Maxwell's equations, show that

$$E_x(t^+) - E_x(0^-) = \frac{jk_o t\mu_r Z_o}{2}\left[H_z(t^+) + H_z(0^-)\right]$$

$$+\frac{t}{2\epsilon_r}\frac{\partial}{\partial x}\left[E_y(t^+)+E_y(0^-)\right]$$

$$E_z(t^+)-E_z(0^-) = -\frac{jk_o t\mu_r Z_o}{2}\left[H_x(t^+)+H_x(0^-)\right]$$

$$+\frac{t}{2\epsilon_r}\frac{\partial}{\partial z}\left[E_y(t^+)+E_y(0^-)\right]$$

(b) The derived conditions in (a) are in terms of the fields at the top and bottom of the layer and the layer has equivalently/mathematically been replaced by these conditions. To derive sheet conditions similar to those for the resistive and conductive sheet, the fields at $y = t^+$ and $y = 0^-$ can be transferred to $y = t/2$. To do so employ the two-term Taylor series expansion

$$F(t) = F\left(\frac{t^+}{2}\right)+\frac{t}{2}\frac{\partial}{\partial y}F\left(\frac{t^+}{2}\right)$$

$$F\left(\frac{t^-}{2}\right) = F(0)+\frac{t}{2}\frac{\partial}{\partial y}F(0)$$

for all field components (since the layer is no longer present) along with Maxwell's equations to derive the sheet conditions

$$E_x\left(\frac{t^+}{2}\right)-E_x\left(\frac{t^-}{2}\right) = Z_o\left[H_z\left(\frac{t^+}{2}\right)+H_z\left(\frac{t^-}{2}\right)\right]\left(\frac{1}{2R_m}+\frac{1}{2R_e'}\right)$$

$$-\frac{1}{jk_oR_e'}\frac{\partial}{\partial y}\left[E_x\left(\frac{t^+}{2}\right)+E_x\left(\frac{t^-}{2}\right)\right]+O(t^2)$$

$$E_z\left(\frac{t^+}{2}\right)-E_z\left(\frac{t^-}{2}\right) = \left[H_x\left(\frac{t^+}{2}\right)+H_x\left(\frac{t^-}{2}\right)\right]-Z_o\left(\frac{1}{2R_m}+\frac{1}{2R_e'}\right)$$

$$-\frac{1}{jk_oR_e'}\frac{\partial}{\partial y}\left[E_z\left(\frac{t^+}{2}\right)+E_z\left(\frac{t^-}{2}\right)\right]+O(t^2)$$

in which

$$R_m = \frac{-j}{k_o t(\mu_r-1)} \quad \text{and} \quad R_e' = \frac{-j\epsilon_r}{k_o t(\epsilon_r-1)}$$

For a complete modeling of the layer, these conditions must be supplemented by their dual.

(c) Compare the conditions derived in (b) with those for the standard resistive and conductive sheets. Explain which of the two sets is more accurate and why.

Chapter 2

Field Solutions and Representations

In this chapter we present formal solutions to Maxwell's equations. These can be cast into a variety of integral representations for computing the radiated field by an antenna or the scattered field from a composite structure. Some of these representations are given here and we will refer to them in the other chapters.

2.1 Field Solutions in Terms of Vector and Hertz Potentials

In the absence of magnetic currents and charges $\nabla \cdot (\mu \mathbf{H}) = 0$, implying that in a homogeneous medium the magnetic field due to electric sources can be written as

$$\mathbf{H} = \mathbf{H}_e = \nabla \times \mathbf{A} \tag{2.1}$$

where $\mathbf{A}$ is an arbitrary unknown vector and is referred to as the *magnetic vector potential.* Its complete specification would, of course, require all point derivatives of $\mathbf{A}$, and we note that (2.1) involves only a subset of those derivatives. Thus one could also independently define the $\nabla \cdot \mathbf{A}$ without interfering with the definition (2.1) and this will be exploited later in the solution for $\mathbf{A}$.

Substituting (2.1) in (1.48) yields

$$\nabla \times \nabla \times \mathbf{A} = \mathbf{J}_i + j\omega\epsilon\mathbf{E}_e \tag{2.2}$$

where $\mathbf{E}_e$ denotes the electric field due to the electric source $\mathbf{J}_i$. Also, from (1.49) we have

$$\nabla \times (\mathbf{E}_e + j\omega\mu\mathbf{A}) = 0 \tag{2.3}$$

implying

$$\mathbf{E}_e + j\omega\mu\mathbf{A} = -\nabla\Phi_e \tag{2.4}$$

with Φ_e being again an arbitrary scalar function commonly referred to as the electric scalar potential. Combining now (2.2) and (2.4) we obtain

$$\nabla \times \nabla \times \mathbf{A} - k^2\mathbf{A} = \mathbf{J}_i - j\omega\epsilon\nabla\Phi_e \tag{2.5}$$

where $k = \omega\sqrt{\mu\epsilon} = 2\pi/\lambda$ is the medium propagation constant associated with the wavelength λ. This can be further simplified by employing the identity

$$\nabla \times \nabla \times \mathbf{A} = \nabla\nabla \cdot \mathbf{A} - \nabla^2\mathbf{A} \tag{2.6}$$

which when introduced in (2.5) gives

$$\nabla^2\mathbf{A} + k^2\mathbf{A} = -\mathbf{J}_i + j\omega\epsilon\nabla\Phi_e + \nabla\nabla \cdot \mathbf{A} \tag{2.7}$$

and in rectangular coordinates

$$\nabla^2\mathbf{A} = \hat{x}\nabla^2 A_x + \hat{y}\nabla^2 A_y + \hat{z}\nabla^2 A_z. \tag{2.8}$$

As stated above, since the derivatives involved in the definition of $\nabla \times \mathbf{A}$ are different from those associated with $\nabla \cdot \mathbf{A}$, we may arbitrarily set

$$\nabla \cdot \mathbf{A} = -j\omega\epsilon\Phi_e \tag{2.9}$$

which is a relation that is often referred to as the Lorentz gauge condition. Substituting (2.9) into (2.7) we obtain

$$\nabla^2\mathbf{A} + k^2\mathbf{A} = -\mathbf{J}_i \tag{2.10}$$

or

$$\left(\nabla^2 + k^2\right)\begin{Bmatrix} A_x \\ A_y \\ A_z \end{Bmatrix} = -\begin{Bmatrix} J_{ix} \\ J_{iy} \\ J_{iz} \end{Bmatrix}$$

in conjunction with the definitions (2.1) and (2.8). Also from (2.4)

$$\mathbf{E}_e = -j\omega\mu\mathbf{A} + \frac{1}{j\omega\epsilon}\nabla\nabla\cdot\mathbf{A} = -jkZ\left(\mathbf{A} + \frac{1}{k^2}\nabla\nabla\cdot\mathbf{A}\right) \tag{2.11}$$

where $Z = \sqrt{\mu/\epsilon}$ denotes the impedance of the medium, and upon substituting this into (1.51) or (1.33), it can be readily shown from (2.9) that Φ_e satisfies

$$\nabla^2\Phi_e + k^2\Phi_e = -\frac{\rho}{\epsilon} \tag{2.12}$$

Given the electric potential $\mathbf{A}$, equation (2.11) provides the solution for the electric field due to the electric sources $\mathbf{J}_i$. The corresponding magnetic field is obtained from (2.1) and to complete the solution of Maxwell's equations we must also find similar expressions in the presence of magnetic sources. If for the moment we assume that only magnetic sources as present, we could then invoke duality to find the corresponding field expressions. In particular, in comparison with (2.1) we now set

$$\mathbf{E}_m = -\nabla\times\mathbf{F} \tag{2.13}$$

where $\mathbf{F}$ is referred to as the *electric vector potential* and $\mathbf{E}_m$ is the field due to $\mathbf{M}_i$. Following, a procedure similar to that in connection with the electric sources or simply by invoking duality we obtain

$$\mathbf{H}_m = -j\omega\epsilon\mathbf{F} + \frac{1}{j\omega\mu}\nabla\nabla\cdot\mathbf{F} = -jkY\left(\mathbf{F} + \frac{1}{k^2}\nabla\nabla\cdot\mathbf{F}\right) \tag{2.14}$$

where $Y = 1/Z = \sqrt{\epsilon/\mu}$ denotes the medium admittance and $\mathbf{F}$ satisfies the partial differential equation

$$\nabla^2\mathbf{F} + k^2\mathbf{F} = -\mathbf{M}_i$$

or

$$\left(\nabla^2 + k^2\right)\begin{Bmatrix} F_x \\ F_y \\ F_z \end{Bmatrix} = -\begin{Bmatrix} M_{ix} \\ M_{iy} \\ M_{iz} \end{Bmatrix} \tag{2.15}$$

In the process of deriving (2.15) we introduced the magnetic scalar potential Φ_m such that

$$\nabla\cdot\mathbf{F} = -j\omega\mu\Phi_m \tag{2.16}$$

By employing this into (2.13) and making use of (1.32) we find that Φ_m satisfies the differential equation

$$\nabla^2\Phi_m + k^2\Phi_m = -\frac{\rho_m}{\mu} \tag{2.17}$$

which is the dual of (2.12).

The fields due to the presence of both electric and magnetic sources $(\mathbf{J}_i, \mathbf{M}_i)$ can now be found by invoking the superposition principle. That is

$$\mathbf{E} = \mathbf{E}_e + \mathbf{E}_m\,, \qquad \mathbf{H} = \mathbf{H}_e + \mathbf{H}_m \tag{2.18}$$

and from (2.1), (2.11), (2.13) and (2.14) we obtain

$$\mathbf{E} = -\nabla \times \mathbf{F} - j\omega\mu\mathbf{A} + \frac{1}{j\omega\epsilon}\nabla\nabla\cdot\mathbf{A} \tag{2.19a}$$

$$\mathbf{H} = \nabla \times \mathbf{A} - j\omega\epsilon\mathbf{F} + \frac{1}{j\omega\mu}\nabla\nabla\cdot\mathbf{F} \tag{2.19b}$$

The vectors

$$\Pi_e = \frac{1}{j\omega\epsilon}\mathbf{A}, \quad \Pi_m = \frac{1}{j\omega\mu}\mathbf{F} \tag{2.20}$$

and usually referred to as the *Hertz Potentials* and in terms of these

$$\mathbf{E} = -jkZ\nabla \times \Pi_m + k^2\Pi_e + \nabla\nabla\cdot\Pi_e \tag{2.21a}$$

$$\mathbf{H} = jkY\nabla \times \Pi_e + k^2\Pi_m + \nabla\nabla\cdot\Pi_m \tag{2.21b}$$

$$\mathbf{E} = \frac{1}{j\omega\epsilon}\nabla \times \mathbf{H} = \frac{jkY}{jkY}\nabla \times \nabla \times \Pi_e + \frac{k^2}{jkY}\nabla \times \Pi_m$$

2.2 Solution for the Vector and Scalar Potentials

Let us first solve (2.10) for the case where $\mathbf{J}_i$ is a small infinitesimal source occupying the volume dv' located at the origin (as illustrated in Fig. 2.1) given that $\mathbf{J}_i = \hat{a}J_a$, (2.10) becomes

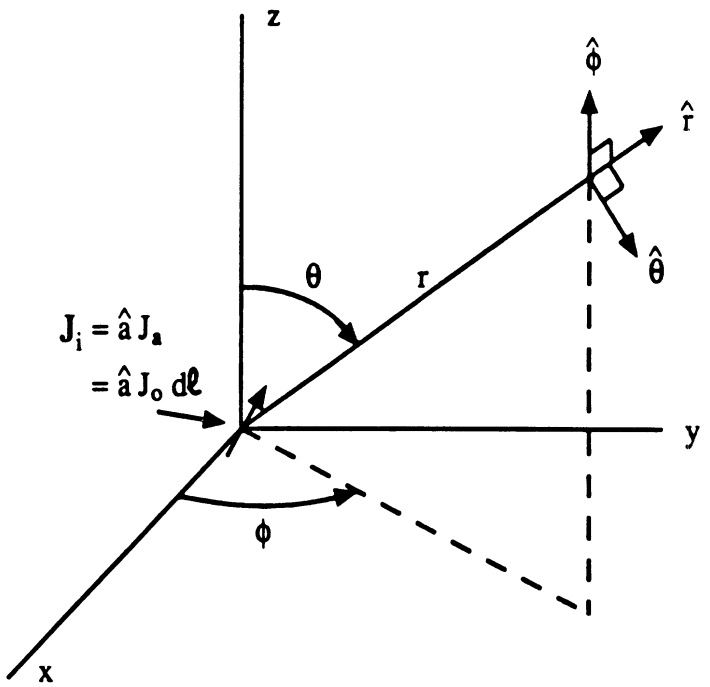

Figure 2.1: Illustration of an infinitesimal source (dipole) at the origin.

$$\nabla^2 A_a + k^2 A_a = -J_a \tag{2.22}$$

where a denotes one of the rectangular coordinates x, y or z and away from the origin A_a satisfies

$$\nabla^2 A_a + k^2 A_a = 0 \tag{2.23}$$

Further since J_a is infinitesimal, A_a is expected to be independent of the spherical angles ϕ and θ implying that (2.23) can be replaced by

$$\frac{1}{r^2}\frac{\partial}{\partial r}\left(r^2 \frac{\partial A_a}{\partial r}\right) + k^2 A_a = 0 \tag{2.24}$$

upon substituting for the spherical form of the Laplace operator ∇^2. Setting

$$A_a = \frac{f(r)}{r} \tag{2.25}$$

(2.24) becomes

$$\frac{\partial^2 f}{\partial r^2} + k^2 f = 0; \quad r \neq 0 \tag{2.26}$$

and by inspection, a solution for $f(r)$ is

$$f(r) = C_1 e^{-jkr} \tag{2.27}$$

Upon restoring the suppressed time dependence $e^{j\omega t}$ it follows that

$$\begin{aligned} f(r,t) &= Re\left\{C_1 e^{-jkr} e^{j\omega t}\right\} \\ &= C_1 \cos(\omega t - kr) = C_1 \cos\left[\omega\left(t - \frac{r}{c}\right)\right] \end{aligned} \tag{2.28}$$

describing an outward propagating wave where r/c denotes the time required for the wave to travel a distance r and consequently c is the speed of the wave. A second solution of (2.25) is associated with the inward propagating wave and is given by

$$f(r) = C_2 e^{+jkr} \tag{2.29}$$

implying that the complete solution for (2.24) is

$$A_a(r) = C_1 \frac{e^{-jkr}}{r} + C_2 \frac{e^{+jkr}}{r} \tag{2.30}$$

For the particular case considered here, the source is expected to generate outward propagating waves and we will thus set $C_2 = 0$. To find the value of the constant C_1 we must return to (2.22). One approach is to note that for $k = 0$ the resulting field obtained from (2.11) should reduce to the known static solution implying that

$$C_1 = \frac{J_a dv'}{4\pi} \tag{2.31}$$

with $J_a dv'$ being the strength of the equivalent point source. Alternatively, we could integrate both sides of (2.22) over a small spherical volume of radius $r_o \to 0$ which encloses the source J_a. In doing so we obtain

$$\int\int\int_{V_o} \nabla^2 A_a dv + k^2 \int\int\int_{V_o} A_a dv = -J_a dv' \tag{2.32}$$

Setting $dv = r^2 \sin\theta \, d\theta \, d\phi \, dr$ and substituting for $A_a = C_1 \frac{e^{-jkr}}{r}$, the second integral vanishes since $r_o \to 0$. The first integral can be rewritten as

$$\begin{aligned} \int\int\int_V \nabla^2 A_a dv &= \int_o^{r_o} \int_0^{2\pi} \int_0^{\pi} \nabla \cdot (\nabla A_a) dv \\ &= \int_o^{2\pi} \int_0^{\pi} \nabla A_a \cdot \hat{r}_o r_o^2 \sin\theta \, d\theta \, d\phi \end{aligned}$$

Evaluating the gradient of A_a gives

$$\nabla A_a \cdot \hat{r} = \frac{\partial A(r_o)}{\partial r_o} = -(1 + jkr_o) C_1 \frac{e^{-jkr_o}}{r_o^2}$$

and when this is introduced into the above integral we obtain

$$\begin{aligned} \int\int\int_{V_o} \nabla^2 A_a dv &= -\int_o^{2\pi} \int_o^{\pi} C_1 e^{-jkr_o} \sin\theta \, d\theta \, d\phi + O(r_o^2) \\ &= -4\pi C_1 \end{aligned}$$

for $r_o \to 0$. Substituting this result into (2.32) yields (2.31).

Based on the above, the electric vector potential is given by

$$\mathbf{A} = \mathbf{J}_i \frac{e^{-jkr}}{4\pi r} dv' \tag{2.33}$$

where $\mathbf{J}_i$ is the electric current density of the source occupying the infinitesimal volume dv' located at the origin. If the infinitesimal volume is moved to $\mathbf{r}'$, then via a coordinate transformation, the corresponding vector potential is given by

$$\mathbf{A} = \mathbf{J}_i \frac{e^{-jk|\mathbf{r}-\mathbf{r}'|}}{4\pi|\mathbf{r}-\mathbf{r}'|} dv' = \mathbf{J}_i \frac{e^{-jkR}}{4\pi R} dv' \tag{2.34}$$

where $R = |\mathbf{r}-\mathbf{r}'|$ is the distance from the source to the observer (see Fig. 2.2). Finally, if the source occupies an arbitrary volume V, then through the superposition principle, the vector potential can be written as an integral over the source (see Fig. 3), i.e.

$$\mathbf{A} = \int\int\int_V \mathbf{J}_i(\mathbf{r}') \frac{e^{-jk|\mathbf{r}-\mathbf{r}'|}}{4\pi|\mathbf{r}-\mathbf{r}'|} dv' = \int\int\int_V \mathbf{J}_i(\mathbf{r}') \frac{e^{-jkR}}{4\pi R} dv' \tag{2.35a}$$

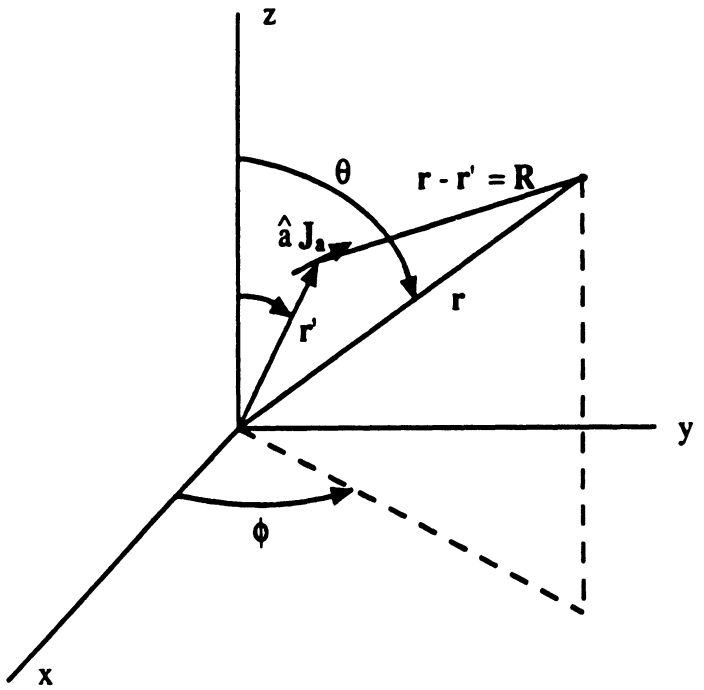

Figure 2.2: Illustration of an infinitesimal source (dipole) away from the origin at $\mathbf{r}'$.

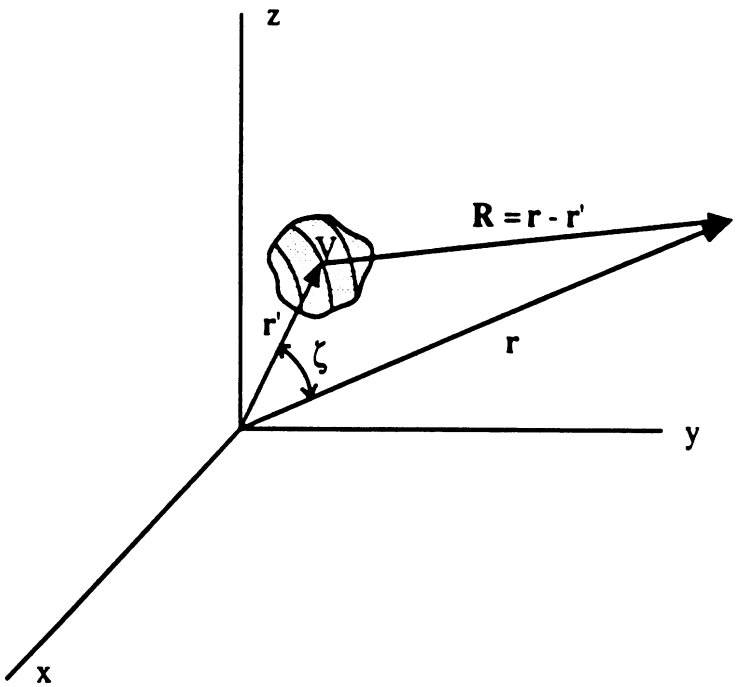

(a)

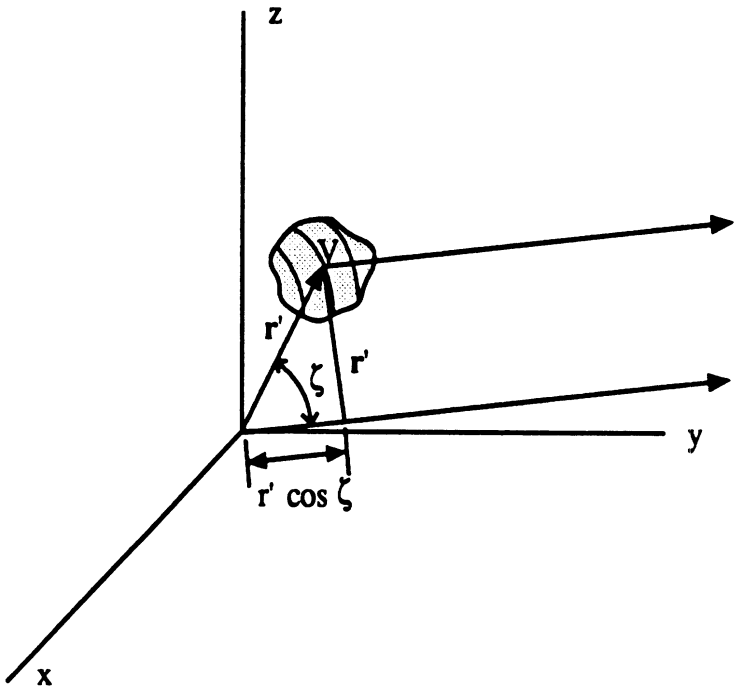

(b)

Figure 2.3: Illustration of the geometrical parameters associated with field representations.

In the case of a surface current density $\mathbf{J}_s$, the electric vector potential is given by

$$\mathbf{A} = \int\int_S \mathbf{J}_s(\mathbf{r}')\frac{e^{-jkR}}{4\pi R}ds' \tag{2.35b}$$

and similarly for a linear source $I(\ell)$ we have

$$\mathbf{A} = \int_C \hat{\ell}'\, I(\ell')\frac{e^{-jkR}}{4\pi R}d\ell'. \tag{2.35c}$$

in which the contour C coincides with the wire supporting the line current $I(\ell)$ and $\hat{\ell}$ is the unit vector tangent to the wire. Expression (2.35b) can be reduced directly from (2.35a) by setting $\mathbf{J}_i = \mathbf{J}_s\delta(\xi - \xi')$ where $\delta(\xi)$ denotes the Dirac delta function and (2.35c) can be obtained in a similar manner. The electric field due to a volume, a surface or a linear electric source is now readily obtained from (2.11) upon substituting for $\mathbf{A}$ as given in (2.35). In case of a combination of volume, surface and/or linear electric sources, the magnetic vector potential is given by the sum of the corresponding integrals.

To solve for the magnetic vector potential we can follow a procedure parallel to that employed for the solution of $\mathbf{A}$. For a volume magnetic source we obtain

$$\mathbf{F} = \int\int\int_V \mathbf{M}_i(\mathbf{r}')\frac{e^{-jkR}}{4\pi R}dv' \tag{2.36a}$$

Similarly, the appropriate solutions for surface and linear magnetic sources are given by

$$\mathbf{F} = \int\int_S \mathbf{M}_s(\mathbf{r}')\frac{e^{-jkR}}{4\pi R}dv' \tag{2.36b}$$

and

$$\mathbf{F} = \int_C \hat{\ell}' I_m(\ell')\frac{e^{-jkR}}{4\pi R}dv' \tag{2.36c}$$

in which $I_m(\ell)$ denotes the linear magnetic current source.

We remark that the common kernel

$$G(\mathbf{r},\mathbf{r}') = \frac{e^{-jk|\mathbf{r}-\mathbf{r}'|}}{4\pi|\mathbf{r}-\mathbf{r}'|} = G(R) = \frac{e^{-jkR}}{4\pi R} \tag{2.37}$$

appearing in the integrals (2.35) and (2.36) is referred to as the *Green's function*. It satisfies the differential equation

$$\nabla^2 G(\mathbf{r},\mathbf{r}') + k^2 G(\mathbf{r},\mathbf{r}') = -\delta(\mathbf{r}-\mathbf{r}') \tag{2.38}$$

and the radiation boundary condition

$$\lim_{r\to\infty} r\left(jkG + \frac{\partial G}{\partial r}\right) = 0 \tag{2.39}$$

In (2.38) $\delta(\mathbf{r}-\mathbf{r}')$ denotes the Dirac delta function satisfying the identity

$$\int\int\int_V f(\mathbf{r}')\delta(\mathbf{r}-\mathbf{r}')dv' = \begin{cases} f(\mathbf{r}) & \mathbf{r} \text{ in } V \\ \\ 0 & \mathbf{r} \text{ not in } V \end{cases} \tag{2.40}$$

When the ambient medium is free space then $k = k_o = 2\pi/\lambda_o$ and $G(\mathbf{r},\mathbf{r}')$ is generally referred to as the free space Green's function, otherwise it is simply the Green's function of the unbounded homogeneous medium.

Were we to begin with the solution of (2.38), it is a straightforward task to derive the solution for the vector potentials as given in (2.36). To do so for $\mathbf{A}$, we first multiply (2.22) by $G(\mathbf{r},\mathbf{r}')$ and (2.38) be $A_a(r)$, and upon adding the resulting expressions we obtain

$$A_a(\mathbf{r})\nabla^2 G(\mathbf{r},\mathbf{r}') - G(\mathbf{r},\mathbf{r}')\nabla^2 A_a(\mathbf{r}) = -A_a(\mathbf{r})\delta(\mathbf{r}-\mathbf{r}') + G(\mathbf{r},\mathbf{r}')J_a(\mathbf{r}) \tag{2.41}$$

Integrating the left side of this equation over the volume V enclosing the source and invoking Green's second identity it follows that

$$\begin{aligned} &\int\int\int_V \left[A_a(\mathbf{r})\nabla^2 G(\mathbf{r},\mathbf{r}') - G(\mathbf{r},\mathbf{r}')\nabla^2 A_a(\mathbf{r})\right] dv \\ &= \oiint_{S_c} \left[A_a(\mathbf{r})\frac{\partial G(\mathbf{r},\mathbf{r}')}{\partial n} - G(\mathbf{r},\mathbf{r}')\frac{\partial A_a(\mathbf{r})}{\partial n}\right] ds \end{aligned} \tag{2.42}$$

where $\frac{\partial}{\partial n}$ denotes differentiation in the direction of the outward surface normal. If S_c (which encloses V) is now allowed to be a sphere of infinite radius, $G(\mathbf{r},\mathbf{r}')$ satisfies the radiation condition (2.39) at each point S_c and if we assume that

$A_a(r)$ satisfies the same condition as well, we observe that the right hand side of (2.42) vanishes. Thus, from (2.41) we have

$$\begin{aligned} 0 &= \int\int\int_V \left[A_a(\mathbf{r})\nabla^2 G(\mathbf{r},\mathbf{r}') - G(\mathbf{r},\mathbf{r}')\nabla^2 A_a(\mathbf{r})\right] dv' \\ &= -\int\int\int_V A_a(r)\delta(\mathbf{r}-\mathbf{r}')dv + \int\int\int_V G(\mathbf{r},\mathbf{r}')J_a(r)dv \end{aligned} \tag{2.43}$$

and upon applying (2.40) we obtain that

$$A_a(\mathbf{r}') = \int\int\int_V J_a(\mathbf{r})G(\mathbf{r},\mathbf{r}')dv \tag{2.44}$$

Since $G(\mathbf{r},\mathbf{r}') = G(\mathbf{r}',\mathbf{r})$, which is a consequence of reciprocity, we may rewrite (2.44) as

$$A_a(\mathbf{r}) = \int\int\int_V J_a(\mathbf{r}')G(\mathbf{r},\mathbf{r}')dv' \tag{2.45}$$

which can be readily generalized to (2.35).

Before closing this section we should note that the solution for the electric scalar potential Φ_e can be readily derived by solving (2.12) through the same procedure followed for the solution of (2.22). This gives

$$\Phi_e(\mathbf{r}) = \frac{1}{\epsilon}\int\int\int_V \rho(\mathbf{r}')G(\mathbf{r},\mathbf{r}')dv' \tag{2.46}$$

and by invoking duality we find that the appropriate expression for the magnetic scalar potential is

$$\Phi_m(\mathbf{r}) = \frac{1}{\mu}\int\int\int_V \rho_m(\mathbf{r}')G(\mathbf{r},\mathbf{r}')dv' \tag{2.47}$$

Corresponding expressions due to the surface charge densities are obtained directly from (2.46) and (2.47) upon replacing the volume integrals with surface integrals over the domain of the surface charges.

2.3 Near and Far Zone Field Expressions

2.3.1 Near Zone Fields

Using the vector potential expressions (2.35) and (2.36), from (2.19) the electric field can be more explicitly written as

$$\mathbf{E} = \int\int\int_V \Big\{ -\nabla\times[\mathbf{M}(\mathbf{r}')G(\mathbf{r},\mathbf{r}')] - jkZ\mathbf{J}(\mathbf{r}')G(\mathbf{r},\mathbf{r}')$$

$$-\frac{jZ}{k}\nabla\left[\nabla\cdot\mathbf{J}(\mathbf{r}')G(\mathbf{r},\mathbf{r}')\right]\Big\}dv' \tag{2.48}$$

where as usual $\mathbf{r}$ and $\mathbf{r}'$ denote the observation and source point, respectively. For simplicity, in this we have dropped the subscript i from the symbols denoting the electric and magnetic currents. As usual, $\mathbf{r}$ and $\mathbf{r}'$ denote the observation and source points, respectively.

To simplify (2.48) it is necessary to carry out the indicated differentiation and as a first step toward this we note that

$$\begin{aligned}\nabla\times[\mathbf{M}(\mathbf{r}')G(\mathbf{r},\mathbf{r}')] &= G(\mathbf{r},\mathbf{r}')\nabla\times\mathbf{M}(\mathbf{r}')-\mathbf{M}(\mathbf{r}')\times\nabla G(\mathbf{r},\mathbf{r}')\\ &= -\mathbf{M}(\mathbf{r}')\times\nabla G(\mathbf{r},\mathbf{r}')\end{aligned} \tag{2.49}$$

since the ∇ operator denotes differentiation only with respect to $\mathbf{r}$ and not the primed coordinates. For the same reason we also have that

$$\begin{aligned}\nabla\cdot[\mathbf{J}(\mathbf{r}')G(\mathbf{r},\mathbf{r}')] &= G(\mathbf{r},\mathbf{r}')\nabla\cdot\mathbf{J}(\mathbf{r}')+\mathbf{J}(\mathbf{r}')\cdot\nabla G(\mathbf{r},\mathbf{r}')\\ &= \mathbf{J}(\mathbf{r}')\cdot\nabla G(\mathbf{r},\mathbf{r}')\end{aligned} \tag{2.50}$$

and thus

$$\begin{aligned}\nabla[\nabla\cdot\mathbf{J}(\mathbf{r}')G(\mathbf{r},\mathbf{r}')] &= \nabla\mathbf{J}(\mathbf{r}')\cdot\nabla G(\mathbf{r},\mathbf{r}')+\mathbf{J}(\mathbf{r}')\cdot\nabla\nabla G(\mathbf{r},\mathbf{r}')\\ &= \mathbf{J}(\mathbf{r}')\cdot\nabla\nabla G(\mathbf{r},\mathbf{r}')\end{aligned} \tag{2.51}$$

When the identities (2.49)-(2.51) are introduced into (2.48) we obtain

$$\begin{aligned}\mathbf{E}(\mathbf{r}) = \int\int\int_V \Big[&\mathbf{M}(\mathbf{r}')\times\nabla G(\mathbf{r},\mathbf{r}')-jkZ\mathbf{J}(\mathbf{r}')G(\mathbf{r},\mathbf{r}')\\ &-\frac{jZ}{k}\mathbf{J}(\mathbf{r}')\cdot\nabla\nabla G(\mathbf{r},\mathbf{r}')\Big]dv'\end{aligned} \tag{2.52a}$$

and by invoking duality we also have that

$$\begin{aligned}\mathbf{H}(\mathbf{r}) = \int\int\int_V \Big[&-\mathbf{J}(\mathbf{r}')\times\nabla G(\mathbf{r},\mathbf{r}')-jkY\mathbf{M}(\mathbf{r}')G(\mathbf{r},\mathbf{r}')\\ &-\frac{jY}{k}\mathbf{M}(\mathbf{r}')\cdot\nabla\nabla G(\mathbf{r},\mathbf{r}')\Big]dv'\end{aligned} \tag{2.52b}$$

To proceed further we must carry out the differentiation on the Green's function. By applying the chain rule of differentiation and noting that $R = |\mathbf{r} - \mathbf{r}'|$, we have

$$\nabla G(\mathbf{r},\mathbf{r}') = \frac{d}{dR}G(R)\nabla R = -\left(jk + \frac{1}{R}\right)G(R)\nabla R \tag{2.53}$$

In addition,

$$\nabla R = \hat{x}\frac{\partial R}{\partial x} + \hat{y}\frac{\partial R}{\partial y} + \hat{z}\frac{\partial R}{\partial z} = \frac{\hat{x}(x-x') + \hat{y}(y-y') + \hat{z}(z-z')}{R} = \frac{\mathbf{R}}{R} = \hat{R} \tag{2.54}$$

where $\hat{R}$ denotes the unit vector along the direction joining the integration and observation points. Using this result in (2.53) we have

$$\nabla G(\mathbf{r},\mathbf{r}') = -\left(jk + \frac{1}{R}\right)G(\mathbf{r},\mathbf{r}')\hat{R} \tag{2.55}$$

Also,

$$\begin{aligned} \nabla\nabla G(\mathbf{r},\mathbf{r}') &= -\nabla\left[\left(jk + \frac{1}{R}\right)G(\mathbf{r},\mathbf{r}')\hat{R}\right] \\ &= -\nabla\left[\left(jk + \frac{1}{R}\right)G(\mathbf{r},\mathbf{r}')\right]\hat{R} - \left(jk + \frac{1}{R}\right)G(\mathbf{r},\mathbf{r}')\nabla\hat{R} \end{aligned} \tag{2.56}$$

where the gradient of the unit vector $\hat{R}$ is interpreted to imply the operation

$$\nabla\mathbf{V} = \hat{x}\nabla V_x + \hat{y}\nabla V_y + \hat{z}\nabla V_z \tag{2.57}$$

Clearly, $\nabla\mathbf{V}$ is a product of two vectors and in that respect it is a *dyadic* whose actual meaning can be realized only when it is dotted with a vector as indicated in the last term of (2.52). To carry out the ∇ operation on $\hat{R}$ we first employ chain rule differentiation to rewrite it as

$$\begin{aligned} \nabla\hat{R} &= \nabla\left(\frac{\mathbf{R}}{R}\right) = \nabla\left(\frac{\mathbf{r}-\mathbf{r}'}{R}\right) = \frac{\nabla(\mathbf{r}-\mathbf{r}')}{R} + (\mathbf{r}-\mathbf{r}')\nabla\left(\frac{1}{R}\right) \\ &= \frac{\nabla\mathbf{r}}{R} - \frac{\mathbf{R}\hat{R}}{R^2} \end{aligned} \tag{2.58}$$

In accordance with (2.57) we can now express $\nabla\mathbf{r}$ as

$$\begin{aligned}\nabla\mathbf{r} &= \hat{x}\nabla(x)+\hat{y}\nabla(y)+\hat{z}\nabla(z)\\ &= \hat{x}\hat{x}+\hat{y}\hat{y}+\hat{z}\hat{z}=\bar{\mathbf{I}}\end{aligned} \tag{2.59}$$

which is referred to as the unit dyad satisfying the identity

$$\mathbf{V}\cdot\bar{\mathbf{I}}=\mathbf{V} \tag{2.60}$$

Substituting (2.59) into (2.58) and then into (2.56) we have

$$\begin{aligned}\nabla\nabla G(\mathbf{r},\mathbf{r}') &= \hat{R}\hat{R}\left[\frac{1}{R^2}+\left(jk+\frac{1}{R}\right)^2\right]G(\mathbf{r},\mathbf{r}')\\ &\quad-(\bar{\mathbf{I}}-\hat{R}\hat{R})\left(jk+\frac{1}{R}\right)\frac{G(\mathbf{r},\mathbf{r}')}{R}\end{aligned} \tag{2.61}$$

and thus

$$\begin{aligned}-jkZ\mathbf{J}(\mathbf{r})G(\mathbf{r},\mathbf{r}')-\frac{jZ}{k}\mathbf{J}(\mathbf{r}')\cdot\nabla\nabla G(\mathbf{r},\mathbf{r}') &= -jkZ\left\{\left[1-\frac{j}{kR}-\frac{1}{(kR)^2}\right]\mathbf{J}(\mathbf{r}')\right.\\ &\quad\left.-\left[1-\frac{3j}{kR}-\frac{3}{(kR)^2}\right]\left(\mathbf{J}(\mathbf{r}')\cdot\hat{R}\right)\hat{R}\right\}G(\mathbf{r},\mathbf{r}')\end{aligned} \tag{2.62}$$

When this result along with (2.55) is introduced into (2.52) we obtain

$$\begin{aligned}\mathbf{E} &= -jk\int\int\int_V\left[\mathbf{M}(\mathbf{r}')\times\hat{R}\right]\left(1+\frac{1}{jkR}\right)G(\mathbf{r},\mathbf{r}')dv'\\ &\quad-jkZ\int\int\int_V\left\{\left[1-\frac{j}{kR}-\frac{1}{(kR)^2}\right]\mathbf{J}(\mathbf{r}')\right.\\ &\quad\left.-\left[1-\frac{3j}{kR}-\frac{3}{(kR)^2}\right]\left(\mathbf{J}(\mathbf{r}')\cdot\hat{R}\right)\hat{R}\right\}G(\mathbf{r},\mathbf{r}')dv'\end{aligned} \tag{2.63a}$$

and similarly

$$\mathbf{H}=+jk\int\int\int_V\left[\mathbf{J}(\mathbf{r}')\times\hat{R}\right]\left(1+\frac{1}{jkR}\right)G(\mathbf{r},\mathbf{r}')dv'$$

$$-jkY\int\int\int_V \left\{ \left[1-\frac{j}{kR}-\frac{1}{(kR)^2}\right]\mathbf{M}(\mathbf{r}') - \left[1-\frac{3j}{kR}-\frac{3}{(kR)^2}\right]\left(\mathbf{M}(\mathbf{r}')\cdot\hat{R}\right)\hat{R}\right\} G(\mathbf{r},\mathbf{r}')dv' \qquad (2.63b)$$

Before closing this section we remark that if $J(\mathbf{r})$ is replaced by an infinitesimal dipole of length $\Delta\ell \to 0$ and carrying a current I, i.e. $\mathbf{J}(\mathbf{r}) = I\hat{\ell}$, from (2.53) the associated near zone fields are given by

$$\mathbf{E}_e = -jkZ(I\Delta\ell)\left[1-\frac{j}{kR}-\frac{1}{(kR)^2}\right]\frac{e^{-jkR}}{4\pi R}\hat{\ell} + jkZ(I\Delta\ell)\left[1-\frac{3j}{kR}-\frac{3}{(kR)^2}\right]\frac{e^{-jkR}}{4\pi R}(\hat{\ell}\cdot\hat{R})\hat{R} \qquad (2.64a)$$

and

$$\mathbf{H}_e = +jk(I\Delta\ell)\left[1+\frac{1}{jkR}\right]\frac{e^{-jkR}}{4\pi R}(\hat{\ell}\times\hat{R}) \qquad (2.64b)$$

If the dipole is z directed ($\hat{\ell} = \hat{z}$) and is located at the origin ($\mathbf{R} = \mathbf{r}$), then upon setting $\hat{z} = \hat{r}\cos\theta - \hat{\theta}\sin\theta$, (2.64) reduce to the usual dipole radiated fields. Similarly, if $\mathbf{M}(\mathbf{r})$ is set equal to an infinitesimal $(I_m)\hat{\ell}$, by referring back to (2.63) or by invoking duality we find that the corresponding radiated fields are given by

$$\mathbf{E}_m = -jk(I_m\Delta\ell)\left[1+\frac{1}{jkR}\right]\frac{e^{-jkR}}{4\pi R}(\hat{\ell}\times\hat{R}) \qquad (2.65a)$$

$$\mathbf{H}_m = -jkY(I_m\Delta\ell)\left[1-\frac{j}{kR}-\frac{1}{(kR)^2}\right]\frac{e^{-jkR}}{4\pi R}\hat{R} + jkY(I_m\Delta\ell)\left[1-\frac{3j}{kR}-\frac{3}{(kR)^2}\right]\frac{e^{-jkR}}{4\pi R}(\hat{\ell}\cdot\hat{R})\hat{R} \qquad (2.65b)$$

Again, upon setting $\hat{\ell} = \hat{z}$ and $\mathbf{r}' = 0$ (implying $\mathbf{R} = \mathbf{r}$), these reduce to the usual magnetic dipole fields.

2.3.2 Field Evaluation in the Source Region

The field expressions (2.63) can be readily evaluated for $r \neq r'$. However, care is required in evaluating the integrals when $\mathbf{r} \to \mathbf{r}'$. In that case $R \to 0$ and the integrand has a non-integrable $1/R^3$ singularity. To circumvent this difficulty we can rewrite the portion of the integral due to the electric current as

$$\begin{aligned}\mathbf{E}_e &= -jkZ \int\int\int_{V-V_o} \left[\mathbf{J}(\mathbf{r}')G(\mathbf{r}_o,\mathbf{r}') + \frac{1}{k^2}\mathbf{J}(\mathbf{r}')\cdot\nabla\nabla G(\mathbf{r}_o,\mathbf{r}')\right] dv' \\ &\quad -jkZ \int\int\int_{V_o} \left[\mathbf{J}(\mathbf{r}')G(\mathbf{r}_o,\mathbf{r}') + \frac{1}{k^2}J(\mathbf{r}')\cdot\nabla\nabla G(\mathbf{r}_o,\mathbf{r}')\right] dv' \quad (2.66)\end{aligned}$$

where V_o is an infinitesimally small spherical volume centered at the observation point $\mathbf{r}_o$ (see Fig. 2.4) and $\mathbf{r}_o$ is in V. It can then be shown that the first term of the second integrand over V_o vanishes and to deal with the second term of the same integral we invoke the identity [Van Bladel, p. 488, Collin; 1986]

$$\int\int\int_{V_o} \nabla f \, dv = \oiint_{S_o} \hat{n}_o f \, ds. \quad (2.67)$$

This is based on a generalization of Gauss' theorem and accordingly $\hat{n}_o$ denotes the outward normal unit vector to the surface S_o enclosing V_o. Using (2.67) and recalling that V_o is a small spherical volume we have

$$\begin{aligned}\int\int\int_{V_o\to 0} \frac{1}{k^2}\mathbf{J}(\mathbf{r}')\cdot\nabla\nabla G(\mathbf{r}_o,\mathbf{r}')dv' &\simeq -\frac{1}{k^2}\mathbf{J}(\mathbf{r}_o)\cdot\nabla\int\int\int_{V_o\to 0}\nabla' G(\mathbf{r}_o,\mathbf{r}')dv' \\ &= +\frac{1}{k^2}\oiint_{S_o}\left(\hat{R}_o\cdot\mathbf{J}(\mathbf{r}_o)\right)\nabla G(\mathbf{r}_o,\mathbf{r}')ds'\end{aligned}$$

where $\hat{R}_o = (\mathbf{r}_o - \mathbf{r}')/|\mathbf{r}_o - \mathbf{r}'|$. For $R_o = |\mathbf{r}_o - \mathbf{r}'| \to 0$, $\nabla G \approx -\frac{\hat{R}_o}{4\pi R_o^2}$ and upon transfering to spherical coordinates we obtain

$$-\lim_{R_o\to 0}\oiint_{S_o}\left(\hat{R}_o\cdot\mathbf{J}(r_o)\right)\nabla G(\mathbf{r}_o,\mathbf{r}')ds' = \frac{1}{4\pi}\int_0^{\pi}\int_0^{2\pi}\left(\hat{R}_o\cdot\mathbf{J}(r_o)\right)\hat{R}_o\sin\theta_o\, d\theta_o d\phi_o$$

Setting now $\hat{R}_o = -[\hat{x}\cos\phi_o\,\sin\theta_o + \hat{y}\sin\phi_o\,\sin\theta_o + \hat{z}\cos\theta_o]$ and dropping those integrals which vanish, we have

$$-\lim_{R_o\to 0}\oiint_{S_o}\left(\hat{R}_o\cdot\mathbf{J}(r_o)\right)\nabla G(\mathbf{r}_o,\mathbf{r}')ds' = \hat{x}(\hat{x}\cdot\mathbf{J}(\mathbf{r}_o))\int_o^{\pi}\int_0^{2\pi}\cos^2\phi_o\sin^3\theta_o d\theta_o d\phi_o$$

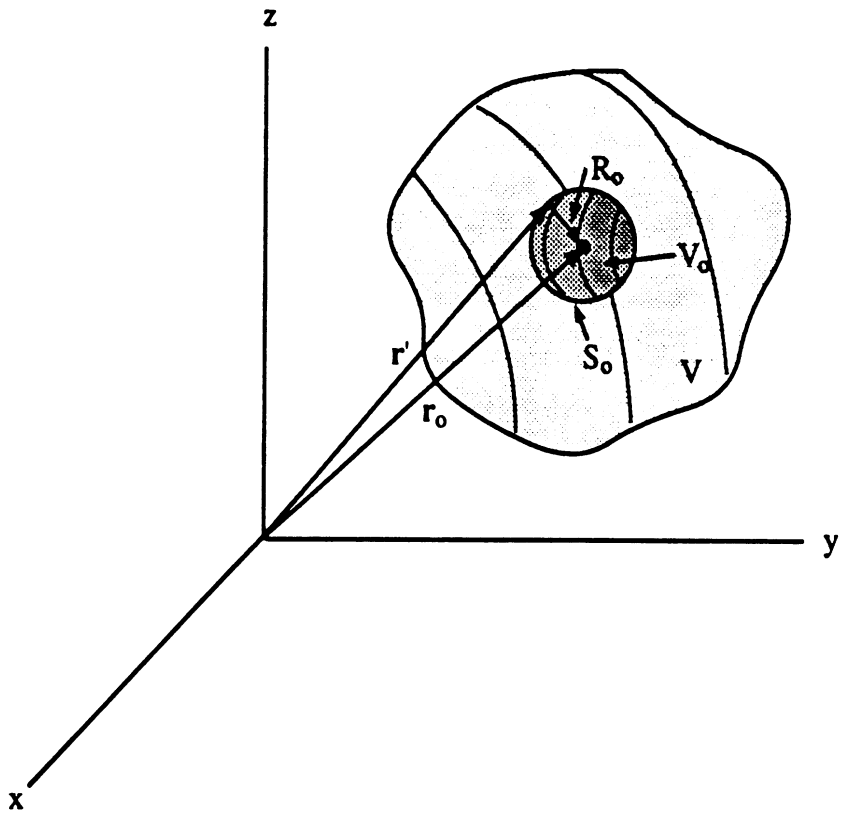

Figure 2.4: Geometry for evaluating the field in the source region.

$$+\hat{y}\,(\hat{y}\cdot\mathbf{J}(\mathbf{r}_o))\int_o^{\pi}\int_0^{2\pi}\sin^2\phi_o\,\sin^3\theta_o\,d\theta_o\,d\phi_o$$

$$+\hat{z}\,(\hat{z}\cdot\mathbf{J}(\mathbf{r}_o))\int_o^{\pi}\int_0^{2\pi}\cos^2\theta_o\,\sin\theta_o\,d\theta_o\,d\phi_o$$

and upon evaluating the trivial integrals we obtain

$$\lim_{R_o\to 0}\oiint_{S_o}\left(\hat{R}_o\cdot\mathbf{J}(r_o)\right)\nabla G(\mathbf{r}_o,\mathbf{r}')ds' = -\frac{1}{3}\mathbf{J}(\mathbf{r}_o) \tag{2.68}$$

Consequently, we may rewrite (2.66) as

$$\mathbf{E}_e(\mathbf{r}) = -jkZ\iiint_V\left[\mathbf{J}(\mathbf{r}')G(\mathbf{r},\mathbf{r}') + \frac{1}{k^2}\mathbf{J}(\mathbf{r}')\cdot\nabla\nabla G(\mathbf{r},\mathbf{r}')\right]dv' + \frac{jZ}{3k}\mathbf{J}(\mathbf{r}) \tag{2.69}$$

where the horizontal bar through the integral denotes the principal value of that integral. That is, if $\mathbf{r} = \mathbf{r}_o$, where $\mathbf{r}_o$ is located in V, the principal value of the integral is evaluated as

$$\iiint\!\!\!\!\!\!-_V f(\mathbf{r}')dv' = \lim_{V\to 0}\int\int\int_{V-V_o} f(\mathbf{r}')dv'. \tag{2.70}$$

Otherwise, if $\mathbf{r}$ is not in the source region V, then $\mathbf{J}(\mathbf{r}) = 0$ and the principal value integral is evaluated as an ordinary integral. This simply implies that for $\mathbf{r}$ not in V, no special care is required for the evaluation of the integrals in (2.63).

2.3.3 Fresnel and Far Zone Fields

When $R = |\mathbf{r} - \mathbf{r}'|$ the field expressions (2.63) can be simplified substantially by neglecting those terms whose amplitude is $O(1/R^2)$ or less. In addition, we may approximate $\hat{R}$ by $\hat{r}$ (see Fig. 2.3) permitting us to simplify (2.63) to

$$\mathbf{E} = -jk\int\int\int_V [\mathbf{M}(\mathbf{r}')\times\hat{r}]\frac{e^{-jk|\mathbf{r}-\mathbf{r}'|}}{4\pi r}dv'$$
$$+ jkZ\int\int\int_V \hat{r}\times[\hat{r}\times\mathbf{J}(\mathbf{r}')]\frac{e^{-jk|\mathbf{r}-\mathbf{r}'|}}{4\pi r}dv' \tag{2.71a}$$

$$\mathbf{H} = jk\int\int\int_V [\mathbf{J}(\mathbf{r}')\times\hat{r}]\frac{e^{-jk|\mathbf{r}-\mathbf{r}'|}}{4\pi r}$$
$$+ jkY\int\int\int_V \hat{r}\times[\hat{r}\times\mathbf{M}(\mathbf{r}')]\frac{e^{-jk|\mathbf{r}-\mathbf{r}'|}}{4\pi r}dv' \tag{2.71b}$$

To proceed further, it is necessary to obtain a more explicit expression for $|\mathbf{r} - \mathbf{r}'|$ and from Figure 2.3, we obtain that

$$R = |\mathbf{r} - \mathbf{r}'| = \sqrt{r^2 + r'^2 - 2rr'\cos\zeta} \tag{2.72}$$

where $r'\cos\zeta = \mathbf{r}'\cdot\hat{r}$ as illustrated in Figure 2.3(b). By employing a binomial expansion for the square root, R can be written as

$$R \approx r + \frac{1}{2}\frac{1}{r}(-2rr'\cos\zeta + r'^2) + \frac{\frac{1}{2}\left(\frac{-1}{2}\right)}{2}(r^2)^{\frac{-3}{2}}(-2rr'\cos\zeta + r'^2) + \cdots$$

and upon some rearrangement we have

$$R \approx r - r'\cos\zeta + \frac{r'^2\sin^2\zeta}{2r} + \frac{r'^2\cos\zeta}{2r^2} - \frac{(r')^4}{8r^3} - \frac{r'^3\cos^3\zeta}{2r^2} + \cdots \tag{2.73}$$

When the first three terms of this expansion are kept, the resulting field expressions become

$$\mathbf{E} \simeq jk\frac{e^{-jkr}}{4\pi r}\int\int\int_V [\hat{r}\times\mathbf{M}(\mathbf{r}') + Z\hat{r}\times\hat{r}\times\mathbf{J}(\mathbf{r}')]\, e^{jk[\mathbf{r}'\cdot\hat{r}+r'\mathbf{r}'\cdot\hat{r}-(r')^2]}dv' \tag{2.74a}$$

$$\mathbf{H} \simeq jk\frac{e^{-jkr}}{4\pi r}\int\int\int_V [-\hat{r}\times\mathbf{J}(\mathbf{r}') + Y\hat{r}\times\hat{r}\times\mathbf{M}(\mathbf{r}')]\, e^{jk[\mathbf{r}'\cdot\hat{r}+r'\mathbf{r}'\cdot\hat{r}-(r')^2]}dv' \tag{2.74b}$$

which were derived by invoking the vector identity

$$\mathbf{a}\times(\mathbf{b}\times\mathbf{c}) = (\mathbf{a}\cdot\mathbf{c})\mathbf{b} - (\mathbf{a}\cdot\mathbf{b})\mathbf{c} \tag{2.75}$$

These expressions give the Fresnel zone fields and if we restrict the maximum phase error due to the three term approximation for R to be less than $\pi/8$, this demands that the next higher order term of the expansion must contribute a phase which is smaller than $\pi/8$. From (2.73), this implies that the sum of the fourth and sixth terms must always be less than $\pi/8k$, i.e.

$$\max\left\{\frac{k\left(\frac{D}{2}\right)^3}{2r^2}\cos\zeta(1-\cos^2\zeta)\right\} \leq \frac{\pi}{8}.$$

where D denotes the maximum linear dimension of the source. Differentiating the left side of the above inequality with respect to ζ and setting the result to zero gives $\zeta_1 = 0$ and $\zeta_2 = \cos^{-1}(1/\sqrt{3})$. Of these solutions the second is associated with a maximum and we thus have

$$\frac{k\left(\frac{D}{2}\right)^3}{2r^2}0.385 \leq \frac{\pi}{8}$$

giving that

$$r \geq 0.62\sqrt{\frac{D^3}{\lambda}} \tag{2.76}$$

if the phase error associated with the approximate expressions (2.74) is to be kept to less than $\pi/8$.

If we retain only the first two terms of the expansion (2.73) the resulting field expressions are

$$\mathbf{E} = \mathbf{E}_{ff} = jk\frac{e^{-jkr}}{4\pi r}\int\int\int_V [\hat{r} \times \mathbf{M}(\mathbf{r}') + Z\hat{r} \times \hat{r} \times \mathbf{J}(\mathbf{r}')]\, e^{jk\mathbf{r}'\cdot\hat{r}}\, dv' \tag{2.77a}$$

$$\mathbf{H} = \mathbf{H}_{ff} = -jkY\frac{e^{-jkr}}{4\pi r}\int\int\int_V [Z\hat{r} \times \mathbf{J}(\mathbf{r}') - \hat{r} \times \hat{r} \times \mathbf{M}(\mathbf{r}')]\, e^{jk\mathbf{r}'\cdot\hat{r}}\, dv' \tag{2.77b}$$

These are referred to as the *far zone fields* and as is the case with (2.74) they are also valid for surface and linear sources upon replacing the volume integrals with surface or line integrals over the domain of the source. Again, by demanding that the maximum phase error due to the two term approximation for R is less than $\pi/8$, we can find the minimum value for r for which this can be achieved. In this case, the third term of the expansion (2.73) must satisfy the inequality

$$\frac{kD^2}{8r} \leq \frac{\pi}{8}$$

implying that

$$r \geq \frac{2D^2}{\lambda} \tag{2.78}$$

and this relation is referred to as the *far zone criterion.*

By comparing the $\mathbf{E}$ and $\mathbf{H}$ expressions given in (2.77) and making use of the identity (2.75) it follows that

$$\mathbf{H}_{ff} = Y\hat{r} \times \mathbf{E}_{ff}, \quad \mathbf{E}_{ff} = -Z\hat{r} \times \mathbf{H}_{ff} \tag{2.79}$$

Which are the usual relations associated with the far zone fields and imply that the far zone field does not have a component along $\hat{r}$, the direction of proagation. Through comparison of (2.77) with (2.35) and (2.36), it also follows that

$$\mathbf{E}_{ff} = jk\hat{r} \times \mathbf{F} + jkZ\hat{r} \times (\hat{r} \times \mathbf{A}) = -Z\hat{r} \times \mathbf{H}_{ff} \tag{2.80a}$$

$$\mathbf{H}_{ff} = -jk\hat{r} \times \mathbf{A} + jkY\hat{r} \times (\hat{r} \times \mathbf{F}) = Y\hat{r} \times \mathbf{E}_{ff} \tag{2.80b}$$

More explicitly, we may also express the far zone fields in terms of the spherical components of the vector potential as

$$\mathbf{E}_{ff} = -\hat{\theta}jk(F_\phi + ZA_\theta) + \hat{\phi}jk(F_\theta - ZA_\phi) \tag{2.81a}$$

$$\mathbf{H}_{ff} = -\hat{\theta}jk(A_\phi - YF_\phi) - \hat{\phi}jk(A_\theta + YF_\phi) \tag{2.81b}$$

By comparison of (2.80a) and (2.80b) we can conclude that the dual quantity of $\mathbf{A}$ is $\mathbf{F}$ and that the dual of $\mathbf{F}$ is $-\mathbf{A}$ and a more complete summary of the dual field quantities is given in Table 2.1.

2.4 Direct Solution of the Vector Wave Equation

2.4.1 Vector wave equations

In many cases it is advantageous and, thus, desirable to work directly with the electric and magnetic fields rather than the vector potentials. To obtain a solution for the fields $\mathbf{E}$ and $\mathbf{H}$ we must then pursue a direct solution of Maxwell's equations (1.48) - (1.51) without invoking the vector or scalar potentials. Because of duality let us concentrate on the electric field solution.

Dividing (1.49) by μ_r, taking its curl and making use of (1.48) we obtain

$$\nabla \times \left(\frac{1}{\mu_r}\nabla \times \mathbf{E}\right) - k_o^2\epsilon_r\mathbf{E} = -j\omega\mu_o\mathbf{J} - \nabla \times \left(\frac{1}{\mu_r}\mathbf{M}\right) \tag{2.82a}$$

where we have again dropped the subscripts i from $\mathbf{J}$ and $\mathbf{M}$. This can be alternatitively written as

$$\nabla \times \nabla \times \mathbf{E} - k^2\mathbf{E} + \mu_r \nabla \left(\frac{1}{\mu_r}\right) \times \nabla \times \mathbf{E} = -j\omega\mathbf{J}$$

$$- \nabla \times \mathbf{M} - \mu_r \nabla \left(\frac{1}{\mu_r}\right) \times \mathbf{M} \tag{2.82b}$$

where we have made use of the identity

$$\nabla \times (\phi\mathbf{A}) = \nabla\phi \times \mathbf{A} + \phi\nabla \times \mathbf{A} \tag{2.83}$$

Equations (2.82) are the most general forms of the electric field *wave equation.* The corresponding magnetic field wave equations are

$$\nabla \times \left(\frac{1}{\epsilon_r}\nabla \times \mathbf{H}\right) - k_o^2\mu_r\mathbf{H} = -j\omega\epsilon_o\mathbf{M} + \nabla \times \left(\frac{1}{\epsilon_r}\mathbf{J}\right) \tag{2.84a}$$

or

$$\nabla \times \nabla \times \mathbf{H} - k^2\mathbf{H} + \epsilon_r \nabla \left(\frac{1}{\epsilon_r}\right) \times \nabla \times \mathbf{H} = -j\omega\epsilon\mathbf{M}$$

$$+ \nabla \times \mathbf{J} + \epsilon_r \nabla \left(\frac{1}{\epsilon_r}\right) \times \mathbf{J} \tag{2.84b}$$

In the case of homogeneous media, $\nabla\left(\frac{1}{\epsilon_r}\right) = \nabla\left(\frac{1}{\mu_r}\right) = 0$ and the wave equation then reduces to

$$\begin{aligned} \nabla \times \nabla \times \mathbf{E} - k^2\mathbf{E} &= -j\omega\mu\mathbf{J} - \nabla \times \mathbf{M} \\ \nabla \times \nabla \times \mathbf{H} - k^2\mathbf{H} &= -j\omega\epsilon\mathbf{M} + \nabla \times \mathbf{J} \end{aligned} \tag{2.85}$$

By employing the identity (2.6) and the relation (1.51), it follows that

$$\begin{aligned} \nabla^2\mathbf{E} + k^2\mathbf{E} &= j\omega\mu\mathbf{J} - \frac{\nabla\nabla \cdot \mathbf{J}}{j\omega\epsilon} + \nabla \times \mathbf{M} \\ \nabla^2\mathbf{H} + k^2\mathbf{H} &= j\omega\epsilon\mathbf{M} - \frac{\nabla\nabla \cdot \mathbf{M}}{j\omega\mu} - \nabla \times \mathbf{J} \end{aligned} \tag{2.86a}$$

In the source free region these reduce to

$$\nabla^2\mathbf{E} + k^2\mathbf{E} = 0$$
$$\nabla\mathbf{H} + k^2\mathbf{H} = 0 \tag{2.86b}$$

which are commonly referred to as the wave equations. These imply that each field component satisfies the scalar Helmholtz equation

$$\nabla^2\psi + k^2\psi = 0 \tag{2.87}$$

where ψ denotes E_x, E_y, E_z, H_x, H_y or H_z.

2.4.2 Dyadic representation

To solve (2.85) we may instead consider the solution of the dyadic equation

$$\nabla \times \nabla \times \overline{\Gamma}(\mathbf{r},\mathbf{r}') - k^2\overline{\Gamma}(\mathbf{r},\mathbf{r}') = -\overline{\mathbf{I}}\delta(\mathbf{r}-\mathbf{r}') \tag{2.88}$$

where $\overline{\Gamma}(\mathbf{r},\mathbf{r}')$ is referred to as the free space dyadic green's function and satisfies the radiation condition

$$\lim_{r\to\infty} r\left[jk\overline{\Gamma} + \hat{r}\times\left(\nabla\times\overline{\Gamma}\right)\right] = 0 \tag{2.89}$$

By setting $\overline{\Gamma} = \mathbf{T}\hat{a}$, where $\hat{a}$ is some arbitrary unit vector, this can be alternatively written as

$$\lim_{r\to\infty} r\left[jk\mathbf{T} + \hat{r}\times(\nabla\times\mathbf{T})\right]\hat{a} = 0 \tag{2.90}$$

By a comparison of (2.85) and (2.88) it is then readily seen that $\mathbf{T}$ represents a field vector and for (2.89) to be a valid radiation condition, (2.90) must be satisfied when $\mathbf{T}$ is replaced by the $\mathbf{E}$ or $\mathbf{H}$ far zone fields. This is easily verified by reverting to the far zone relation (2.74) and in conjunction with the source free Maxwell's equation, we find that

$$\nabla\times\mathbf{T} = -jk\hat{r}\times\mathbf{T} \tag{2.91}$$

where $\mathbf{T}$ represents the $\mathbf{E}$ or $\mathbf{H}$ fields, and from which it is seen that (2.90) is satisfied .

To solve for $\overline{\Gamma}$ we first take the divergence of both sides of (2.88) and this gives

$$-\nabla \cdot \left[k^2 \overline{\Gamma}(\mathbf{r}, \mathbf{r}')\right] = -\nabla \cdot \left[\bar{\mathbf{I}} \delta(\mathbf{r} - \mathbf{r}')\right] \tag{2.92}$$

Also, by invoking the identity (2.6), equation (2.88) can be written as

$$\nabla^2 \overline{\Gamma}(\mathbf{r}, \mathbf{r}') + k^2 \overline{\Gamma}(\mathbf{r}, \mathbf{r}') = \bar{\mathbf{I}} \delta(\mathbf{r} - \mathbf{r}') + \nabla \left[\nabla \cdot \overline{\Gamma}(\mathbf{r}, \mathbf{r}')\right] \tag{2.93}$$

which can be combined with (2.92) to give

$$(\nabla^2 + k^2) \overline{\Gamma}(\mathbf{r}, \mathbf{r}') = \left[\bar{\mathbf{I}} + \frac{\nabla\nabla}{k^2}\right] \delta(\mathbf{r} - \mathbf{r}'). \tag{2.94}$$

Setting

$$\overline{\Gamma}(\mathbf{r}, \mathbf{r}') = -\left[\bar{\mathbf{I}} + \frac{\nabla\nabla}{k^2}\right] G(\mathbf{r}, \mathbf{r}') \tag{2.95}$$

it follows from (2.94) that $G(\mathbf{r}, \mathbf{r}')$ must satisfy the differential equation

$$(\nabla^2 + k^2) G(\mathbf{r}, \mathbf{r}') = -\delta(\mathbf{r} - \mathbf{r}')$$

This is identical to (2.38) and since it can be shown from (2.89) that $G(\mathbf{r}, \mathbf{r}')$ must also satisfy the scalar radiation condition (2.39), it is then given by (2.37).

By referring to section 2.3.1, it is readily seen that $\overline{\Gamma}$ can be expressed as

$$\begin{aligned} \overline{\Gamma}(\mathbf{r}, \mathbf{r}') &= \left(\frac{j}{kR} + \frac{1}{(kR)^2} - 1\right) G(R) \bar{\mathbf{I}} \\ &= +\left(1 - \frac{3}{(kR)^2} - \frac{3j}{kR}\right) G(R) \hat{R}\hat{R} \end{aligned} \tag{2.96}$$

Also,

$$\begin{aligned} \nabla \times \overline{\Gamma}(\mathbf{r}, \mathbf{r}') &= -\nabla \times \left(\bar{\mathbf{I}} + \frac{\nabla\nabla}{k^2}\right) G(R) \\ &= -\nabla \times \bar{\mathbf{I}} G(R) + \nabla \times \frac{\nabla\nabla}{k^2} G(R) \\ &= -\nabla \times \bar{\mathbf{I}} G(R) = -\nabla G(R) \times \bar{\mathbf{I}} \end{aligned} \tag{2.97a}$$

$$\nabla \times \overline{\Gamma}(\mathbf{r}, \mathbf{r}') = \left(jk + \frac{1}{R}\right) G(R) \hat{R} \times \bar{\mathbf{I}} \tag{2.97b}$$

since $\nabla R = \hat{R}$. However, before proceeding with field representations in terms of the dyadic Green's function, it is instructive to look at more explicit expressions of $\overline{\Gamma}$ aimed at clarifying its use in subsequent integral equations.

Any dyadic can be written in terms of its components, and for the case of $\overline{\Gamma}$ we have

$$\begin{aligned}\overline{\Gamma} = {} & \hat{x}\hat{x}\Gamma_{xx} + \hat{x}\hat{y}\Gamma_{xy} + \hat{x}\hat{z}\Gamma_{xz} \\ & + \hat{y}\hat{x}\Gamma_{yx} + \hat{y}\hat{y}\Gamma_{yy} + \hat{y}\hat{z}\Gamma_{yz} \\ & + \hat{z}\hat{x}\Gamma_{zx} + \hat{z}\hat{y}\Gamma_{zy} + \hat{z}\hat{z}\Gamma_{zz} \end{aligned} \tag{2.98a}$$

which can be more conveniently written in matrix form as

$$\overline{\Gamma} = \begin{pmatrix} \Gamma_{xx} & \Gamma_{xy} & \Gamma_{xz} \\ \Gamma_{yx} & \Gamma_{yy} & \Gamma_{yz} \\ \Gamma_{zx} & \Gamma_{zy} & \Gamma_{zz} \end{pmatrix} \tag{2.98b}$$

Again, it should be noted that the meaning of the dyadic can only be realized when it is dotted with another vector. Using (2.98b) this operation becomes the matrix product

$$\overline{\Gamma} \cdot \mathbf{V} = \begin{pmatrix} \Gamma_{xx} & \Gamma_{xy} & \Gamma_{xz} \\ \Gamma_{yx} & \Gamma_{yy} & \Gamma_{yz} \\ \Gamma_{zx} & \Gamma_{zy} & \Gamma_{zz} \end{pmatrix} \begin{pmatrix} V_x \\ V_y \\ V_z \end{pmatrix}$$

which is convenient for numerical implementations.

To find the individual matrix components of $\overline{\Gamma}$ we may return to (2.95) and upon replacing the ∇ operators with their cartesian forms we find

$$\overline{\Gamma}(\mathbf{r}, \mathbf{r}') = -\frac{1}{4\pi k^2} \begin{pmatrix} k^2 + \frac{\partial^2}{\partial x^2} & \frac{\partial^2}{\partial x \partial y} & \frac{\partial^2}{\partial x \partial z} \\ \frac{\partial^2}{\partial x \partial y} & k^2 + \frac{\partial^2}{\partial y^2} & \frac{\partial^2}{\partial y \partial z} \\ \frac{\partial^2}{\partial x \partial z} & \frac{\partial^2}{\partial y \partial z} & k^2 + \frac{\partial^2}{\partial z^2} \end{pmatrix} \frac{e^{-jkR}}{R} \tag{2.99}$$

and

$$\nabla \times \overline{\Gamma}(\mathbf{r},\mathbf{r}') = -\frac{1}{4\pi}\begin{pmatrix} 0 & -\frac{\partial}{\partial z} & \frac{\partial}{\partial y} \\ \frac{\partial}{\partial z} & 0 & -\frac{\partial}{\partial x} \\ -\frac{\partial}{\partial y} & \frac{\partial}{\partial x} & 0 \end{pmatrix}\frac{e^{-jkR}}{R} \tag{2.100}$$

One could now carry out the differentiations or more conveniently (2.96) and (2.97) could be employed along with the cartesian expressions of $\hat{R}$ and $\overline{\mathbf{I}}$ given by (2.59) and (2.54), respectively. The cartesian components of $\overline{\Gamma}$ are then readily found by collecting the like terms. The corresponding matrix components of $\overline{\Gamma}$ in the cylindrical coordinate systems are found by replacing the ∇ operators in (2.95) with their corresponding cylindrical forms. Upon collecting like terms, this gives

$$\overline{\Gamma}(\mathbf{r},\mathbf{r}') = -\frac{1}{4\pi k^2}\begin{pmatrix} k^2+\frac{\partial^2}{\partial\rho^2} & \frac{1}{\rho}\frac{\partial}{\partial\rho\partial\phi} & \frac{\partial^2}{\partial\rho\partial z} \\ \frac{1}{\rho}\frac{\partial^2}{\partial\phi\partial\rho} & k^2+\frac{1}{\rho^2}\frac{\partial^2}{\partial\phi^2} & \frac{1}{\rho}\frac{\partial^2}{\partial\phi\partial z} \\ \frac{\partial^2}{\partial z\partial\rho} & \frac{1}{\rho}\frac{\partial^2}{\partial z\partial\phi} & k^2+\frac{\partial^2}{\partial z^2} \end{pmatrix}\frac{e^{-jkR}}{R} \tag{2.101}$$

where (ρ,ϕ,z) denote the usual cylindrical coordinates. In carrying out the differentiations, it should be noted that now

$$R = \sqrt{\rho^2+\rho'^2-2\rho\rho'\cos(\phi-\phi')+(z-z')^2}.$$

To express the $\mathbf{E}$ and $\mathbf{H}$ fields in terms of the free space dyadic green's function we may examine (2.52) and identify the presence of $\overline{\Gamma}(\mathbf{r},\mathbf{r}')$ and $\nabla\times\overline{\Gamma}(\mathbf{r},\mathbf{r}')$ which are given in (2.95) and (2.97a), respectively. Then, upon making use of the identity (2.60) and that $-\nabla G\times\mathbf{M} = -\nabla G\times\overline{\mathbf{I}}\cdot\mathbf{M}$,we can rewrite (2.52) as

$$\mathbf{E}(\mathbf{r}) = \int\int\int\left\{\left[\nabla\times\overline{\Gamma}(\mathbf{r},\mathbf{r}')\right]\cdot\mathbf{M}(\mathbf{r}')+jkZ\overline{\Gamma}(\mathbf{r},\mathbf{r}')\cdot\mathbf{J}(\mathbf{r}')\right\}dv' \tag{2.102a}$$

$$\mathbf{H}(\mathbf{r}) = \int\int\int\left\{jkY\overline{\Gamma}(\mathbf{r},\mathbf{r}')\cdot\mathbf{M}(\mathbf{r}')-\left[\nabla\times\overline{\Gamma}(\mathbf{r},\mathbf{r}')\right]\cdot\mathbf{J}(\mathbf{r}')\right\}dv' \tag{2.102b}$$

A more formal derivation of (2.102), though, directly from the vector wave equations (2.85) and the dyadic equations (2.88) requires use of the vector-dyadic second Green's identity. This is given by

$$\int\int\int_V \left\{[\nabla \times \nabla \times \mathbf{E}(\mathbf{r})] \cdot \overline{\Gamma}(\mathbf{r},\mathbf{r}') - \mathbf{E}(\mathbf{r}) \cdot \nabla \times \nabla \times \overline{\Gamma}(\mathbf{r},\mathbf{r}')\right\} dv =$$

$$\oiint_{S_c} \left\{[\hat{n} \times \mathbf{E}(\mathbf{r})] \cdot \nabla \times \overline{\Gamma}(\mathbf{r},\mathbf{r}') + [\hat{n} \times \nabla \times \mathbf{E}(\mathbf{r})] \cdot \overline{\Gamma}(\mathbf{r},\mathbf{r}')\right\} ds \tag{2.103}$$

where $\hat{n}$ is the outward unit normal to the surface S_c enclosing V. Also, $\mathbf{E}$ and $\overline{\Gamma}$ can be any vector or dyadic but in this case they are chosen to represent the electric field and the free space dyadic green's function. We note that the identity (2.103) can be derived directly from the scalar second green's identity (2.42) and this is discussed in the Appendix.

Upon making use of (2.85) and (2.88) in (2.103) along with the property of the delta function, the left hand side of (2.103) becomes

$$\mathbf{E}(\mathbf{r}') - \int\int\int_V \left\{j\omega\mu\mathbf{J}(\mathbf{r}) \cdot \overline{\Gamma}(\mathbf{r},\mathbf{r}') + [\nabla \times \mathbf{M}(\mathbf{r})] \cdot \overline{\Gamma}(\mathbf{r},\mathbf{r}')\right\} dv$$

To evaluate the right hand side surface integral we may assume that S_c is a spherical surface at infinity since V encompasses all space. Then, upon invoking the radiation condition (2.89) and (2.91) it can be shown that the right hand side of (2.103) vanishes. Thus, we have

$$\mathbf{E}(\mathbf{r}') = \int\int\int_V \left\{j\omega\mu\mathbf{J}(\mathbf{r}) \cdot \overline{\Gamma}(\mathbf{r},\mathbf{r}') + [\nabla \times \mathbf{M}(\mathbf{r})] \cdot \overline{\Gamma}(\mathbf{r},\mathbf{r}')\right\} dv \tag{2.104}$$

and by noting that

$$\int\int\int_V \nabla \cdot \left\{\mathbf{M}(\mathbf{r}) \times \overline{\Gamma}(\mathbf{r},\mathbf{r}')\right\} dv = \oiint_{S_c} \left\{\mathbf{M}(\mathbf{r}) \times \overline{\Gamma}(\mathbf{r},\mathbf{r}')\right\} \cdot \hat{n} ds = 0 \tag{2.105}$$

(since $\mathbf{M}(\mathbf{r})$ is zero on S_c) and the identity

$$\nabla \cdot \left\{\mathbf{M}(\mathbf{r}) \times \overline{\Gamma}(\mathbf{r},\mathbf{r}')\right\} = \nabla \times \mathbf{M}(\mathbf{r}) \cdot \overline{\Gamma}(\mathbf{r},\mathbf{r}') - \mathbf{M}(\mathbf{r}) \cdot \nabla \times \overline{\Gamma}(\mathbf{r},\mathbf{r}') \tag{2.106}$$

it follows that

$$\mathbf{E}(\mathbf{r}') = \int\int\int_V \left\{ j\omega\mu \mathbf{J}(\mathbf{r}) \cdot \overline{\Gamma}(\mathbf{r},\mathbf{r}') + \mathbf{M}(\mathbf{r}) \cdot \left[\nabla \times \overline{\Gamma}(\mathbf{r},\mathbf{r}') \right] \right\} dv \quad (2.107)$$

To cast this into the integral form given in (2.102) it is necessary to invoke some properties of the dyadic green's function. We note that

$$\tilde{\overline{\Gamma}}(\mathbf{r},\mathbf{r}') = \overline{\Gamma}(\mathbf{r},\mathbf{r}') \quad (2.108a)$$

$$\widetilde{\nabla \times} \overline{\Gamma}(\mathbf{r},\mathbf{r}') = -\nabla \times \overline{\Gamma}(\mathbf{r},\mathbf{r}') = \nabla' \times \overline{\Gamma}(\mathbf{r},\mathbf{r}') \quad (2.108b)$$

where the tilde over the dyadic quantity denotes the transpose of their associated matrix. Thus

$$\mathbf{M}(\mathbf{r}) \cdot \nabla \times \overline{\Gamma}(\mathbf{r},\mathbf{r}') = -\nabla \times \overline{\Gamma}(\mathbf{r},\mathbf{r}') \cdot \mathbf{M}(\mathbf{r}) = \nabla' \times \overline{\Gamma}(\mathbf{r},\mathbf{r}') \cdot \mathbf{M}(\mathbf{r}')$$

and

$$\mathbf{J}(\mathbf{r}) \cdot \overline{\Gamma}(\mathbf{r},\mathbf{r}') = \tilde{\overline{\Gamma}}(\mathbf{r},\mathbf{r}') \cdot \mathbf{J}(\mathbf{r}) = \overline{\Gamma}(\mathbf{r},\mathbf{r}') \cdot \mathbf{J}(\mathbf{r})$$

Further, since $\overline{\Gamma}(\mathbf{r},\mathbf{r}') = \overline{\Gamma}(\mathbf{r}',\mathbf{r})$ and $\nabla' \times \overline{\Gamma}(\mathbf{r},\mathbf{r}') = \nabla \times \overline{\Gamma}(\mathbf{r}',\mathbf{r})$, it follows that (2.107) is identical to (2.102).

When making practical use of the integral expressions (2.102) it is necessary to work with the individual field components. In the case of the cartesian components, these can be readily found by introducing the matrices (2.99) and (2.100) for $\overline{\Gamma}$ and $\nabla \times \overline{\Gamma}$, respectively. We have

$$E_x(\mathbf{r}) = \frac{-jZ}{k} \int\int\int_V \left[J_x(\mathbf{r}') \left(k^2 + \frac{\partial^2}{\partial x^2} \right) + J_y(\mathbf{r}') \frac{\partial^2}{\partial x \partial y} + J_z(\mathbf{r}') \frac{\partial^2}{\partial x \partial z} \right]$$
$$\cdot G(R) dv' - \int\int\int_V \left[M_z(\mathbf{r}') \frac{\partial}{\partial y} - M_y(\mathbf{r}') \frac{\partial}{\partial z} \right] G(R) dv' \quad (2.109a)$$

$$E_y(\mathbf{r}) = \frac{-jZ}{k} \int\int\int_V \left[J_x(\mathbf{r}') \frac{\partial^2}{\partial x \partial y} + J_y(\mathbf{r}') \left(k^2 + \frac{\partial^2}{\partial y^2} \right) + J_z(\mathbf{r}') \frac{\partial^2}{\partial y \partial z} \right]$$
$$\cdot G(R) dv' - \int\int\int_V \left[M_x(\mathbf{r}') \frac{\partial}{\partial z} - M_z(\mathbf{r}') \frac{\partial}{\partial x} \right] G(R) dv' \quad (2.109b)$$

$$E_z(\mathbf{r}) = \frac{-jZ}{k}\int\int\int_V \left[J_x(\mathbf{r}')\frac{\partial^2}{\partial x \partial z} + J_y(\mathbf{r}')\frac{\partial^2}{\partial y \partial z} + J_z(\mathbf{r}')\left(k^2 + \frac{\partial^2}{\partial z^2}\right)\right]$$

$$\cdot G(R)dv' - \int\int\int_V \left[-M_x(\mathbf{r}')\frac{\partial}{\partial y} + M_y(\mathbf{r}')\frac{\partial}{\partial x}\right] G(R)dv' \qquad (2.109c)$$

and the corresponding cartesian components of $\mathbf{H}$ follow by duality. To obtain the ideal dipole fields from (2.102) or (2.109) and their dual we simply set

$$\begin{aligned} J(\mathbf{r}) &= \hat{\ell}(I\Delta\ell)\delta(\mathbf{r}-\mathbf{r}') = d\mathbf{p}_e\delta(\mathbf{r}-\mathbf{r}') \\ M(\mathbf{r}) &= \hat{\ell}(I_m\Delta\ell)\delta(\mathbf{r}-\mathbf{r}') = d\mathbf{p}_m\delta(\mathbf{r}-\mathbf{r}') \end{aligned} \qquad (2.110)$$

where $d\mathbf{p}_{e,m}$ are referred to as the electric and magnetic dipole moments. From (2.102) we then have

$$\begin{aligned} \mathbf{E}(\mathbf{r}) &= jkZ\overline{\Gamma}(\mathbf{r},\mathbf{r}')\cdot d\mathbf{p}_e + \nabla\times\overline{\Gamma}(\mathbf{r},\mathbf{r}')\cdot d\mathbf{p}_m \\ \mathbf{H}(\mathbf{r}) &= jkY\overline{\Gamma}(\mathbf{r},\mathbf{r}')\cdot d\mathbf{p}_m - \nabla\times\overline{\Gamma}(\mathbf{r},\mathbf{r}')\cdot d\mathbf{p}_e \end{aligned} \qquad (2.111)$$

which can be shown to be identical to the expressions (2.64) and (2.65) upon making use of (2.96) and (2.97).

2.5 Two-Dimensional Fields

Two dimensional fields are generally referred to as those fields which do not exhibit a dependence on one coordinate variable. For example, the problem of propagation in a parallel plate waveguide is two-dimensional in nature and so is that of plane wave scattering by a circular cylinder (see Fig. 2.5). Of course, neither the parallel plate waveguide nor the infinitely long cylinder are physically realizable structures but nevertheless their study can provide important results which are applicable to the three dimensional structures which they approximate. For example, results based on the parallel plate waveguide are useful in the analysis of striplines and the general theory of transmission lines. In the case of scattering, elongated bodies can often be

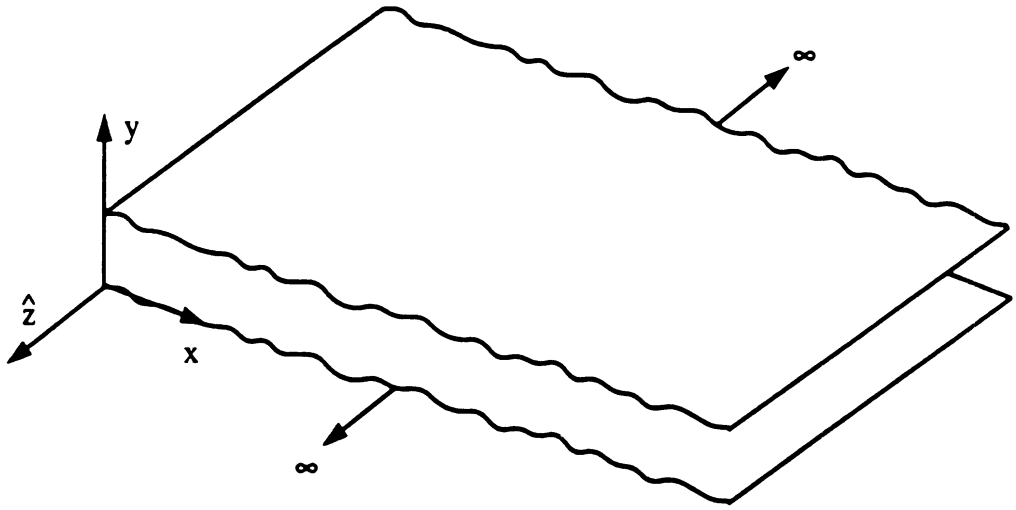

(a)

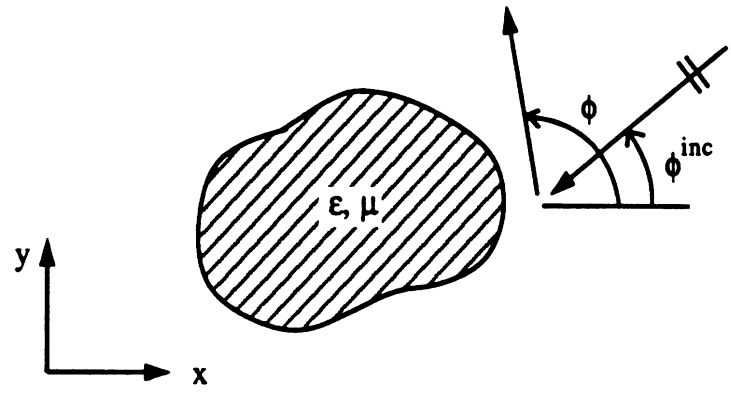

(b)

Figure 2.5: Examples of two-dimensional problems: (a) Propagation in a parallel plate waveguide whose plates are infinite in the z-direction. (b) Scattering by an infinitely long cylinder infinite in the z-direction.

treated as infinite in one dimension to simplify the analysis. Results based on the two-dimensional model can then be applied to the corresponding three dimensional problem through scaling.

2.5.1 Two-dimensional sources

The most elemental two dimensional source is an electric or a magnetic line source. Referring to Fig. 2.6, these are z-directed current filaments carrying a constant current. They may thus be represented by

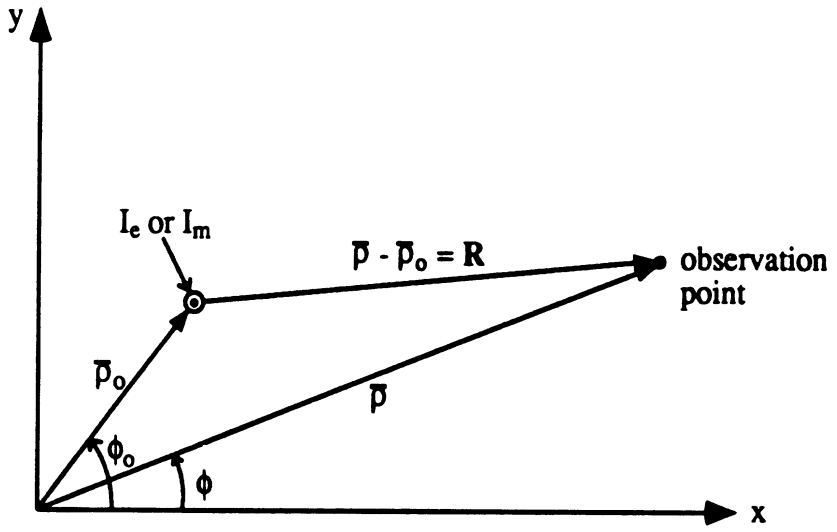

Figure 2.6: Illustration of geometrical parameters associated with a line source.

$$\mathbf{J}(\mathbf{r}) = \hat{z} I_e \delta(\bar{\rho} - \bar{\rho}_o) = \hat{z} I_e \frac{\delta(\rho - \rho_o)\delta(\phi - \phi_o)}{\rho} \qquad (2.112a)$$

$$\mathbf{M}(\mathbf{r}) = \hat{z} I_m \delta(\bar{\rho} - \bar{\rho}_o) = \hat{z} I_m \frac{\delta(\rho - \rho_o)\delta(\rho - \phi_o)}{\rho} \qquad (2.112b)$$

where $\bar{\rho} = x\hat{x} + y\hat{y} = \rho(\hat{x}\cos\phi + \hat{y}\sin\phi) = \rho\hat{\rho}$ denotes the vector to the observation point and $\bar{\rho}_o = x_o\hat{x} + y_o\hat{y} = \rho_o(\hat{x}\cos\phi_o + \hat{y}\sin\phi_o)$ is the vector to the source point. To find the field radiated by these sources we refer to

expression (2.52) or (2.102). Upon setting $dv = \rho\, d\rho\, d\phi\, dz$ and noting that

$$\int_{-\infty}^{\infty} \frac{e^{-jkR}}{R} dz' = \int_{-\infty}^{\infty} \frac{e^{-jk\sqrt{|\overline{\rho}-\overline{\rho}_o|^2+(z')^2}}}{\sqrt{|\overline{\rho}-\overline{\rho}_o|^2+(z')^2}} dz' = -j\pi H_o^{(2)}(k|\overline{\rho}-\overline{\rho}_o|) \quad (2.113)$$

the field due to the electric source is found to be

$$\begin{aligned} \mathbf{E}_e &= -\hat{z}\frac{jkZI_e}{4\pi}\left[-j\pi H_o^{(2)}(k|\overline{\rho}-\overline{\rho}_o|)\right] - \frac{jZI_e}{4\pi k}\hat{z}\cdot\nabla\nabla\left\{-j\pi H_o^{(2)}(k|\overline{\rho}-\overline{\rho}_o|)\right\} \\ &= -\hat{z}I_e\frac{kZ}{4}H_o^{(2)}(k|\overline{\rho}-\overline{\rho}_o|) = -\hat{z}jkZI_eG_{2d}(R) \end{aligned} \quad (2.114)$$

since the dot product in the second term is zero. In this $H_o^{(2)}(\cdot)$ denotes the zero order Hankel function of the second kind. The quantity $R = |\overline{\rho} - \overline{\rho}_o| = \sqrt{\rho^2+\rho_o^2-2\rho\rho_o\cos(\phi-\phi_o)} = \sqrt{(x-x_o)^2+(y-y_o)^2}$ is now the distance between the source and the observer and

$$G_{2d}(R) = G_{2d}(\overline{\rho},\overline{\rho}_o) = -\frac{j}{4}H_o^{(2)}(k|\overline{\rho}-\overline{\rho}_o|) = -\frac{j}{4}H_o^{(2)}(kR) \quad (2.115)$$

is referred to as the two-dimensional Green's function for the unbounded homogeneous media. It satisfies the differential equation

$$\nabla^2 G_{2d}(\overline{\rho},\overline{\rho}') + k^2 G_{2d}(\overline{\rho},\overline{\rho}') = -\delta(\overline{\rho}-\overline{\rho}') \quad (2.116)$$

and the radiation condition

$$\lim_{\rho\to\infty}\sqrt{\rho}\left(jkG_{2d}+\frac{\partial G_{2d}}{\partial\rho}\right) = 0. \quad (2.117)$$

As can be expected (2.115) can be obtained by integrating (2.38) with respect to z and setting $z' = 0$. Also, the validity of the radiation condition (2.117) can be readily established by noting that as $\rho \to \infty$

$$H_o^{(2)}(k|\overline{\rho}-\overline{\rho}'|) \underset{\rho\to\infty}{\longrightarrow} \sqrt{\frac{2j}{\pi}}e^{jk\hat{\rho}\cdot\overline{\rho}'}\frac{e^{-jk\rho}}{\sqrt{\rho}} \quad (2.118)$$

and when this is used in (2.115) it follows that (2.117) is satisfied.

To find the electric field radiated by the magnetic line source, we substitute (2.112b) into (2.52), yielding

$$\mathbf{E}_m = \frac{-j}{4} I_m \hat{z} \times \nabla H_o^{(2)}(k|\overline{\rho} - \overline{\rho}_o|) \tag{2.119}$$

Since (see section 2.3.1)

$$\nabla H_o^{(2)}(k|\overline{\rho} - \overline{\rho}_o|) = \nabla H_o^{(2)}(kR) = k\frac{d}{d(kR)} H_o^{(2)}(kR)\nabla R = -kH_1^{(2)}(kR)\hat{R} \tag{2.120}$$

where $H_1^{(2)}(\cdot)$ is the first order Hankel function of the second kind, (2.119) simplifies to

$$\mathbf{E}_m = I_m \frac{jk}{4} H_1^{(2)}(k_o R)\hat{z} \times \hat{R} \tag{2.121}$$

where $\hat{R} = (\overline{\rho} - \overline{\rho}_o)/|\overline{\rho} - \overline{\rho}_o|$. The corresponding magnetic field due to the magnetic line source is given by

$$\mathbf{H}_m = -\hat{z} I_m \frac{kY}{4} H_o^{(2)}(k|\overline{\rho} - \overline{\rho}_o|) \tag{2.122}$$

which is the dual of (2.114). Also by invoking duality, the magnetic field due to an electric current is given by

$$\begin{aligned} \mathbf{H}_e &= \frac{j}{4} I_e \hat{z} \times \nabla H_o^{(2)}(k|\overline{\rho} - \overline{\rho}_o|) \\ &= -I_e \frac{jk}{4} H_1^{(2)}(kR)\hat{z} \times \hat{R} \end{aligned} \tag{2.123}$$

Upon comparing this to (2.114), it is observed that for two-dimensional z-directed electric sources

$$\mathbf{H}_e = -\frac{jY}{k} \hat{z} \times \nabla(\mathbf{E}_e \cdot \hat{z}) \tag{2.124a}$$

and for z-directed magnetic sources

$$\mathbf{E}_m = \frac{jZ}{k} \hat{z} \times \nabla(\mathbf{H}_m \cdot \hat{z}) \tag{2.124b}$$

Above, we discussed the radiated fields by two-dimensional z-directed line sources. However, it should be noted that in subsequent studies we will encounter two-dimensional sources which may be invariant in z but are not necessarily z-directed. That is,

$$\mathbf{J}(\mathbf{r}) = \hat{a} I_e \delta(\overline{\rho} - \overline{\rho}_o) \tag{2.125}$$

and this represents a current filament as illustrated in Figure 2.7. Such sources,

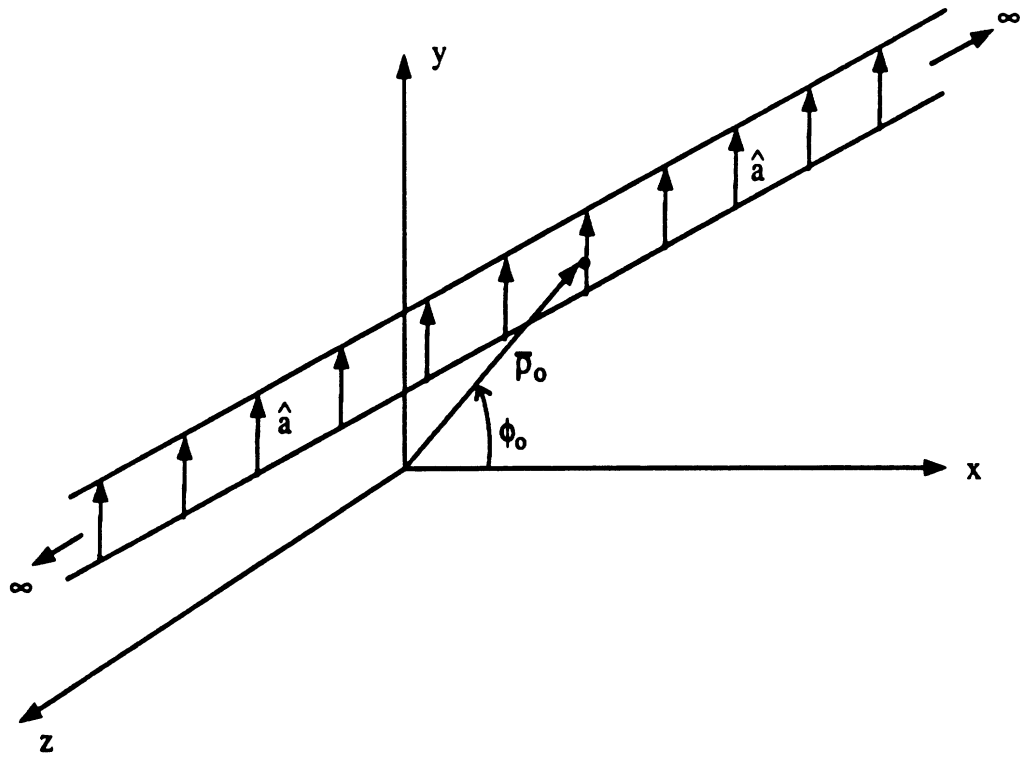

Figure 2.7: Illustration of two dimensional current filament.

although not physical are useful as equivalent sources in formulating a given radiation or scattering problem (as is the case with magnetic sources). Their associated fields can be found by following a procedure similar to that outlined for the z-directed two-dimensional sources. Alternatively, they can be obtained from the more general expressions given in the next section which refer to completely arbitrary two-dimensional source distributions.

2.5.2 Exact Integral Expressions

Let us assume the presence of the general two-dimensional sources $\{\mathbf{J}(\overline{\rho}), \mathbf{M}(\overline{\rho})\}$ occupying the cross sectional areas A as illustrated in Figure 2.8. As discussed in the previous section, to find the field radiated by these

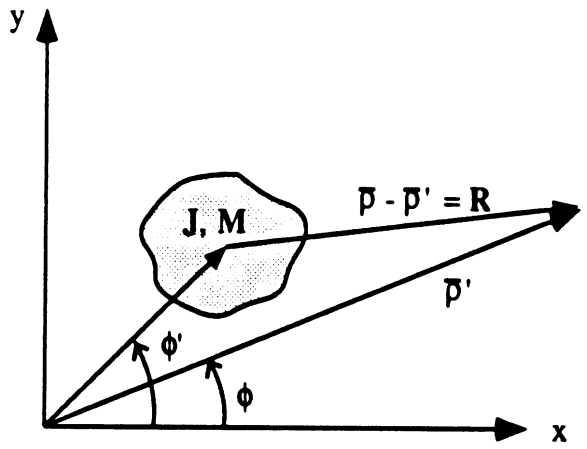

Figure 2.8: Radiation by two-dimensional sources.

sources we refer to the integral expressions (2.52) and set

$$\begin{aligned} \mathbf{J}(\mathbf{r}) &\rightarrow \mathbf{J}(\overline{\rho}) \\ \mathbf{M}(\mathbf{r}) &\rightarrow \mathbf{M}(\overline{\rho}) \end{aligned} \tag{2.126}$$

By making use of the identity (2.113) we then readily find

$$\mathbf{E}(\overline{\rho}) = \int\int_A \Big[\mathbf{M}(\overline{\rho}') \times \nabla G_{2d}(\overline{\rho}, \overline{\rho}') - jkZ\mathbf{J}(\overline{\rho}')G_{2d}(\overline{\rho}, \overline{\rho}') - \frac{jZ}{k}\mathbf{J}(\overline{\rho}') \cdot \nabla\nabla G_{2d}(\overline{\rho}, \overline{\rho}')\Big] ds' \tag{2.127a}$$

$$\mathbf{H}(\overline{\rho}) = \int\int_A \Big[-\mathbf{J}(\overline{\rho}') \times \nabla G_{2d}(\overline{\rho}, \overline{\rho}') - jkY\mathbf{M}(\overline{\rho}')G_{2d}(\overline{\rho}, \overline{\rho}') - \frac{jY}{k}\mathbf{M}(\overline{\rho}') \cdot \nabla\nabla G_{2d}(\overline{\rho}, \overline{\rho}')\Big] ds' \tag{2.127b}$$

where $G_{2d}(\overline{\rho},\overline{\rho}')$ is given by (2.115) upon replacing $\overline{\rho}_o$ by $\overline{\rho}' = \rho'(\hat{x}\cos\phi' + \hat{y}\sin\phi')$.

Clearly, (2.127) are identical to (2.52) other than the replacement of the three-dimensional Green's function with the two-dimensional one. Also, the volume integral has been replaced by a double integral over the domain of the sources in the xy plane. For computational purposes it is necessary to carry out the gradient operations which necessitates that we write out the dyadic $\nabla\nabla G_{2d}$ in its explicit form. This can be readily done by following the procedure employed for the three dimensional case along with the identities (2.120) and

$$\begin{aligned} H_\nu'^{(2)}(kR) &= H_{\nu-1}^{(2)}(kR) - \frac{\nu}{kR}H_\nu(kR) \\ H_\nu'(kR) &= -H_{\nu+1}(kR) + \frac{\nu}{kR}H_\nu(kR) \end{aligned} \tag{2.128}$$

where ν denotes the order of the Hankel function. We obtain

$$\nabla\nabla G^{2d}(\overline{\rho},\overline{\rho}') = \frac{jk}{4}\left\{\left[kH_o^{(2)}(kR) - \frac{2}{R}H_1^{(2)}(kR)\right]\hat{R}\hat{R} + \frac{H_1^{(2)}(kR)}{R}\bar{\mathbf{I}}_{2d}\right\} \tag{2.129}$$

and in this case $\bar{\mathbf{I}}_{2d} = \hat{x}\hat{x} + \hat{y}\hat{y}$, $R = |\overline{\rho} - \overline{\rho}'| = \sqrt{(x-x')^2 + (y-y')^2}$ and $\hat{R} = (\overline{\rho} - \overline{\rho}')/|\overline{\rho} - \overline{\rho}'|$. Substituting (2.129) into (2.127) yields

$$\begin{aligned} \mathbf{E}(\overline{\rho}) = {} & \frac{jk}{4}\int\int_A \mathbf{M}(\overline{\rho}') \times \hat{R}\, H_1^{(2)}(kR)ds' \\ & - \frac{kZ}{4}\int\int_A \mathbf{J}(\overline{\rho}')H_0^{(2)}(kR)ds' + \frac{kZ}{4}\int\int_A \mathbf{J}(\overline{\rho}')\cdot\bar{\mathbf{I}}_{2d}\frac{H_1^{(2)}(kR)}{kR}ds' \\ & + \frac{kZ}{4}\int\int_A \hat{R}\left(\mathbf{J}(\overline{\rho}')\cdot\hat{R}\right)\left[H_o^{(2)}(kR) - \frac{2}{kR}H_1^{(2)}(kR)\right]ds' \end{aligned} \tag{2.130a}$$

$$\begin{aligned} \mathbf{H}(\overline{\rho}) = {} & -\frac{jk}{4}\int\int_A \mathbf{J}(\overline{\rho}') \times \hat{R}\, H_1^{(2)}(kR)ds' \\ & - \frac{kY}{4}\int\int_A \mathbf{M}(\overline{\rho}')H_0^{(2)}(kR)ds' + \frac{kY}{4}\int\int_A \mathbf{M}(\overline{\rho}')\cdot\bar{\mathbf{I}}_{2d}\frac{H_1^{(2)}(kR)}{kR}ds' \end{aligned}$$

$$-\int\int_A \hat{R}(\mathbf{M}(\overline{\rho}')\cdot\hat{R})\left[H_0^{(2)}(kR)-\frac{2}{kR}H_1^{(2)}(kR)\right]ds' \qquad (2.130b)$$

Alternatively, we may expand the del operators in their cartesian form and in doing so we can rewrite (2.127) as

$$\begin{aligned}
E_x &= \frac{-jZ}{k}\int\int_A\left[J_x(\overline{\rho}')\left(k^2+\frac{\partial^2}{\partial x^2}\right)+J_y(\overline{\rho}')\frac{\partial}{\partial x\partial y}\right]G_{2d}(\overline{\rho},\overline{\rho}')ds' \\
&\quad -\int\int_A M_z(\overline{\rho}')\frac{\partial}{\partial y}G_{2d}(\overline{\rho},\overline{\rho}')ds' \\
E_y &= \frac{-jZ}{k}\int\int_A\left[J_x(\overline{\rho}')\frac{\partial^2}{\partial y\partial x}+J_y(\overline{\rho}')\left(k^2+\frac{\partial^2}{\partial y^2}\right)\right]G_{2d}(\overline{\rho},\overline{\rho}')ds' \\
&\quad +\int\int_A M_z(\overline{\rho}')\frac{\partial}{\partial x}G_{2d}(\overline{\rho},\overline{\rho}')ds' \\
E_z &= -jkZ\int\int_A J_z(\overline{\rho}')G_{2d}(\overline{\rho},\overline{\rho}')ds' \\
&\quad -\int\int_A\left[M_y(\overline{\rho}')\frac{\partial}{\partial x}-M_x(\overline{\rho}')\frac{\partial}{\partial y}\right]G_{2d}(\overline{\rho},\overline{\rho}')ds' \\
H_x &= -\frac{jY}{k}\int\int_A\left[M_x(\overline{\rho}')\left(k^2+\frac{\partial^2}{\partial x^2}\right)+M_y\frac{\partial^2}{\partial x\partial y}\right]G_{2d}(\overline{\rho},\overline{\rho}')ds' \\
&\quad +\int\int_A J_z(\overline{\rho}')\frac{\partial}{\partial y}G_{2d}(\overline{\rho},\overline{\rho}')ds' \\
H_y &= -\frac{jY}{k}\int\int_A\left[M_x(\overline{\rho}')\frac{\partial^2}{\partial y\partial x}+M_y(\overline{\rho}')\left(k^2+\frac{\partial^2}{\partial y^2}\right)\right]G_{2d}(\overline{\rho},\overline{\rho}')ds' \\
&\quad -\int\int_A J_z(\overline{\rho}')\frac{\partial}{\partial x}G_{2d}(\overline{\rho},\overline{\rho}')ds' \\
H_z &= -jkY\int\int_A M_z(\overline{\rho}')G_{2d}(\overline{\rho},\overline{\rho}')ds' \\
&\quad +\int\int_A\left[J_y(\overline{\rho}')\frac{\partial}{\partial x}-J_x(\overline{\rho}')\frac{\partial}{\partial y}\right]G_{2d}(\overline{\rho},\overline{\rho}')ds' \qquad (2.131)
\end{aligned}$$

Obviously, (2.130) are more useful for computing the radiation of given sources, but the representations (2.131) are more appropriate in numerical solutions to

be discussed later. We note that (2.131) can be deduced directly from the corresponding three dimensional expressions (2.109) upon setting to zero all derivatives with respect to zero and making use of the identity (2.113).

2.5.3 Far Zone Fields

In the far zone, (2.130) can be simplified by introducing the asymptotic approximation

$$H_\nu^{(2)}(kR) \underset{k\rho \simeq \infty}{\simeq} \sqrt{\frac{2j}{\pi}} j^\nu \frac{e^{-jk|\overline{\rho}-\overline{\rho}'|}}{\sqrt{k|\overline{\rho}-\overline{\rho}'|}} \approx \sqrt{\frac{2j}{\pi\kappa}} j^\nu \frac{e^{-jk\rho}}{\sqrt{\rho}} e^{jk\hat{\rho}\cdot\overline{\rho}'} \tag{2.132}$$

Then, on letting $R \to \rho$, $\hat{R} \to \hat{\rho}$ and keeping only terms of $O(1/\sqrt{\rho})$ we have

$$\mathbf{E}_{ff} \approx +\sqrt{\frac{k}{8\pi}} \frac{e^{-j\left(k\rho-\frac{\pi}{4}\right)}}{\sqrt{\rho}} \int\int_A \left[\hat{\rho} \times \mathbf{M}(\overline{\rho}') + Z\hat{\rho} \times \hat{\rho} \times \mathbf{J}(\overline{\rho}')\right] e^{jk\hat{\rho}\cdot\overline{\rho}'} ds' \tag{2.133a}$$

and

$$\mathbf{H}_{ff} \approx +\sqrt{\frac{k}{8\pi}} \frac{e^{-j\left(k\rho-\frac{\pi}{4}\right)}}{\sqrt{\rho}} \int\int_A \left[\mathbf{J}(\overline{\rho}') \times \hat{\rho} + Y\hat{\rho} \times \hat{\rho} \times \mathbf{M}(\overline{\rho}')\right] e^{jk\hat{\rho}\cdot\overline{\rho}'} ds' \tag{2.133b}$$

and from Fig. 2.9, it is seen that $\hat{\rho}\cdot\overline{\rho}' = x\cos\phi + y\sin\phi = \rho\cos(\phi-\phi')$.

By comparing (2.133a) with (2.133b) and making use of the identity (2.75) it is then readily seen that

$$\mathbf{H}_{ff} = Y\hat{\rho} \times \mathbf{E}_{ff}, \quad \mathbf{E}_{ff} = -Z\hat{\rho} \times \mathbf{H}_{ff} \tag{2.134}$$

which are identical to (2.79) except for the replacement of $\hat{r}$ with $\hat{\rho}$. We can rewrite (2.133) in a more compact form by introducing the two-dimensional vector potential definitions

$$\mathbf{A} = \frac{-j}{4} \int\int_A \mathbf{J}(\overline{\rho}') H_0^{(2)}(k|\overline{\rho}-\overline{\rho}'|) ds' \tag{2.135}$$

$$\mathbf{F} = \frac{-j}{4} \int\int_A \mathbf{M}(\overline{\rho}') H_0^{(2)}(k|\overline{\rho}-\overline{\rho}'|) ds' \tag{2.136}$$

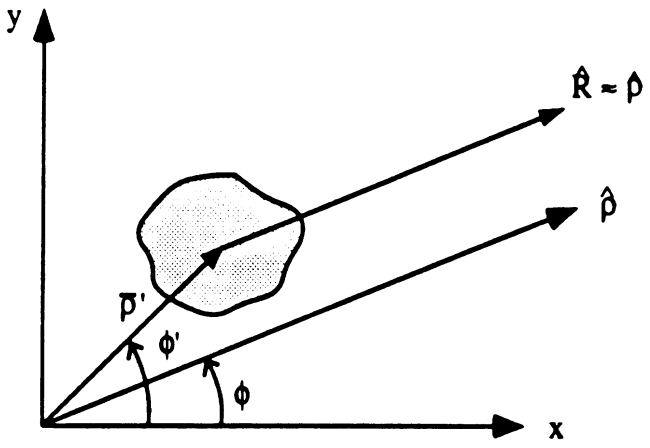

Figure 2.9: Far zone radiation by two-dimensional sources.

On making use of (2.132) we have that in the far zone,

$$\mathbf{A} \approx \frac{-j}{\sqrt{8\pi k}} \frac{e^{-j(k\rho-\pi/4)}}{\sqrt{\rho}} \int\int_A \mathbf{J}(\vec{\rho}') e^{jk\hat{\rho}\cdot\vec{\rho}'} ds' \tag{2.137}$$

$$\mathbf{F} \approx \frac{-j}{\sqrt{8\pi k}} \frac{e^{-j(k\rho-\pi/4)}}{\sqrt{\rho}} \int\int_A \mathbf{M}(\vec{\rho}') e^{jk\hat{\rho}\cdot\vec{\rho}'} ds' \tag{2.138}$$

and thus from (2.132) we obtain

$$\mathbf{E}_{ff} = +jk\hat{\rho} \times \mathbf{F} + jkZ\hat{\rho} \times \hat{\rho} \times \mathbf{A} = -Z\hat{\rho} \times \mathbf{H}_{ff} \tag{2.139a}$$

$$\mathbf{H}_{ff} = -jk\hat{\rho} \times \mathbf{A} + jkY\hat{\rho} \times \hat{\rho} \times \mathbf{F} = Y\hat{\rho} \times \mathbf{E}_{ff} \tag{2.139b}$$

These are identical to those for the three-dimensional case given in (2.80). They imply that the two dimensional far zone fields have only ϕ and z components since the field propagation is along the $\hat{\rho}$ direction. More explicitly, upon carrying out the cross products in (2.139) we find that

$$\mathbf{E}_{ff} = \hat{z}jk(F_\phi - ZA_z) - \hat{\phi}jk(F_z + ZA_\phi) \tag{2.140a}$$

$$\mathbf{H}_{ff} = -\hat{z}jk(A_\phi + YF_z) + \hat{\phi}jk(A_z - YF_\phi) \tag{2.140b}$$

2.5.4 Field evaluation in the source region

When the observation point is in the source region, (i.e. $\rho \rightarrow \rho'$) the integrands in (2.127) and (2.130) contain a non-integrable $\frac{1}{R^2}$ singularity because

$$H_1^{(2)}(kR) \underset{R \simeq 0}{} \frac{j}{\pi} \frac{2}{kR} \tag{2.141}$$

for $kR \rightarrow 0$. To treat this situation we must proceed in a manner analogous to that described in section 2.3.2. That is, we first rewrite (2.127a) as

$$\mathbf{E}_e = -jkZ \int\int_{A-A_o} \left[\mathbf{J}(\overline{\rho}') G_{2d}(\overline{\rho}_o, \overline{\rho}') + \frac{1}{k^2} \mathbf{J}(\overline{\rho}') \cdot \nabla\nabla G_{2d}(\overline{\rho}_o, \overline{\rho}') \right] ds'$$

$$-jkZ \int\int_{A_o} \left[\mathbf{J}(\overline{\rho}') G_{2d}(\overline{\rho}_o, \overline{\rho}') + \frac{1}{k^2} \mathbf{J}(\overline{\rho}') \cdot \nabla\nabla_{2d}(\overline{\rho}_o, \overline{\rho}') \right] ds' \tag{2.142}$$

where we kept only those terms associated with electric currents. Further, A_o is arbitrarily chosen as the cross section of a circular cylinder of radius $a \rightarrow 0$ and is centered at the observation point $\overline{\rho} = \overline{\rho}_o$. Setting $ds' = \rho' d\rho' d\phi'$, and noting that

$$H_o^{(2)}(kR) \underset{R \simeq 0}{} \frac{2}{\pi} \ln(1.123kR) \tag{2.143}$$

it is readily seen that the first term of the integral over A_o vanishes as $A_o \rightarrow 0$. To deal with the second term of the same integral we invoke the identity

$$\int\int_{A_o} \nabla f ds = \oint_{C_o} \hat{n}_o f d\ell \tag{2.144}$$

which is reduced directly from (2.67) and thus $\hat{n}_o$ is the outward unit normal to the contour C_o enclosing A_o (see Fig. 2.10). Thus,

$$\frac{1}{k^2} \int\int_{A_o \rightarrow 0} \mathbf{J}(\overline{\rho}') \cdot \nabla\nabla G_{2d}(\overline{\rho}_o, \overline{\rho}') ds' \approx -\frac{1}{k^2} \mathbf{J}(\overline{\rho}_o) \cdot \nabla \int\int_{A_o \rightarrow 0} \nabla' G_{2d}(\overline{\rho}_o, \overline{\rho}') ds'$$

$$\approx +\frac{1}{k^2} \oint_{C_o} [\hat{R}_o \cdot \mathbf{J}(\overline{\rho}_o)] \nabla G_{2d}(\overline{\rho}_o, \overline{\rho}') d\ell' \tag{2.145}$$

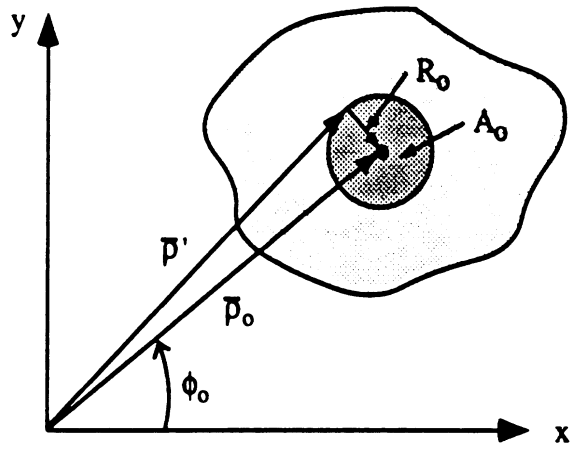

Figure 2.10: Geometry for evaluating the field in the source region.

where $\hat{R}_o = (\overline{\rho}_o - \overline{\rho}')/|\overline{\rho}_o - \overline{\rho}'|$ and $\overline{\rho}'$ is on C_o. For $|\overline{\rho}_o - \overline{\rho}'| = a \to 0$, $\nabla G_{2d} \approx -\left(\frac{-j}{4}\right)\frac{j2}{\pi k a}\nabla(kR_o) = -\frac{\hat{R}_o}{2\pi a}$ and upon setting $d\ell' = a d\phi_o$ we get

$$\frac{1}{k^2}\int\int_{A_o\to 0} \mathbf{J}(\overline{\rho}')\cdot\nabla\nabla G_{2d}(\overline{\rho}_o,\overline{\rho}')ds' = -\frac{1}{2\pi k^2}\int_0^{2\pi}\left(\hat{R}_o\cdot\mathbf{J}(\overline{\rho}_o)\right)\hat{R}_o d\phi_o$$

$$= -\frac{1}{2\pi k^2}\left[\hat{x}J_x(\overline{\rho}_o)\int_0^{2\pi}\cos^2\phi_o d\phi_o + \hat{y}J_y(\overline{\rho}_o)\int_0^{2\pi}\sin^2\phi_o d\phi_o\right]$$

We thus conclude that

$$\frac{1}{k^2}\int\int_{A_o\to 0} \mathbf{J}(\overline{\rho}')\cdot\nabla\nabla G_{2d}(\overline{\rho}_o,\overline{\rho}')ds' = -\frac{\mathbf{J}(\overline{\rho}_o)}{2k^2} \tag{2.146}$$

and consequently, (2.142) can be rewritten as

$$\mathbf{E}_e = -jkZ\overline{\iint}_A\left[\mathbf{J}(\overline{\rho}')G_{2d}(\overline{\rho},\overline{\rho}') + \frac{1}{k^2}\mathbf{J}(\overline{\rho}')\cdot\nabla\nabla G_{2d}(\overline{\rho},\overline{\rho}')\right]ds' + \frac{jZ}{2k}\mathbf{J} \tag{2.147}$$

As usual the horizontal bar through the integral denotes its principal value.

2.6 Spectral Field Representations

One readily observes that the field representations given in this chapter are convolution integrals involving the Green's function and the source current

density. Consequently, by taking the Fourier transform of the integrals in (2.109) or (2.131), it follows that the Fourier transform of the fields is a simple algebraic function. From the convolution theorem, this function is the product of the transforms associated with the Green's function and the current densities. To find explicit expressions for the field transform or spectrum we must first introduce the appropriate Fourier transform pair and evaluate the transform of the Green's function. For simplicity, let us first consider the two-dimensional case.

Two-Dimensions

In two dimensions there is no dependence in z and the Fourier transform pair is thus defined as

$$\tilde{f}(k_x, k_y) = \int_{-\infty}^{\infty}\int_{-\infty}^{\infty} f(x,y)e^{-j(k_x x + k_y y)}dx\,dy \tag{2.148a}$$

$$f(x,y) = \frac{1}{(2\pi)^2}\int_{-\infty}^{\infty}\int_{-\infty}^{\infty} \tilde{f}(k_x, k_y)e^{j(k_x x + k_y y)}dk_x\,dk_y \tag{2.148b}$$

In these, k_x and k_y are the Fourier or spectral variables and in the future we shall use the notation

$$\tilde{f}(k_x, k_y) = \mathcal{F}\{f(x,y)\} \tag{2.149a}$$

$$f(x,y) = \mathcal{F}^{-1}\{f(k_x, k_y)\} \tag{2.149b}$$

to imply the integral expressions (2.148). By differentiating both sides of (2.148b) with respect to x or y, it readily follows that

$$\mathcal{F}\left\{\frac{\partial}{\partial x}f(x,y)\right\} = jk_x\tilde{f}(k_x, k_y) \tag{2.150}$$

$$\mathcal{F}\left\{\frac{\partial}{\partial y}f(x,y)\right\} = jk_y\tilde{f}(k_x, k_y) \tag{2.151}$$

$$\mathcal{F}\left\{\frac{\partial}{\partial x\partial y}f(x,y)\right\} = -k_x k_y\tilde{f}(k_x, k_y) \tag{2.152}$$

$$\mathcal{F}\left\{\frac{\partial^2}{\partial x^2}f(x,y)\right\} = -k_x^2\tilde{f}(k_x, k_y) \tag{2.153}$$

etc. Also, from the convolution theorem we have

$$f(x,y) * g(x,y) = \int_{-\infty}^{\infty}\int_{-\infty}^{\infty} f(x',y')g(x-x',y-y')dx'dy'$$

$$= \tilde{f}(k_x,k_y)\tilde{g}(k_x,k_y) \tag{2.154}$$

in which $\tilde{g}(k_x,k_y) = \mathcal{F}\{g(x,y)\}$. When this identity in conjunction with (2.150) - (2.153) is now applied to the integral expressions (2.131) we obtain

$$\begin{pmatrix} \tilde{E}_x \\ \tilde{E}_y \\ \tilde{E}_z \end{pmatrix} = -\frac{jZ}{k}\tilde{G}_{2d}(k_x,k_y)\begin{pmatrix} k^2-k_x^2 & -k_xk_y & 0 \\ -k_xk_y & k^2-k_y^2 & 0 \\ 0 & 0 & k^2 \end{pmatrix}\begin{pmatrix} \tilde{J}_x \\ \tilde{J}_y \\ \tilde{J}_z \end{pmatrix}$$

$$+\tilde{G}_{2d}(k_x,k_y)\begin{pmatrix} 0 & 0 & +jk_y \\ 0 & 0 & -jk_x \\ -jk_x & -jk_y & 0 \end{pmatrix}\begin{pmatrix} \widetilde{M}_x \\ \widetilde{M}_y \\ \widetilde{M}_z \end{pmatrix} \tag{2.155a}$$

$$\begin{pmatrix} \widetilde{H}_x \\ \widetilde{H}_y \\ \widetilde{H}_z \end{pmatrix} = -\frac{jY}{k}\tilde{G}_{2d}(k_x,k_y)\begin{pmatrix} k^2-k_x^2 & -k_xk_y & 0 \\ -k_xk_y & k^2-k_y^2 & 0 \\ 0 & 0 & k^2 \end{pmatrix}\begin{pmatrix} \widetilde{M}_x \\ \widetilde{M}_y \\ \widetilde{M}_z \end{pmatrix}$$

$$-\tilde{G}_{2d}(k_x,k_y)\begin{pmatrix} 0 & 0 & jk_y \\ 0 & 0 & -jk_x \\ jk_x & -jk_y & 0 \end{pmatrix}\begin{pmatrix} \tilde{J}_x \\ \tilde{J}_y \\ \tilde{J}_z \end{pmatrix} \tag{2.155b}$$

In these, $\tilde{G}_{2d}(k_x,k_y)$ is the Fourier transform of the two dimensional Green's function with $\overline{\rho}' = 0$, i.e.

$$\tilde{G}_{2d}(k_x,k_y) = \mathcal{F}\left\{\frac{-j}{4}H_o^{(2)}\left(k\sqrt{x^2+y^2}\right)\right\} \tag{2.156}$$

and likewise $\tilde{J}_{x,y,z}$ and $\widetilde{M}_{x,y,z}$ denote the Fourier transforms of the electric and magnetic current densities.

One can rewrite (2.155) more compactly by referring to (2.127) and noting that the transform of the gradient function $\nabla f(x,y)$ is

$$\mathcal{F}(\nabla f(x,y)) = \widetilde{\nabla}\tilde{f}(k_x,k_y)j(\hat{x}k_x+\hat{y}k_y)\tilde{f}(k_x,k_y) = j\mathbf{k}_{2d}\tilde{f}(k_x,k_y)$$

where

$$\mathbf{k}_{2d} = \hat{x}k_x + \hat{y}k_y$$

and we may also write that $\widetilde{\nabla} = j\mathbf{k}_{2d}$. Thus, upon application of the convolution theorem we obtain

$$\begin{aligned}\tilde{\mathbf{E}}(k_x,k_y) &= \Big[-jkZ\tilde{\mathbf{J}}(k_x,k_y)+\frac{jZ}{k}\tilde{\mathbf{J}}(k_x,k_y)\cdot\mathbf{k}_{2d}\mathbf{k}_{2d}\\ &\quad +j\widetilde{\mathbf{M}}(k_x,k_y)\times\mathbf{k}_{2d}\Big]\tilde{G}_{2d}(k_x,k_y)\\ \widetilde{\mathbf{H}}(k_x,k_y) &= \Big[-jkY\widetilde{\mathbf{M}}(k_x,k_y)+\frac{jY}{k}\widetilde{\mathbf{M}}(k_x,k_y)\cdot\mathbf{k}_{2d}\mathbf{k}_{2d}\\ &\quad -j\tilde{\mathbf{J}}(k_x,k_y)\times\mathbf{k}_{2d}\Big]\tilde{G}_{2d}(k_x,k_y)\end{aligned} \tag{2.157}$$

where $\tilde{\mathbf{J}} = \hat{x}\tilde{\mathbf{J}}_x+\hat{y}\tilde{\mathbf{J}}_y+\hat{z}\tilde{\mathbf{J}}_z$ and $\widetilde{\mathbf{M}} = \hat{x}\widetilde{\mathbf{M}}_x+\hat{y}\widetilde{\mathbf{M}}_y+\hat{z}\widetilde{\mathbf{M}}_z$. It remains to compute the transform of the Green's function and to do so we recall the differential equation

$$\left(\frac{\partial^2}{\partial x^2}+\frac{\partial^2}{\partial y^2}+k^2\right)G_{2d}(\overline{\rho},0) = -\delta(x)\delta(y) \tag{2.158}$$

obtained from (2.116) by setting $\overline{\rho}' = 0$. Then from (2.156)

$$\begin{aligned}G_{2d}(\overline{\rho},0) &= \frac{-j}{4}H_o^{(2)}\left(k\sqrt{x^2+y^2}\right)\\ &= \frac{1}{(2\pi)^2}\int_{-\infty}^{\infty}\int_{-\infty}^{\infty}\tilde{G}_{2d}(k_x,k_y)e^{j(k_xx+k_yy)}dk_x\,dk_y\end{aligned} \tag{2.159}$$

Also, in accordance with distribution theory [Papoulis, *Fourier Int.*, 1962] we may express the Dirac delta function as

$$\delta(x)\delta(y) = \frac{1}{(2\pi)^2}\int_{-\infty}^{\infty}\int_{-\infty}^{\infty} e^{j(k_x x + k_y y)} dk_x\, dk_y \tag{2.160}$$

Substituting (2.159) and (2.160) into (2.158) and taking the d ·vatives inside the integral, we obtain

$$\frac{1}{(2\pi)^2}\int_{-\infty}^{\infty}\int_{-\infty}^{\infty}(-k_x^2 - k_y^2 + k^2)\tilde{G}_{2d}(k_x, k_y)e^{j(k_x x + k_y y)}dk_x \quad _y$$

$$= -\frac{1}{(2\pi)^2}\int_{-\infty}^{\infty}\int_{-\infty}^{\infty} e^{j(k_x x + k_y y)}dx\, dy$$

from which it follows that

$$\tilde{G}_{2d}(k_x, k_y) = \frac{1}{k_y^2 + k_x^2 - k^2} \tag{2.161}$$

Consequently we may write

$$H_o^{(2)}\left(k\sqrt{k^2 + y^2}\right) = \frac{j}{\pi^2}\int_{-\infty}^{\infty}\int_{-\infty}^{\infty}\frac{1}{k_y^2 + k_x^2 - k^2}e^{j(k_x x + k_y y)}dk_x\, dk_y \tag{2.162}$$

which can be referred to as the plane wave spectral representation of the Hankel function. This is because the Fourier integral can be thought as a sum of inhomogeneous plane waves, i.e. plane waves whose amplitude is a function of the spectral variables k_x and k_y which can be associated with the propagation constants along the x and y directions, respectively.

For the existance of the Fourier transform pair in the classical sence, it is necessary that the function and its transform be integrable. However, as seen from (2.162) the transform of $H_o^{(2)}(k_o\sqrt{x^2 + y^2})$ has poles in the k_y plane located at (see Figure 2.11)

$$k_y = \pm\sqrt{k^2 - k_x^2} \tag{2.163}$$

For real k, these poles are on the $Re(k_y)$ axis and in this case the integral in (2.162) is non-convergent. This difficulty, though, can be avoi by introducing a small loss in the medium. That is, we assume that $k = \quad - jk''$, where $k'' \to 0^+$ and the poles (2.163) are then located off the real axi

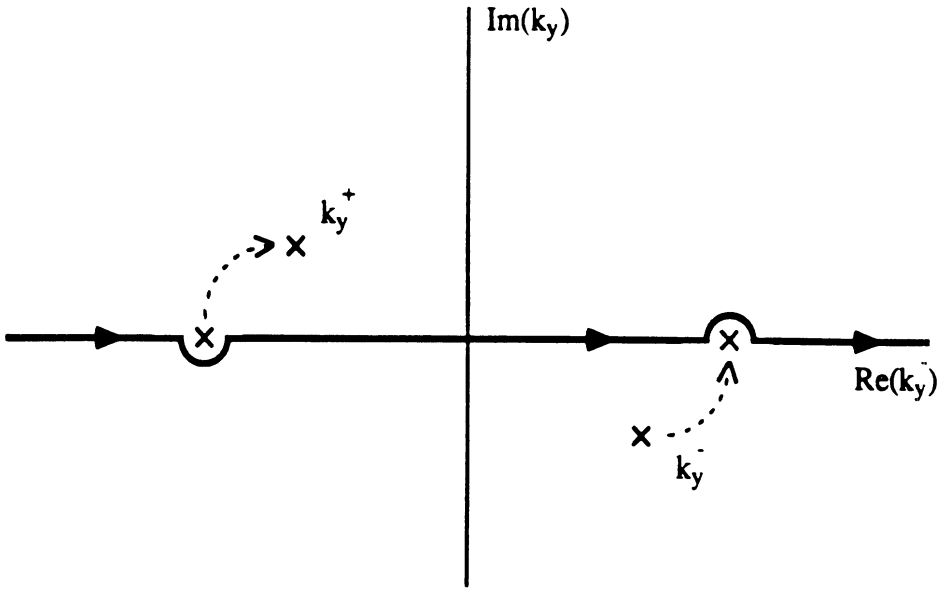

Figure 2.11: Integration path for Fourier transform integral.

By closing the integral over k_y with a semi-infinite contour in the upper half of the k_y plane, Cauchy's theorem gives

$$H_o^{(2)}(k_o\sqrt{x^2+y^2}) = -\frac{1}{\pi}\int_{-\infty}^{\infty}\frac{e^{jk_y^+ y}}{k_y^+}e^{jk_x x}dk_x\,; \quad y>0 \tag{2.164}$$

in which

$$k_y^+ = k_y\,, \quad Im(k_y) > 0\,. \tag{2.165}$$

This is valid only for $y > 0$ to ensure a vanishing semi-infinite contour in the application of Cauchy's theorem. For $y < 0$, the path of integration is closed in the lower half of the k_y plane and this gives

$$H_o^{(2)}\left(k_o\sqrt{x^2+y^2}\right) = \frac{1}{\pi}\int_{-\infty}^{\infty}\frac{e^{jk_y^- y}}{k_y^-}e^{jk_x x}dk_x\,; \quad y<0 \tag{2.166}$$

in which

$$k_y^- = k_y, \quad Im(k_y) < 0. \tag{2.167}$$

and as such $k_y^- = -k_y^+$. Combining (2.164) - (2.167) we may write

$$H_o^{(2)}\left(k\sqrt{x^2+y^2}\right) = \frac{1}{\pi}\int_{-\infty}^{\infty} \frac{e^{-jk_y^-|y|}}{k_y^-} e^{jk_x x} dk_x \tag{2.168}$$

and since $Im(k) < 0$, then $Im(\sqrt{k^2 - k_x^2}) < 0$, implying that $k_y^- = \sqrt{k^2 - k_x^2}$. In the case of a lossless medium and for $k > k_x$, the factor k_y^- becomes real and from figure 2.11, it is now clear how the path of integration is chosen in (2.162) and (2.168). In particular it must be indented around the poles and/or branch points to ensure the convergence of the integrals and avoid the branch cuts of k_y^-.

When $|y| \to 0$, from (2.168) we obtain

$$H_o^{(2)}(k|x|) = \frac{1}{\pi}\int_{-\infty}^{\infty} \frac{e^{jk_x x}}{k_y^-} dk_x \tag{2.169}$$

and in accordance with (2.167)

$$k_y^- = \begin{cases} \sqrt{k^2 - k_x^2} & k > k_x \\ -j\sqrt{k_x^2 - k^2} & k < k_x \end{cases} \tag{2.170}$$

Introducing the one-dimensional Fourier transform pair

$$\tilde{f}(k_x) = \int_{-\infty}^{\infty} f(x) e^{-jk_x x} dx \tag{2.171a}$$

$$f(x) = \frac{1}{2\pi}\int_{-\infty}^{\infty} \tilde{f}(k_x) e^{+jk_x x} dk_x \tag{2.171b}$$

the result in (2.169) simply implies that the transform of $H_o^{(2)}(k|x|)$ is given by

$$\widetilde{H}_o^{(2)}(k_x) = \mathcal{F}\left\{H_o^{(2)}(k|x|)\right\} = \begin{cases} \frac{2}{\sqrt{k^2 - k_x^2}} & k > k_x \\ \frac{2j}{\sqrt{k_x^2 - k^2}} & k < k_x \end{cases} \tag{2.172}$$

We note that the integral relations (2.168) and (2.169) are often the starting point for deriving a variety of integral identities relating to the Hankel and Bessel functions. For example, by taking the real part of (2.169) we obtain

$$J_o(k|x|) = Re\left\{H_o^{(2)}(k|x|)\right\} = \frac{1}{\pi}\int_{-k}^{k} \frac{e^{jk_x x}}{\sqrt{k^2 - k_x^2}} dk_x \tag{2.173}$$

where $J_o(k)$ denotes the zeroth order Bessel function. Introducing now the variable transformation $k_x = k\cos\alpha$, permits us to rewrite (2.173) as

$$\begin{aligned} J_o(k|x|) &= \frac{1}{\pi}\int_{-\pi/2}^{\pi/2} e^{jkx\sin\alpha} d\alpha = \frac{2}{\pi}\int_0^{\pi/2} \cos(kx\sin\alpha) d\alpha \\ &= \frac{1}{2\pi}\int_0^{2\pi} e^{jk_x\cos\alpha} d\alpha = \frac{1}{2\pi}\int_0^{2\pi} e^{jk\rho\cos(\alpha-\phi)} d\alpha \end{aligned} \tag{2.174}$$

which is one of the usual integral expressions for the Bessel function. Other formulas can be derived in a similar manner.

Now that we have evaluated the transform of the two-dimensional Green's function and its implications, we are in a position to examine the behavior of the field spectra given in (2.157). Substituting (2.161) into the first of (2.157) yields

$$\tilde{\mathbf{E}}(k_x, k_y) = -\frac{jZ}{k}\tilde{\mathbf{J}} \cdot \frac{(k^2\bar{\mathbf{I}}_{2d} - \mathbf{k}_{2d}\mathbf{k}_{2d})}{k_x^2 + k_y^2 - k^2} + j\frac{\widetilde{\mathbf{M}}(k_x, k_y) \times \mathbf{k}_{2d}}{k_x^2 + k_y^2 - k^2} \tag{2.175}$$

Taking the limit of this expression as $k_x \to \infty$ with k_y finite or alternatively as $k_y \to \infty$ with k_x finite yields

$$\begin{aligned} \tilde{\mathbf{E}}(k_x \to \infty, k_y) &\to \frac{jZ}{k}\tilde{J}_x \\ \tilde{\mathbf{E}}(k_x, k_y \to \infty) &\to \frac{jZ}{k}\tilde{J}_y \end{aligned} \tag{2.176}$$

These results imply that the transformation of the electric field is bandlimited only if the transform of the current is also bandlimited. Thus, strictly speaking, the inverse Fourier integral is not convergent for impulsive currents which is a consequence of the singular kernel associated with the field integrals given by

(2.127). The evaluation of these integrals in the source region required special treatment as discussed in section 2.5.4 and a similar procedure can be used for the evaluation of the inverse Fourier integral. Specifically, we may express $\mathbf{E}(\overline{\rho})$ as

$$\begin{aligned}\mathbf{E}(\overline{\rho}) \;=\; \mathbf{E}(x,y) &= \frac{-jZ}{(2\pi)^2 k}\int_{-\infty}^{\infty}\int_{-\infty}^{\infty}\tilde{\mathbf{J}}(k_x,k_y)\\ &\cdot\left[\left(\frac{k^2\bar{\mathbf{I}}_{2d}-\mathbf{k}_{2d}\mathbf{k}_{2d}}{k_x^2+k_y^2-k^2}\right)+\bar{\mathbf{I}}_{2d}\right]e^{j(k_x x+k_y y)}dk_x\,dk_y\\ &+\frac{jZ}{(2\pi)^2 k}\int_{-\infty}^{\infty}\int_{-\infty}^{\infty}\left(\tilde{\mathbf{J}}(k_x,k_y)\cdot\bar{\mathbf{I}}_{2d}\right)e^{j(k_x x+k_y y)}dk_x\,dk_y\\ &+\frac{j}{(2\pi)^2}\int_{-\infty}^{\infty}\int_{-\infty}^{\infty}\frac{\widetilde{\mathbf{M}}(k_x,k_y)\times\mathbf{k}_{2d}}{k_x^2+k_y^2-k^2}e^{j(k_x x+k_y y)}dk_x\,dk_y\end{aligned}\tag{2.177}$$

where we have added and substracted the term

$$\begin{aligned}&\frac{jZ}{(2\pi)^2 k}\int_{-\infty}^{\infty}\int_{-\infty}^{\infty}\left(\tilde{\mathbf{J}}(k_x,k_y)\cdot\bar{\mathbf{I}}_{2d}\right)e^{j(k_x x+k_y y)}dk_x\,dk_y\\ &\qquad=\frac{jZ}{(2\pi)^2 k}\int_{-\infty}^{\infty}\int_{-\infty}^{\infty}\tilde{\mathbf{J}}(k_x,k_y)e^{j(k_x x+k_y y)}dk_x\,dk_y\end{aligned}\tag{2.178}$$

so that the first integral of (2.177) is now convergent and the same is true for the third integral. In accordance with the definitions (2.148), the second integral is simply equal to $\frac{jZ}{k}\mathbf{J}$ and thus we can rewrite (2.177) as

$$\begin{aligned}\mathbf{E}(\overline{\rho}) \;=\; &\frac{jZ}{k}\mathbf{J}(\overline{\rho})-\frac{jZ}{(2\pi)^2 k}\int_{-\infty}^{\infty}\int_{-\infty}^{\infty}\tilde{\mathbf{J}}(k_x,k_y)\\ &\cdot\left[\frac{k^2\bar{\mathbf{I}}_{2d}-\mathbf{k}_{2d}\mathbf{k}_{2d}}{k_x^2+k_y^2-k^2}+\bar{\mathbf{I}}_{2d}\right]e^{j(k_x x+k_y y)}dk_x\,dk_y\\ &+\frac{j}{(2\pi)^2}\int_{-\infty}^{\infty}\int_{-\infty}^{\infty}\frac{\widetilde{\mathbf{M}}(k_x,k_y)\times\mathbf{k}_{2d}}{k_x^2+k_y^2-k^2}e^{j(k_x x+k_y y)}dk_x\,dk_y\end{aligned}\tag{2.179}$$

which is compatible and completely equivalent to the representation given by (2.147), provided we set $\mathbf{M}=0$.

Three-Dimensions

The Fourier transform pair in three dimensions is defined by

$$\tilde{f}(k_x,k_y,k_z) = \int_{-\infty}^{\infty}\int_{-\infty}^{\infty}\int_{-\infty}^{\infty} f(x,y,z)e^{-j(k_x+k_y y+k_z z)}dx\,dy\,dz$$

$$f(\overline{\rho}) = f(x,y,z) = \frac{1}{(2\pi)^3}\int_{-\infty}^{\infty}\int_{-\infty}^{\infty}\int_{-\infty}^{\infty} f(k_x,k_y,k_z)e^{j(k_x x+k_y y+k_z z)}dk_x\,dk_y\,dk_z \tag{2.180}$$

with k_x, k_y and k_z being the Fourier or spectral variables. In subsequent references we shall more compactly write this transform pair using the notation

$$\begin{aligned}\tilde{f}(k_x,k_y,k_z) &= \mathcal{F}\{f(x,y,z)\}\\ f(x,y,z) &= \mathcal{F}^{-1}\left\{\tilde{f}(k_x,k_y,k_z)\right\}\end{aligned} \tag{2.181}$$

It follows directly from (2.180) that

$$\begin{aligned}\mathcal{F}\left\{\frac{\partial^2}{\partial\alpha\partial\beta}f(x,y,z)\right\} &= (+jk_\alpha)(+jk_\beta)\tilde{f}(k_x,k_y,k_z)\\ &= -k_\alpha k_\beta\tilde{f}(k_x,k_y,k_z)\end{aligned} \tag{2.182}$$

where α and β represent either of the cartesian coordinates x, y or z. Also, from the convolution theorem we have

$$\begin{aligned}f(x,y,z)*g(x,y,z) &= \int_{-\infty}^{\infty}\int_{-\infty}^{\infty}\int_{-\infty}^{\infty} f(x',y',z')\\ &\quad\cdot g(x-x',y-y',z-z')dx'dy'dz'\\ &= \tilde{f}(k_x,k_y,k_z)\tilde{g}(k_x,k_y,k_z).\end{aligned} \tag{2.183}$$

When the identities (2.181) - (2.183) are applied to the integral representations (2.109) we obtain

$$\tilde{\mathbf{E}}(k_x,k_y,k_z) = \frac{-jZ}{k}\tilde{G}(k_x,k_y,k_z)\begin{pmatrix}(k^2-k_x^2) & -k_xk_y & -k_xk_z\\ -k_xk_y & k^2-k_y^2 & -k_yk_z\\ -k_xk_z & -k_yk_z & k^2-k_z^2\end{pmatrix}\begin{pmatrix}\tilde{J}_x\\ \tilde{J}_y\\ \tilde{J}_z\end{pmatrix}$$

$$-j\tilde{G}(k_x,k_y,k_z)\begin{pmatrix} 0 & -k_z & k_y \\ k_z & 0 & -k_x \\ -k_y & k_x & 0 \end{pmatrix}\begin{pmatrix} \widetilde{M}_x \\ \widetilde{M}_y \\ \widetilde{M}_z \end{pmatrix} \tag{2.184}$$

as the transform of the electric field. In this,

$$\tilde{G}(k_x,k_y,k_z) = \mathcal{F}\left\{\frac{e^{-jk\sqrt{x^2+y^2+z^2}}}{4\pi\sqrt{x^2+y^2+z^2}}\right\} \tag{2.185}$$

denotes the transform of the unbounded space Green's function,

$$\tilde{\mathbf{J}}(k_x,k_y,k_z) = \hat{x}\tilde{J}_x + \hat{y}\tilde{J}_y + \hat{z}\tilde{J}_z \tag{2.186}$$

is the transform of the electric current and likewise

$$\widetilde{\mathbf{M}}(k_x,k_y,k_z) = \hat{x}\widetilde{M}_x + \hat{y}\widetilde{M}_y + \hat{z}\widetilde{M}_z \tag{2.187}$$

is the transform of the magnetic current. By duality the transform of the magnetic field is explicitly given by

$$\begin{aligned}\widetilde{\mathbf{H}}(k_x,k_y,k_z) &= \frac{-jY}{k}\tilde{G}(k_x,k_y,k_z)\begin{pmatrix} k^2-k_x^2 & -k_xk_y & -k_xk_z \\ -k_xk_y & k^2-k_y^2 & -k_yk_z \\ -k_xk_z & -k_yk_z & k^2-k_z^2 \end{pmatrix}\begin{pmatrix} \widetilde{M}_x \\ \widetilde{M}_y \\ \widetilde{M}_z \end{pmatrix} \\ &\quad + j\tilde{G}(k_x,k_y,k_z)\begin{pmatrix} 0 & -k_z & k_y \\ k_z & 0 & -k_x \\ -k_y & k_x & 0 \end{pmatrix}\begin{pmatrix} \tilde{J}_x \\ \tilde{J}_y \\ \tilde{J}_z \end{pmatrix}\end{aligned} \tag{2.188}$$

As was the case in two-dimensions, these matrices may be written more completely by introducing the transform pair

$$\begin{aligned}\mathcal{F}\{\nabla f(x,y,z)\} &= \widetilde{\nabla}\tilde{f}(k_x,k_y,k_z) \\ &= j\mathbf{k}\tilde{f}(k_x,k_y,k_z)\end{aligned} \tag{2.189}$$

in which

$$\mathbf{k} = \hat{x}k_x + \hat{y}k_y + \hat{z}k_z \tag{2.190}$$

From (2.52) we then have

$$\begin{aligned}\tilde{\mathbf{E}}(k_x,k_y,k_z) &= -jkZ\tilde{\mathbf{J}}(k_x,k_y,k_z)\cdot\left(\bar{\mathbf{I}}-\frac{\mathbf{kk}}{k^2}\right)\tilde{G}(k_x,k_y,k_z)\\ &\quad +j\widetilde{\mathbf{M}}(k_x,k_y,k_z)\times\mathbf{k}\tilde{G}(k_x,k_y,k_z)\\ \widetilde{\mathbf{H}}(k_x,k_y,k_z) &= -jkY\widetilde{\mathbf{M}}(k_x,k_y,k_z)\cdot\left(\bar{\mathbf{I}}-\frac{\mathbf{kk}}{k^2}\right)\tilde{G}(k_x,k_y,k_z)\\ &\quad -j\tilde{\mathbf{J}}(k_x,k_y,k_z)\times\mathbf{k}\tilde{G}(k_x,k_y,k_z)\end{aligned} \tag{2.191}$$

Also, from (2.95) we find that the transform of the dyadic Green's function is given by

$$\tilde{\bar{\Gamma}}(k_x,k_y,k_z) = \mathcal{F}\left\{\bar{\Gamma}(\mathbf{r},\mathbf{r}')\right\} = -\left(\bar{\mathbf{I}}-\frac{\mathbf{kk}}{k^2}\right)\tilde{G}(k_x,k_y,k_z) \tag{2.192}$$

Needless to mention, (2.191) are identical to the matrix representations (2.184) and (2.188).

It remains to explicitly determine $\tilde{G}(k_x,k_y,k_z)$ defined in (2.185). However, instead of integrating the unbounded Green's function directly we recall the identity (2.38)

$$(\nabla^2+k^2)G(\mathbf{r},0) = -\delta(\mathbf{r}) \tag{2.193}$$

where $\delta(\mathbf{r}) = \delta(x)\delta(y)\delta(z)$. Taking the Fourier transform of this equation yields

$$(-\mathbf{k}\cdot\mathbf{k}+k^2)\tilde{G}(k_x,k_y,k_z) = -1 \tag{2.194}$$

which gives

$$\tilde{G}(k_x,k_y,k_z) = \frac{1}{k_x^2+k_y^2+k_z^2-k^2} \tag{2.195}$$

and when this result is compared to (2.185) we deduce the identity

$$\frac{e^{-jkr}}{4\pi r}=\frac{e^{-jk\sqrt{x^2+y^2+z^2}}}{4\pi\sqrt{x^2+y^2+z^2}}=\frac{1}{(2\pi)^3}\int_{-\infty}^{\infty}\int_{-\infty}^{\infty}\int_{-\infty}^{\infty}\frac{e^{j(k_x x+k_y y+k_z z)}}{k_x^2+k_y^2+k_z^2-k^2}dk_x\,dk_y\,dz \tag{2.196}$$

As was the case for two-dimensions, the Fourier integral in (2.196) does not exist in the classical sense because of the poles at

$$k_z=\pm\sqrt{k^2-k_x^2-k_y^2} \tag{2.197}$$

This difficulty though can be alleviated by assuming a small loss in the medium which amounts to setting $k=k'-jk''$ with $k''\neq 0$. The poles (2.197) are then shifted away from the real axis. Consequently, by closing the integral over k_z with a semi- infinite contour in the upper half of the k_z plane we capture one of the poles. Upon invoking Cauchy's theorem we then obtain

$$\frac{e^{-jkr}}{4\pi r}=\frac{j}{2(2\pi)^2}\int_{-\infty}^{\infty}\int_{-\infty}^{\infty}\frac{e^{jk_z^+ z}}{k_z^+}e^{j(k_x x+k_y y)}dk_x\,dk_y;\quad z>0 \tag{2.198}$$

in which

$$k_z^+=k_z,\quad Im(k_z)>0 \tag{2.199}$$

this is valid only for $z>0$ to ensure a vanishing semi-infinite contour in the application of Cauchy's theorem. For $z<0$, the path of integration is closed by semi-infinite contour in the lower half of the k_z plane giving

$$\frac{e^{-jkr}}{4\pi r}=\frac{-j}{2(2\pi)^2}\int_{-\infty}^{\infty}\int_{-\infty}^{\infty}\frac{e^{jk_z^- z}}{k_z^-}e^{j(k_x x+k_y y)}dk_x\,dk_y;\quad z<0 \tag{2.200}$$

in which

$$k_z^-=k_z,\quad Im(k_z)<0 \tag{2.201}$$

and as such $k_z^-=-k_z^+$. Combining (2.198) - (2.201) we deduce the well known Weyl identity

$$\frac{e^{-jkr}}{4\pi r}=\frac{-j}{8\pi^2}\int_{-\infty}^{\infty}\int_{-\infty}^{\infty}\frac{e^{-jk_z^-|z|}}{k_z^-}e^{j(k_x x+k_y y)}dk_x\,dk_y \tag{2.202}$$

In the case of a lossless medium and for $k^2 > k_x^2 + k_y^2$, the factor k_z^- is real and the path of integration must then be identical to that shown in fig. 2.12, thus avoiding the branch cuts and ensuring the convergence of the integrals.

We remark that Weyl's identity is the starting point for deriving a variety of other identities involving Bessel and Hankel functions whose arguments are functions of both x and y or the standard cylindrical variables (ρ, ϕ). For example, by setting

$$\mathbf{k}_{2d} = \hat{x}k_x + \hat{y}k_y = k_\rho(\hat{x}\cos\alpha + \hat{y}\sin\alpha) \tag{2.203}$$

with $k_\rho = \sqrt{k_x^2 + k_y^2}$, it can be shown from (2.202) that

$$\frac{e^{-jkr}}{4\pi r} = \frac{-j}{8\pi^2}\int_0^\infty \int_0^{2\pi} \frac{k_\rho e^{-j[k_\rho\cos(\alpha-\phi)+k_z^-|z|]}}{k_z^-} d\alpha\, dk_\rho \tag{2.204}$$

Further, by invoking the identity (2.174) it follows that

$$\frac{e^{-jkr}}{4\pi r} = \frac{-j}{4\pi}\int_0^\infty \frac{k_\rho}{k_z^-} J_o(k_\rho\rho)e^{-jk_z^-|z|}dk_\rho \tag{2.205}$$

and in accordance with (2.201),

$$k_z^- = \begin{cases} \sqrt{k^2 - k_\rho^2} = \sqrt{k^2 - k_x^2 - k_y^2} & k^2 > k_\rho^2 \\ -j\sqrt{k^2 - k_\rho^2} = -j\sqrt{k^2 - k_x^2 - k_y^2} & k^2 < k_\rho^2 \end{cases} \tag{2.206}$$

Expression (2.205) is known as Sommerfeld's identity and several variations of this can be derived by employing various relations among the Bessel and Hankel functions. For example, we may introduce in (2.205) the relation

$$J_o(k_\rho\rho) = \frac{H_o^{(1)}(k_\rho\rho) + H_o^{(2)}(k_\rho\rho)}{2} \tag{2.207}$$

where $H_o^{(1)}$ is the zeroth order Hankel function of the first kind, and since

$$H_o^{(1)}(-k_\rho\rho) = H_o^{(1)}(e^{j\pi}k_\rho\rho) = -H_o^{(2)}(k_\rho\rho) \tag{2.208}$$

it follows that

$$\frac{e^{-jkr}}{4\pi r} = \frac{-j}{8\pi}\int_{-\infty}^\infty \frac{k_\rho}{k_z^-} H_o^{(2)}(k_\rho\rho)e^{-jk_z^-|z|}dk_\rho \tag{2.209}$$

From the wave equation or through a change of variables in (2.210) it can also be shown that

$$\frac{e^{-jkr}}{4\pi r} = \frac{-j}{8\pi}\int_{-\infty}^{\infty} H_0^{(2)}(\sqrt{k^2-k_z^2}\rho)e^{\pm jk_z z}dk_z \tag{2.210}$$

In closing this section we also note that when $|z| \to 0$, from (2.202) we deduce the identity

$$\frac{e^{-jk\sqrt{x^2+y^2}}}{4\pi\sqrt{x^2+y^2}} = \frac{-j}{8\pi^2}\int_{-\infty}^{\infty}\int_{-\infty}^{\infty}\frac{e^{+j(k_x x+k_y y)}}{k_z^-}dk_x\,dk_y \tag{2.211}$$

and upon recalling the definitions for the two-dimensional transform pair, it is seen that this identity implies that

$$\mathcal{F}\left\{\frac{e^{-jk\sqrt{x^2+y^2}}}{4\pi\sqrt{x^2+y^2}}\right\} = \begin{cases} \frac{1}{2j\sqrt{k^2-k_x^2-k_y^2}} & k^2 > k_x^2+k_y^2 \\ \frac{1}{2\sqrt{k_x^2+k_y^2-k^2}} & k^2 < k_x^2+k_y^2 \end{cases} \tag{2.212}$$

This transform will be found useful in the study and modeling of thin planar layers of material and flat metallic plates.

2.7 Radiation over a Dielectric Half Space

A particular utility of (2.202) is in solving boundary value problems associated with boundary conditions that are invarient with respect to x and y. As an example, let us consider the radiation of an electric source $\mathbf{J} = \hat{x}J_x(x,y)$ located at a dielectric interface as shown in fig. 2.12. Transforming the fields with respect to x and y only as given in (2.148), from (2.202) we can readily write down the transform of the field generated by $\hat{x}J_x(x,y)$. For example, in the case of the x-component we have

$$\tilde{E}_x^g(k_x,k_y,z) = \frac{-jZ_1}{k_1}\tilde{J}_x(k_x,k_y)\left(k_1^2-k_x^2\right)\left(\frac{-j}{2}\right)\frac{e^{\mp jk_{1z}^- z}}{k_{1z}^-} \tag{2.213}$$

in which $k_1 = \omega\sqrt{\mu_1\epsilon_1}$ is the wave number in region 1 and $Z_1 = \sqrt{\mu_1/\epsilon_1}$ is the intrinsic impedance in the same region. Clearly, this represents a plane

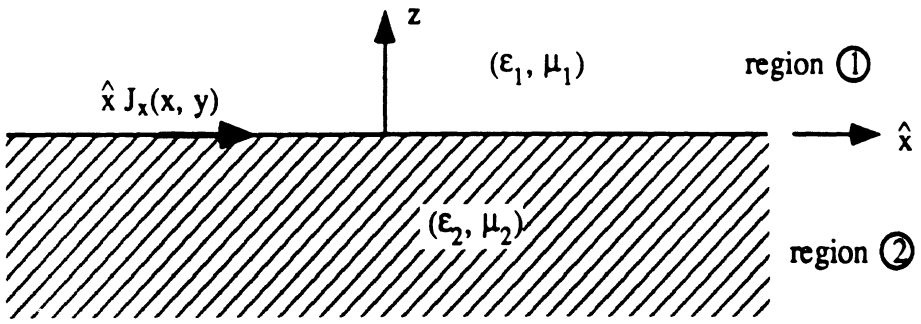

Figure 2.12: Geometry of a source on a dielectric interface.

wave traveling along the z-direction with a propagation constant of $k_{1z}^- = \sqrt{k_1^2 - k_\rho^2}$. To consider the reflection of this wave from the dielectric interface, it is instructive to decompose it into transverse-electric (TE) and transverse-magnetic (TM) components. For the TE field, $E_z = 0$ and for the TM field $H_z = 0$, and thus such a decomposition can be accomplished once the fields are expressed in terms of their E_z and H_z components. Since $\frac{\partial}{\partial z} \to \pm jk_{1z}^-$, from Maxwell's equations it is not difficult to show that[1]

$$\tilde{\mathbf{E}}_t(k_x, k_y, z) = \frac{1}{k_1^2 - (k_{1z}^-)^2}\left[\widetilde{\nabla}_t\left(\frac{\partial \tilde{E}_z}{\partial z}\right) + jk_1 Z_1 \hat{z} \times \nabla_t \widetilde{H}_z\right] \tag{2.214}$$

where $\tilde{\mathbf{E}}_t = \tilde{\mathbf{E}} - \hat{z}\tilde{E}_z$ and $\nabla_t = \nabla - \hat{z}\frac{\partial}{\partial z}$. From (2.184) and (2.202) the transforms of the z components generated by the source alone are found to be

$$\tilde{E}_z^g(k_x, k_y, z) = \mp\frac{jZ_1}{k_1}\tilde{J}_x(k_x, k_y)k_x k_{1z}^-\left(\frac{-j}{2}\right)\frac{e^{\mp jk_{1z}^- z}}{k_{1z}^-} \tag{2.215}$$

$$\widetilde{H}_z^g(k_x, k_y, z) = -j\tilde{J}_x(k_x, k_y)k_y\left(\frac{-j}{2}\right)\frac{e^{-jk_{1z}^-|z|}}{k_{1z}^-} \tag{2.216}$$

Each of these wave components in (2.215) and (2.216) independently gives rise to a reflected field which is simply given by

$$E_z^r(k_x, k_y, z > 0) = -R^{TM}\tilde{E}_z^g(k_x, k_y, z = 0)e^{-jk_{1z}^- z} \tag{2.217}$$

[1]Separate in Maxwell's equation the z and transverse components. Then by crossing one of them with $\hat{z}$, eliminate from the other the transverse electric/magnetic field.

$$H_z^r(k_x, k_y, z > 0) = R^{TE}\widetilde{H}_z^g(k_x, k_y, z = 0)e^{-jk_{1z}^- z} \tag{2.218}$$

where

$$R^{TM} = -\frac{\epsilon_1 k_{2z}^- - \epsilon_2 k_{1z}^-}{\epsilon_1 k_{2z}^- + \epsilon_2 k_{1z}^-} \tag{2.219}$$

$$R^{TE} = \frac{\mu_2 k_{1z}^- - \mu_1 k_{2z}^-}{\mu_2 k_{1z}^- + \mu_1 k_{2z}^-} \tag{2.220}$$

are the TM and TE plane wave reflection coefficients, respectively, in which $k_{2z}^- = \sqrt{(k_2)^2 - k_\rho^2}$ with $k_2 = \omega\sqrt{\mu_2\epsilon_2}$. The z components of the total TE and TM fields above the interface can now be expressed as

$$\tilde{E}_z(k_x, k_y, z > 0) = \tilde{E}_z^g + \tilde{E}_z^r = -\frac{jZ_1}{k_1}\tilde{J}_x(k_x, k_y)k_x k_{1z}^-(1 - R^{TM})\left(\frac{-j}{2}\right)\frac{e^{-jk_{1z}^- z}}{k_{1z}^-} \tag{2.221}$$

$$\widetilde{H}_z(k_x, k_y, z > 0) = \widetilde{H}_z^g + \widetilde{H}_z^r = -j\tilde{J}_x(k_x, k_y)k_y(1 + R^{TE})\left(\frac{-j}{2}\right)\frac{e^{-jk_{1z}^- z}}{k_{1z}^-} \tag{2.222}$$

To obtain the fields in terms of the spatial variables x, y, and z, (2.221) and (2.222) must first be substituted in (2.213) and the result be then inverse transformed via (2.148b). This results in an integral of the form

$$I(\Omega) = \int_{-\infty}^{\infty}\int_{-\infty}^{\infty} f(x, y)e^{j\Omega g(x,y)}dxdy \tag{2.223}$$

(where $g(x, y)$ is real) whose evaluation must take account of any possible integrand poles and branch cuts when the observation point is near or on the surface of the dielectric interface [Collin: Field Theory of Guided Waves, 1991; Felsen and Marcuvitz, 1973]. The residues of the integrand poles provide the contribution of surface/guided and leaky wave modes which will be present in the case of a layered reflecting medium (i.e. a grounded slab) or simply any reflecting surface which can support guided waves below the dielectric interface. For the particular problem illustrated in fig. 2.13, the reflecting surface is a homogeneous half space and cannot support any surface waves

other than those below the Brewster angle which can be considered as part of the reflected field. The last along with direct source contribution are the only fields which are present in the far zone and can be explicitly determined as $r \rightarrow \infty$ by considering an asymptotic evaluation of the integral (2.223). This type of evaluation relies on the principle that since $\Omega g(x,y) = rg(x,y)$, the exponential part of the integrand is rapidly oscillating and thus any contribution must come from the portion of integration near the region where

$$\frac{\partial g(x,y)}{\partial x} = 0, \quad \frac{\partial g(x,y)}{\partial y} = 0 \tag{2.224}$$

These relations define one or more points (x_s, y_s) referred to as the stationary points. Based on the analysis given in the Appendix it follows that for large Ω

$$I(\Omega) \sim f(x_s,y_s)\left(\frac{2\pi}{\Omega}\right) e^{j\Omega g(x_s,y_s)} \frac{e^{j(\pi/4)\sigma}}{\left|det\left(\frac{\partial^2 g}{\partial x \partial y}\right)\right|^{1/2}_{x=x_s,y=y_s}} \tag{2.225}$$

where

$$\sigma = sgnd_1 + sgnd_2$$

in which (d_1, d_2) are the eigenvalues of the matrix comprising the elements of $\frac{\partial^2 g}{\partial x \partial y}$ evaluated at $x = x_s, y = y_s$. Also, the function $sgn(x) = sign(x) = \pm 1$.

From (2.214) and (2.148b), the pertinent inverse Fourier integral to be evaluated for the TM field is

$$\mathbf{E}^{TM}(x,y,z) = -\frac{Z_1}{2k_1}\left(\frac{1}{2\pi}\right)^2 \int_{-\infty}^{\infty}\int_{-\infty}^{\infty} \frac{(\hat{x}k_x k_{1z}^- + \hat{y}k_y k_{1z}^- + \hat{z})k_x}{k_1^2 - (k_{1z}^-)^2}$$

$$\cdot(1 - R^{TM})\tilde{J}_x(k_x,k_y)e^{-jk_{1z}^- z}e^{j(k_x x + k_y y)}dk_x dk_y \tag{2.226}$$

Upon setting $x = r\sin\theta\sin\phi$, $y = r\sin\theta\sin\phi$ and $z = r\cos\theta$, $g(k_x,k_y)$ is identified to be

$$g(k_x,k_y) = k_x\sin\theta\cos\phi + k_y\sin\theta\sin\phi - \cos\theta\sqrt{k_1^2 - k_x^2 - k_y^2} \tag{2.227}$$

from which we find that the stationary point is located at

$$k_x = k_{xs} = -k_1\sin\theta\cos\phi \quad k_y = k_{ys} = -k_1\sin\theta\sin\phi \tag{2.228}$$

and consequently $\sigma = 2$ and

$$\left| det \left(\frac{\partial^2 q}{\partial k_x \partial ky} \right) \right|^{1/2}_{k_x = k_{xs}, k_y = y_{ys}} = \frac{1}{k_1 \cos\theta} \tag{2.229}$$

From the asymptotic formula (2.224), it then follows that the TM far zone field is given by

$$E_\theta(r,\phi,\theta) = \hat{\theta} \cdot \mathbf{E}^{TM}(x,y,z) \sim -\frac{jk_o Z_o}{4\pi} \frac{e^{-jkr}}{r} \cos\theta \cos\phi (1 - R^{TM}) J_x(k_{xs}, k_{ys}) \tag{2.230}$$

where we have set $k_1 = k_o = 2\pi/\lambda_o$ (i.e. $\epsilon_1 = \epsilon_o, \mu_1 = \mu_o$) and $Z_1 = Z_o = \sqrt{\mu_o/\epsilon_o}$. Also upon setting $\epsilon_r = \epsilon_2/\epsilon_o$ and $\mu_r = \mu_2/\mu_o$, R_{TM} can be reduced to

$$R^{TM} = \frac{\sqrt{\epsilon_r \mu_r - \sin^2\theta} - \epsilon_r \cos\theta}{\sqrt{\epsilon_r \mu_r - \sin^2\theta} + \epsilon_r \cos\theta} \tag{2.231}$$

which is the plane wave reflection coefficient associated with the planar dielectric interface. Clearly, this result is the sum of the far zone field generated directly from the source and that reflected from the interface.

By following a similar analysis we find that in general the far zone fields due to the current distribution $\mathbf{J}(x,y,z) = [\hat{x} J_x(x,y) + \hat{y} J_y(x,y)]\,\delta(z)$ located on a dielectric interface can be expressed as

$$E_\theta(r,\phi,\theta) = -\frac{jk_o Z_o}{4\pi} \frac{e^{-jk_o r}}{r} (1 - R^{TM}) \Big[\cos\theta \cos\phi \tilde{J}_x(k_{xs}, k_{ys}) + \cos\theta \sin\phi \tilde{J}_y(k_{xs}, k_{ys}) \Big] \tag{2.232}$$

and

$$E_\phi(r,\phi,\theta) = -\frac{jk_o Z_o}{4\pi} \frac{e^{-jk_o r}}{r} (1 + R^{TE}) \Big[-\sin\phi \tilde{J}_x(k_{xs}, k_{ys}) + \cos\phi \tilde{J}_y(k_{xs}, k_{ys}) \Big] \tag{2.233}$$

The first of these is the TM (to z) field and the second represents the TE (to z) component. The expressions for k_{xs} and k_{ys} are again given by (2.228) whereas R^{TM} is as given by (2.231) and

$$R^{TE} = \frac{\mu_r \cos\theta - \sqrt{\mu_r \epsilon_r - \sin^2\theta}}{\mu_r \cos\theta + \sqrt{\mu_r \epsilon_r - \sin^2\theta}} \tag{2.234}$$

is the TE plane wave reflection coefficient.

The above elementary exercise demonstrates rather well the usefulness of the spectral representations presented in this chapter. Of importance is that the outlined method can be easily generalized to other source distributions and layered dielectric planar interfaces. Further, for near zone observations, the spectral integrand characteristics yield the physical wave mechanisms which take place near and below the dielectric interface. However, a more elementary and customary approach for this analysis is to consider the radiation of an infinitesimal dipole source above the dielectric interface, and in this case we may write the result in terms of a single integral by invoking one of Sommerfeld's identities. This problem was first solved by Sommerfeld and is briefly discussed below.

Consider again the problem illustrated in figure 2.12 with the source now being replaced by the horizontal infinitesimal dipole

$$\mathbf{J}(x,y) = \hat{x} I \Delta\ell \, \delta(x) \, \delta(y) \tag{2.235}$$

and as such $\tilde{\mathbf{J}}(k_x, k_y) = \hat{x} I \Delta\ell$. Substituting this into (2.221) - (2.222) and inverse transforming yields

$$E_z(x,y,z>0) = -\frac{Z_1}{2k_1}\left(\frac{1}{2\pi}\right)^2 (I\Delta\ell)\int_{-\infty}^{\infty}\int_{-\infty}^{\infty} \frac{\partial}{\partial x \partial z}(1-R^{TM})\frac{e^{-jk_{1z}^- z}}{k_{1z}^-} dk_x dk_y \tag{2.236}$$

$$H_z(x,y,z>0) = -\frac{j}{2}\left(\frac{1}{2\pi}\right)^2 (I\Delta\ell)\int_{-\infty}^{\infty}\int_{-\infty}^{\infty} \frac{\partial}{\partial y}(1+R^{TE})\frac{e^{-jk_{1z}^- z}}{k_{1z}^-} dk_x dk_y \tag{2.237}$$

where we have also made the replacements $jk_x \to \frac{\partial}{\partial x}$, $jk_y \to \frac{\partial}{\partial y}$ and $-jk_{1z}^- = \frac{\partial}{\partial z}$. Since R^{TM} and R^{TE} are functions of $k_\rho^2 = k_x^2 + k_y^2$, the above double

integrals can be reduced to a single integral by invoking Sommerfeld's identity (2.209). In particular, for $z > 0$ we have

$$E_z(\rho,\phi,z) = -\frac{Z_1}{k_1}\frac{(I\Delta\ell)}{8\pi}\frac{\partial}{\partial x\partial z}\int_{-\infty}^{\infty}\frac{k_\rho}{k_{1z}^-}(1-R^{TM})H_o^{(2)}(k_\rho\rho)e^{-jk_{1z}^-z}dk_\rho \quad (2.238)$$

$$H_z(\rho,\phi,z) = -j\frac{(I\Delta\ell)}{8\pi}\frac{\partial}{\partial y}\int_{-\infty}^{\infty}\frac{k_\rho}{k_{1z}^-}(1+R^{TE})H_o^{(2)}(k_\rho\rho)e^{-jk_{1z}^-z}dk_\rho \quad (2.239)$$

and upon carrying out the derivatives we obtain

$$E_z(\rho,\phi,z) = -\frac{jZ_1}{k_1}\frac{(I\Delta\ell)}{8\pi}(\hat\rho\cdot\hat x)\int_{-\infty}^{\infty}k_\rho^2(1-R^{TM})H_1^{(2)}(k_\rho\rho)e^{-jk_{1z}^-z}dk_\rho \quad (2.240)$$

$$H_z(\rho,\phi,z) = j\frac{(I\Delta\ell)}{8\pi}(\hat\rho\cdot\hat y)\int_{-\infty}^{\infty}\frac{k_\rho^2}{k_{1z}^-}(1+R^{TE})H_1^{(2)}(k_\rho\rho)e^{-jk_{1z}^-z}dk_\rho \quad (2.241)$$

Upon introducing the large argument approximation for the Hankel function (see (2.132))

$$H_1^{(2)}(k_\rho\rho)\sim j\sqrt{\frac{2}{\pi k}}e^{j\frac{\pi}{4}}\frac{e^{-jk\rho}}{\sqrt{\rho}} \quad (2.242)$$

these integrals can be evaluated via the stationary phase method when the observation point is in the far zone. When the result is substituted into (2.214) we again obtain the far zone field expressions (2.232) and (2.233) with $\tilde J_x(k_{xs},k_{ys}) = (I\Delta\ell)$ and $\tilde J_y(k_{xs},k_{ys}) = 0$.

An alternative and more rigorous approach for evaluating the integrals is the steepest descent method. In this case the integration path illustrated in fig. 2.11 is deformed to one on which the rapidly varying exponential portion of the integrand has constant phase and is decaying. To illustrate this idea let us consider the integral (Ω is large)

$$I_c(\Omega) = \int_C F(\zeta)e^{\Omega g(\zeta)}d\zeta\,; \quad \zeta = \zeta_r + j\zeta_i \quad (2.243)$$

where the path C is illustrated in fig. 2.11 and $g(\zeta) = u(\zeta_r,\zeta_i) + jv(\zeta_r,\zeta_i)$. We now define the saddle point to be such that

$$\frac{dg(\zeta)}{d\zeta}\Big|_{\zeta=\zeta_s} = 0 \quad (2.244)$$

where $\zeta_s = \zeta_{rs} + j\zeta_{is}$, and an integration path C_{SDP} on which

$$\begin{aligned} u(\xi_r, \xi_i) &\leq u(\xi_{rs}, \xi_{is}) \\ v(\xi_r, \xi_i) &= v(\xi_{rs}, \xi_{is}) \end{aligned} \tag{2.245}$$

Then upon rewriting $I_c(\Omega)$ as

$$I_c(\Omega) = e^{\Omega g(\zeta_s)} \int_C F(\zeta) e^{\Omega[g(\zeta) - g(\zeta_s)]} d\zeta \tag{2.246}$$

It is clear from the definitions in (2.244) to (2.245) that the exponent $[g(\zeta) - g(\zeta_s)]$ is real and negative along the path C_{SDP} which is consequently referred to as the steepest descent path. It is thus instructive to rewrite $I_c(\Omega)$ as

$$I_c(\Omega) = 2\pi j \sum Res + I_b(\Omega) + I_{SDP}(\Omega) \tag{2.247}$$

where

$$I_{SDP}(\Omega) = e^{\Omega g(\zeta_s)} \int_{C_{SDP}} F(\zeta) e^{\Omega[g(\zeta) - g(\zeta_s)]} d\zeta, \tag{2.248}$$

$I_b(\Omega)$ provides the contribution of any branch points/cuts crossed in the deformation of the contour C to C_{SDP} and $2\pi j \sum Res$ is the residue contribution of the crossed poles. From the appendix

$$I_{SDP}(\Omega) \sim e^{\Omega g(\zeta_s)} \sqrt{\frac{-2\pi}{\Omega g''(\zeta_s)}} F(\zeta_s) + O(\Omega) \tag{2.249}$$

and when this formula is employed in conjunction with the pertinent integrals (2.140) and (2.241) we recover the same results obtained via the stationary phase method.

2 PL/P7

Problems

1. Given that

$$R = |\mathbf{r} - \mathbf{r}'| = \sqrt{(x-x')^2 + (y-y')^2 + (z-z')^2}$$

and

$$G(R) = \frac{e^{-jk|\mathbf{r}-\mathbf{r}'|}}{4\pi|\mathbf{r}-\mathbf{r}'|} = f(\mathbf{r}-\mathbf{r}')$$

Show that
(a)

$$\nabla R = \hat{R}$$

$$\nabla \cdot \hat{R} = \frac{2}{R}$$

$$\nabla \hat{R} = \nabla\left(\frac{\mathbf{r}-\mathbf{r}'}{R}\right) = \frac{\bar{\mathbf{I}}}{R} - \frac{\mathbf{R}\hat{R}}{R^2}$$

note: $\nabla \mathbf{A} = \hat{x}\nabla A_x + \hat{y}\nabla A_y + \hat{z}\nabla A_z$ and $\bar{\mathbf{I}} = \hat{x}\hat{x} + \hat{y}\hat{y} + \hat{z}\hat{z}$

(b) Write out the dyadic operator $\nabla\nabla$ in matrix form and show that

$$\nabla\nabla f(\mathbf{r}-\mathbf{r}') = \nabla\nabla \cdot f(\mathbf{r}-\mathbf{r}')\bar{\mathbf{I}} = -\nabla'\nabla \cdot f(\mathbf{r}-\mathbf{r}')$$

(c) Show that

$$\nabla \cdot (\psi\bar{\mathbf{I}}) = \nabla\psi$$

$$\nabla \cdot (\bar{\mathbf{I}} \times \mathbf{A}) = \nabla \times \mathbf{A}$$

$$\bar{\mathbf{I}} \times \mathbf{A} = -\mathbf{A} \times \bar{\mathbf{I}}$$

2. (a) Beginning with (2.82) show that if $\mathbf{E} = \hat{z}u$, the wave equation in the source free region reduces to

$$\nabla \cdot \left[\frac{1}{\mu_r}\nabla u\right] + k_o^2 \epsilon_r u = 0$$

provided u is independent of z.
(b) Multiply this by the weighting functions $W(\bar{\rho})$ and integrate over the region A to obtain

$$\int\int_A W(\bar{\rho})\left\{\nabla \cdot \left[\frac{1}{\mu_r(\bar{\rho})}\nabla u(\bar{\rho})\right] + k_o^2 \epsilon_r u(\bar{\rho})\right\} ds = 0$$

Starting from here, show that

$$\int\int_A \left\{\frac{1}{\mu_r}\nabla W \cdot \nabla u - k_o^2 \epsilon_r W u\right\} ds - \oint_\Gamma \frac{1}{\mu_r} W \frac{\partial u}{\partial n} d\ell = 0$$

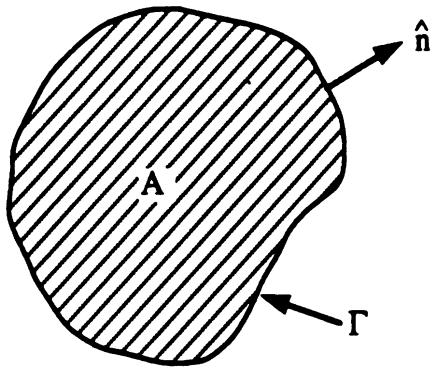

where

$$\frac{\partial u}{\partial n} = \hat{n} \cdot \nabla u$$

and Γ encloses A. In carrying out this proof, you must employ a standard identity along with the divergence theorem. Note that this integral equation is the starting point in developing field solutions based on the finite element method for two dimensional problems.

3. (a) Show that the x-component of the near zone magnetic field can be written as

$$H_x = \int\int\int [(z-z')J_y(\mathbf{r}') - (y-y')J_z(\mathbf{r}')]\, K(R)\, dv'$$

where

$$K(R) = (1+jkR)\frac{e^{-jkR}}{4\pi R^3}$$

(b) Show that the far zone E_θ spherical component due to the electric current can be written as

$$E_\theta = \frac{j\omega\mu}{4\pi r}e^{-jkr}\int\int\int [-J_\rho(\mathbf{r}')\cos(\phi-\phi')\cos\theta - J_\phi(\mathbf{r}')\sin(\phi-\phi')\cos\theta + J_z(\mathbf{r}')\sin\theta]e^{jkg}\,dv'$$

with

$$g = \rho'\cos(\phi-\phi')\sin\theta + z'\cos\theta, \quad dv' = \rho'\,d\rho'\,d\phi'\,dz'$$

or as

$$E_\theta = \frac{j\omega\mu}{4\pi r}e^{-jkr}\int\int\int \Big\{ [\sin\theta\cos\theta' - \cos\theta\sin\theta'\cos(\phi-\phi')]\, J_r(\mathbf{r}') - [\sin\theta\sin\theta' + \cos\theta\cos\theta'\cos(\phi-\phi')]\, J_\theta(\mathbf{r}') - \cos\theta\sin(\phi-\phi')J_\phi(\mathbf{r}')\Big\} e^{jkg}\,dv'$$

with

$$g = [\cos\theta\cos\theta' + \sin\theta\sin\theta'\cos(\phi-\phi')]\, r'$$

and

$$dv' = r'^2\sin\theta'\,dr'\,d\theta'\,d\phi'$$

In these J_ρ, J_ϕ and J_z are the cylindrical components of the current and likewise J_r, J_θ and J_ϕ are the spherical components of $\mathbf{J}$. Depending on the integration volume or surface, one of these expressions is likely to be more convenient than the other.

(c) Obtain similar expressions to those in (b) for the E_ϕ component.

(d) Obtain the E_θ and E_ϕ far zone field components due to the magnetic current using

(1) cylindrical coordinates for integration and spherical for observation.

(2) spherical coordinates for integration and observation.

4. Consider the plane wave

$$\mathbf{E}^i = \hat{z} E_o e^{-jkx}$$

incident upon a small dielectric sphere of radius $a \ll \lambda$. Based on the volume equivalence principle, the presence of the sphere can be replaced by the radiation of the equivalent volume current

$$\mathbf{J} = j\omega(\epsilon - \epsilon_o)\mathbf{E}$$

where $\mathbf{E} = \mathbf{E}^i + \mathbf{E}^s$ with $\mathbf{E}^s$ being the scattered field which is that radiated by $\mathbf{J}$.

(a) Since the sphere is small, assume that $\mathbf{E} = \hat{z} E_1$ in the sphere with E_1 being a constant. Determine E_1 (hint: see equ. (2.69))

(b) Determine the scattered field in the far zone

(c) Show that

$$\sigma = \underset{r \to \infty}{4\pi r^2} \frac{|\mathbf{E}^s|^2}{|\mathbf{E}^i|^2} = \frac{4\pi k_o^4 (\epsilon_r - 1)^2 a^6 \sin^2\theta}{(\epsilon_r + 2)^2}$$

where σ is the bistatic echo area of the sphere. This result is a form of the Rayleigh law of scattering.

(d) repeat (a) - (c) if the sphere is replaced by a small cube of volume h^3, where $h \ll \lambda$. hint: You must derive a replacement for the last term of (2.69).

(e) repeat (a) - (c) if the sphere is replaced by a small cylinder having length h and radius a, such that $h \ll \lambda$ and $a \ll \lambda$.

5. Give the explicit matrix or components of the free space dyadic Green's function using spherical coordinates. Do not carry out the derivatives.

6. Give the explicit matrix of the two dimensional dyadic Green's function in cylindrical and rectangular coordinates. Do not carry out the derivatives.

7. Show that the right hand side of (2.103) vanishes when S_c is placed at infinity.

8. Find the explicit components of the dyadics $\overline{\mathbf{g}}_{1,2}$ such that

$$\mathbf{A} = \int\int\int \overline{\mathbf{g}}_1 \cdot \mathbf{J}\, dv'$$

and

$$\mathbf{F} = \int\int\int \overline{\mathbf{g}}_2 \cdot \mathbf{M}\, dv'$$

where $\mathbf{A}$ and $\mathbf{F}$ denote the magnetic and electric potentials, respectively.

9. Verify equation (2.128).

10. Derive appropriate replacements for the last term of (2.147) if A_o in (2.142) is chosen to be the cross section of a small rectangular cylinder having width w and height h.

11. Consider the plane wave

$$\mathbf{E}^i = \hat{z} e^{-jkz}$$

incident upon an infinitely long (along the z direction) dielectric cylinder having $\epsilon = \epsilon_o \epsilon_r$ and $\mu = \mu_o$. Given that the echowidth is defined by

$$\sigma = \lim_{\rho \to \infty} 4\pi\rho \frac{|\mathbf{E}^s|^2}{|\mathbf{E}^i|^2}$$

where $\mathbf{E}^s$ denotes the scattered field and ρ is the usual cylindrical distance, find:

(a) The echowidth of a circular dielectric cylinder of radius $a \ll \lambda$.

(b) The echowidth of a rectangular dielectric cylinder whose dimensions are much smaller than the wavelength in the dielectric.

12. Show that

$$\frac{e^{-jkr}}{4\pi r} = -\frac{j}{8\pi}\int_{-\infty}^{\infty} H_o^{(2)}\left(\sqrt{k_o^2 - k_2^2}\rho\right) e^{\pm jk_z z} dk_z$$

hint: Take the transform of the wave equations (2.193) with respect to z to obtain an equation similar to (2.116)

13. Consider the planar current distribution $\mathbf{J} = \hat{x} J_x(x,y)\delta(z)$ over the dielectric interface, as shown

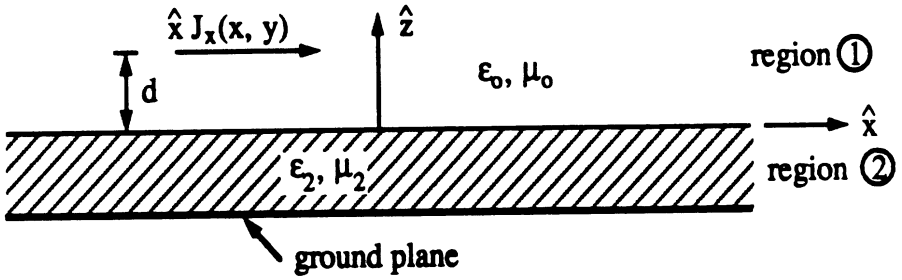

(a) Using the plane wave spectrum representation (2.202) show that for $z > d = 0$

$$H_z = \frac{1}{8\pi^2}\iint_{-\infty}^{\infty} \frac{k_y}{k_z^-}\tilde{J}_x(k_x,k_y)e^{-j\mathbf{k}\cdot\mathbf{r}}(1+R^{TE})dk_x\,dk_y$$

Generalize this result to the case when $d \neq 0$ and identify R^{TE}.
(b) repeat for $\mathbf{J} = \hat{y} J_y(x,y)\delta(z)$.

14. (Sommerfeld problem) Assume a $\hat{z}$ directed vertical electric dipole (VED) located a distance d over the interface of problem 3. Using the Sommerfeld indentity (see class notes) show that the radiated field by this dipole in the presence of the interface is

$$E_z = C\int_{-\infty}^{\infty} \frac{(k\rho)^3}{k_z^-} H_o^{(2)}(k_\rho \rho)\left[e^{-jk_z^-|z|} + R^{TM} e^{-jk_z^-(z+2d)}\right] dk_\rho$$

Identify R^{TM} and the constant C.
Note: $k_\rho = \sqrt{k_x^2 + k_y^2}$, $k_z^- = \sqrt{k_o^2 - k_\rho^2}$.

15. Give explicit expressions for the transform $\tilde{\mathbf{E}}(k_x, k_y, k_z)$ is terms of $\widetilde{\mathbf{H}}(k_x, k_y, k_z)$ for all rectalinear components.

16. Verify equation (2.129) and derive (2.130)

17. Evaluate the integral

$$\iiint_{V_0} J(\bar{r}) \times \nabla G(\bar{r}, \bar{r}')\, dv'$$

When V_0 is a vanishingly small volume

18. Modify the right hand side of 3.10 to account for the case when the observation point r is at P, where P coincides with the tip of a cone.

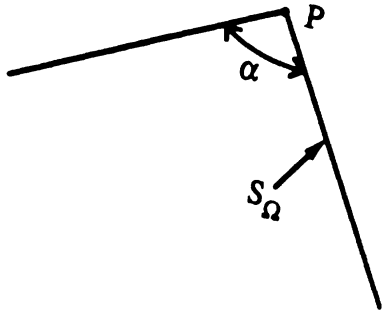

Chapter 3

Integral Equations and Other Field Representations

The field integral representations given in the last chapter, although of sufficient generality are often inconvenient and possibly inefficient for specific applications. Also, their integrands are highly singular requiring special treatment, when the observation point is in the source region. This difficulty cannot be eliminated but any reduction in the integrand's singularity is desirable for achieving higher accuracies in numerical computations involving such integrals. Obviously, there are a variety of field representations, integral equations and formal solutions that could be derived, many of which can be only applicable to a specific situation. Below we shall consider some alternative field representations from which we then construct integral equations that are among the most frequently used. First we shall develop three dimensional representations. Many of the two-dimensional representations can then be reduced from the three dimensional ones. However, for scattering applications a larger variety of two-dimensional representations are available primarily because the topic has been extensively studied.

3.1 Three-Dimensional Integral Equations

3.1.1 Kirchhoff's Integral Equation

Perhaps the simplest integral representation can be derived by considering the wave equations (2.86) in conjunction with Green's second identity (see (2.42)). To proceed, we assume the existance of certain structures whose surfaces will be denoted by $S_1, S_2, \ldots, S_N$. The collection of these surfaces, henceforth referred to as S_Ω (enclosing the volume V_Ω), are illuminated by sources which are enclosed within the volume V_{is}. The volume region exterior to S_Ω shall be denoted by V_∞ which as seen is also bounded by the surface S_∞ placed at infinity.

Without loss of generality let us consider one of the electric field component, say E_a. Then from (2.86)

$$\nabla^2 E_a + k^2 E_a = \begin{cases} F_a(\mathbf{r}) & r \in V_{is} \\ 0 & r \notin V_{is} \end{cases} \tag{3.1}$$

in which $F_a(\mathbf{r}) = \mathbf{F}(r) \cdot \hat{a}$ represents the source terms in the right hand side of (2.86). Multiplying this by the free space Green's function and integrating yields

$$\iiint_{V_\infty} G(\mathbf{r},\mathbf{r}')\left[\nabla^2 E_a(\mathbf{r}) + k^2 E_a(\mathbf{r})\right] dv = \begin{cases} \iiint_{V_{is}} F_a(\mathbf{r}) G(\mathbf{r},\mathbf{r}') dv & \mathbf{r} \in V_{is} \\ 0 & \mathbf{r} \notin V_{is} \end{cases} \tag{3.2}$$

Also, from Green's second identity (see (2.42)) we have

$$\begin{aligned} &\iiint_{V_\infty} \left[E_a(\mathbf{r})\nabla^2 G(\mathbf{r},\mathbf{r}') - G(\mathbf{r},\mathbf{r}')\nabla^2 E_a(\mathbf{r})\right] dv \\ &= -\oiint_{S_\Omega} \left[E_a(\mathbf{r})\frac{\partial G(\mathbf{r},\mathbf{r}')}{\partial n} - G(\mathbf{r},\mathbf{r}')\frac{\partial E_a(\mathbf{r})}{\partial n}\right] ds \\ &+ \oiint_{S_\infty} \left[E_a(\mathbf{r})\frac{\partial G(\mathbf{r},\mathbf{r}')}{\partial n} - G(\mathbf{r},\mathbf{r}')\frac{\partial E_a(\mathbf{r},\mathbf{r}')}{\partial n}\right] ds \end{aligned} \tag{3.3}$$

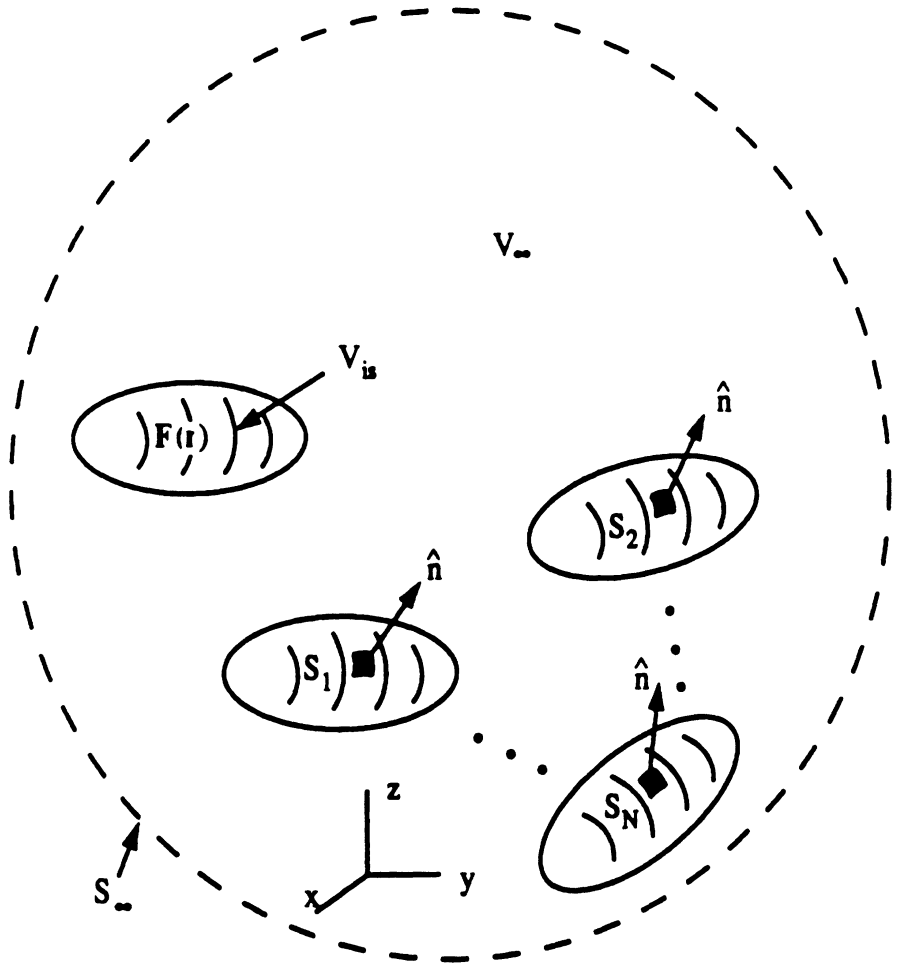

Figure 3.1: Geometry for the application of Green's second identity.

where $\frac{\partial}{\partial n} = \hat{n} \cdot \nabla$ and we remark that the negative sign in front of the integral over S_Ω was introduced because the unit normal $\hat{n}$ points toward the interior of V_∞. Further, by noting that $G(\mathbf{r}, \mathbf{r}')$ and $E_a(\mathbf{r})$ satisfy the radiation condition (2.39), it follows that the integral over S_∞ in (3.3a) vanishes. Thus we have

$$\int\int\int_{V_\infty + V_{is}} G(\mathbf{r}, \mathbf{r}') \nabla^2 E_a(\mathbf{r}) dv = \int\int\int_{V_\infty + V_{is}} E_a(\mathbf{r}) \nabla^2 G(\mathbf{r}, \mathbf{r}') dv$$
$$+ \oiint_{S_\Omega} \left[E_a(\mathbf{r}) \frac{\partial G(\mathbf{r}, \mathbf{r}')}{\partial n} - G(\mathbf{r}, \mathbf{r}') \frac{\partial E_a(\mathbf{r})}{\partial n} \right] ds \qquad (3.4)$$

and when this is combined with (3.2) we obtain

$$\int\int\int_{V_\infty} E_a(\mathbf{r})\left[\nabla^2 G(\mathbf{r},\mathbf{r}') + k^2 G(\mathbf{r},\mathbf{r}')\right] dv = -\oiint_{S_\Omega}\left[E_a(\mathbf{r})\frac{\partial G(\mathbf{r},\mathbf{r}')}{\partial n}\right.$$

$$\left. -G(\mathbf{r},\mathbf{r}')\frac{\partial E_a(\mathbf{r})}{\partial n}\right] + \int\int\int_{V_{i_a}} F_a(\mathbf{r})G(\mathbf{r},\mathbf{r}')dv \qquad (3.5)$$

We now recall the differential equation (2.38) satisfied by the Green's function and when this is introduced into (3.5), upon interchanging $\mathbf{r}$ and $\mathbf{r}'$ we obtain

$$\oiint_{S_\Omega}\left[E_a(\mathbf{r}')\frac{\partial G(\mathbf{r},\mathbf{r}')}{\partial n'} - G(\mathbf{r},\mathbf{r}')\frac{\partial E_a(\mathbf{r}')}{\partial n'}\right] ds' - \int\int\int_{V_{i_a}} F_a(\mathbf{r}')G(\mathbf{r},\mathbf{r}')dv'$$

$$= \begin{cases} E_a(\mathbf{r}) & \mathbf{r} \text{ in } V_\infty \\ 0 & \mathbf{r} \text{ not in } V_\infty \end{cases} \qquad (3.6)$$

in which the differentiation is on the primed coordinates and is taken along the normal directed away from $S_1, S_2, \ldots, S_N$.

The above result given by (3.6) is often referred to as the *extinction or Kirchhoff's integral equation* and is valid for all field components provided these satisfy the radiation condition. No other boundary condition is required to be satisfied by the field and since $E_a(\mathbf{r})$ is completely arbitrary we can generalize it to the case of vector fields. We have

$$\oiint_{S_\Omega}\left[\mathbf{E}(\mathbf{r}')\frac{\partial G(\mathbf{r},\mathbf{r}')}{\partial n'} - G(\mathbf{r},\mathbf{r}')\frac{\partial \mathbf{E}(\mathbf{r}')}{\partial n'}\right] ds' - \int\int\int_{V_{i_a}} \mathbf{F}_E(\mathbf{r})G(\mathbf{r},\mathbf{r}')dv'$$

$$= \begin{cases} \mathbf{E}(\mathbf{r}) & \mathbf{r} \text{ in } V_\infty \\ 0 & \mathbf{r} \text{ not in } V_\infty \end{cases} \qquad (3.7a)$$

and by duality

$$\oiint_{S_\Omega}\left[\mathbf{H}(\mathbf{r}')\frac{\partial G(\mathbf{r},\mathbf{r}')}{\partial n'} - G(\mathbf{r},\mathbf{r}')\frac{\partial \mathbf{E}(\mathbf{r}')}{\partial n'}\right] ds' - \int\int\int_{V_{i_a}} \mathbf{F}_H(\mathbf{r})G(\mathbf{r},\mathbf{r}')dv'$$

$$= \begin{cases} \mathbf{H}(\mathbf{r}) & \mathbf{r} \text{ in } V_\infty \\ 0 & \mathbf{r} \text{ not in } V_\infty \end{cases} \qquad (3.7b)$$

in which

$$\mathbf{F}_E(\mathbf{r}) = j\omega\mu\mathbf{J}(\mathbf{r}) - \frac{\nabla\nabla\cdot\mathbf{J}(\mathbf{r}')}{j\omega\epsilon} + \nabla\times\mathbf{M}(\mathbf{r}).$$

and

$$\mathbf{F}_H(\mathbf{r}) = j\omega\epsilon\mathbf{M}(\mathbf{r}) - \frac{\nabla\nabla\cdot\mathbf{M}(\mathbf{r}')}{j\omega\mu} - \nabla\times\mathbf{J}(\mathbf{r}).$$

If no external sources are present or if all sources are located on or within the surfaces S_1, S_2, etc, then $\mathbf{F}_E = \mathbf{F}_M = 0$. In that case $\mathbf{E}, \mathbf{H}$, $\frac{\partial\mathbf{E}}{\partial n'}$, or $\frac{\partial\mathbf{H}}{\partial n'}$ when integrated over S_Ω play the role of equivalent sources of the same type as $\mathbf{F}_E$ and $\mathbf{F}_H$. This will become apparent in later applications. Alternatively, the integrals associated with $\mathbf{F}_E$ and $\mathbf{F}_M$ can be recognized to yield the fields radiated by the sources within V_∞ and we may thus set

$$-\int\int\int \mathbf{F}_E(\mathbf{r}')G(\mathbf{r},\mathbf{r}')dv' \;\rightarrow\; \mathbf{E}^i(\mathbf{r})$$

$$-\int\int\int \mathbf{F}_H(\mathbf{r}')G(\mathbf{r},\mathbf{r}')dv' \;\rightarrow\; \mathbf{H}^i(\mathbf{r})$$

where $(\mathbf{E}^i, \mathbf{H}^i)$ denote the excitation or incident fields. For scattering computations these are usually plane waves whose source is at infinity.

In practice, additional boundary conditions would be imposed on the fields at the surfaces S_1, S_2, etc. This leads to the construction of integral equations for a unique solution of the fields. However, in their present form, (3.6) and (3.7) are not applicable to the case where $\mathbf{r}$ is on S_Ω, i.e. at the boundary of V_Ω coinciding with S_Ω. To make them applicable to this case we shall consider the limit as the observation point P at $\mathbf{r} = \mathbf{r}_o$ approaches the surface from outside or inside S_Ω. In order to simulate the last situation, we distort the surface S_Ω about the observation point P as shown in Fig. 3.2, i.e. by adding a hemispherical surface to S_Ω of radius $R_o \rightarrow 0$ which has its center at the observation point P. Accordingly, from (3.7a)

$$\int\int_{S_\Omega - S_o}\left[\mathbf{E}(\mathbf{r}')\frac{\partial G(\mathbf{r},\mathbf{r}')}{\partial n'} - G(\mathbf{r},\mathbf{r}')\frac{\partial\mathbf{E}(\mathbf{r}')}{\partial n'}\right]ds'$$
$$= -\int\int_{S_o}\left[\mathbf{E}(\mathbf{r}')\frac{\partial G(\mathbf{r},\mathbf{r}')}{\partial n'} - G(\mathbf{r},\mathbf{r}')\frac{\partial\mathbf{E}(\mathbf{r}')}{\partial n'}\right]ds'$$

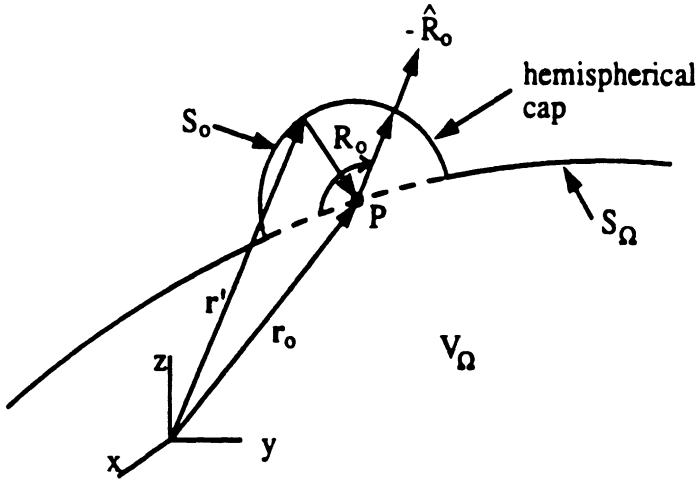

Figure 3.2: Geometry for evaluating the field on S_Ω.

For the integral over the hemispherical surface S_o we have $ds' = R_o^2 \sin\theta_o d\phi_o d\theta_o$,

$$G(\mathbf{r},\mathbf{r}') = \frac{e^{-jkR_o}}{4\pi R_o}$$

and

$$\frac{\partial G(\mathbf{r},\mathbf{r}')}{\partial n'} = -\hat{R}_o \cdot \nabla' G(\mathbf{r},\mathbf{r}') = \hat{R}_o \cdot \nabla G(\mathbf{r},\mathbf{r}') = \frac{\partial G}{\partial R_o} = -\left(jk + \frac{1}{R_o}\right)\frac{e^{-jkR_o}}{4\pi R_o}$$

Substituting these into the integral gives

$$-\int\int_{S_o \to 0} [\ ]\, ds' = \mathbf{E}(\mathbf{r}_o)\int_0^{\frac{\pi}{2}}\int_0^{2\pi}\left(jk + \frac{1}{R_o}\right)\frac{e^{-jkR_o}}{4\pi R_o} R_o^2 \sin\theta_o d\phi_o d\theta_o$$

$$-\int_0^{\pi}\int_0^{2\pi}\frac{\partial \mathbf{E}}{\partial n'}\frac{e^{-jkR_o}}{4\pi R_o} R_o^2 \sin\theta_o d\phi_o d\theta_o$$

and it is seen that the last integral vanishes as $R_o \to 0$. Also,

$$\mathbf{E}(\mathbf{r}_o)\int_0^{\frac{\pi}{2}}\int_0^{2\pi}\left(jk + \frac{1}{R_o}\right)\frac{e^{-jkR_o}}{4\pi R_o} R_o^2 \sin\theta_o d\phi_o d\theta_o = \frac{1}{2}\mathbf{E}(\mathbf{r}_o) \qquad (3.8)$$

and thus we can write

$$\oiint_{S_\Omega}\left[\mathbf{E}(\mathbf{r}')\frac{\partial G(\mathbf{r},\mathbf{r}')}{\partial n'} - G(\mathbf{r},\mathbf{r}')\frac{\partial \mathbf{E}(\mathbf{r}')}{\partial n'}\right] ds' = \frac{1}{2}\mathbf{E}(\mathbf{r}) \tag{3.9}$$

for $\mathbf{r}$ on S_Ω. This simply states that the field on the surface S_Ω is obtained by averaging its values just inside and just outside S_Ω. Using (3.9) we can now revise the integral expressions (3.7) to read

$$\oiint_{S_\Omega}\left[\mathbf{E}(\mathbf{r}')\frac{\partial G(\mathbf{r},\mathbf{r}')}{\partial n'} - G(\mathbf{r},\mathbf{r}')\frac{\partial \mathbf{E}(\mathbf{r}')}{\partial n'}\right] ds' + \mathbf{E}^i(\mathbf{r})$$
$$= \begin{cases} \mathbf{E}(\mathbf{r}) & \mathbf{r} \text{ in } V_\infty \\ \frac{1}{2}\mathbf{E}(\mathbf{r}) & \mathbf{r} \text{ on } S_\Omega \\ 0 & \mathbf{r} \text{ within } S_\Omega \end{cases} \tag{3.10a}$$

$$\oiint_{S_\Omega}\left[\mathbf{H}(\mathbf{r}')\frac{\partial G(\mathbf{r},\mathbf{r}')}{\partial n'} - G(\mathbf{r},\mathbf{r}')\frac{\partial \mathbf{H}(\mathbf{r}')}{\partial n'}\right] ds' + \mathbf{H}^i(\mathbf{r})$$
$$= \begin{cases} \mathbf{H}(\mathbf{r}) & \mathbf{r} \text{ in } V_\infty \\ \frac{1}{2}\mathbf{H}(\mathbf{r}) & \mathbf{r} \text{ on } S_\Omega \\ 0 & \mathbf{r} \text{ within } S_\Omega \end{cases} \tag{3.10b}$$

and it should be noted that these are valid provided the observation point is not at a corner or an edge formed by S_Ω. They are evocative of Huygen's principle which states that the fields caused by the presence of the volume enclosed by the surface(s) S_Ω can be determined uniquely everywhere from a knowledge of that field and its normal derivative on S_Ω. Alternatively, it will be shown in the next section that a knowledge of the tangential electric and magnetic fields on S_Ω is sufficient to uniquely determine the fields exterior to S_Ω regardless of the volume composition enclosed by S_Ω. These statements are valid even if $(\mathbf{E}^i, \mathbf{H}^i)$ are zero and sources exist within S_Ω. In that case we can state that the fields exterior to S_Ω can be determined uniquely from a knowledge of the surface tangential electric and magnetic fields or a knowledge of the electric/magnetic field and its normal derivative. By referring to chapter 1, one concludes that the surface equivalence principle can be thought as another statement of Huygen's principle.

Equations (3.10) can be referred to as the vector form of Kirchhoff's equations who first employed (a scalar form of) these for computing diffraction by apertures. To obtain the standard Kirchhoff's scalar equations the vector

field in (3.10) is replaced by a scalar function or a component of the field. Because of their simplicity, Kirchhoff's equations are widely used for obtaining the diffraction by apertures or scattering by closed surfaces whose surface fields are known or can be reasonably approximated (using physical optics, for example).

3.1.2 Stratton-Chu Integral Equations

The Stratton-Chu integral formulae for field representations are among the most popular in scattering and antenna related problems. Perhaps a primary reason for their popularity is their reduced kernel singularity in comparison to the representations (2.52) or (2.102), which integrate the current sources directly over the volume. The main feature of the Stratton-Chu representations is the transferring of one of the del operators from the Green's function to the current reducing the kernel singularity from R^{-3} to R^{-2} (see (2.63)). There are several ways to derive the Stratton-Chu equations but it is instructive to begin their derivation by considering one of the integral expansions given earlier. Let us for example begin with equation (2.52a) where our goal is to reduce the singularity of the integrand (or kernel) associated with the last right hand side term of this equation. This term can be written as

$$-\frac{jZ}{k}\int\int\int_V \mathbf{J}(\mathbf{r}')\cdot\nabla\nabla G(\mathbf{r},\mathbf{r}')dv' = -\frac{jZ}{k}\nabla\left\{\int\int\int_V \mathbf{J}(\mathbf{r}')\cdot\nabla G(\mathbf{r},\mathbf{r}')dv'\right\}$$

$$= \frac{jZ}{k}\nabla\left\{\int\int\int_V \mathbf{J}(\mathbf{r}')\cdot\nabla' G(\mathbf{r},\mathbf{r}')dv'\right\}$$

and by invoking the identity (2.50) we have

$$\int\int\int_V \mathbf{J}(\mathbf{r}')\cdot\nabla' G(\mathbf{r},\mathbf{r}')dv' = \int\int\int \nabla'\cdot\{\mathbf{J}(\mathbf{r}')G(\mathbf{r},\mathbf{r}')\}\,dv'$$

$$-\int\int\int_V [\nabla'\cdot\mathbf{J}(\mathbf{r}')]\,G(\mathbf{r},\mathbf{r}')dv'.$$

Next, by employing the divergence theorem we obtain

$$\int\int\int_V \nabla'\cdot\{\mathbf{J}(\mathbf{r}')G(\mathbf{r},\mathbf{r}')\}\,dv' = \oiint_{S_c} G(\mathbf{r},\mathbf{r}')\,[\mathbf{J}(\mathbf{r}')\cdot\hat{n}(\mathbf{r}')]\,ds' \qquad (3.11)$$

where $\hat{n}$ is the unit normal pointing outward of the surface S_c enclosing the volume V containing the source $\mathbf{J}(\mathbf{r}')$. A natural boundary condition is that

the current be confined within the volume V implying that the component of $\mathbf{J}$ normal to the surface S_c must be zero. Thus, the integral in (3.11) vanishes and we can then write

$$\frac{-jZ}{k}\int\int\int_V \mathbf{J}(\mathbf{r}')\cdot\nabla\nabla G(\mathbf{r},\mathbf{r}')dv' = \frac{-jZ}{k}\int\int\int_V [\nabla'\cdot\mathbf{J}(\mathbf{r}')]\,\nabla G(\mathbf{r},\mathbf{r}')dv' \tag{3.12}$$

When this identity and its dual is used in (2.52) we obtain the equations

$$\mathbf{E}(\mathbf{r}) = \int\int\int_V \Big[\mathbf{M}(\mathbf{r}')\times\nabla G(\mathbf{r},\mathbf{r}') - jkZ\mathbf{J}(\mathbf{r}')G(\mathbf{r},\mathbf{r}') - \frac{jZ}{k}\nabla'\cdot\mathbf{J}(\mathbf{r}')\nabla G(\mathbf{r},\mathbf{r}')\Big]dv' \tag{3.13a}$$

$$\mathbf{H}(\mathbf{r}) = \int\int\int_V \Big[-\mathbf{J}(\mathbf{r}')\times\nabla G(\mathbf{r},\mathbf{r}') - jkY\mathbf{M}(\mathbf{r}')G(\mathbf{r},\mathbf{r}') - \frac{jY}{k}\nabla'\cdot\mathbf{M}(\mathbf{r}')\nabla G(\mathbf{r},\mathbf{r}')\Big]dv' \tag{3.13b}$$

Alternative representations can be obtained by invoking the continuity equations (1.38) and (1.39) to replace the divergence of the current quantities with volume charges. Doing so yields

$$\mathbf{E}(\mathbf{r}) = \int\int\int_V \Big[\mathbf{M}(\mathbf{r}')\times\nabla G(\mathbf{r},\mathbf{r}') - jkZ\mathbf{J}(\mathbf{r}')G(\mathbf{r},\mathbf{r}') - \frac{\rho(\mathbf{r}')}{\epsilon}\nabla G(\mathbf{r},\mathbf{r}')\Big]dv' \tag{3.14a}$$

$$\mathbf{H}(\mathbf{r}) = \int\int\int_V \Big[-\mathbf{J}(\mathbf{r}')\times\nabla G(\mathbf{r},\mathbf{r}') - jkY\mathbf{M}(\mathbf{r}')G(\mathbf{r},\mathbf{r}') - \frac{\rho_m(\mathbf{r}')}{\mu}\nabla G(\mathbf{r},\mathbf{r}')\Big]dv' \tag{3.14b}$$

which are the natural equations that result if we introduce the scalar potentials Φ_e and Φ_m in equations (2.19).

When the above expressions (3.13) and (3.14) are applied to an antenna or scattering configuration such as that shown in Figure 2.10 it is convenient to employ Love's equivalence principle. This allows one to replace the presence

of the volume enclosed by the surfaces $S_1, S_2, \ldots, S_N$ (comprising the surface S_Ω) by a set of equivalent sources

$$\mathbf{J} = \hat{n} \times \mathbf{H}, \quad \mathbf{M} = \mathbf{E} \times \hat{n} \tag{3.15}$$

placed on the surfaces $S_1, S_2, \ldots, S_N$. Also, in accordance with the boundary conditions (1.62) and (1.63) we may set

$$\rho_s = \epsilon(\hat{n} \cdot \mathbf{E}), \quad \rho_{ms} = \mu(\hat{n} \cdot \mathbf{H}) \tag{3.16}$$

Introducing these into (3.14) yields

$$\mathbf{E}(\mathbf{r}) = \mathbf{E}^i + \oiint_{S_\Omega} \Big\{ [\mathbf{E}(\mathbf{r}') \times \hat{n}'] \times \nabla G(\mathbf{r}, \mathbf{r}') - jkZ\,[\hat{n}' \times \mathbf{H}(\mathbf{r}')]\, G(\mathbf{r}, \mathbf{r}') - \hat{n}' \cdot \mathbf{E}(\mathbf{r}') \nabla G(\mathbf{r}, \mathbf{r}') \Big\} ds' \tag{3.17a}$$

$$\mathbf{H}(\mathbf{r}) = \mathbf{H}^i + \oiint_{S_\Omega} \Big\{ [\mathbf{H}(\mathbf{r}') \times \hat{n}'] \times \nabla G(\mathbf{r}, \mathbf{r}') - jkY\,[\mathbf{E}(\mathbf{r}') \times \hat{n}']\, G(\mathbf{r}, \mathbf{r}') - \hat{n}' \cdot \mathbf{H}(\mathbf{r}') \nabla G(\mathbf{r}, \mathbf{r}') \Big\} ds' \tag{3.17b}$$

in which $\hat{n}' = \hat{n}(\mathbf{r}')$, where $\hat{n}(\mathbf{r}')$ denotes the outward unit normal outward to S_Ω at $\mathbf{r}$. We have also included the incident fields $(\mathbf{E}^i, \mathbf{H}^i)$ to account for any source exterior to S_Ω. We remark that (3.17) give the most common form of the Stratton-Chu equations.

An alternative field representation in terms of the dyadic Green's function can be obtained by substituting (3.15) into (2.102). Since the equivalent sources are only over the surface(s) S_Ω we have

$$\mathbf{E}(\mathbf{r}) = \mathbf{E}^i + \iint_{S_\Omega} \Big\{ \big[\nabla \times \overline{\Gamma}(\mathbf{r}, \mathbf{r}')\big] \cdot [\mathbf{E}(\mathbf{r}') \times \hat{n}'] + jkZ\overline{\Gamma}(\mathbf{r}, \mathbf{r}') \cdot [\hat{n}' \times \mathbf{H}(\mathbf{r}')] \Big\} ds' \tag{3.18a}$$

$$\mathbf{H}(\mathbf{r}') = \mathbf{H}^i \iint_{S_\Omega} \Big\{ jkY\overline{\Gamma}(\mathbf{r}, \mathbf{r}') \cdot [\mathbf{E}(\mathbf{r}') \times \hat{n}'] - \big[\nabla \times \overline{\Gamma}(\mathbf{r}, \mathbf{r}')\big] \cdot [\hat{n}' \times \mathbf{H}(\mathbf{r}')] \Big\} ds' \tag{3.18b}$$

and this is equivalent to (3.17) only for closed surfaces in which case the identity [Van Bladel, p. 503]

$$\oiint_{S_\Omega} \nabla \cdot [\mathbf{J}(\mathbf{r}')G(\mathbf{r},\mathbf{r}')]\,ds' = -\oiint_{S_\Omega} \left[\frac{1}{R_1}+\frac{1}{R_2}\right] G(\mathbf{r},\mathbf{r}')\,[\mathbf{J}(\mathbf{r}')\cdot\hat{n}(\mathbf{r}')]\,ds' = 0 \tag{3.19}$$

holds when $\mathbf{J}$ is replaced by $\hat{n}' \times \mathbf{H}(\mathbf{r}')$ or $\mathbf{E}(\mathbf{r}') \times \hat{n}(\mathbf{r}')$. In (3.19), R_1 and R_2 denote the principle radii of curvature at the surface point $\mathbf{r}'$ but in the event S_Ω is not closed (i.e. S_Ω is the surface of a flat or curved conducting sheet as shown in Fig. 1.1) then this identity must be replaced by [Van Bladel, p. 502]

$$\begin{aligned}\int\int_{S_\Omega} \nabla \cdot [\mathbf{J}(\mathbf{r}')G(\mathbf{r},\mathbf{r}')]\,ds' &= +\oint_C \hat{b}' \cdot \mathbf{J}(\mathbf{r}')G(\mathbf{r},\mathbf{r}')d\ell' \\ &\quad - \int\int_{S_\Omega} \left[\frac{1}{R_1}+\frac{1}{R_2}\right] G(\mathbf{r},\mathbf{r}')\,[\mathbf{J}(\mathbf{r}')\cdot\hat{n}(\mathbf{r}')]\,ds' \\ &= \oint_C \hat{b}' \cdot \mathbf{J}(\mathbf{r}')G(\mathbf{r},\mathbf{r}')d\ell' \end{aligned} \tag{3.20}$$

in which C denotes the contour defining the outer perimeter of S_Ω and $\hat{b}' = \hat{\ell}' \times \hat{n}'$ where $\hat{\ell}'$ is the unit tangent to C at $\mathbf{r}'$. Thus, one cannot specialize (3.13) to open surfaces such as curved plates (see Fig. 3.3) by simply changing

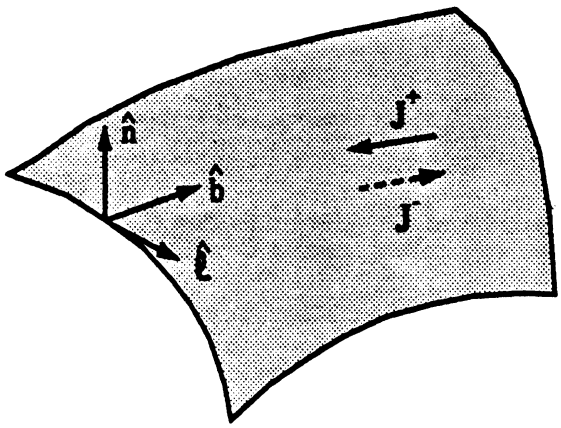

Figure 3.3: Geometry of a curved plate representing an open surface.

the volume integral to one over the boundary domain of $\mathbf{J}$ and $\mathbf{M}$. Such an

interchange of the volume and surface integral is permitted for the dyadic representations (2.102) or (2.42) which are similar to Franz's integral formulas whose precise form is given in one of the problems. However, in the case of (3.13) it is permitted only if the contour integral in (3.20) also vanishes. The last is often referred to as Kottler's boundary line integral and its presence is necessary to ensure the divergenceless of the field for all $\mathbf{r}$. If, however, one thinks of $\mathbf{J}$ and $\mathbf{M}$ as representing the net currents on the open surface, then $\mathbf{J}\cdot\hat{b} = (\mathbf{J}^+ - \mathbf{J}^+)\cdot\hat{b} = 0$ and $\mathbf{M}\cdot\hat{b} = (\mathbf{M}^+ - \mathbf{M}^-)\cdot\hat{b} = 0$ at the boundary line C. Consequently, the Kottler integral in (3.20) again vanishes implying that with this interpretation of $\mathbf{J}$ and $\mathbf{M}$, (3.13) remains valid when the volume integrals are replaced by ones over the surface of the curved plate.

We remark that (3.18) are again evocative of Huygen's principle as discussed in the previous section in connection with Kirchhoff's integral equation. In practice, however, the Stratton-Chu equations are more attractive than (3.18) because of the lower singularity of their kernel leading to a more accurate numerical implementation.

Integral equations such as those in (3.17) can be used for solving the fields on S_Ω by enforcing the specific boundary conditions associated with the surfaces comprising S_Ω. To enforce these boundary conditions it is necessary to have the observation point directly on S_Ω leading to singular kernels which must be carefully integrated as done in the previous section. As before we refer to figure 3.2 and rewrite (3.17a) as

$$\begin{aligned}\mathbf{E}(\mathbf{r}_o) &= \mathbf{E}^i(\mathbf{r}_o) + \int\int_{S_\Omega - S_o}\Big\{[\mathbf{E}(\mathbf{r}')\times\hat{n}']\times\nabla G(\mathbf{r}_o,\mathbf{r}') \\ &\quad - jkZ\,[\hat{n}'\times\mathbf{H}(\mathbf{r}')]\,G(\mathbf{r}_o,\mathbf{r}') - \hat{n}'\cdot\mathbf{E}(\mathbf{r}')\nabla G(\mathbf{r}_o,\mathbf{r}')\Big\}ds' \\ &\quad + \int\int_{S_o}\Big\{[\mathbf{E}(\mathbf{r}')\times\hat{n}']\times\nabla G(\mathbf{r}_o,\mathbf{r}') - jkZ\,[\hat{n}'\times\mathbf{H}(\mathbf{r}')]\,G(\mathbf{r}_o,\mathbf{r}') \\ &\quad - \hat{n}'\cdot\mathbf{E}(\mathbf{r}')\nabla G(\mathbf{r}_o,\mathbf{r}')\Big\}ds' \qquad (3.21)\end{aligned}$$

in which S_o is a vanishingly small hemispherical surface. Noting the identities

$$(\mathbf{E}\times\hat{n}')\times\nabla G \;=\; \nabla G\times(\hat{n}'\times\mathbf{E})$$

$$= \hat{n}'(\mathbf{E}\cdot\nabla G) - \mathbf{E}(\hat{n}'\cdot\nabla G) \tag{3.22}$$

$$-(\hat{n}'\cdot\mathbf{E})\nabla G = -\hat{n}'(\mathbf{E}\cdot\nabla G) + \mathbf{E}\times(\hat{n}'\times\nabla G) \tag{3.23}$$

it follows that

$$(\mathbf{E}\times\hat{n}')\times\nabla G - (\hat{n}'\cdot\mathbf{E})\nabla G = \mathbf{E}\times(\hat{n}'\times\nabla G) - \mathbf{E}(\hat{n}'\cdot\nabla G) \tag{3.24}$$

When the last is substituted into (3.21) the surface integral over S_o becomes

$$\int\int_{S_o}\Big\{\mathbf{E}(\mathbf{r}')\times[\hat{n}'\times\nabla G(\mathbf{r}_o,\mathbf{r}')] - \mathbf{E}(\mathbf{r}')\,[\hat{n}'\cdot\nabla G(\mathbf{r}_o,\mathbf{r}')]$$

$$-jkZ\,[\hat{n}'\times\mathbf{H}(\mathbf{r}')]\,G(\mathbf{r}_o,\mathbf{r}')\Big\}ds'$$

For this integral $\hat{n}' = \hat{R}_o$, $ds' = R_o^2\sin\theta_o d\phi_o d\theta_o$ and since $S_o \to 0$ we may set $\mathbf{E}(\mathbf{r}') \approx \mathbf{E}(\mathbf{r}_o)$ and $\mathbf{H}(\mathbf{r}') = \mathbf{H}(\mathbf{r}_o)$. When we substitute for ∇G as given in (2.55) with $R = R_o$, we find that the first term of the integral vanishes because $\nabla G = \hat{R}_o|\nabla G|$ and $\hat{n}\times\hat{R}_o$. Also the third term goes to zero as $R_o \to 0$. The second term (see (3.8)) when integrated gives $-\frac{1}{2}\mathbf{E}(\mathbf{r}_o)$ and thus we can rewrite (3.21) as

$$\mathbf{E}(\mathbf{r}_o) = 2\mathbf{E}^i(r_o) + 2\oiint_{S_\Omega}\Big\{[\mathbf{E}(\mathbf{r}')\times\hat{n}']\times\nabla G(\mathbf{r}_o,\mathbf{r}')$$

$$-jkZ\,[\hat{n}'\times\mathbf{H}(\mathbf{r}')]\,G(\mathbf{r}_o,\mathbf{r}') - \hat{n}'\cdot\mathbf{E}(\mathbf{r}')\nabla G(\mathbf{r}_o,\mathbf{r}')\Big\}ds' \tag{3.25}$$

Incorporating this result into (3.17) we have

$$\oiint_{S_\Omega}\Big\{[\mathbf{E}(\mathbf{r}')\times\hat{n}']\times\nabla G(\mathbf{r},\mathbf{r}') - jkZ\,[\hat{n}'\times\mathbf{H}(\mathbf{r})]\,G(\mathbf{r},\mathbf{r}')$$

$$-\hat{n}'\cdot\mathbf{E}(\mathbf{r}')\nabla G(\mathbf{r},\mathbf{r}')\Big\}ds' + \mathbf{E}^i(\mathbf{r}) = \begin{cases}\mathbf{E}(\mathbf{r}) & \mathbf{r}\text{ in }V_\infty\\ \frac{1}{2}\mathbf{E}(\mathbf{r}) & \mathbf{r}\text{ on }S_\Omega\\ 0 & \text{rwithin }S_\Omega\end{cases} \tag{3.26a}$$

$$\oiint_{S_\Omega}\Big\{[\mathbf{H}(\mathbf{r}')\times\hat{n}']\times\nabla G(\mathbf{r},\mathbf{r}') - jkY\,[\mathbf{E}(\mathbf{r})\times\hat{n}']\,G(\mathbf{r},\mathbf{r}')$$

$$-\hat{n}'\cdot\mathbf{H}(\mathbf{r}')\nabla G(\mathbf{r},\mathbf{r}')\Big\}ds'+\mathbf{H}^i(\mathbf{r})=\begin{cases}\mathbf{H}(\mathbf{r}) & \mathbf{r}\text{ in }V_\infty\\ \frac{1}{2}\mathbf{H}(\mathbf{r}) & \mathbf{r}\text{ on }S_\Omega\\ 0 & \text{within }S_\Omega\end{cases}\qquad(3.26b)$$

For completeness we note that the impressed fields $(\mathbf{E}^i,\mathbf{H}^i)$ may be replaced by their volume integral representations (3.13) or (2.52), However, when the observation point is within the volume of the impressed or equivalent volume sources $(\mathbf{J},\mathbf{M})$ we must then revert to the principle-value integral representation given in (2.69). It should also be noted that the Stratton-Chu equations are completely equivalent to the vector Kirchhoff equations (3.10). Notably, both sets of integral equations involve the normal and tangential field components on the surface S_Ω but Kirchhoff's equations decouple each field component from the others. However, these are unavoidably coupled upon application of the boundary conditions on S_Ω. Nevertheless, in the case of two-dimensional applications where only a z-directed electric or magnetic field exists, Kirchhoff's equations are the most simple to use. By setting $\mathbf{E}=\hat{z}E_z$ or $\mathbf{H}=\hat{z}H_z$ in (3.10) a scalar equation is obtained instead of the vector integral equation resulting from (3.26). Consequently, the extinction or Kirchhoff's integral equations are, generally, the preferred choice in formulating two-dimensional problems.

3.1.3 Integral Equations for Homogeneous Dielectrics

Man-made structures such as vehicles made of composites and microstrip antennas are typically composed of piecewise homogeneous dielectrics. The effects of these materials must therefore be accounted for in computing the radiated or scattered fields. So far, field representations were given which apply in the presence of structures enclosed within a surface S_Ω by invoking the equivalence theorem. In this section we will specialize these expressions to the case where the surface S_Ω encloses a piecewise homogeneous dielectric body. We shall first consider the simplest case, i.e. that pertinent to a homogeneous dielectric body.

Consider the homogeneous dielectric body enclosed by the surface $S_\Omega = S_d$ as shown in Fig. 3.4. The dielectric is immersed in some excitation field $(\mathbf{E}^i,\mathbf{H}^i)$ generated by the sources $(\mathbf{J}^i,\mathbf{M}^i)$ which are exterior to S_d and we are interested in finding a representation of the field in the exterior region (region

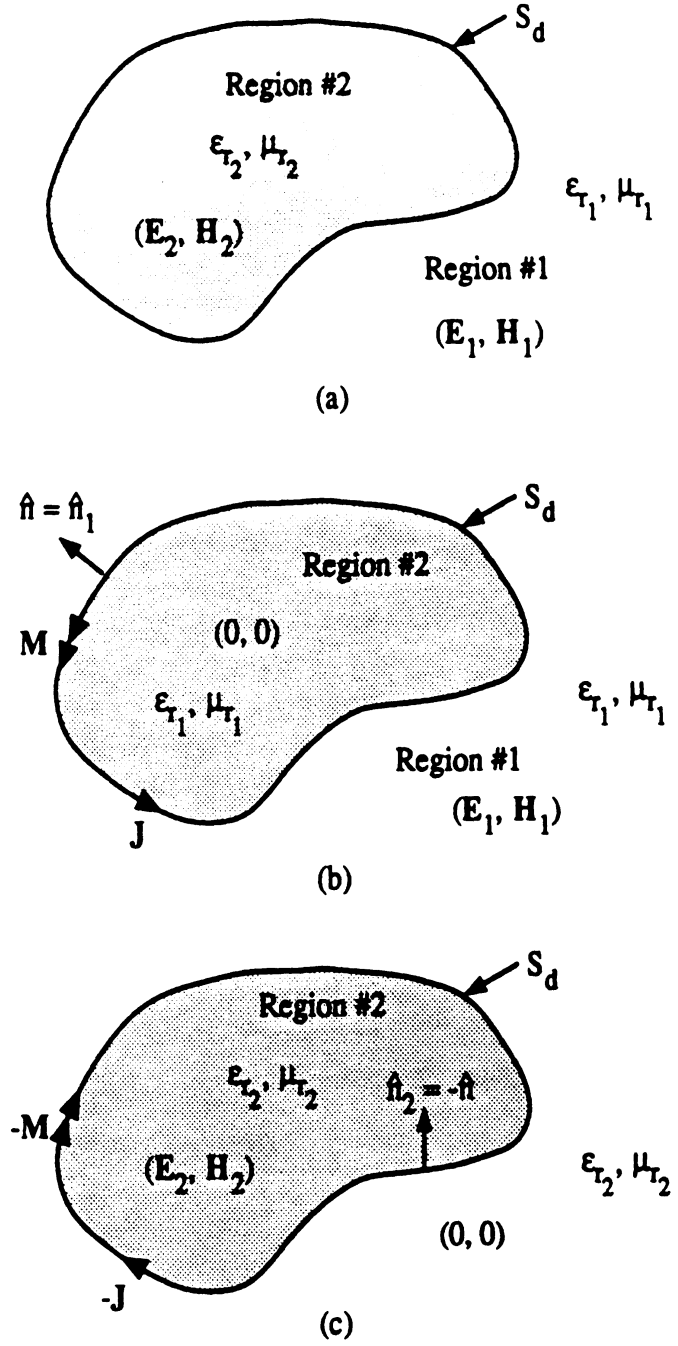

Figure 3.4: Application of the equivalence principle for a dielectric. (a) original problem (b) equivalent problem for Region #1, (c) equivalent problem for Region #2.

#1) and perhaps interior to S_d (region #2). One of the simplest integral expressions in this case is obtained by invoking the surface equivalence theorem and with this in mind we set up the two problems illustrated in Figure 3.4. The set-up in Figure 3.4(a) assumes zero field interior to S_d and thus the equivalent current $(\mathbf{J}_1, \mathbf{M}_1)$ can be used for computing the fields $(\mathbf{E}_1, \mathbf{H}_1)$ exterior to S_d. In contrast, the set-up in Figure 3.4(b) assumes zero exterior fields and thus the equivalent currents $(\mathbf{J}_2, \mathbf{M}_2)$ can be used for computing the interior fields $(\mathbf{E}_2, \mathbf{H}_2)$.

It should be remarked that the set-up assumed here, where the fields are set to zero in the indicated region, is not unique. Any other non-zero field could have been used and this would result in a different, albeit equivalent, formulation. In fact, certain judicious choices for the interior fields of the set-up in figure 4(b) or the exterior fields in figure 4(c) lead to formulations which may involve a single surface equivalent current [Glisson, AP-T, 1984]. An alternative approach will be to eliminate the introduction of the equivalent surface currents altogether and express the scattered fields in terms of the tangential electric and magnetic fields at the dielectric interface. In this case, the representation (3.18) may be used (or some other equivalent expression) to set-up integral equations for the tangential fields upon invoking field continuity at the interface. Nevertheless, below we shall consider the solution of the scattered/radiated fields in the presence of a dielectric via the set-up in fig. 4 since this appears to be one of the most often used approaches.

The introduced equivalent current illustrated in fig. 4 can be substituted into (3.13) to obtain integral expressions for the exterior and interior fields upon changing the volume integral to one over the closed surface S_d. However before doing so, it is important to note that by enforcing the tangential field continuity equations

$$\hat{n}_1 \times \mathbf{E}_1 = \hat{n}_1 \times \mathbf{E}_2, \quad \hat{n}_1 \times \mathbf{H}_1 = \hat{n}_1 \times \mathbf{H}_2 \tag{3.27}$$

($\hat{n}_1$ denotes the unit normal pointing away from S_d) across the surface S_d, it follows that

$$\mathbf{J}_1 = -\mathbf{J}_2 = \mathbf{J}, \quad \mathbf{M}_1 = -\mathbf{M}_2 = -\mathbf{M} \tag{3.28}$$

In arriving at (3.28) we could have also implied that (see section 1.10)

$$\mathbf{J}_1 = \hat{n}_1 \times \mathbf{H}_1, \quad \mathbf{M}_1 = -\hat{n}_1 \times \mathbf{E}_1$$

$$\mathbf{J}_2 = \hat{n}_2 \times \mathbf{H}_2 = -\hat{n}_1 \times \mathbf{H}_2 \qquad \mathbf{M}_2 = -\hat{n}_2 \times \mathbf{E}_2 = \hat{n}_1 \times \mathbf{E}_2 \tag{3.29}$$

However, it is not necessary to introduce these expressions since the surface fields are unknown and it is thus more convenient to retain $(\mathbf{J}, \mathbf{M})$ as the variable functions to be determined by enforcing the boundary conditions associated with problems defined in Figure 3.4. From Figure 3.4a, since the interior fields have been set to zero, we have that on S_d (actually just inside S_d)

$$\begin{aligned} \hat{n}_1 \times \mathbf{E}_1 &= 0 \\ \hat{n}_1 \times \mathbf{H}_1 &= 0 \end{aligned} \tag{3.30}$$

By defining the total fields $(\mathbf{E}_1, \mathbf{H}_1)$ to be the sum of the source fields and those radiated by $(\mathbf{J}, \mathbf{M})$ we may rewrite (3.30) as

$$\begin{aligned} \hat{n}_1 \times \mathbf{E}^i &= -\hat{n}_1 \times \mathbf{E}_1^s \\ \hat{n}_1 \times \mathbf{H}^i &= -\hat{n}_1 \times \mathbf{H}_1^s \end{aligned} \tag{3.31a}$$

where

$$\mathbf{E}_1^s = \oiint_{S_d} \Big[\mathbf{M}(\mathbf{r}') \times \nabla G_1(\mathbf{r}, \mathbf{r}') - jk_o Z_o \mu_{r_1} \mathbf{J}(\mathbf{r}') G_1(\mathbf{r}, \mathbf{r}') - j \frac{Z_o}{k_o \epsilon_{r_1}} \nabla_s' \cdot \mathbf{J}(\mathbf{r}') \nabla G_1(\mathbf{r}, \mathbf{r}') \Big] ds' \tag{3.31b}$$

$$\mathbf{H}_1^s = \oiint_{S_d} \Big[-\mathbf{J}(\mathbf{r}') \times \nabla G_1(\mathbf{r}, \mathbf{r}') - jk_o Y_o \epsilon_{r_1} \mathbf{M}(\mathbf{r}') G_1(\mathbf{r}, \mathbf{r}') - j \frac{Y_o}{k_o \mu_{r_1}} \nabla_s' \cdot \mathbf{M}(\mathbf{r}') \nabla G_1(\mathbf{r}, \mathbf{r}') \Big] ds' \tag{3.31c}$$

In these k_o, Z_o, Y_o are the free space wavenumber impedance and admittance, respectively, whereas ϵ_{r_1} and μ_{r_1} are the relative material constants of the exterior medium and are usually unity. Also,

$$G_1(\mathbf{r}, \mathbf{r}') = \frac{e^{-jk_1|\mathbf{r}-\mathbf{r}'|}}{4\pi|\mathbf{r}-\mathbf{r}'|} = \frac{e^{-jk_o\sqrt{\mu_{r_1}\epsilon_{r_1}}|\mathbf{r}-\mathbf{r}'|}}{4\pi|\mathbf{r}-\mathbf{r}'|} \tag{3.32}$$

is the Green's function associated with the exterior region. The fields $(\mathbf{E}_1^s, \mathbf{H}_1^s)$ are customarily referred to as those scattered by the dielectric body due to the excitation $(\mathbf{E}^i, \mathbf{H}^i)$. Instead of repeatedly using the explicit integral representation (3.31) it is convenient to define the operators

$$L_{1E_m}(\mathbf{M}) = \oiint_{S_d} \mathbf{M}(\mathbf{r}') \times \nabla G_1(\mathbf{r}, \mathbf{r}') ds' \tag{3.33}$$

$$L_{1H_m}(\mathbf{M}) = -\oiint_{S_d} \left[jk_o Y_o \epsilon_{r_1} \mathbf{M}(\mathbf{r}') G_1(\mathbf{r}, \mathbf{r}') + \frac{jY_o}{k_o \mu_{r1}} \nabla_s' \cdot \mathbf{M}(\mathbf{r}') \nabla G_1(\mathbf{r}, \mathbf{r}') \right] ds' \tag{3.34}$$

$$L_{1E_e}(\mathbf{J}) = -\oiint_{S_d} \left[jk_o Z_o \mu_{r1} \mathbf{J}(\mathbf{r}') G_1(\mathbf{r}, \mathbf{r}') + \frac{jZ_o}{k_o \epsilon_{r1}} \nabla_s' \cdot \mathbf{J}(\mathbf{r}') \nabla G_1(\mathbf{r}, \mathbf{r}') \right] ds' \tag{3.35}$$

$$L_{1H_e}(\mathbf{J}) = -\oiint_{S_d} \mathbf{J}(\mathbf{r}') \times \nabla G_1(\mathbf{r}, \mathbf{r}') ds' \tag{3.36}$$

Then, since

$$\hat{n}_1 \times \oiint_{S_d} \mathbf{A}(\mathbf{r}') \times \nabla G_1(\mathbf{r}_o^{\pm}, \mathbf{r}') ds' = \frac{1}{2} \mathbf{A}(\mathbf{r}_o)$$

$$+\hat{n}_1 \times \oiint_{S_d} \mathbf{A}(\mathbf{r}') \times \nabla G_1(\mathbf{r}_o, \mathbf{r}') \tag{3.37}$$

where $\mathbf{r}_o^{\pm}$ implies that the observation point is just exterior (+) or interior (-) to S_d, we can rewrite (3.31) more explicitly as

$$\begin{aligned} -\frac{1}{2}\mathbf{M}(\mathbf{r}) - \hat{n}_1 \times L_{1E_m}(\mathbf{M}) - \hat{n}_1 \times L_{1E_e}(\mathbf{J}) &= \hat{n}_1 \times \mathbf{E}^i \\ +\frac{1}{2}\mathbf{J}(\mathbf{r}) - \hat{n}_1 \times L_{1H_e}(\mathbf{J}) - \hat{n}_1 \times L_{1H_m}(\mathbf{M}) &= \hat{n}_1 \times \mathbf{H}^i \end{aligned} \tag{3.38}$$

valid for $\mathbf{r}$ on S_d. We note that (3.37) can be proven by following a similar procedure to that employed for the derivation of (3.9).

Another set of equations to be coupled with (3.38) can be obtained by enforcing the boundary conditions on $(\mathbf{E}_2, \mathbf{H}_2)$. From Fig. 3.4(b) we have that on S_d (actually just outside S_d)

$$\hat{n}_1 \times \mathbf{E}_2 = \hat{n}_1 \times \mathbf{E}_2^s = 0$$

$$\hat{n}_1 \times \mathbf{H}_2 = \hat{n}_1 \times \mathbf{H}_2^s = 0 \tag{3.39}$$

and upon making use of (3.37) these can be more explicitly written as

$$-\frac{1}{2}\mathbf{M}(\mathbf{r}) - \hat{n}_1 \times L_{2E_m}(-\mathbf{M}) - \hat{n}_1 \times L_{2E_e}(-\mathbf{J}) = 0$$

$$+\frac{1}{2}\mathbf{J}(\mathbf{r}) - \hat{n}_1 \times L_{2H_e}(-\mathbf{J}) - \hat{n}_1 \times L_{2H_m}(-\mathbf{M}) = 0 \tag{3.40a}$$

In these, the integral operators $L_{2E_m}, L_{2E_e}, L_{2H_e}$ and L_{2H_m} are identical to those defined in (3.33) - (3.36) provided ϵ_{r_1} and μ_{r_1} are replaced by ϵ_{r_2} and μ_{r_2}, respectively. By inspection, it is also seen that the minus sign in the argument of the operators can be factored out giving

$$\frac{1}{2}\mathbf{M}(\mathbf{r}) - \hat{n}_1 \times L_{2E_m}(\mathbf{M}) - \hat{n}_1 \times L_{2E_e}(\mathbf{J}) = 0$$

$$-\frac{1}{2}\mathbf{J}(\mathbf{r}) - \hat{n}_1 \times L_{2H_e}(\mathbf{J}) - \hat{n}_1 \times L_{2H_m}(\mathbf{M}) = 0 \tag{3.40b}$$

valid for $\mathbf{r}$ on S_d.

It is apparent that (3.38) and (3.40) are four integral equations involving only two unknowns. This is because we had initially enforced the continuity conditions (3.27) to relate the equivalent currents introduced for representing the exterior and interior fields. It is also a consequence of the fact that only the tangential electric or magnetic fields are needed over a closed surface for determining the fields away from S_d. Thus, we are essentially free to use one from each set of equations (3.38) and (3.40) to obtain a pair of them to be solved (usually numerically, and this will be discussed later) for $(\mathbf{J}, \mathbf{M})$. For example, we could select the equation resulting from the pair of conditions

$$\hat{n}_1 \times \mathbf{E}^i = -\hat{n}_1 \times \mathbf{E}_1^s$$

$$\hat{n}_1 \times \mathbf{E}_2^s = 0 \tag{3.41a}$$

or from

$$\hat{n}_1 \times \mathbf{H}^i = -\hat{n}_1 \times \mathbf{H}_1^s$$

$$\hat{n}_1 \times \mathbf{H}_2^s = 0 \tag{3.41b}$$

The integral equations resulting from (3.41a) are usually referred to as the *electric field integral equations* (EFIE) whereas those implied by (3.41b) are referred as the *magnetic field integral equations* (MFIE).

3.1.4 Integral Equations for Metallic Bodies

When S_d encloses a conducting surface (i.e. $\epsilon_{r_2} \to 1 - j\infty$) we may then set $\mathbf{M} = 0$ (see sections 1.4 and 1.10) and in that case the first of (3.41a) gives

$$jk_o Z_o \mu_{r1} \hat{n}_1 \times \oiint_{S_d} \left[\mathbf{J}(\mathbf{r}') G_1(\mathbf{r}, \mathbf{r}') + \frac{1}{k_o^2 \mu_{r1} \epsilon_{r1}} \nabla_s' \cdot \mathbf{J}(\mathbf{r}') \nabla G_1(\mathbf{r}, \mathbf{r}') \right] ds'$$

$$= \hat{n}_1 \times \mathbf{E}^i \qquad (3.42a)$$

whereas from the first of (3.41b) we have

$$\frac{1}{2}\mathbf{J}(\mathbf{r}') + \hat{n}_1 \times \oiint_{S_d} \mathbf{J}(\mathbf{r}') \times \nabla G_1(\mathbf{r}, \mathbf{r}') ds' = \hat{n}_1 \times \mathbf{H}^i \qquad (3.42b)$$

These are, respectively, the well known EFIE and MFIE for perfectly conducting surfaces. This MFIE is also known as *Maue's integral equation* and is the most common for solving the fields scattered by a closed conducting surface. It will be shown later that Maue's MFIE leads to a better conditioned matrix than (3.42a), and this is a primary reason for its popularity in simulating closed conducting surfaces. An EFIE which is of the same form as the MFIE (3.42b), can however be derived from (3.41a) by invoking image theory to eliminate the electric currents (since S_d is perfectly conducting). This gives

$$\frac{1}{2}\mathbf{M}(\mathbf{r}) + \hat{n}_1 \times \oiint_{S_d} \mathbf{M}(\mathbf{r}') \times \nabla G_1(\mathbf{r}, \mathbf{r}') ds' = -\hat{n}_1 \times \mathbf{E}^i \qquad (3.42c)$$

which is clearly the dual of (3.42b). Since (3.42c) and (3.42b) simulate the same metallic surface, it is not surprising that one can be derived from the other. Specifically, (3.42b) can be derived from (3.42c) by taking the curl of the last and making use of the equivalence relation (see (1.111))

$$\mathbf{J} = \frac{\nabla \times \mathbf{M}}{j\omega \mu_o \mu_{r1}}.$$

The fact that (3.42b) and (3.42c) are equivalent (i.e. they predict the same scattered fields) is a vivid demonstration that in the case of perfectly conducting surfaces, one could formulate the fields in terms of electric or magnetic currents.

We should remark that neither of (3.42) are valid for open conducting surfaces such as a metallic flat or curved plate (see figure 3.5). This is because

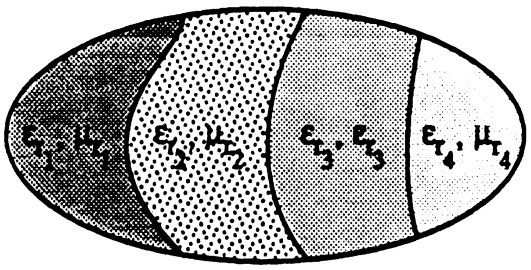

Figure 3.5: Piecewise homogeneous dielectric body.

the surface equivalence principle was used to introduce the equivalent surface currents. To construct an integral equation for the surface currents on a curved plate we may return to the original integral expression (2.52a) or (2.147) and set $\mathbf{M} = 0$. Then upon enforcing the boundary condition $\hat{n} \times (\mathbf{E}^s + \mathbf{E}^i) = 0$, we obtain the integral equation (also an EFIE)

$$+jk_o Z_o \mu_{r1} \hat{n} \times \int\int_S \left[\mathbf{J}(\mathbf{r}') G_1(\mathbf{r}, \mathbf{r}') + \frac{1}{k_o^2 \epsilon_{r1} \mu_{r1}} \mathbf{J}(\mathbf{r}') \cdot \nabla\nabla G_1(\mathbf{r}, \mathbf{r}') \right] ds'$$

$$= \hat{n} \times \mathbf{E}^i \qquad (3.43)$$

In contrast to the current appearing in (3.42), the one in this integral equation should be interpreted to represent the net flow between the top and bottom surfaces of the plate as illustrated in figure 3.3. With this interpretation of $\mathbf{J}$ and from the discussion in section 3.1.2, it is then seen that (3.43) is equivalent to (3.42a). Nevertheless, (3.43) is more difficult to implement than (3.42a) because of its higher kernel singularity.

3.1.5 Combined Field Integral Equations

Returning now to the original integral equation for the dielectric body we must address their uniqueness. Since they were formulated by assuming a null field

within certain enclosed volumes, in accordance with the uniqueness theorem (3.41) or (3.42) will fail at those frequencies associated with a resonant mode within S_d. Fortunately, the EFIE is associated with different resonant modes than the MFIE and this has been exploited to construct sets of equations which yield a unique solution. The most obvious approach is to consider various linear combinations of (3.41). For example, we could consider the combination [Mautz and Harrington, AEU, 1978]

$$\begin{aligned} \hat{n}_1 \times [\mathbf{E}_1^s + \alpha \mathbf{E}_2^s] &= -\hat{n}_1 \times \mathbf{E}^i \\ \hat{n}_1 \times [\mathbf{H}_1^s + \beta \mathbf{H}_2^s] &= -\hat{n}_1 \times \mathbf{H}^i \end{aligned} \tag{3.44}$$

where α and β are arbitrary non-zero scalars. If we set $\alpha = \beta = 1$ we obtain the PMCHW formulation [Poggio and Miller, 1973, Mittra, ed.] while the choice of $\alpha = -\epsilon_{r_2}/\epsilon_{r_1}$ and $\beta = -\mu_{r_2}/\mu_{r_1}$ leads to the Müeller formulation. Another combination which was proposed [Govind and Wilton, 1979] is

$$\begin{aligned} \hat{n}_1 \times \left[\mathbf{H}_1^s + \frac{\alpha}{Z_1}\mathbf{E}_1^s\right] &= -\hat{n}_1 \times \left[\mathbf{H}_1^i + \frac{\alpha}{Z_1}\mathbf{E}^i\right] \\ \hat{n}_1 \times \left[\mathbf{H}_2^s - \frac{\beta}{Z_2}\mathbf{E}_2^s\right] &= 0 \end{aligned} \tag{3.45}$$

in which $Z_1 = Z_0\sqrt{\mu_{r_1}/\epsilon_{r_1}}$, $Z_2 = Z_0\sqrt{\mu_{r_2}/\epsilon_{r_2}}$ whereas α and β are again arbitrary scalars. Finally, a third coupled set of integral was proposed by Yagjian [Radio Science, Nov.-Dec. 1981] who noted that the continuity equations are not necessarily satisfied when resonant modes are present. On this basis, the continuity equations can be combined with (3.41) and (3.42) to yield the conditions

$$\begin{aligned} \hat{n}_1 \times \mathbf{E}_1^s + \nabla \cdot \mathbf{J} + j\omega\epsilon_o\epsilon_{r_1}\hat{n}_1 \cdot \mathbf{E} &= -\hat{n}_1 \times \mathbf{E}^i \\ \hat{n}_1 \times \mathbf{H}_1^s + \nabla \cdot \mathbf{M} + j\omega\mu_o\mu_{r_1}\hat{n}_1 \cdot \mathbf{H} &= -\hat{n}_1 \times \mathbf{H}^i \end{aligned} \tag{3.46}$$

From these we can readily derive integral equations for $(\mathbf{J}, \mathbf{M})$ upon substituting for the fields as given in (3.31). The integral equations based on (3.44) or (3.45) are generally referred to the literature as the *combined field integral equations* (CFIE) whereas the integral equations resulting from (3.46) is

referred to as the *augmented field integral equations* (AFIE). They have all been used primarily for scattering computations and their solution will be considered later. The CFIE have also been used for radiation problems relating to various types of cavity antennas. As can be expected, the CFIE cannot yield unique solutions at those frequencies where the electric and magnetic field integral equations fall concurrently. In addition, for very large structures the spurious resonant modes of S_d are congruent leading to inaccuracies in the solution of CFIE. Further, it has been noted that the AFIE does not ensure the removal of all spurious resonances and later we will discuss other remedies which can ensure uniqueness at the resonant frequencies of the cavity enclosed by S_d.

3.1.6 Integral Equations for Piecewise Homogeneous Dielectrics

The formulation presented in the previous section for treating homogeneous dielectrics can be readily extended to bodies composed of various homogeneous dielectric sections as shown in Figure 3.5. Let us for example consider the structure in Figure 3.6 consisting of a dielectric and a perfectly conducting section. We shall denote the surface of the conducting section which borders the exterior region (region #1) as S_{dc_1} and that which borders the dielectric region of the body (region #2) as S_{dc_2}. Also, the surface of the dielectric which borders the exterior regions will be denoted as S_{dc}. The exterior region has relative dielectric constants $(\epsilon_{r_1}, \mu_{r_1})$ and a characteristic impedance $Z_1 = Z_o\sqrt{\frac{\mu_{r_1}}{\epsilon_{r_1}}}$. Correspondingly, the interior dielectric region has relative dielectric constants $(\epsilon_{r_2}, \mu_{r_2})$ and a characteristic impedance $Z_2 = Z_o\sqrt{\frac{\mu_{r_2}}{\epsilon_{r_2}}}$. We shall assume that the excitation fields $(\mathbf{E}^i, \mathbf{H}^i)$ will be in the exterior region although they can also be placed within the interior dielectric region as is likely the case with cavity type antennas [IEEE AP-S Magazine, April 1991].

Following the formulation presented in the previous section, we refer to Fig. 3.5 and introduce the equivalent currents $\mathbf{J}_{c_1}$ and $\mathbf{J}_{c_2}$ on the conducting surfaces S_{dc_1} and S_{dc_2}, respectively. Since S_{dc_1} and S_{dc_2} border perfect conductors we choose to retain only the electric equivalent currents although one could also choose to formulate the fields in terms of magnetic currents as discussed in the previous section. On the dielectric surface S_{de} which borders the exterior region we introduce the equivalent electric and magnetic currents $(\mathbf{J}_d, \mathbf{M}_d)$. In

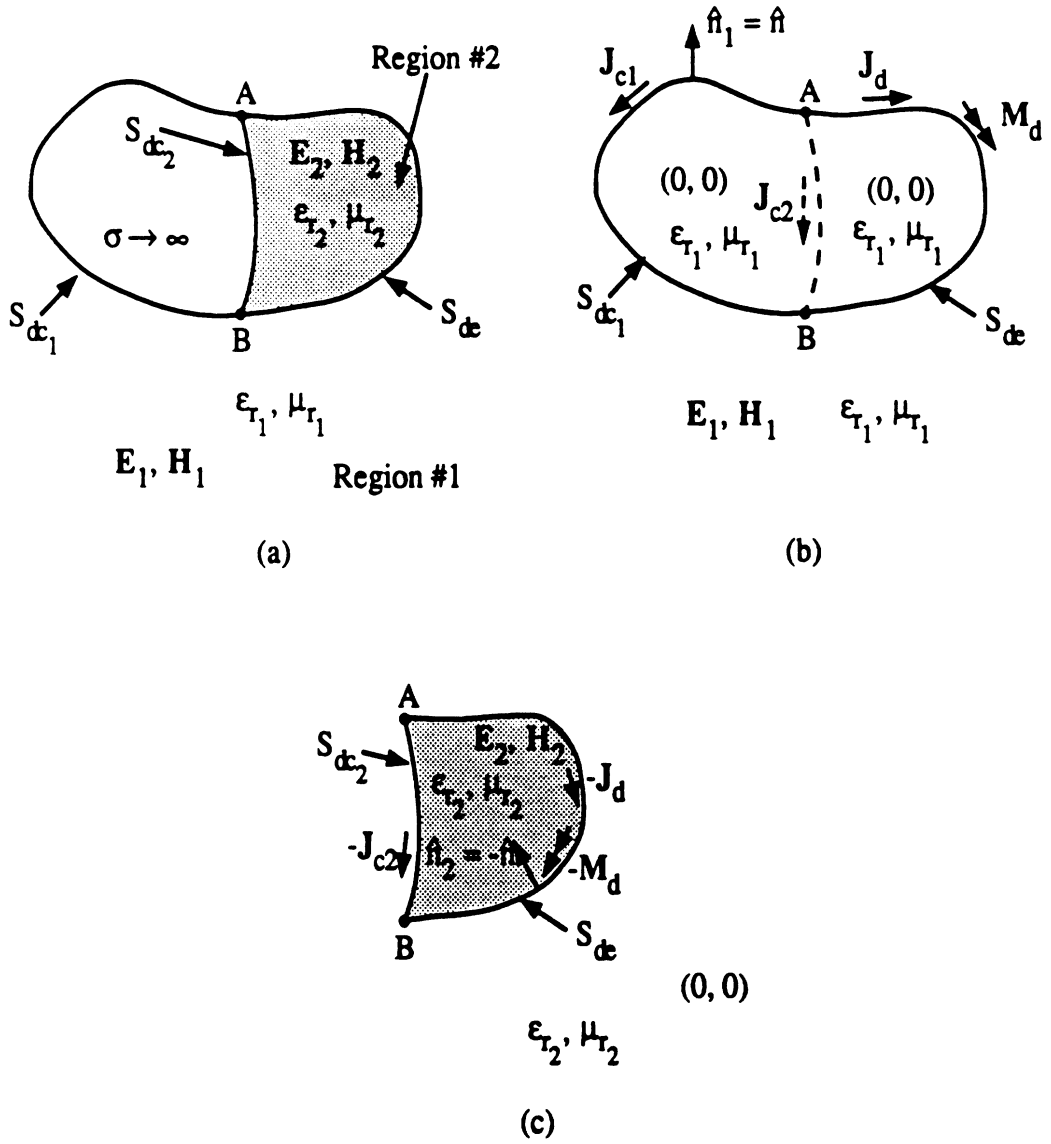

Figure 3.6: Application of equivalence principle for a conductor dielectric body. (a) original problem (b) equivalent problem for the exterior fields (c) equivalent problem for the interior fields.

accordance with the model in Figure 3.6(b) the boundary conditions are

$$\begin{aligned}
\hat{n} \times \mathbf{E}_1 &= \hat{n} \times (\mathbf{E}^i + \mathbf{E}_1^s) = 0 \quad \text{on } S_{dc_1} \\
\hat{n} \times \mathbf{H}_1 &= \hat{n} \times (\mathbf{H}^i + \mathbf{H}_1^s) = 0 \quad \text{on } S_{dc_1} \\
\hat{n} \times \mathbf{E}_1 &= \hat{n} \times (\mathbf{E}^i + \mathbf{E}_1^s) = 0 \quad \text{on } S_{de} \\
\hat{n} \times \mathbf{H}_1 &= \hat{n} \times (\mathbf{H}_1 + \mathbf{H}_1^s) = 0 \quad \text{on } S_{de}
\end{aligned} \tag{3.47}$$

in which the scattered fields are given by

$$\begin{aligned}
\mathbf{E}_1^s = &- \int\int_{S_{dc_1}} \left[jk_o Z_o \mu_{r_1} \mathbf{J}_{c_1}(\mathbf{r}') G_1(\mathbf{r}, \mathbf{r}') + \frac{jZ_o}{k_o \epsilon_{r_1}} \nabla_s' \cdot \mathbf{J}_{c_1}(\mathbf{r}') \nabla G_1(\mathbf{r}, \mathbf{r}') \right] ds' \\
&+ \int\int_{S_{de}} \left[\mathbf{M}_d(\mathbf{r}') \times \nabla G_1(\mathbf{r}, \mathbf{r}') - jk_o Z_o \mu_{r_1} \mathbf{J}_d(\mathbf{r}) G_1(\mathbf{r}, \mathbf{r}') \right. \\
&\left. - \frac{jZ_o}{k_o \epsilon_{r_1}} \nabla_s' \cdot \mathbf{J}_d(\mathbf{r}') \nabla G_1(\mathbf{r}, \mathbf{r}') \right] ds'
\end{aligned} \tag{3.48a}$$

$$\begin{aligned}
\mathbf{H}_1^s = &- \int\int_{S_{dc_1}} \mathbf{J}_{c_1}(\mathbf{r}') \times \nabla G_1(\mathbf{r}, \mathbf{r}') ds' + \int\int_{S_{de}} \left[-\mathbf{J}_d(\mathbf{r}') \times \nabla G_1(\mathbf{r}, \mathbf{r}') \right. \\
&\left. - jk_o Y_o \epsilon_{r_1} \mathbf{M}_d(\mathbf{r}') G_1(\mathbf{r}, \mathbf{r}') - \frac{jY_o}{k_o \mu_{r_1}} \nabla_s' \cdot \mathbf{M}_d(\mathbf{r}') \nabla G_1(\mathbf{r}, \mathbf{r}') \right] ds'
\end{aligned} \tag{3.48b}$$

It should be noted that $\mathbf{J}_{c_2}$ does not enter into the representation of the exterior fields $(\mathbf{E}_1, \mathbf{H}_1)$ because it is completely enclosed by the surface S_{dc_1} and S_{de}. Thus, in accordance with the equivalence principle it does not contribute to $(\mathbf{E}_1, \mathbf{H}_1)$. However, it does radiate in the dielectric region and its effect in the exterior region is observed through the modifications it causes to $(\mathbf{J}_d, \mathbf{M}_d)$. This will be more apparent when the interior fields $(\mathbf{E}_2, \mathbf{H}_2)$ are formulated. To solve for the current densities, (3.48) are substituted into the boundary conditions (3.47) and upon making use of the identity (3.37) and the operator definitions (3.33) - (3.36), we obtain the integral equations

$$-\hat{n} \times L_{1E_m}(\mathbf{M}_d) - \hat{n} \times L_{1E_e}(\mathbf{J}_d) - \hat{n} \times L_{1E_e}(\mathbf{J}_{c_1}) = \hat{n} \times \mathbf{E}^i$$

$$\mathbf{r} \text{ on } S_{dc_1} \quad (3.49a)$$

$$+\frac{1}{2}\mathbf{J}_{c_1}(\mathbf{r}) - \hat{n} \times L_{1H_e}(\mathbf{J}_{c_1}) - \hat{n} \times L_{1H_e}(\mathbf{J}_d) - \hat{n} \times L_{1H_m}(\mathbf{M}_d) = \hat{n} \times \mathbf{H}^i$$
$$\mathbf{r} \text{ on } S_{dc_1} \quad (3.49b)$$

$$-\frac{1}{2}\mathbf{M}_d(\mathbf{r}) - \hat{n} \times L_{1E_m}(\mathbf{M}_d) - \hat{n} \times L_{1E_e}(\mathbf{J}_d) - \hat{n} \times L_{1E_e}(\mathbf{J}_{c_1}) = \hat{n} \times \mathbf{E}^i$$
$$\mathbf{r} \text{ on } S_{de} \quad (3.49c)$$

$$\frac{1}{2}\mathbf{J}_d(\mathbf{r}) - \hat{n} \times L_{1H_e}(\mathbf{J}_{c_1}) - \hat{n} \times L_{1H_e}(\mathbf{J}_d) - \hat{n} \times L_{1H_m}(\mathbf{M}_d) = \hat{n} \times \mathbf{H}^i$$
$$\mathbf{r} \text{ on } S_{de} \quad (3.49d)$$

In addition to these, we can derive another set of four integral equations by referring to Figure 3.6 and enforcing the boundary conditions relating to the interior fields $(\mathbf{E}_2, \mathbf{H}_2)$.

Since we have assumed that no sources exist within the dielectric region the boundary condition for the interior fields are

$$\begin{aligned} \hat{n} \times \mathbf{E}_2 &= \hat{n} \times \mathbf{E}_2^s = 0 \quad \text{on } S_{dc_2} \\ \hat{n} \times \mathbf{H}_2 &= \hat{n} \times \mathbf{H}_2^s = 0 \quad \text{on } S_{dc_2} \\ \hat{n} \times \mathbf{E}_2 &= \hat{n} \times \mathbf{E}_2^s = 0 \quad \text{on } S_{de} \\ \hat{n} \times \mathbf{H}_2 &= \hat{n} \times \mathbf{H}_2^s = 0 \quad \text{on } S_{de} \end{aligned} \quad (3.50)$$

By invoking tangential field continuity across the dielectric boundary S_{de}, it follows that the interior fields are generated by the negative of the currents used for formulating the exterior fields. Thus, the interior fields are given by

$$\mathbf{E}_2 = \mathbf{E}_2^s = \int\int_{S_{dc_2}} \left[jk_o Z_o \mu_{r_2} \mathbf{J}_{c_2}(\mathbf{r}') G_2(\mathbf{r}, \mathbf{r}') + \frac{jZ_o}{k_o \epsilon_{r_2}} \nabla_s' \cdot \mathbf{J}_{c_1}(\mathbf{r}') \nabla G_2(\mathbf{r}, \mathbf{r}') \right] ds'$$

$$- \int\int_{S_{de}} \left[\mathbf{M}_d(\mathbf{r}') \times \nabla G_2(\mathbf{r},\mathbf{r}') - jk_o Z_o \mu_{r_2} \mathbf{J}_d(\mathbf{r}') G_2(\mathbf{r},\mathbf{r}') \right.$$
$$\left. - \frac{jZ_o}{k_o \epsilon_{r_2}} \nabla'_s \cdot \mathbf{J}_d(\mathbf{r}') \nabla G_2(\mathbf{r},\mathbf{r}') \right] ds' \qquad (3.51a)$$

$$\mathbf{H}_2 = \mathbf{H}_2^s = \int\int_{S_{dc_2}} \mathbf{J}_{c_2}(\mathbf{r}') \times \nabla G_2(\mathbf{r},\mathbf{r}')$$
$$+ \int\int_{S_{de}} \left[\mathbf{J}_d(\mathbf{r}') \times \nabla G_2(\mathbf{r},\mathbf{r}') - jk_o Y_o \epsilon_{r_2} \mathbf{M}_d(\mathbf{r}') G_2(\mathbf{r},\mathbf{r}') \right.$$
$$\left. - \frac{jY_o}{k_o \mu_{r_2}} \nabla'_s \cdot \mathbf{M}_d(\mathbf{r}') \nabla G_2(\mathbf{r},\mathbf{r}') \right] ds' \qquad (3.51b)$$

in which

$$G_2(\mathbf{r},\mathbf{r}') = \frac{e^{-jk_o\sqrt{\mu_{r_2}\epsilon_{r_2}}|\mathbf{r}-\mathbf{r}'|}}{4\pi|\mathbf{r}-\mathbf{r}'|}$$

Substituting these into the boundary conditions (3.50) and making use of the identity (3.37) and definitions similar to those in (3.33) - (3.36) we obtain the integral equations

$$-\hat{n} \times L_{2E_m}(\mathbf{M}_d) - \hat{n} \times L_{2E_e}(\mathbf{J}_d) - \hat{n} \times L_{2E_e}(\mathbf{J}_{c_2}) = 0 \quad \mathbf{r} \text{ on } S_{dc_2} \qquad (3.52a)$$

$$-\frac{1}{2}\mathbf{J}_{c_2}(\mathbf{r}) - \hat{n} \times L_{2H_e}(\mathbf{J}_{c2}) - \hat{n} \times L_{2H_e}(\mathbf{J}_d) - \hat{n} \times L_{2H_m}(\mathbf{M}_d) = 0 \quad \mathbf{r} \text{ on } S_{dc_2} \qquad (3.52b)$$

$$\frac{1}{2}\mathbf{M}_d(\mathbf{r}) - \hat{n} \times L_{2E_m}(\mathbf{M}_d) - \hat{n} \times L_{2E_e}(\mathbf{J}_d) - \hat{n} \times L_{2E_e}(\mathbf{J}_{c_2}) = 0 \quad \mathbf{r} \text{ on } S_{de} \qquad (3.52c)$$

$$-\frac{1}{2}\mathbf{J}_d(\mathbf{r}) - \hat{n} \times L_{2H_e}(\mathbf{J}_d) - \hat{n} \times L_{2H_e}(\mathbf{J}_{c_2}) - \hat{n} \times L_{2H_m}(\mathbf{M}_d) = 0 \quad \mathbf{r} \text{ on } S_{de} \qquad (3.52d)$$

which can be combined with (3.49) for a solution of the surface current densities. We have, of course, eight vector equations whereas only four are needed

to solve for $\mathbf{J}_{c_1}$, $\mathbf{J}_{c_2}$, $\mathbf{J}_d$ and $\mathbf{M}_d$. We may choose the four EFIE which result from the boundary conditions

$$\begin{aligned}
\hat{n} \times \left(\mathbf{E}^i + \mathbf{E}_1^s\right) &= 0 \quad \text{on } S_{dc_1} \\
\hat{n} \times \mathbf{E}_2 &= 0 \quad \text{on } S_{dc_2} \\
\hat{n} \times \left(\mathbf{E}^i + \mathbf{E}_1^s\right) &= 0 \quad \text{on } S_{de} \\
\hat{n} \times \mathbf{E}_2 &= 0 \quad \text{on } S_{de}
\end{aligned} \tag{3.53}$$

or the four MFIE which result from the boundary conditions

$$\begin{aligned}
\hat{n} \times \left(\mathbf{H}^i + \mathbf{H}_1^s\right) &= 0 \quad \text{on } S_{dc_1} \\
\hat{n} \times \mathbf{H}_2 &= 0 \quad \text{on } S_{dc_2} \\
\hat{n} \times \left(\mathbf{H}^i + \mathbf{H}_1^s\right) &= 0 \quad \text{on } S_{de} \\
\hat{n} \times \mathbf{H}_2 &= 0 \quad \text{on } S_{de}
\end{aligned} \tag{3.54}$$

However, as noted in the previous section the integral equation set based on (3.53) or (3.54) fail to yield unique solutions when the excitation frequency coincides with an internal resonance. In this case we may again combine (3.53) and (3.54) to obtain, for example, the CFIE set resulting from the boundary condition

$$\begin{aligned}
\hat{n} \times [\mathbf{E}_1^s + \alpha \mathbf{E}_2] &= -\hat{n} \times \mathbf{E}^i \quad \text{on } S_{de} \\
\hat{n} \times [\mathbf{H}_1^s + \beta \mathbf{H}_2] &= -\hat{n} \times \mathbf{H}^i \quad \text{on } S_{de} \\
\hat{n} \times \left(\mathbf{E}^i + \mathbf{E}_1^s\right) &= 0 \quad \text{on } S_{dc_1} \\
\hat{n} \times \mathbf{E}_2 &= 0 \quad \text{on } S_{dc_2}
\end{aligned} \tag{3.55}$$

in which α and β are arbitrary scalars and can be set equal to the values discussed below equation (3.44). Another CFIE set can be obtained by enforcing the boundary conditions

$$\begin{aligned}
\hat{n} \times \left[\mathbf{E}^i + \mathbf{E}_1^s\right] + \frac{\alpha}{Z_1}\hat{n} \times \left[\mathbf{H}^i + \mathbf{H}_1^s\right] &= 0 \quad \text{on } S_{dc_1} \\
\hat{n} \times \mathbf{E}_2 + \frac{\beta}{Z_2}\hat{n} \times \mathbf{H}_2 &= 0 \quad \text{on } S_{dc_2} \\
\hat{n} \times (\mathbf{E}^i + \mathbf{E}_1^s) + \frac{\gamma}{Z_1}\hat{n} \times (\mathbf{H}^i + \mathbf{H}_1^s) &= 0 \quad \text{on } S_{de} \\
\hat{n} \times \mathbf{E}_2 + \frac{\delta}{Z_2}\hat{n} \times \mathbf{H}_2 &= 0 \quad \text{on } S_{de}
\end{aligned} \tag{3.56}$$

where again α, β, γ, and δ are arbitrary scalars similar to those appearing in (3.45). As can be realized there are several other CFIE which could be generated through various combinations of the EFIE and HFIE [Shafai, etc., AP Magazine, April 1991], [Rao and Wilton, Electromagnetics, 1990, pp. 407-421]. Alternatively, one could combine the EFIE and HFIE with the integral equations derived from the continuity equations as discussed in the previous section in connection with the augmented field integral equations (AFIE).

3.1.7 Integral Equations for Inhomogeneous Dielectrics

In the previous section we developed integral equations for piecewise homogeneous structures. This was accomplished by treating each homogeneous section separately in a manner permitting us to employ a uniform set of dielectric constants over the entire region of interest. The fields and equations generated from each homogeneous section were then coupled by enforcing tangential field continuity at the transition boundaries of the different dielectric regions. An important aspect of this approach was the use of the unbounded space Green's function for the treatment of each homogeneous region. Obviously in the case of an inhomogeneous dielectric region (i.e. a region in which the permittivity and permeability are arbitrary functions of $\mathbf{r}$) this approach cannot be used because of a lack of an appropriate Green's function.

A standard approach in modeling inhomogeneous dielectrics is to employ the volume equivalence principle rather than the surface equivalence principle

used for sectionally homogeneous dielectrics. Let us consider the inhomogeneous dielectric volume V_d as shown in Figure 3.7 in the presence of some excitation field $(\mathbf{E}^i, \mathbf{H}^i)$ whose source may be within V_d or exterior to it. The total

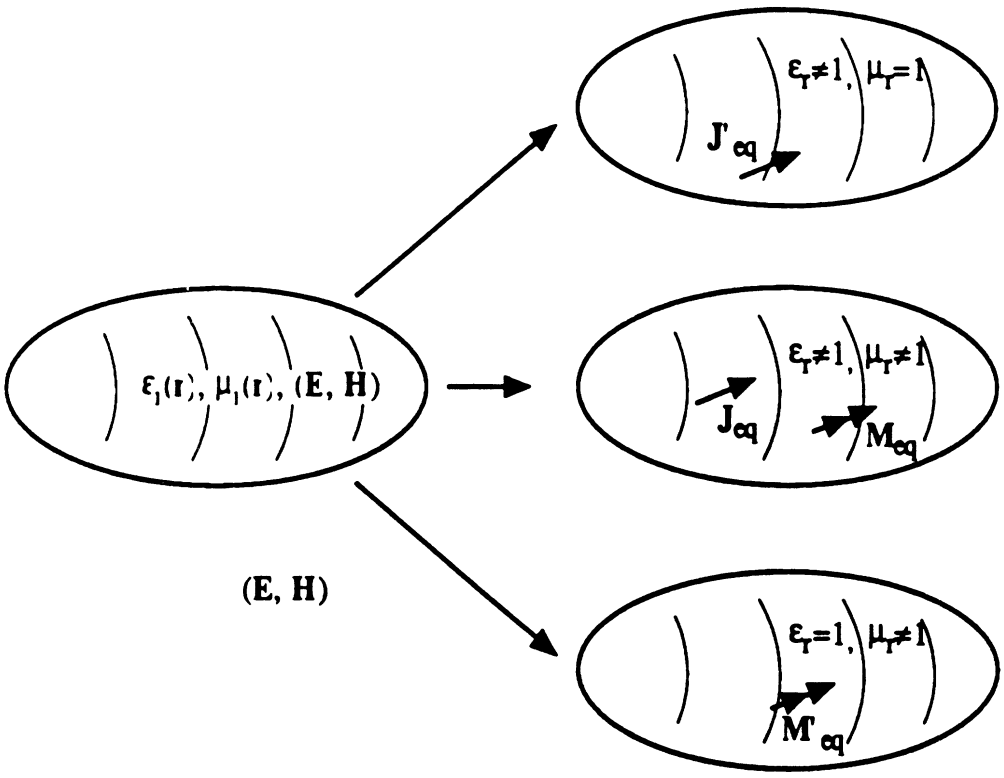

Figure 3.7: Volume equivalences for an inhomogeneous dielectric. The equivalent sources $\mathbf{J}_{eq}, \mathbf{M}_{eq}, \mathbf{J}'_{eq}$ and $\mathbf{M}'_{eq}$ are respectively defined in (3.58), (1.112) and (1.113).

field $(\mathbf{E}, \mathbf{H})$ in the presence of the dielectric volume V_d can then be written as

$$\mathbf{E} = \mathbf{E}^i + \mathbf{E}^s \quad \mathbf{H} = \mathbf{H}^i + \mathbf{H}^s \tag{3.57}$$

where $(\mathbf{E}^s, \mathbf{H}^s)$ are the scattered fields caused by the presence of the dielectric (i.e. they may comprise the reflected, diffracted fields and their interactions). In accordance with the volume equivalence principle (see section 1.9), the scattered fields may be represented by the field generated from the equivalent volume sources

$$\mathbf{J}_{eq} = j\omega\epsilon_o(\epsilon_r - 1)\mathbf{E}, \quad \mathbf{M}_{eq} = j\omega\mu_o(\mu_r - 1)\mathbf{H} \tag{3.58}$$

where ϵ_r and μ_r can be arbitrary functions of position. Obviously, since ϵ_r and μ_r are unity exterior to V_d, these equivalent currents exist only within the dielectric volume (see Fig. 3.7). From (2.52), (2.69), (2.102) or (3.13) the scattered electric field can now be expressed as

$$\begin{aligned}
\mathbf{E}^s &= \iiint_{V_d} \Big[\mathbf{M}_{eq}(\mathbf{r}') \times \nabla G_o(\mathbf{r},\mathbf{r}') - jk_o Z_o \mathbf{J}_{eq}(\mathbf{r}') G_o(\mathbf{r},\mathbf{r}') \\
&\quad - \frac{jZ_o}{k} \mathbf{J}_{eq}(\mathbf{r}') \cdot \nabla\nabla G_o(\mathbf{r},\mathbf{r}') \Big] dv' + \frac{jZ_o}{3k_o} \mathbf{J}_{eq}(\mathbf{r}) \\
&= \iiint_{V_d} \Big[\mathbf{M}_{eq}(\mathbf{r}') \times \nabla G_o(\mathbf{r},\mathbf{r}') - jk_o Z_o \mathbf{J}_{eq}(\mathbf{r}') G_o(\mathbf{r},\mathbf{r}') \\
&\quad - \frac{jZ_o}{k_o} \nabla' \cdot \mathbf{J}_{eq}(\mathbf{r}') \nabla G_o(\mathbf{r},\mathbf{r}') \Big] dv' + \frac{jZ_o}{3k_o} \mathbf{J}_{eq}(\mathbf{r}) \\
&= \iiint_{V_d} \Big[\nabla \times \overline{\Gamma}_o(\mathbf{r},\mathbf{r}') \cdot \mathbf{M}_{eq}(\mathbf{r}') + jk_o Z_o \overline{\Gamma}_o(\mathbf{r},\mathbf{r}') \cdot \mathbf{J}_{eq}(\mathbf{r}') \Big] dv' \\
&\quad + \frac{jZ_o}{3k_o} \mathbf{J}_{eq}(\mathbf{r}) \qquad (3.59)
\end{aligned}$$

and $\mathbf{H}^s$ can be obtained by duality. In this, $G_o(\mathbf{r},\mathbf{r}')$ denotes the free space Green's function given by (2.37) with $k = k_o\omega\sqrt{\mu_o\epsilon_o}$, i.e.

$$G_o(\mathbf{r},\mathbf{r}') = \frac{e^{-jk_o|\mathbf{r}-\mathbf{r}'|}}{4\pi|\mathbf{r}-\mathbf{r}'|} = \frac{e^{-jk_oR}}{4\pi R} \qquad (3.60)$$

and $Z_o = 1/Y_o$ is the free space intrinsic impedance. Also, $\overline{\Gamma}_o$ is the free space dyadic Green's function given by (2.95) upon replacing k with k_o, i.e.

$$\overline{\Gamma}_o(\mathbf{r},\mathbf{r}') = -\left[\overline{\mathbf{I}} + \frac{\nabla\nabla}{k_o^2}\right] G_o(\mathbf{r},\mathbf{r}') \qquad (3.61)$$

To obtain an integral equation for the solution of the currents $(\mathbf{J}_{eq}, \mathbf{M}_{eq})$ we substitute (3.57) into (3.58) and this yields

$$\mathbf{J}_{eq} = jk_oY_o(\epsilon_r - 1)\left[\mathbf{E}^i + \mathbf{E}^s\right] \qquad (3.62a)$$

$$\mathbf{M}_{eq} = jk_oZ_o(\mu_r - 1)\left[\mathbf{H}^i + \mathbf{H}^s\right] \qquad (3.62b)$$

By introducing the integral expression for the scattered electric field and its dual we then obtain a coupled set of integral equations for the solution of $(\mathbf{J}_{eq}, \mathbf{M}_{eq})$. The solution of such an integral set will be considered later.

By this time, it should be obvious to the reader that the introduction of the equivalent currents is a matter of convenience since one could instead formulate the scattered fields without invoking such currents. For example, the Stratton-Chu surface integral equation can be written in terms of the surface fields as given by (3.17) or in terms of equivalent currents as given by (3.13). Also, the integral equations presented in the previous section for homogeneous dielectrics could be rewritten by replacing the equivalent surface currents with tangential surface fields. This amounts to substituting, for example, (3.28) - (3.29) into the integral equations (3.38) or (3.40). These can then be solved to find the unknown surface fields from which we can obtain the fields elsewhere by employing, for example, the Stratton-Chu integral equation (3.17) or some other equivalent expression. Not surprising therefore, we can rewrite the scattered field expressions (3.59) by replacing the equivalent currents with quantities which involve the electric and magnetic fields within the volume. For example, (3.58) can be substituted into (3.59) and then (3.57) provide a coupled set of integral equations for the solution of the fields within the dielectric's volume V_d. This integral equation set, as well as that implied by (3.62) in conjunction with (3.59) involve a total of six unknown field or current components per volume location for non-trivial ϵ_r and μ_r. If $\mu_r = 1$ then $\mathbf{M}_{eq} = 0$ or $\mu_r - 1 = 0$ and the number of unknowns reduce to three, involving the three components of the electric field within each point in the volume V_d. Alternatively, if $\epsilon_r = 1$ only the three components of magnetic field or the magnetic equivalent current are required for determining the fields everywhere.

As will be seen later, the traditional numerical implementation of the coupled set (3.62) for non-trivial ϵ_r and μ_r demands substantial computer memory and it is thus of interest to reduce the number of unknown quantities as much as possible. One approach is to employ the equivalent current expression (1.112)

$$\mathbf{J}'_{eq} = \frac{\epsilon_r - 1}{\epsilon_r} \nabla \times \mathbf{H} + \nabla \times [(\mu_r - 1)\mathbf{H}]$$

which combines the radiation effects of $\mathbf{J}_{eq}$ and $\mathbf{M}_{eq}$ given by (3.58). The

scattered fields can then be expressed as

$$\mathbf{E}^s = jk_oZ_o \int\int\int_{V_d} \overline{\Gamma}_o(\mathbf{r},\mathbf{r}') \cdot \left\{ \frac{\epsilon_r - 1}{\epsilon_r} \nabla' \times \mathbf{H}(\mathbf{r}') + \nabla' \times [(\mu_r - 1)\mathbf{H}(\mathbf{r}')] \right\} dv' \tag{3.63a}$$

$$\mathbf{H}^s = -\int\int\int_{V_d} \nabla \times \overline{\Gamma}_o(\mathbf{r},\mathbf{r}') \cdot \left\{ \frac{\epsilon_r - 1}{\epsilon_r} \nabla' \times \mathbf{H}(\mathbf{r}') + \nabla' \times [(\mu_r - 1)\mathbf{H}(\mathbf{r}')] \right\} dv' \tag{3.63b}$$

in which the primed del operator ∇' implies differentiation with respect to the primed variables and in the integrals ϵ_r and μ_r may be functions of $\mathbf{r}'$. By substituting (3.63b) into the second of (3.57), we obtain the integral equation

$$\mathbf{H} = \mathbf{H}^i - \int\int\int_{V_d} \nabla \times \overline{\Gamma}_o(\mathbf{r},\mathbf{r}') \cdot \left\{ \frac{\epsilon_r - 1}{\epsilon_r} \nabla' \times \mathbf{H}(\mathbf{r}') + \nabla' \times [(\mu_r - 1)\mathbf{H}(\mathbf{r}')] \right\} dv' \tag{3.64}$$

We may also substitute (3.63a) into the first of (3.57) and by taking the curl of the resulting equation we recover (3.64). Alternatively, we may formulate an integral equation for the electric field by introducing the magnetic equvalent current (1.113)

$$\mathbf{M}'_{eq} = -\frac{\mu_r - 1}{\mu_r} \nabla \times \mathbf{E} - \nabla \times [(\epsilon_r - 1)\mathbf{E}]$$

to replace $\mathbf{J}_{eq}$ and $\mathbf{M}_{eq}$ of (3.58). The scattered fields are then given by

$$\mathbf{E}^s = -\int\int\int_{V_d} \nabla \times \overline{\Gamma}_o(\mathbf{r},\mathbf{r}') \cdot \left\{ \frac{\mu_r - 1}{\mu_r} \nabla' \times \mathbf{E}(\mathbf{r}') + \nabla' \times [(\epsilon_r - 1)\mathbf{E}(\mathbf{r}')] \right\} dv' \tag{3.65a}$$

$$\mathbf{H}^s = -jk_oY_o \int\int\int_{V_d} \overline{\Gamma}_o(\mathbf{r},\mathbf{r}') \cdot \left\{ \frac{\mu_r - 1}{\mu_r} \nabla' \times \mathbf{E}(\mathbf{r}') + \nabla' \times [(\epsilon_r - 1)\mathbf{E}(\mathbf{r}')] \right\} dv' \tag{3.65b}$$

and when these are substituted into (3.57) we obtain the integral equation

$$\mathbf{E} = \mathbf{E}^i - \int\int\int_{V_d} \nabla \times \overline{\Gamma}_o(\mathbf{r},\mathbf{r}') \cdot \left\{ \frac{\mu_r - 1}{\mu_r} \nabla' \times \mathbf{E}(\mathbf{r}') + \nabla' \times [(\epsilon_r - 1)\mathbf{E}(\mathbf{r}')] \right\} dv' \tag{3.66}$$

which as expected is the dual of (3.64).

From (3.63) - (3.66) it is seen that one could formulate the fields in an inhomogeneous dielectric volume, either in terms of the magnetic field or the electric field. In contrast, the integral expressions (3.59) require knowledge of both the electric and the magnetic fields. Clearly, the numerical solution of (3.64) or (3.66) requires only three unknown components per volume point but the presence of the curl operations on the unknown volume fields complicates their implementation. It is, thus, instructive to find alternative expressions to (3.63) or (3.65) which do not involve the curl of the unknown field. This is possible, and to develop the resulting integral expression let us begin with (3.59) which upon introducing the volume equivalent current expressions (3.58) becomes

$$\mathbf{E}^s = -k_o^2 \int\int\int_{V_d} (\epsilon_r - 1)\mathbf{E}(\mathbf{r}') \cdot \overline{\Gamma}_o(\mathbf{r},\mathbf{r}') dv' - j\omega\mu_o \nabla \times \int\int\int_{V_d} (\mu_r - 1)\mathbf{H}(\mathbf{r}') G_o(\mathbf{r},\mathbf{r}') dv' \tag{3.67}$$

We can rewrite the second integral in this by introducing Maxwell's equation $\nabla \times \mathbf{E} = -j\omega\mu_o\mu_r\mathbf{H}$ giving

$$\mathbf{E}_m^s = -j\omega\mu_o \nabla \times \int\int\int_{V_d} (\mu_r - 1)\mathbf{H}(\mathbf{r}') G_o(\mathbf{r},\mathbf{r}') dv'$$

$$= \nabla \times \int\int\int_{V_d} \left(1 - \frac{1}{\mu_r}\right) G_o(\mathbf{r},\mathbf{r}') \nabla' \times \mathbf{E}(\mathbf{r}') dv' \tag{3.68}$$

Further by using the identities

$$\nabla \times [\nabla' \times (\phi\mathbf{E})] = \nabla \times [\nabla'\phi \times \mathbf{E}] + \nabla \times [\phi \nabla' \times \mathbf{E}] \tag{3.69}$$

$$\nabla(\phi\psi) = \psi\nabla\phi + \phi\nabla\psi \tag{3.70}$$

we obtain

$$\begin{aligned}\mathbf{E}_m^s &= \nabla \times \iiint_{V_d} \nabla' \times \left\{ \left(1 - \frac{1}{\mu_r}\right) G_o(\mathbf{r},\mathbf{r}')\mathbf{E}(\mathbf{r}') \right\} dv' \\ &\quad - \nabla \times \iiint_{V_d} \left\{ \left(1 - \frac{1}{\mu_r}\right) \nabla' G_o(\mathbf{r},\mathbf{r}') \times \mathbf{E}(\mathbf{r}') \right\} dv' \\ &\quad + \nabla \times \iiint_{V_d} \left\{ G_o(\mathbf{r},\mathbf{r}') \nabla' \left(\frac{1}{\mu_r}\right) \times \mathbf{E}(\mathbf{r}') \right\} dv' \\ &= \mathbf{F}_{I_1} + \mathbf{F}_{I_2} + \mathbf{F}_{I_3} \end{aligned} \tag{3.71}$$

The first of the integrals in (3.71) can be transformed to a surface integral by invoking the vector Stokes identity

$$\iiint_V (\nabla \times \mathbf{F}) dv = \oiint_{S_c} (\hat{n} \times \mathbf{F}) ds \tag{3.72}$$

This gives

$$\begin{aligned}\mathbf{F}_{I_1} &= \nabla \times \iiint_{V_d} \nabla' \times \left\{ \left(1 - \frac{1}{\mu_r}\right) G_o(\mathbf{r},\mathbf{r}')\mathbf{E}(\mathbf{r}') \right\} dv' \\ &= \nabla \times \oiint_{S_d} \left(1 - \frac{1}{\mu_r}\right) G_o(\mathbf{r},\mathbf{r}')\hat{n}' \times \mathbf{E}(\mathbf{r}') ds' \\ &= -\oiint_{S_d} \left(1 - \frac{1}{\mu_r}\right) [\hat{n}' \times \mathbf{E}(\mathbf{r}')] \times \nabla G_o(\mathbf{r},\mathbf{r}') ds' \end{aligned} \tag{3.73}$$

in which $\hat{n}' = \hat{n}(\mathbf{r}')$ is the outward unit surface normal to the surface S_d and $\mu_r = \mu_r(\mathbf{r}')$. For the second integral in (3.71) we have

$$\begin{aligned}\mathbf{F}_{I_2} &= -\nabla \times \iiint_{V_d} \left(1 - \frac{1}{\mu_r}\right) \nabla' G_o(\mathbf{r},\mathbf{r}') \times \mathbf{E}(\mathbf{r}') dv' \\ &= -\iiint_{V_d} \left(1 - \frac{1}{\mu_r}\right) \nabla \times [\nabla' G_o(\mathbf{r},\mathbf{r}') \times \mathbf{E}(\mathbf{r}')] dv' \end{aligned} \tag{3.74}$$

and by employing the identity [Van Bladel, p. 487]

$$\begin{aligned}\nabla \times (\nabla' G_o \times \mathbf{E}) &= \nabla' G_o \nabla \cdot \mathbf{E} - \mathbf{E}\nabla \cdot \nabla' G_o + \mathbf{E} \cdot \nabla\nabla' G_o - \nabla' G_o \cdot \nabla \mathbf{E} \\ &= \mathbf{E}\nabla^2 G_o - \mathbf{E} \cdot \nabla\nabla G_o \end{aligned} \tag{3.75}$$

(since $\nabla G = -\nabla' G$ and $\mathbf{E}$ is a function of $\mathbf{r}'$), it follows that

$$\begin{aligned}\mathbf{F}_{I_2} &= +k_o^2 \iiint_{V_d} \left(1 - \frac{1}{\mu_r}\right) \mathbf{E}(\mathbf{r}') \cdot \left[\bar{\mathbf{I}} + \frac{\nabla\nabla}{k_o^2}\right] G_o(\mathbf{r}, \mathbf{r}') dv' + \left(1 - \frac{1}{\mu_r}\right) \mathbf{E}(\mathbf{r}) \\ &= -k_o^2 \iiint_{V_d} \left(1 - \frac{1}{\mu_r}\right) \mathbf{E}(\mathbf{r}') \cdot \bar{\mathbf{\Gamma}}_o(\mathbf{r}, \mathbf{r}') dv' + \left(1 - \frac{1}{\mu_r}\right) \mathbf{E}(\mathbf{r})\end{aligned} \tag{3.76}$$

for $\mathbf{r}$ in V_d. In deriving this expression we also employed the differential equation (2.38) satisfied by the scalar Green's function and the definition for the free space dyadic Greens' function (3.61). Clearly, with the derivation of (3.73) and (3.76), the first two integrals in (3.71) have been rewritten only in terms of undifferentiated electric fields and we would like to do the same for the last integral of (3.71). We have

$$\begin{aligned}\mathbf{F}_{I_3} &= \nabla \times \int\int\int_{V_d} \left\{ G_o(\mathbf{r}, \mathbf{r}') \nabla' \left(\frac{1}{\mu_r}\right) \times \mathbf{E}(\mathbf{r}') \right\} dv' \\ &= \int\int\int_{V_d} \nabla \times \left\{ G_o(\mathbf{r}, \mathbf{r}') \nabla' \left(\frac{1}{\mu_r}\right) \times \mathbf{E}(\mathbf{r}') \right\} dv' \\ &= \int\int\int_{V_d} \nabla G_o(\mathbf{r}, \mathbf{r}') \times \left[\nabla' \left(\frac{1}{\mu_r}\right) \times \mathbf{E}(\mathbf{r}') \right] dv'\end{aligned} \tag{3.77}$$

where again the last integral involves only the undifferentiated electric field within the volume of the dielectric.

We can now rewrite $\mathbf{E}_m$ by using the simplified expressions (3.73), (3.76) and (3.77). When the result is substituted in (3.66), the complete electric field expression involving undifferentiated volume fields is

$$\begin{aligned}&- k_o^2 \iiint_{V_d} \left(\epsilon_r - \frac{1}{\mu_r}\right) \mathbf{E}(\mathbf{r}') \cdot \bar{\mathbf{\Gamma}}_o(\mathbf{r}, \mathbf{r}') dv' \\ &+ \int\int\int_{V_d} \left[\mathbf{E}(\mathbf{r}') \times \nabla' \left(\frac{1}{\mu_r}\right) \right] \times \nabla G_o(\mathbf{r}, \mathbf{r}') dv' \\ &- \oiint_{S_d} \left(1 - \frac{1}{\mu_r}\right) [\hat{n}' \times \mathbf{E}(\mathbf{r}')] \times \nabla G_o(\mathbf{r}, \mathbf{r}') dv' + \mathbf{E}^i\end{aligned}$$

$$= \begin{cases} \mathbf{E}(\mathbf{r}) & \mathbf{r} \text{ not in } V_d \\ \frac{1}{2}\left(1+\frac{1}{\mu_r}\right)\mathbf{E}(\mathbf{r}) & \mathbf{r} \text{ on } S_d \\ \frac{1}{3}(\epsilon_r+2\mu_r)\mathbf{E}(\mathbf{r}) & \mathbf{r} \text{ in } V_d \end{cases} \tag{3.78a}$$

and by duality

$$-k_o^2 \iiint_{V_d}\left(\mu_r-\frac{1}{\epsilon_r}\right)\mathbf{H}(\mathbf{r}')\cdot\overline{\Gamma}_o(\mathbf{r},\mathbf{r}')dv'$$

$$+\int\int\int_{V_d}\left[\mathbf{H}(\mathbf{r}')\times\nabla'\left(\frac{1}{\epsilon_r}\right)\right]\times\nabla G_o(\mathbf{r},\mathbf{r}')dv'$$

$$-\oiint_{S_d}\left(1-\frac{1}{\epsilon_r}\right)[\hat{n}'\times\mathbf{H}(\mathbf{r}')]\times\nabla G_o(\mathbf{r},\mathbf{r}')dv'+\mathbf{H}^i$$

$$= \begin{cases} \mathbf{H}(\mathbf{r}) & \mathbf{r} \text{ not in } V_d \\ \frac{1}{2}\left(1+\frac{1}{\epsilon_r}\right)\mathbf{H}(\mathbf{r}) & \mathbf{r} \text{ on } S_d \\ \frac{1}{3}(\mu_r+2\epsilon_r)\mathbf{H}(\mathbf{r}) & \mathbf{r} \text{ in } V_d \end{cases} \tag{3.78b}$$

It should be noted that in evaluating the right hand side of (3.78) we made use of (2.69) and (3.25). Either (3.78a) or (3.78b) can be used for a solution of the fields within the volume of the dielectric. As seen, these integral expressions/equations contain both surface and volume integrals and we shall therefore refer to them as ***volume-surface integral equations*** (VSIE). The second integral of (3.78a) involves the gradient of the dielectric constant (which vanishes for a homogeneous dielectric) whose effect is indistinguishable from the equivalent volume magnetic current $\mathbf{E}\times\nabla\left(\frac{1}{\mu_r}\right)$. Similarly, the surface integral in (3.78a) involves the tangential electric field which can be thought as representing equivalent surface magnetic currents.

3.2 Two-Dimensional Representations

All integral equations and expressions presented in the previous section can be readily modified for two-dimensional structures which are invarient with respect to the z variable. As discussed in section 2.5, in this case the excitation

is an electric or a magnetic line source. Typically, this is a z-directed source generating z-polarized electric or magnetic fields, respectively, which become the excitation fields (E_z^i or H_z^i). Consequently, the corresponding total fields and scattered fields will be z-directed as well. This fact along with the field's independence on the z variable leads to a substantial simplification of the three-dimensional integral equations and expressions given earlier. In addition, by introducing the two-dimensional Green's function (see equ. (2.113)), the volume integrals reduce to surface integrals over the cross section of the structure, and those over a three-dimensional surface reduce to a line integral over the boundary of the two-dimensional cross-section. Below we consider some two-dimensional boundary (surface) and domain (volume) integral equations which are among the most popular in the literature.

3.2.1 Boundary Integral Equations

Upon setting $\mathbf{E} = \hat{z}E_z$ and $\mathbf{H} = \hat{z}H_z$, directly from (3.10) we have

$$\oint_C \left[E_z(\rho') \frac{\partial G_{2d}(\overline{\rho}, \overline{\rho}')}{\partial n'} - G_{2d}(\overline{\rho}, \overline{\rho}') \frac{\partial E_z(\overline{\rho}')}{\partial n'} \right] d\ell' + E_z^i(\overline{\rho}) = \begin{cases} E_z(\overline{\rho}) & \overline{\rho} \text{ in } A_\infty \\ 0 & \overline{\rho} \text{ in } A \end{cases} \tag{3.79a}$$

$$\oint_C \left[H_z(\rho') \frac{\partial G_{2d}(\overline{\rho}, \overline{\rho}')}{\partial n'} - G_{2d}(\overline{\rho}, \overline{\rho}') \frac{\partial H_z(\overline{\rho}')}{\partial n'} \right] d\ell' + H_z^i(\overline{\rho}) = \begin{cases} H_z(\overline{\rho}) & \overline{\rho} \text{ in } A_\infty \\ 0 & \overline{\rho} \text{ in } A \end{cases} \tag{3.79b}$$

In these $G_{2d}(\overline{\rho}, \overline{\rho}')$ is the two-dimensional Green's function defined in (2.115). Also as illustrated in fig. 3.8 C is the sum of all contours $C_1, C_2, \ldots, C_N$ which enclose the regions $A_1, A_2, \ldots, A_N$, respectively, and A_∞ is the region outside $A = \sum_n A_n$.

As usual the contour integrals in the left hand side of (3.79) contains non-integrable singularities when $\overline{\rho}$ is on A and must thus be evaluated by distorting the contour C at that point and take the limit as this distortion vanishes. In parallel with the previous approaches, we proceed by rewritting (3.79a) as

$$\int_{C-C_o} \left[E_z(\overline{\rho}') \frac{\partial G_{2d}(\overline{\rho}_o, \overline{\rho}')}{\partial n'} - G_{2d}(\overline{\rho}_o, \overline{\rho}') \frac{\partial E_z(\overline{\rho}')}{\partial n'} \right] d\ell'$$

$$= -\int_{C_o}\left[E_z(\overline{\rho}')\frac{\partial G_{2d}(\overline{\rho}_o,\overline{\rho})}{\partial n'} - G_{2d}(\overline{\rho}_o,\overline{\rho})\frac{\partial E_z(\overline{\rho}')}{\partial n'}\right]d\ell' \qquad (3.80)$$

where C_o is a vanishingly small semi-circular contour whose center is at the observation point $\overline{\rho}_o$ and this is illustrated in figure 3.9. To evaluate the right hand side integral of (3.80) as $C_o \to 0$ we let $d\ell' = a\,d\phi$, where $|\overline{\rho}_o - \overline{\rho}'| = R_o \to 0$ and recall the small argument expression for the Hankel function (2.141) and (2.143). In particular from (2.143) it follows that the second term of the right hand side integral in (3.80) vanishes as $a \to 0$ and the first term can be written as

$$\begin{aligned}
-\int_{C_o} E_z(\overline{\rho}')\frac{\partial G_{2d}(\overline{\rho}_o,\overline{\rho}')}{\partial n'}d\ell' &= -\int_{C_o} E_z(\overline{\rho}')\,[\hat{n}\cdot\nabla' G_{2d}(\overline{\rho}_o,\overline{\rho}')]\,d\ell' \\
&= -\int_0^{\pi} E_z(\overline{\rho}')\left[\hat{R}_o\cdot\nabla G_{2d}(\overline{\rho}_o,\overline{\rho}')\right]a\,d\phi' \\
&\approx +E_z(\overline{\rho}_o)\int_0^{\pi}\frac{\hat{R}_o\cdot\hat{R}_o}{2\pi a}a\,d\phi' \\
&= +\frac{1}{2}E_z(\overline{\rho}_o)
\end{aligned}$$

In general, one can also show that

$$\oint_C \phi(\overline{\rho}')\frac{\partial G_{2d}(\overline{\rho}_o^{\pm},\overline{\rho}')}{\partial n'}d\ell' = \pm\frac{1}{2}\phi(\overline{\rho}_o) + \oint_C \phi(\overline{\rho}')\frac{\partial G_{2d}}{\partial n'}(\overline{\rho}_o,\overline{\rho}')d\ell' \qquad (3.81)$$

where $\overline{\rho}_o^{\pm}$ is the observation point just exterior (+) or interior (-) to the contour C. This identity (generalization of the result in (3.8)) can be viewed as the scalar form of the vector identity (3.37) and as stated earlier, the field discontinuity at the boundary C is due to the implied surface currents responsible for the scattered field.

When the identity (3.81) is incorporated into the integral equations (3.79) we have

$$\oint_C\left[E_z(\overline{\rho}')\frac{\partial G_{2d}(\overline{\rho},\overline{\rho}')}{\partial n'} - G_{2d}(\overline{\rho},\overline{\rho}')\frac{\partial E_z(\overline{\rho}')}{\partial n'}\right]d\ell' + E_z^i(\overline{\rho}) = \begin{cases} E_z(\overline{\rho}) & \overline{\rho}\text{ in } A_\infty \\ \frac{1}{2}E_z(\overline{\rho}) & \overline{\rho}\text{ on } C \\ 0 & \overline{\rho}\text{ in } A \end{cases}$$

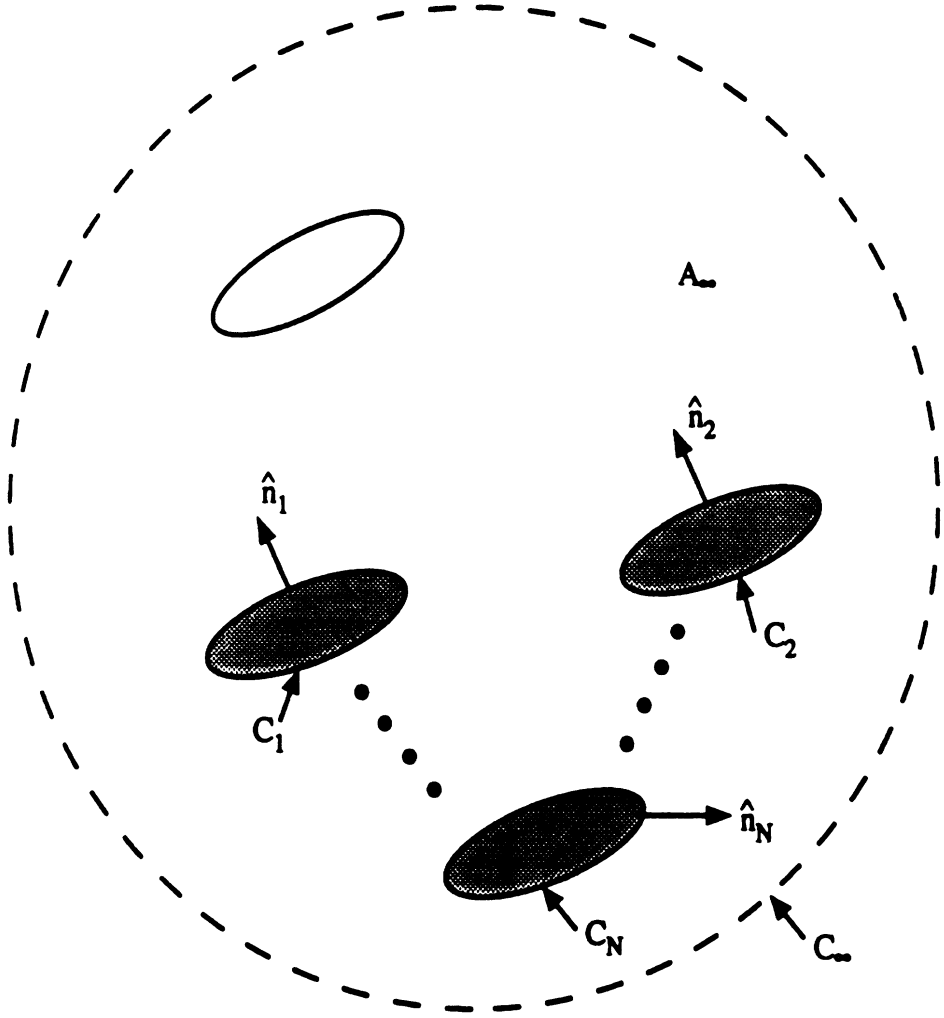

Figure 3.8: Geometry for the two-dimensional application of the excitation integral equations.

(3.82a)

$$\oint_C \left[H_z(\overline{\rho}') \frac{\partial G_{2d}(\overline{\rho}, \overline{\rho}')}{\partial n'} - G_{2d}(\overline{\rho}, \overline{\rho}') \frac{\partial E_z(\overline{\rho}')}{\partial n'} \right] d\ell' + H_z^i(\overline{\rho}) = \begin{cases} H_z(\overline{\rho}) & \overline{\rho} \text{ in } A_\infty \\ \frac{1}{2} H_z(\overline{\rho}) & \overline{\rho} \text{ on } C \\ 0 & \overline{\rho} \text{ in } A \end{cases}$$

(3.82b)

These should be compared with (3.10) which apply to three dimensional surfaces. Of course, one could have derived (3.82) directly from (3.10) by integrating with respect to z' (see (2.113)). Also, the Stratton-Chu integral equations (3.26) can be shown to reduce to (3.82) upon making use of (2.124) and noting that $\hat{n} \cdot \mathbf{E} = 0$ on the boundary C. The first of (3.82) is commonly referred to as the E-polarization or transverse magnetic (TM) boundary integral equation since the electric field is transverse to the plane of incidence. Correspondingly, (3.82b) is referred to as the H-polarization or transverse electric (TE) integral equation.

3.2.2 Homogeneous Dielectrics

The boundary integral equations for two-dimensional homogeneous dielectric cylinders can be derived directly from the corresponding three dimensional ones given in (3.38) and (3.40). However, it is simpler to consider their derivation beginning with the boundary integral equations (3.82)

Let us consider the dielectric cylinder whose cross-section is illustrated in figure 3.9. The cylinder's constitutive parameters are $(\epsilon_{r2}, \mu_{r2})$ whereas those of the exterior region are $(\epsilon_{r1}, \mu_{r1})$, and $\hat{n}$ denotes the unit normal pointing in the outward direction of the cylinder. We shall denote the total field in medium #1 as E_{z1} or H_{z1} and that in medium #2 as E_{z2} or H_{z2}. Then, from (3.82) if we let $\overline{\rho}$ approach C from the exterior (medium #1) we have

$$\oint_C \left[E_{z1}(\overline{\rho}') \frac{\partial G_{2d_1}(\overline{\rho}, \overline{\rho}')}{\partial n'} - G_{2d_1}(\overline{\rho}, \overline{\rho}') \frac{\partial E_{z1}(\overline{\rho}')}{\partial n'} \right] d\ell' + E_z^i(\overline{\rho}) = \frac{1}{2} E_{z1}(\overline{\rho}) \quad \overline{\rho} \in C$$

(3.83a)

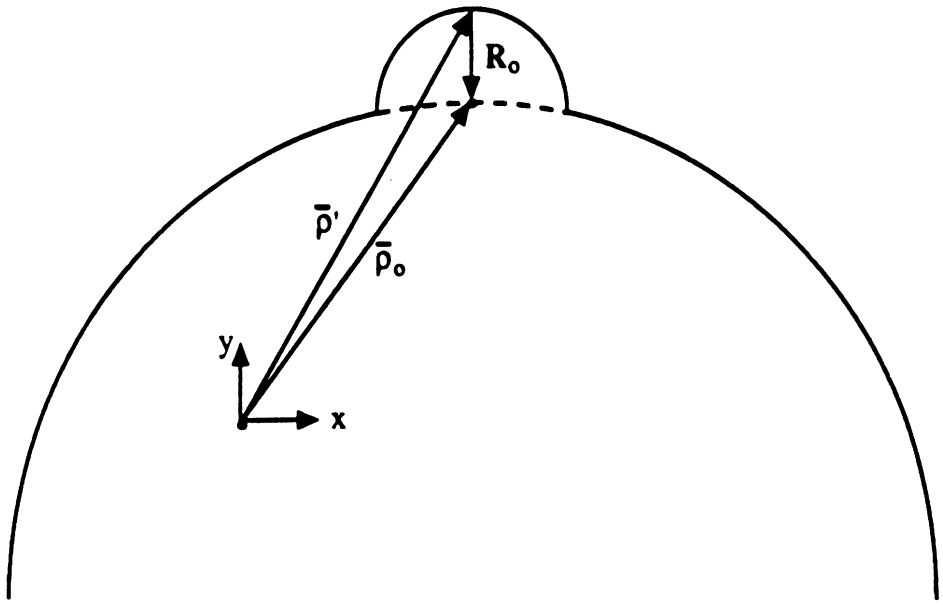

Figure 3.9: Geometry for evaluating the fields on C.

for TM excitation and

$$\oint_C \left[H_{z1}(\bar{\rho}') \frac{\partial G_{2d_1}(\bar{\rho},\bar{\rho}')}{\partial n'} - G_{2d_1}(\bar{\rho},\bar{\rho}') \frac{\partial H_{z1}(\bar{\rho}')}{\partial n'} \right] d\ell' + H_z^i(\bar{\rho}) = \frac{1}{2} H_{z1}(\bar{\rho}) \quad \bar{\rho} \in C \tag{3.83b}$$

for TE excitation with

$$G_{2d_1}(\bar{\rho},\bar{\rho}') = \frac{-j}{4} H_0^{(2)}\left(k_o \sqrt{\epsilon_{r1}\mu_{r1}}\, |\bar{\rho} - \bar{\rho}'|\right) \tag{3.84}$$

Alternatively, if we let $\bar{\rho}$ approach from the interior of C (3.82) yields

$$-\oint_C \left[E_{z2}(\bar{\rho}') \frac{\partial G_{2d_2}(\bar{\rho},\bar{\rho}')}{\partial n'} - G_{2d_2}(\bar{\rho},\bar{\rho}') \frac{\partial E_{z2}(\bar{\rho}')}{\partial n'} \right] d\ell' = \frac{1}{2} E_{z2}(\bar{\rho}) \quad \bar{\rho} \in C \tag{3.85a}$$

for TM incidence and

$$-\oint_C \left[H_{z2}(\bar{\rho}') \frac{\partial G_{2d_2}(\bar{\rho},\bar{\rho}')}{\partial n'} - G_{2d_2}(\bar{\rho},\bar{\rho}') \frac{\partial H_{z2}(\bar{\rho}')}{\partial n'} \right] d\ell' = \frac{1}{2} H_{z2}(\bar{\rho}) \quad \bar{\rho} \in C \tag{3.85b}$$

for TE incidence with

$$G_{2d_2}(\overline{\rho},\overline{\rho}') = \frac{-j}{4} H_o^{(2)}\left(k_o\sqrt{\epsilon_{r2}\mu_{r2}}\,|\overline{\rho}-\overline{\rho}'|\right). \tag{3.86}$$

We remark that in (3.86) there is no explicit appearance of the excitation field since this is confined in the exterior region of the dielectric (i.e. there are no sources in the dielectric).

To obtain an integral equation set for the unique solution of the boundary fields and their derivatives it is necessary to couple the respective equations of (3.83) and (3.85). This can be accomplished by enforcing the tangential field continuity conditions

$$\begin{aligned} \hat{n}\times\mathbf{E}_1 &= \hat{n}\times\mathbf{E}_2 \\ \hat{n}\times\mathbf{H}_1 &= \hat{n}\times\mathbf{H}_2 \end{aligned}$$

For the TM case, the first of these conditions implies

$$E_{z1} = E_{z2} \tag{3.87a}$$

and from the second condition, in conjunction with (2.124), we have

$$\frac{1}{\mu_{r1}}\frac{\partial E_{z1}}{\partial n} = \frac{1}{\mu_{r2}}\frac{\partial E_{z2}}{\partial n} \tag{3.87b}$$

Likewise, for the TE case the appropriate boundary conditions are

$$\begin{aligned} H_{z1} &= H_{z2} \\ \frac{1}{\epsilon_{r1}}\frac{\partial H_{z1}}{\partial n} &= \frac{1}{\epsilon_{r2}}\frac{\partial H_{z2}}{\partial n} \end{aligned} \tag{3.88}$$

Substituting now (3.87) and (3.88) into (3.85) yields

$$-\oint\left[E_{z1}(\overline{\rho}')\frac{\partial G_{2d}(\overline{\rho},\overline{\rho}')}{\partial n'} - \frac{\mu_{r2}}{\mu_{r1}}G_{2d_2}(\overline{\rho},\overline{\rho}')\frac{\partial E_{z1}(\overline{\rho})}{\partial n'}\right]d\ell' = \frac{1}{2}E_{z1}(\overline{\rho}) \tag{3.89a}$$

and

$$-\oint \left[H_{z1}(\overline{\rho}') \frac{\partial G_{2d}(\overline{\rho}, \overline{\rho}')}{\partial n'} - \frac{\epsilon_{r2}}{\epsilon_{r1}} G_{2d_2}(\overline{\rho}, \overline{\rho}') \frac{\partial H_{z1}(\overline{\rho}')}{\partial n'} \right] d\ell' = \frac{1}{2} H_{z1}(\overline{\rho}) \tag{3.89b}$$

The integral equations (3.83a) and (3.89a) now form a coupled set of integral equations for the solution of E_{z1} and $\frac{\partial E_{z1}}{\partial n}$ on the boundary C. Similarly, the H-polarization integral equations (3.83b) and (3.85b) form another set of coupled integral equations which can be solved for H_{z1} and $\frac{\partial H_{z1}}{\partial n}$ on C. The solution of these integral equations will be considered in a later chapter.

Upon solution of the boundary field and its derivative, the fields in the exterior (medium #1) and interior (medium #2) regions can be found by returning to (3.82). For example, the exterior field is given by

$$\phi = \phi^s + \phi^i \tag{3.90}$$

where

$$\phi^s = \int_C \left[\phi(\overline{\rho}') \frac{\partial G_{2d_1}(\overline{\rho}, \overline{\rho}')}{\partial n'} - G_{2d_1}(\overline{\rho}, \overline{\rho}') \frac{\partial \phi(\overline{\rho}')}{\partial n'} \right] d\ell' \tag{3.91}$$

is the scattered field and ϕ represents the E_{z1} or H_{z1} field depending on the polarization of the excitation field. For computational purposes, we may write (see also (1.120))

$$\frac{\partial G_{2d_1}}{\partial n} = \hat{n} \cdot \nabla G_{2d_1} = -\frac{j}{4} (\hat{n} \cdot \hat{R}) H_o^{(2)'}(kR) = (\hat{n} \cdot \hat{R}) \frac{jk_o \sqrt{\mu_{r_1} \epsilon_{r_1}}}{4}$$

$$\cdot H_1^{(2)}(k_o \sqrt{\mu_{r_1} \epsilon_{r_1}}\, R) \tag{3.92}$$

and when this is substituted in (3.91) along with the large argument expressions for $H_o^{(2)}(kR)$ and $H_1^{(2)}(kR)$ given by (2.132), it follows that in the far zone ($\rho \to \infty$)

$$\phi^s{}_{k_o\rho \simeq \infty} \; -\sqrt{\frac{k_1}{8\pi}} \frac{e^{-j(k\rho + \pi/4)}}{\sqrt{\rho}} \int_C [j(\hat{n}' \cdot \hat{\rho}) \phi(\overline{\rho}') + \psi(\overline{\rho}')] \, e^{jk_1 \hat{\rho} \cdot \overline{\rho}'} d\ell' \tag{3.93}$$

where we have set

$$\psi(\overline{\rho}) = \frac{\partial \phi(\overline{\rho})}{\partial n}$$

and $k_1 = k_o\sqrt{\mu_{r_1}\epsilon_{r_1}}$. The evaluation of the field in the interior region can be accomplished in a similar manner. It follows that the interior total field is given by the negative of the right hand side of (3.88) provided G_{2d_1} is also replaced by G_{2d_2} and ϕ is identified as E_{z2} or H_{z2}. That is

$$E_{z2} = -\int_C \left[E_{z1}(\overline{\rho}')\frac{\partial G_{2d_2}(\overline{\rho},\overline{\rho}')}{\partial n'} - \frac{\mu_{r2}}{\mu_{r1}}G_{2d_2}(\overline{\rho},\overline{\rho}')\frac{\partial E_{z1}}{\partial n'}(\overline{\rho}')\right] d\ell' \quad (3.94a)$$

for the TM case and

$$H_{z2} = -\int_C \left[H_{z1}(\overline{\rho}')\frac{\partial G_{2d_2}(\overline{\rho},\overline{\rho}')}{\partial n'} - \frac{\epsilon_{r2}}{\epsilon_{r1}}G_{2d_2}(\overline{\rho},\overline{\rho}')\frac{\partial H_{z1}}{\partial n'}(\overline{\rho}')\right] d\ell' \quad (3.94b)$$

for the TE case.

3.2.3 Metallic Cylinders

A special case of a homogeneous cylinder is the perfectly conducting or metallic cylinder. Then, on the boundary C the tangential electric field vanishes, implying

$$E_{z1} = E_z = 0 \quad (3.95a)$$

for E-polarization and

$$\frac{\partial H_{z1}}{\partial n} = \frac{\partial H_z}{\partial n} = 0 \quad (3.95b)$$

for H-polarization. Incorporating these into (3.83) we obtain the integral equations

$$\oint \frac{\partial E_z(\overline{\rho}')}{\partial n'}G_{2d_1}(\overline{\rho},\overline{\rho}')d\ell' = E_z^i(\overline{\rho}) \quad \overline{\rho} \in C \quad (3.96a)$$

and

$$\oint_C H_z(\overline{\rho}')\frac{\partial G_{2d_1}(\overline{\rho},\overline{\rho}')}{\partial n'}d\ell' + H_z^i(\overline{\rho}) = \frac{1}{2}H_z(\overline{\rho}) \quad \overline{\rho} \in C \quad (3.96b)$$

for E and H polarizations, respectively.

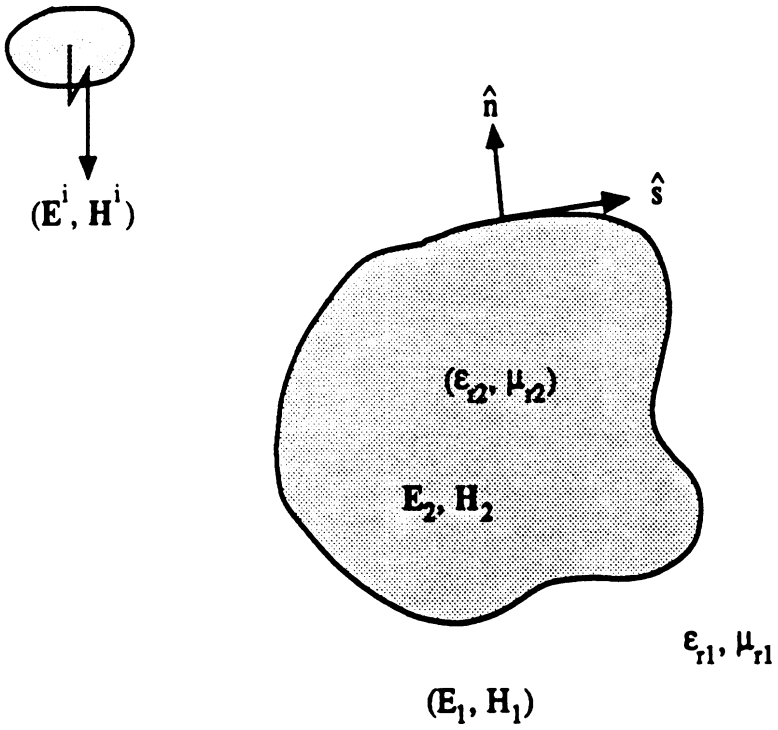

Figure 3.10: Geometry of an inhomogeneous dielectric cylinder.

As noted earlier, we could have instead formulated the problem by introducing on C the equivalent current

$$\begin{aligned} \mathbf{J} &= \hat{n} \times \mathbf{H} \\ &= \begin{cases} \hat{n} \times \left(\frac{-jY_1}{k_1} \hat{z} \times \nabla E_z\right) = -\hat{z} \frac{jY_1}{k_1} \frac{\partial E_z}{\partial n}, & \text{TM case} \\ \hat{\ell} H_z, & \text{TE case} \end{cases} \end{aligned} \tag{3.97}$$

where $\hat{\ell} = \hat{z} \times \hat{n}$ denotes the unit vector tangent to C as illustrated in figure 3.11. Substituting (3.97) into (3.96) yields

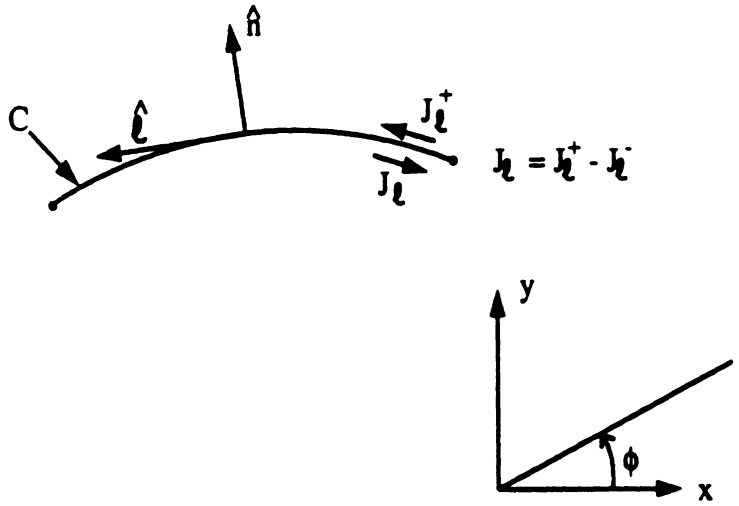

Figure 3.11: Geometry of a metallic curved strip.

$$jk_1 Z_1 \int_C J_z(\overline{\rho}') G_{2d_1}(\overline{\rho}, \overline{\rho}') d\ell' = E_z^i(\overline{\rho}), \quad \overline{\rho} \in C \tag{3.98a}$$

for the TM case and

$$\oint_C J_\ell(\overline{\rho}') \frac{\partial G_{2d_1}(\overline{\rho}, \overline{\rho}')}{\partial n'} d\ell' + H_z^i(\overline{\rho}') = \frac{1}{2} J_\ell(\overline{\rho}), \quad \overline{\rho} \in C \tag{3.98b}$$

for the TE case, with $\mathbf{J} = \hat{\ell} J_s$. It is now readily recognized that (3.98b) is the two-dimensional counterpart of the MFIE given by (3.42b). As was the case

in three-dimensions, this is only valid for closed boundaries. In contrast, the EFIE (3.98a) which is the counterpart of (3.42a) for three dimensions, can be shown to be valid for closed as well as open surfaces such as a curved strip. This can be verified by rederiving it from (2.217a) upon setting $\mathbf{M} = 0$ and then enforcing the boundary condition $\hat{n} \times \mathbf{E} = 0$ on the boundary. Using the same procedure for H-polarization, we find directly from (2.127a) the integral equation

$$E_\ell^i = \int_C jk_1 Z_1 (\hat{\ell} \cdot \hat{\ell}') J_\ell(\overline{\rho}') G_{2d_1}(\overline{\rho}, \overline{\rho}') d\ell' - \frac{jZ_1}{k_1} \frac{\partial}{\partial \ell} \int_C J_\ell(\overline{\rho}') \frac{\partial}{\partial \ell'} G_{2d_1}(\overline{\rho}, \overline{\rho}') d\ell' \tag{3.99}$$

in which $\mathbf{E}_\ell^i = \hat{\ell} \cdot \mathbf{E}^i$, and $\frac{\partial}{\partial \ell} = \hat{\ell} \cdot \nabla$ implies differentiation along the direction tangential to the boundary C. The three-dimensional counterpart of (3.99) is (3.43) and it is readily seen that the EFIEs (3.98a) and (3.99) can be deduced directly from (3.43) through the application of the identity (2.113). As explained in connection with (3.43), when the EFIEs (3.98) and (3.99) are applied to open surfaces, the current density in those equations represents the net current flow on the curved strip (see fig. 3.11). It should be noted that the non-integrable singularity of the kernel in the second integral of the EFIE (3.99) requires special attention when this integral equation is solved numerically. Thus, although (3.45) is valid for both open and closed surfaces, it is preferable to use the MFIE whenever possible.

3.2.4 Piecewise Homogeneous Dielectrics

The treatment of piecewise homogeneous dielectrics is important in many industrial and biomedical applications involving the characterization of the field behavior in materials. The structure in figure 3.12 is a typical configuration of interest. To compute the interior and scattered fields from this configuration due to an exterior TE or TM excitation one approach is to formulate appropriate boundary integral equations at each of the dielectric interfaces [Wu and Tsai; MTT-T, 1977; AP-T, 1977]. Following the procedure discussed earlier for three dimensional structures, we can proceed with the construction of the boundary integral equations by setting-up the three equivalent problems illustrated in figures 3.12 (b)-(c). As before, we can then introduce equivalent surface currents at the interface boundaries C_1 and C_2 satisfying (3.28), thus

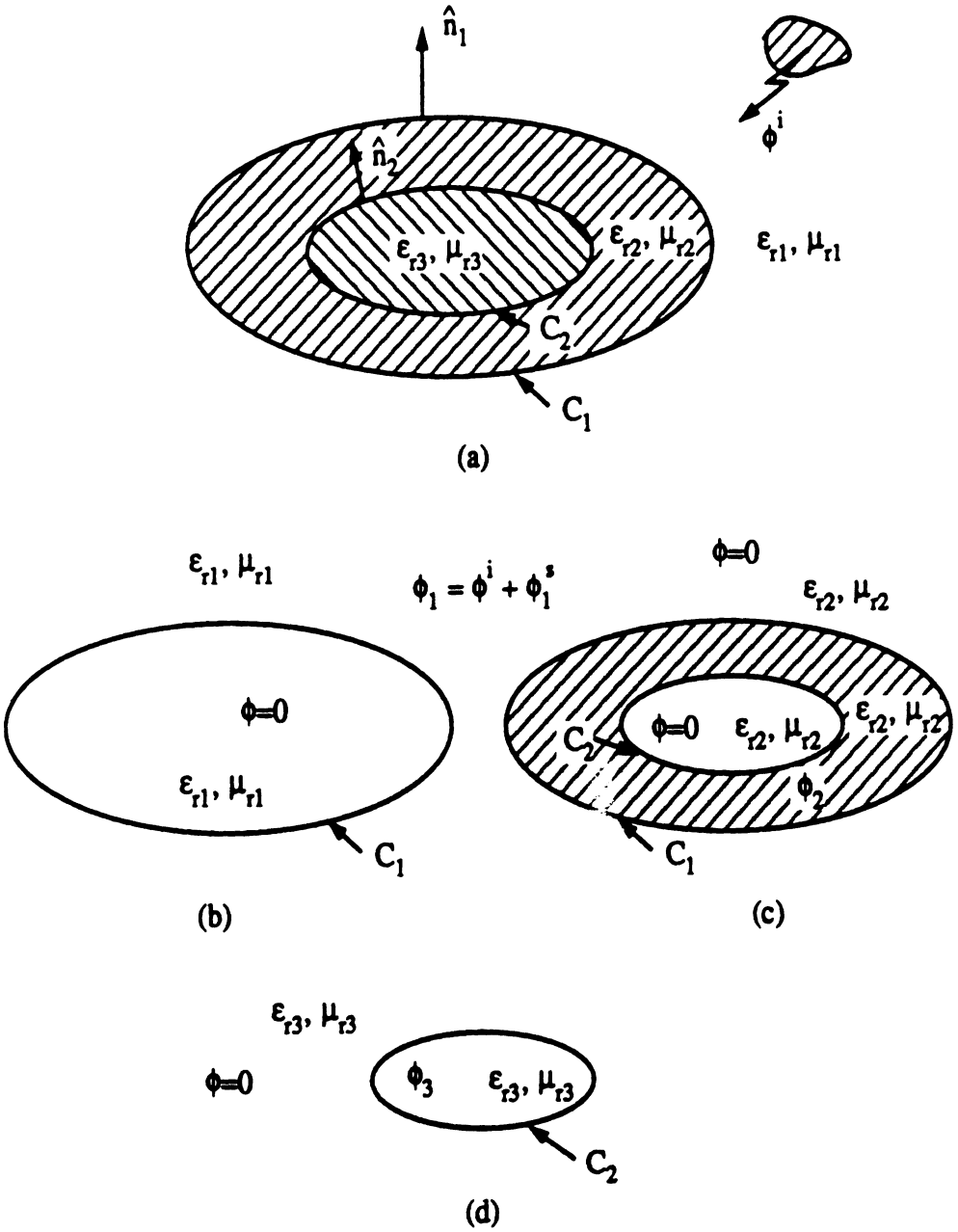

Figure 3.12: Geometry of the layered dielectric cylinder and equivalent problems to formulate the field in each region.

ensuring tangential field continuity. Integral equations for the solution of the equivalent current can then be constructed by enforcing conditions such as those in (3.47).

An alternative to the above procedure is to bypass the introduction of the equivalent currents and work directly with the z-directed field and its normal derivative as was done in the previous section for homogeneous dielectrics. Such an approach could also be used in the three dimensional formulation and in this case use of (3.26) or (3.18) would be required. However, when employing (3.26), one must deal with the presence of $\hat{n} \cdot \mathbf{H}$ and $\hat{n} \cdot \mathbf{E}$. These can be replaced by

$$\hat{n} \cdot \mathbf{H} = -\frac{\nabla_s \cdot \mathbf{M}}{j\omega\mu} = \frac{\nabla_s \cdot (\hat{n} \times \mathbf{E})}{jkZ} \tag{3.100a}$$

$$\hat{n} \cdot \mathbf{E} = -\frac{\nabla_s \cdot \mathbf{J}}{j\omega\mu} = \frac{\nabla_s \cdot (\hat{n} \times \mathbf{H})}{jkY} \tag{3.100b}$$

implying that we could derive integral equations similar to those in sections 3.1.3 - 3.1.6 which involve only the tangential electric and magnetic fields instead of the equivalent surface currents. Thus, mathematically the two procedures are equivalent but one could argue that the introduction of the equivalent surface currents is physically more appealing. With this understanding, we now proceed to construct boundary integral equations for the layered dielectric in figure 3.11(a).

Assuming TM excitation and denoting the field exterior to C_1 by E_{z1}, from (3.83a) we have

$$\oint_{C_1} \left[E_{z1}(\overline{\rho}') \frac{\partial G_{2d_1}(\overline{\rho}, \overline{\rho}')}{\partial n_1'} - G_{2d_1}(\overline{\rho}, \overline{\rho}') \frac{\partial E_{z1}(\overline{\rho}')}{\partial n_1'} \right] + E_z^i(\overline{\rho}') = \frac{1}{2} E_z(\overline{\rho}) \quad \overline{\rho} \in C. \tag{3.101a}$$

When we approach the observation point on C_1 from its interior surface, it is convenient to choose the closed boundary to be the sum of C_1 and C_2 when making use of (3.82). Then, since there are no sources in region #2, it follows that (E_{z2} is the field between C_1 and C_2)

$$+ \oint_{C_2} \left[E_{z2}(\overline{\rho}') \frac{\partial G_{2d_2}(\overline{\rho}, \overline{\rho}')}{\partial n_2'} - G_{2d_2}(\overline{\rho}, \overline{\rho}') \frac{\partial E_{z2}}{\partial n_2'} \right] d\ell'$$

$$-\oint_{C_1}\left[E_{z1}(\overline{\rho}')\frac{\partial G_{2d_2}(\overline{\rho},\overline{\rho}')}{\partial n_1'}-\frac{\mu_{r2}}{\mu_{r1}}G_{2d_2}(\overline{\rho},\overline{\rho}')\frac{\partial E_{z1}}{\partial n_1'}\right]d\ell'=\begin{cases}\frac{1}{2}E_{z1}(\overline{\rho}), & \overline{\rho}\in C_1\\ \frac{1}{2}E_{z2}(\overline{\rho}), & \overline{\rho}\in C_2\end{cases} \tag{3.101b}$$

which except for the appearance of the integral over C_2 is identical to (3.89). Finally, by approaching the observation point on C_2 from its interior surface, we obtain

$$-\oint_{C_3}\left[E_{z2}(\overline{\rho}')\frac{\partial G_{2d_3}(\overline{\rho},\overline{\rho}')}{\partial n_2'}-\frac{\mu_{r3}}{\mu_{r2}}G_{2d_3}(\overline{\rho},\overline{\rho}')\frac{\partial E_{z2}(\overline{\rho}')}{\partial n_2'}\right]d\ell'=\frac{1}{2}E_{z2}(\overline{\rho})\quad \overline{\rho}\in C_2 \tag{3.101c}$$

where

$$G_{2d_3}(\overline{\rho},\overline{\rho}')=-\frac{j}{4}H_o^{(2)}\left(k_o\sqrt{\epsilon_{r3}\mu_{r3}}\,|\overline{\rho}-\overline{\rho}'|\right) \tag{3.102}$$

Together, the integral equations (3.101) form a coupled set for the solution of the fields and their derivatives on the boundaries C_1 and C_2. The corresponding set of integral equations for the TE case is obtained directly from (3.101) by invoking duality. Once (3.101) are solved via some numerical procedure, the exterior fields can be found from (3.90) - (3.91) with $C = C_1$. The interior fields can be evaluated using one of the equations given in (3.82). For example, the field in medium #2 between the boundaries C_1 and C_2 is given by

$$\begin{aligned}E_{z2}(\overline{\rho})=&\oint_{C_2}\left[E_{z2}(\overline{\rho}')\left(\hat{n}_2'\cdot\nabla' G_{2d_2}(\overline{\rho},\overline{\rho}')\right)-G_{2d_2}(\overline{\rho},\overline{\rho}')\frac{\partial E_{z2}}{\partial n_2'}\right]d\ell'\\ &-\oint_{C_1}\left[E_{z1}(\overline{\rho}')\left(\hat{n}_1'\cdot\nabla' G_{2d_2}(\overline{\rho},\overline{\rho}')\right)-\frac{\mu_{r2}}{\mu_{r1}}G_{2d_2}(\overline{\rho},\overline{\rho}')\frac{\partial E_{z2}}{\partial n_1'}\right]d\ell'\end{aligned} \tag{3.103}$$

and the dual of this must be used for TE incidence.

3.2.5 Domain Integral Equations

In modeling the cross section of inhomogeneous dielectric cylinders we must resort to a volume/domain formulation as discussed in section 3.1.7 for three-dimensional dielectrics. Consider the inhomogeneous cylinders shown in figure

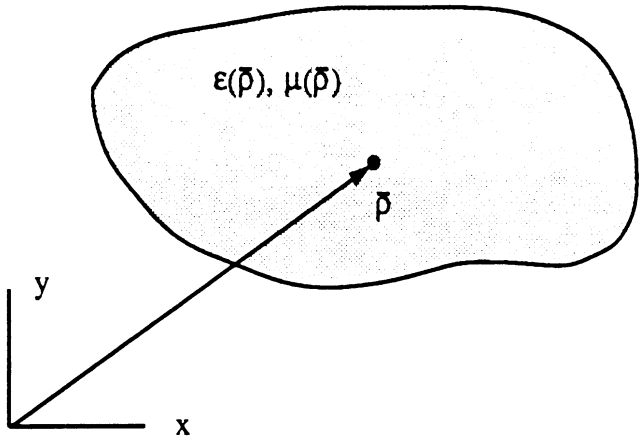

Figure 3.13: Inhomogeneous dielectric cylinder of arbitrary cross section.

3.13 whose relative permittivity and permeability are $\epsilon_r(\overline{\rho})$ and $\mu_r(\overline{\rho})$. In accordance with the volume equivalence principle, for TM incidence/excitation, we may replace the presence of the cylinder by the two-dimensional currents

$$J_z = jk_oY_o(\epsilon_r - 1)(E_z^s + E_z^i) \tag{3.104a}$$

$$\mathbf{M} = \hat{x}M_x + \hat{y}M_y = jk_oZ_o(\mu_r - 1)(\mathbf{H}^s + \mathbf{H}^i) \tag{3.104b}$$

Then, from (2.127) or (2.130) we obtain

$$E_z^s = \frac{jk_o}{4}\int\int_A \hat{z}\cdot\left(\mathbf{M}(\overline{\rho}')\times\hat{R}\right)H_1^{(2)}(k_oR)ds' - \frac{k_oZ_o}{4}\int\int_A J_z(\overline{\rho}')H_o^{(2)}(k_oR)ds' \tag{3.105a}$$

$$\mathbf{H}^s = \int\int_A \Big[J_z(\overline{\rho}')\hat{z}\times\nabla G_{2d_o}(\overline{\rho},\overline{\rho}') - jk_oY_o\mathbf{M}(\overline{\rho}')G_{2d_o}(\overline{\rho},\overline{\rho}') - \frac{jY_o}{k_o}\mathbf{M}(\overline{\rho}')\cdot\nabla\nabla G_{2d_o}(\overline{\rho},\overline{\rho}')\Big]ds' \tag{3.105b}$$

with

$$G_{2d_o}(\overline{\rho},\overline{\rho}') = \frac{-j}{4}H_o^{(2)}(k_o|\overline{\rho}-\overline{\rho}'|) \tag{3.106}$$

Substituting these expressions into (3.104) results in a coupled set of integral equations for the currents J_z and $\mathbf{M}$. The corresponding equations for the TE

case are

$$\frac{M_z}{jk_oZ_o(\mu_r-1)} = H_z^i + H_z^s \tag{3.107a}$$

$$\frac{\mathbf{J}}{jk_oY_o(\epsilon_r-1)} = \mathbf{E}^i + \mathbf{E}^s \tag{3.107b}$$

where

$$H_z^s = -\frac{jk_o}{4}\int\int_A \hat{z}\cdot\left(\mathbf{J}(\overline{\rho}')\times\hat{R}\right)H_1^{(2)}(k_oR)ds' - \frac{k_oY_o}{4}\int\int_A M_z(\overline{\rho}')H_o^{(2)}(k_oR)ds' \tag{3.108a}$$

and

$$\mathbf{E}^s = -\int\int_A M_z(\overline{\rho}')\hat{z}\times\nabla G_{2d_o}(\overline{\rho},\overline{\rho}')ds' - \int\int_A\left[jk_oZ_o\mathbf{J}(\overline{\rho}')G_{2d_o}(\overline{\rho},\overline{\rho}') + \frac{jZ_o}{k_o}\mathbf{J}(\overline{\rho}')\cdot\nabla\nabla G_{2d_o}(\overline{\rho},\overline{\rho}')\right]ds' \tag{3.108b}$$

are the associated scattered fields.

When $\mu_r = 1$ in (3.104), $\mathbf{M}$ vanishes and thus the solution of (3.104) - (3.105) involves a single unknown. However, for non-unity μ_r, the integral equations involve three unknowns which can be reduced in number by following the procedure discussed in section 3.1.7. That is, the effect of the currents (3.104) may be replaced by the single magnetic equivalent current

$$\begin{aligned}\mathbf{M}' &= -\frac{\mu_r-1}{\mu_r}\nabla\times(\hat{z}E_z) - \nabla\times[\hat{z}(\epsilon_r-1)E_z] \\ &= \frac{\mu_r-1}{\mu_r}\hat{z}\times\nabla E_z + \hat{z}\times\nabla[(\epsilon_r-1)E_z]\end{aligned} \tag{3.109}$$

which can be used in the first integral (3.105a) to obtain the scattered field expression

$$\hat{z}E_z^s = -\frac{jk_o}{4}\int\int_A \hat{R}\times\left\{\frac{\mu_r-1}{\mu_r}\hat{z}\times\nabla E_z(\overline{\rho}') + \hat{z}\times\nabla[(\epsilon_r-1)E_z(\overline{\rho}')]\right\}H_1^{(2)}(k_oR)ds' \tag{3.110}$$

When this is substituted into (3.57) we have

$$\hat{z}E_z(\overline{\rho}) = \hat{z}E_z^i(\overline{\rho}) - \frac{jk_o}{4}\int\int_A \hat{R}\times\left\{\frac{\mu_r-1}{\mu_r}\hat{z}\times\nabla E_z(\overline{\rho}')\right.$$
$$\left.+\,\hat{z}\times\nabla\left[(\epsilon_r-1)E_z(\overline{\rho}')\right]\right\}H_1^{(2)}(k_oR)ds' \qquad (3.111)$$

which is an integral equation for the solution of the field E_z across the cross-section of the cylinder. Similarly, by invoking duality the corresponding integral equation for the TE case is

$$\hat{z}H_z(\overline{\rho}) = \hat{z}H_z^i(\overline{\rho}) - \frac{jk_o}{4}\int\int_A \hat{R}\times\left\{\frac{\epsilon_r-1}{\epsilon_r}\hat{z}\times\nabla H_z(\overline{\rho}')\right.$$
$$\left.+\,\hat{z}\times\nabla\left[(\mu_r-1)H_z(\overline{\rho}')\right]\right\}H_1^{(2)}(k_oR)ds' \qquad (3.112)$$

and the implied equivalent source for this field is the electric current

$$\mathbf{J}' = -\frac{\epsilon_r-1}{\epsilon_r}\hat{z}\times\nabla H_z - \hat{z}\times\nabla\left[(\mu_r-1)H_z\right] \qquad (3.113)$$

which can be deduced from (1.112).

Special forms of (3.111) and (3.112) have been solved by Peterson and Klock [AP-T, 1988] and Peterson [JEWA, 1989] (see also AP-T, April 1991). Because they involve derivatives of the unknown quantities E_z or H_z, their solution requires use of higher order expansion functions. However these can be replaced by domain-boundary integral equations which again involve a single undifferentiated unknown quantity. Such a domain-boundary integral equation can be deduced directly from the volume-surface integral formulation described in section 3.1.7. In particular, by making use of (2.113) and setting $\mathbf{E} = \hat{z}E_z$ in (3.67) - (3.77), it follows that [Jin, etc., JEWA 1988]

$$E_z = E_{ze} + E_{zm} + E_z^i \qquad (3.114a)$$

where

$$E_{ze}(\overline{\rho}) = k_o^2\int\int_A(\epsilon_r-1)E_z(\overline{\rho}')G_o(\mathbf{r},\mathbf{r}')ds' \qquad (3.114b)$$

$$E_{zm}(\overline{\rho}) = k_o^2\int\int_A\left(1-\frac{1}{\mu_r}\right)E_z(\overline{\rho}')G_o(\overline{\rho},\overline{\rho}')ds'$$

$$
\begin{aligned}
&- \int\int_A \nabla' \left(\frac{1}{\mu_r}\right) \cdot [E_z(\overline{\rho}')\nabla G_o(\overline{\rho},\overline{\rho}')]\, ds' \\
&+ \oint_C \left(1 - \frac{1}{\mu_r}\right) E_z(\overline{\rho}') \frac{\partial G_o(\overline{\rho},\overline{\rho}')}{\partial n'} d\ell' \\
&+ \begin{cases} \left(1 - \frac{1}{\mu_r}\right) E_z(\overline{\rho}) & \overline{\rho} \in A \\ \frac{1}{2}\left(1 - \frac{1}{\mu_r}\right) E_z(\overline{\rho}) & \overline{\rho} \in C \\ 0 & \text{elsewhere} \end{cases}
\end{aligned} \tag{3.114c}
$$

which is an integral equation for the solution of $E_z(\overline{\rho})$ in the domain A and on the boundary C. Clearly, $E_{ze} + E_{zm} = E_z^s$ is the scattered field from the dielectric cylinder. To derive the corresponding expression for H-polarization we follow the same procedure which yields the dual of (3.114).

We remark that an alternative and equivalent integral equation to (3.114) was derived by Ricoy and Volakis [IEE Proc.-H, 1989] who chose to work with equivalent currents rather than the fields themselves. In this case, the scattered field by the cylinder is expressed as

$$
E_z^s = -jk_o Z_o \int\int_A J_z'(\overline{\rho}') G_o(\overline{\rho},\overline{\rho}') ds' + Z_o \int_C M_z'(\overline{\rho}') G_o(\overline{\rho},\overline{\rho}') \tag{3.115}
$$

where J_z' and M_z' are some unknown equivalent current density quantities. They can be found by solving the integral equation

$$
\begin{aligned}
&\left[-\nabla\left(\frac{\mu_r - 1}{\mu_r}\right) \times \mathbf{H}^i(\overline{\rho}) - \left(\frac{\epsilon_r\mu_r - 1}{\mu_r}\right) \nabla \times \mathbf{H}^i(\overline{\rho})\right] \cdot \hat{z} \\
&= -\frac{1}{\mu_r} J_z'(\overline{\rho}) - jk_o \int\int_A J_z'(\overline{\rho}') K(\overline{\rho},\overline{\rho}') ds' + \int_C M_z'(\overline{\rho}') K(\overline{\rho},\overline{\rho}') d\ell'
\end{aligned} \tag{3.116}
$$

in which the kernel $K(\overline{\rho},\overline{\rho}')$ is given by

$$
K(\overline{\rho},\overline{\rho}') = \left[\frac{jk_o(\epsilon_r\mu_r - 1)}{\mu_r} - \frac{j}{k_o}\nabla\left(\frac{\mu_r - 1}{\mu_r}\right) \cdot \nabla\right] G_o(\mathbf{r},\mathbf{r}') \tag{3.117}
$$

Both integral equations (3.114) and (3.116) involve the same (undifferentiated) number of unknown quantities and have the same kernel singularity. As a result, there is no advantage between the two integral equations.

Chapter 4

Solution of Integral Equations for Wire Radiators and Scatterers

4.1 Formulation

Let us consider a wire of length 2ℓ and radius a ($\ell \gg a$), as shown in Figure 4.1. The wire is excited by an incident field $\mathbf{E}^i$ and we are interested in computing the current generated on the wire due to this excitation. Upon determination of the current we can then compute the radiated field in the usual manner.

To solve for the wire surface currents, we must enforce the boundary condition demanding that the total tangential electric field vanishes on the surface of the perfectly conducting wire. That is,

$$E_z^{tot} = E_z^i + E_z^r = 0 \tag{4.1}$$

where E_z^r is the field radiated by the wire surface current density $\mathbf{J}(\phi, z) = \hat{z}J_z(\phi, z) + \hat{\phi}J_\phi(\phi, z)$. However, on the assumption of a very thin wire, i.e. $k_o a \ll 1$, where $k_o = 2\pi/\lambda_o$ is the free space wavenumber, $J_\phi(\phi, z)$ will either be negligible or not effect the radiated field. Thus, from (2.52a), (2.109c) or (2.102a) in conjunction with (2.101) we may express the wire radiated field as

$$\mathbf{E}^r(\rho, \phi, z) = -jk_o Z_o \hat{z} \int_{-\ell}^{\ell} \int_0^{2\pi} J_z(\phi', z') \left(1 + \frac{1}{k_o^2} \frac{\partial^2}{\partial z^2}\right) \frac{e^{-jk_o R}}{4\pi R} a d\phi' dz' \tag{4.2}$$

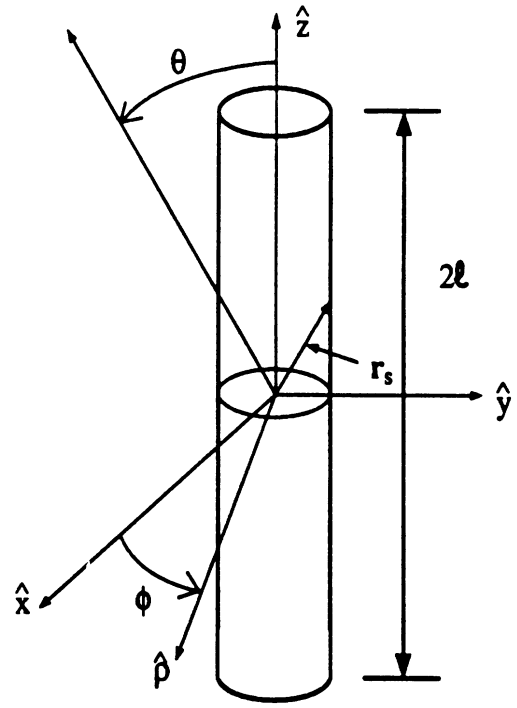

Figure 4.1: Cylindrical wire geometry.

in which $Z_o = 1/Y_o$ denotes the free space intrinsic impedance and

$$R = |\mathbf{r} - \mathbf{r}'| = \sqrt{\rho^2 + a^2 - 2\rho a \cos(\phi - \phi') + (z - z')^2} \tag{4.3}$$

since $\mathbf{r} = \rho\hat{\rho} + z\hat{z}$ and $\mathbf{r}' = a\hat{\rho}' + z'\hat{z}$. This expression can be further simplified by assuming that $J_z(\phi, z)$ is symmetric with respect to ϕ, a reasonable assumption since the wire is very thin and is typically part of a transmission line fed by a voltage source at its center. The surface current $J_z(\phi, z)$ can then be equivalently replaced by a filamentary line current $I(z)$ placed at the center of the tubular conductor. For the two currents to generate the same field when $\rho \gg a$, it is necessary that they satisfy the relation

$$I(z) = \int_0^{2\pi} J_z(\phi, z) a d\phi = 2\pi a J_z(z). \tag{4.4}$$

Introducing this into (4.2) yields

$$E_z^r(\rho, \phi = 0, z) = E_z^r(\rho, z) = -jk_o Z_o \int_{-\ell}^{\ell} I(z') \left(1 + \frac{1}{k_o^2} \frac{d^2}{dz^2}\right) G_w(z - z') dz' \tag{4.5}$$

where

$$G_w(z - z') = \frac{1}{2\pi} \int_0^{2\pi} \frac{e^{-jk_o\sqrt{\rho^2 + a^2 - 2\rho a \cos\phi' + (z-z')^2}}}{4\pi\sqrt{\rho^2 + a^2 - 2\rho a \cos\phi' + (z - z')^2}} d\phi' \tag{4.6}$$

and we have arbitrarily set $\phi = 0$ since by symmetry the radiated field is expected to be independent of ϕ.

To construct the integral equation for the solution of the current $I(z)$ we set $\rho = a$ in (4.6) and substitute (4.5) into (4.1). This gives

$$E_z^i(\rho = a, z) = +jk_o Z_o \int_{-\ell}^{\ell} I(z') \left(1 + \frac{1}{k_o^2} \frac{d^2}{dz^2}\right) G_{wu}(z - z') dz' \tag{4.7}$$

The kernel $G_{wu}(z - z')$ is now given by

$$G_{wu}(z - z') = \frac{1}{2\pi} \int_0^{2\pi} \frac{e^{-jk_o R_u}}{4\pi R_u} d\phi' \tag{4.8}$$

with

$$R_u = \sqrt{(z-z')^2 + 4a^2 \sin^2(\phi'/2)} \tag{4.9}$$

G_{wu} is often referred to as the unreduced thin wire kernel. In practice, though, to avoid the integration over ϕ', $G_{wu}(z-z')$ is replaced by the reduced kernel

$$G_{wr}(z-z') = \frac{e^{-jk_o\sqrt{(z-z')^2+a^2}}}{4\pi\sqrt{(z-z')^2+a^2}} = \frac{e^{-jk_oR_o}}{4\pi R_o} \tag{4.10}$$

which is obtained by letting $\mathbf{r} = z'\hat{z}$. That is, the reduced kernel refers to the problem where the filamentary current is introduced from the start of the analysis. Substituting (4.10) into the integral equation (4.7) gives

$$E_z^i(\rho = a, z) = jk_oZ_o \int_{-\ell}^{\ell} I(z') \left(1 + \frac{1}{k_o^2}\frac{d^2}{dz^2}\right) \frac{e^{-jk_oR_o}}{4\pi R_o} dz' \tag{4.11}$$

with R_o as defined in (4.10). One readily observes that the right hand side of this equations is simply the negative of the field radiated by the filamentary current $I(z)$ and evaluated at $\rho = a$, (i.e. on the surface of the perfectly conducting wire as shown in Fig. 4.2. Obviously, (4.11) could have been derived in a more direct manner by first invoking the approximation (4.4) and then referring to the integral representation (2.109c). Nevertheless, the above steps should serve to clarify the implied approximations. Also, as will be shown later (4.7) and (4.11) can be solved with equal efforts when an iterative solution scheme is employed.

The thin wire integral equation (4.11) is commonly referred to as Pocklington's integral equation. More generally, it belongs to the general class of Fredholm integral equations of the first kind. These are characterized by the presence of the unknown function only under the integral whose limits are constant. Integral equations which have the unknown quantity both under and outside the integral are of the second kind and we shall consider them at the end of this chapter. Also, if the integral limits are not constant, then the corresponding integral equations are of the Voltera type which are the typical equations for non-harmonic (time-dependent) field quantities.

An analytical solution of (4.11) is not possible unless the wire is semi-infinite in which case function theoretic techniques such as the Weiner-Hopf method [ ] can be employed for its solution in the transform domain. However,

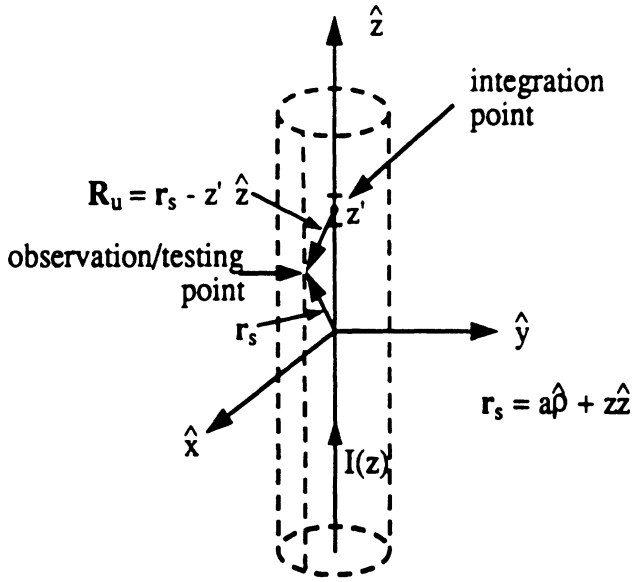

Figure 4.2: Geometry for testing on the wire surface.

Pocklington's integral equation can be numerically solved without difficulty, particularly because the integral's kernel is never singular since $R_o > a$ for all values of z and z'. Nevertheless, to reduce the kernel's singularity, it is still instructive to transfer one of the derivatives from the Green's function to the current as was done in section 3.1.2 in conjunction with the Stratton-Chu integral equation. In particular, from the one-dimensional form of (3.12) via integration by parts we have (note $\frac{d}{dz}G_{wr} = -\frac{d}{dz'}G_{wr}$)

$$\int_{-\ell}^{\ell} I(z')\frac{d^2}{dz^2}G_{wr}(z-z')dz' = \int_{-\ell}^{\ell} \frac{dI(z')}{dz'}\frac{d}{dz}G_{wr}(z-z')dz' - \frac{d}{dz}\left[G_{wr}(z-z')I(z')\right]_{z'=-\ell}^{z'=\ell} \tag{4.12}$$

Since the current at the wire ends must vanish, we observe that the last term of (4.12) is zero and thus Pocklington's integral equation can be rewritten as

$$E_z^i(\rho = a, z) = jk_oZ_o\int_{-\ell}^{\ell}\left[I(z')G_{wr}(z-z') + \frac{1}{k_o^2}\frac{d}{dz'}I(z')\frac{d}{dz}G_{wr}(z-z')\right]dz' \tag{4.13}$$

An alternative way to derive Pocklington's equation is through the use of the vector and scalar potentials. Accordingly, from (2.4) E_z^r can be expressed as

$$E_z^r(\rho, z) = -jk_o Z_o A_z - \frac{\partial \Phi_e}{\partial z} \tag{4.14}$$

where

$$A_z(\rho = a, z) = \int_{-\ell}^{\ell} I(z') \frac{e^{-jk_o R_o}}{4\pi R_o} dz' \tag{4.15}$$

and

$$\Phi_e(\rho = a, z) = \int_{-\ell}^{\ell} \frac{\rho(z')}{\epsilon_o} \frac{e^{-jk_o R_o}}{4\pi R_o} dz' \tag{4.16}$$

From the continuity equation (1.33) we have

$$\frac{\rho(z)}{\epsilon_o} = -\frac{Z_o}{jk_o} \frac{dI(z)}{dz} \tag{4.17}$$

and, thus, when (4.14) along with (4.15) - (4.17) is substituted into (4.1) we obtain (4.13).

The standard procedure for solving the above integral equation amounts to first expanding the currents in terms of a class of basis functions. That is, $I(z)$ is approximately expressed as a linear sum of N known expansion functions. Upon substitution of this expansion into (4.13) we obtain an equation for the coefficients of the expansion which is a function of the surface observation point z. The second step in the numerical solution process is the enforcement of the integral equation at specific values of z. In this manner we obtain a single linear equation for each enforcement point. If we have N expansion coefficients, a total of N linear equations must then be generated by changing the location of the testing point. These comprise a system which can be solved for the unknown expansion coefficients. Depending on the type of expansion functions or enforcement scheme, different linear systems will be obtained. The procedure of expanding the current in terms of a finite set of functions and then enforcing the boundary condition is referred to as the discretization of the integral equation. Discretization is therefore the procedure which generates the linear system. In turn, the resulting system can be solved through various

direct or iterative methods to obtain the coefficients of the expansion. A knowledge of these provides an approximation for the current distribution and once the current is known we can proceed with the computation of the radiated field, input impedance, radiated power and gain of the antenna using standard formulae.

Before proceeding with the discretization of the integral equation (4.11) as discussed above, we first present some of the most commonly used expansion basis for the current distributions.

4.2 Basis Functions

A first step in discretizing (4.9) is to expand the current distribution as

$$I(z) = \sum_{n=0}^{N-1} I_n f_n(z) = \sum_{n=0}^{N-1} I_n f(z - z_n) \tag{4.18}$$

where $f_n(z)$ are the basis functions of the expansion and I_n are unknown expansion coefficients. Referring to Figure 4.3, some of the most popular choices for $f_n(z)$ are

(1) Pulse basis functions/Piecewise constant (PWC):

$$f_n(x) = P_{\Delta x}(x - x_n) = \begin{cases} 1 & x_n - \frac{\Delta x}{2} < x < x_n + \frac{\Delta x}{2} \\ 0 & \text{elsewhere} \end{cases} \tag{4.19}$$

(2) Triangular function/Piecewise linear:

$$f_n(x) = T_n(x) = \left(1 - \frac{|x - x_n|}{\Delta x}\right) P_{2\Delta x}(x - x_n) \tag{4.20}$$

(3) Piecewise sinusoidal (PWS):

$$f_n(x) = S_n(x) = \frac{\sin k_o(\Delta x - |x - x_n|)}{\sin k_o \Delta x} P_{2\Delta x}(x - x_n) \tag{4.21}$$

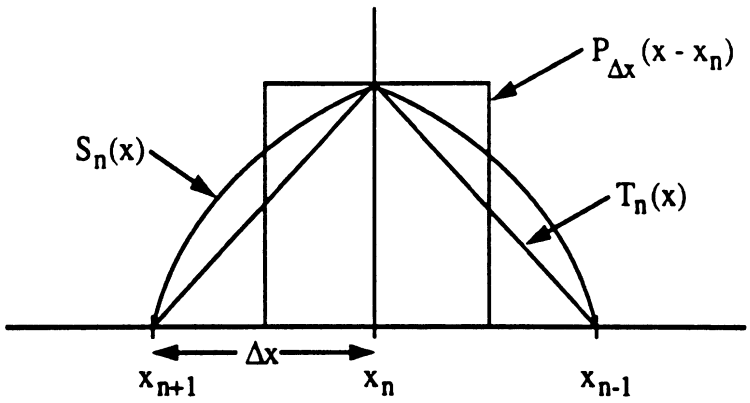

Figure 4.3: Three subsectional expansion functions.

where Δx is usually small (of the order $\lambda_o/10$) and $N = 2\ell/\Delta x$. Because their domain is confined to a small section of the wire, they are commonly referred to as subsectional or subdomain basis functions. A major reason for their popularity is owed to their capability to model any arbitrary function provided Δx is sufficiently small.

As illustrated though in figure 4.4, they cause artificial discontinuities in the current or its derivatives at the transition between two consecutive expansion functions. Specifically, the current expansion with the PWC basis is inherently discontinuous at the junction of two adjacent segments and from (4.17) this implies the existance of a fictitious charge at that point. Nevertheless, in spite of this difficiency when the segments are sufficiently small, they provide a reasonable approximation to the current distribution. In that case, the constant value over the segment should be interpreted to represent the average of the true current over that segment. Because of their simplicity, and this will soon be apparent in the next section, they have been used extensively in electromagnetics but more so for scattering than antenna parameter computations. In the last case, excessive sampling may be required for the correct evaluation of the antenna's input impedance.

The piecewise linear basis are seen to generate continuous current distributions. This is because the adjacent basis are overlaid as shown in figure 4.4(b). Thus, the current at any point on the wire is obtained by summing the overlaid basis. From their definition, though, when one of the overlaying expansion functions is at a maximum, the left and right adjacent expansion

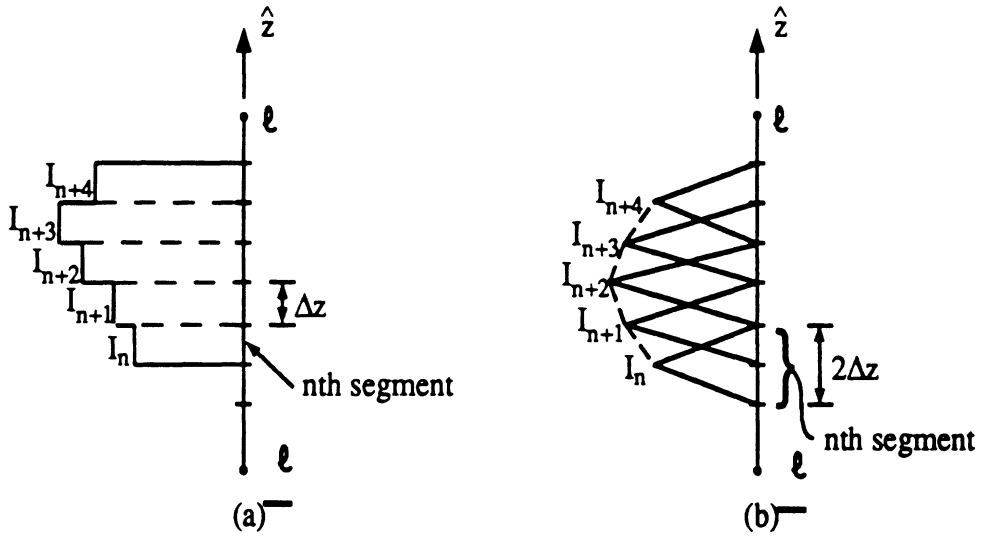

Figure 4.4: Illustration of wire segmentation and current approximation with subdomain basis (a) pulse basis expansion (b) triangular basis expansion.

functions are zero. Further, because each expansion is normalized, the coefficients correspond to the current's value at the middle of the nth segment. The PWS expansion functions are very similar to the linear basis in nearly all respects. One difference between the two is that the PWS basis can be differentiated any arbitrary number of times within its range without vanishing. Nevertheless, similarly to the piecewise linear basis they also yield a current expansion that has a discontinuous first derivative at the middle of each wire segment. The only advantage of the PWS basis is drawn from their property to yield potential integrals which can be evaluated analytically once $S_n(x)$ is expressed as a sum of two exponentials.

Instead of using the above subsectional or subdomain basis to represent the wire current one could alternatively employ the usual full basis expansions such as $\cos nx$ and $\sin nx$. For example, noting that $I(\pm\ell) = 0$, an appropriate expansion for the wire current would be

$$I(z) = \sum_{n=1}^{N} C_n \cos\left[\frac{(2n-1)\pi z}{2\ell}\right] \tag{4.22}$$

or

$$I(z) = \sum_{n=1}^{N} C_n \sin\left[\frac{(2n-1)\pi z}{\ell}\right] \tag{4.23}$$

In contrast to the expansions (4.19) - (4.21), the coefficients of these expansions do not coincide with specific values of the current $I(z)$. More importantly, N may have to be quite large in case $I(z)$ is rapidly varying or not sinusoidal in form. However, for wire antennas $I(z)$ is generally sinusoidal, particularly when the wire is excited by an external incident field. In this case only a few terms of the full basis expansions (4.22) or (4.23) may be required, making them attractive. Generally, though, (4.22) - (4.23) cannot be effectively used for curved wires or other complex wire structures on which the current's distribution is much more irregular. In the following, we shall therefore concentrate on the discretization and solution of Pocklington's integral equation using subdomain/basis functions since such a solution is less specific to the straight wire.

4.3 Pulse Basis–Point Matching Solution

For simplicity, let us first consider the pulse basis expansion to represent the wire current distribution. This results in a summation of shifted pulses over the total length of the wire, i.e.

$$I(z) = \sum_{n=0}^{N-1} I_n P_{\Delta z}(z - z_n) \tag{4.24}$$

where

$$N = \frac{2\ell}{\Delta z} \tag{4.25}$$

are the number of pulses used to approximate the current distribution on the wire and

$$z_n = -\ell + \left(n - \frac{1}{2}\right)\Delta z; \quad n = 0, 1, 2, \ldots \tag{4.26}$$

Substituting (4.24) into (4.13) yields

$$E_z^i = \frac{jk_oZ_o}{4\pi}\left\{\sum_{n=0}^{N-1} I_n \int_{z_n-\frac{\Delta z}{2}}^{z_n+\frac{\Delta z}{2}} \frac{e^{-jk_oR_o}}{R_o}dz' + \frac{1}{k_o^2}\sum_{n=0}^{N-1} I_n \frac{d}{dz}\right. \cdot \left.\left[\frac{e^{-jk_oR_{1n}}}{R_{1n}} - \frac{e^{-jk_oR_{2n}}}{R_{2n}}\right]\right\} \tag{4.27}$$

where

$$R_{1n} = \sqrt{\left(z - z_n + \frac{\Delta z}{2}\right)^2 + a^2}\,, \qquad R_{2n} = \sqrt{\left(z - z_n - \frac{\Delta z}{2}\right)^2 + a^2} \tag{4.28}$$

and we have invoked the expression

$$\frac{dI(z)}{dz} = \sum_{n=-N/2}^{N/2} I_n\left[\delta\left(z - z_n + \frac{\Delta z}{2}\right) - \delta\left(z - z_n - \frac{\Delta z}{z}\right)\right] \tag{4.29}$$

in deriving (4.27). After differentiating the last term of (4.27) with respect to z, we obtain

$$E_z^i(\rho = a, z) = \frac{jZ_o}{2\lambda_o}\sum_{n=0}^{N-1} I_n\left[\Psi_n(z) + \Phi_n(z)\right] \tag{4.30}$$

where

$$\Psi_n(z) = \int_{z_n-\frac{\Delta z}{2}}^{z_n+\frac{\Delta z}{2}} \frac{e^{-jk_oR_o}}{R_o}dz' \tag{4.31}$$

and

$$\Phi_n(z) = -k_o\left[\left(z - z_n + \frac{\Delta z}{2}\right)\frac{(jkR_{1n}+1)}{(k_oR_{1n})^3}e^{-jk_oR_{1n}} - \left(z - z_n - \frac{\Delta z}{2}\right)(jk_oR_{2n}+1)\frac{e^{-jk_oR_{2n}}}{(k_oR_{2n})^3}\right] \tag{4.32}$$

Equation (4.30) can now be solved for I_n by demanding that it be satisfied (matched) at N points on the surface of the wire. A convenient set of such points is

$$z = z_m = -\ell + \left(m - \frac{1}{2}\right)\Delta z, \quad m = 0, 1, 2, 3, \ldots$$

with $\phi = 0$, i.e. along the line formed by the wire surface and the xy plane. This results in a set of matrix equations which are commonly written as

$$[Z_{mn}]\{I_n\} = \{V_m\} \tag{4.33}$$

In (4.25)

$$\{I_n\} = \left\{I_0, I_1, I_2, \ldots, I_{N/2}, \ldots, I_{N-1}\right\}^T \tag{4.34}$$

is a column matrix, $[Z_{mn}]$ is a square matrix referred to as the impedance matrix and $\{V_m\}$ is the excitation column whose elements are given by

$$V_m = -E_z^i(\rho = a, z_m) \tag{4.35}$$

The corresponding elements of the impedance matrix can be obtained directly from (4.30) - (4.32). We find

$$Z_{mn} = -\frac{jZ_o}{2\lambda_o}\left[\Psi_n(z_m) + \Phi_n(z_m)\right] \tag{4.36}$$

where $\Psi_n(z_m)$ can be rewritten as

$$\Psi_n(z_m) = \int_{(z_m - z_n) - \frac{\Delta z}{2}}^{(z_m - z_n) + \frac{\Delta z}{2}} \frac{e^{-jk_o\sqrt{t^2+a^2}}}{\sqrt{t^2+a^2}} dt.$$

It is seen that $Z_{nm} = Z_{mn}$ indicating that the impedance matrix is symmetric. It is also observed that $[Z_{mn}]$ is completely independent of the excitation.

The integral $\Psi_n(z_m)$ cannot be evaluated analytically but can be approximated in closed form with sufficient acccuracy. For $m \neq n$, $\sqrt{t^2+a^2}$ is not very small and we may therefore employ midpoint integration to approximately express it as

$$\Psi_n(z_m) \approx \Delta z \frac{e^{-jk_o\sqrt{(z_m - z_n)^2 + a^2}}}{\sqrt{(z_m - z_n)^2 + a^2}}; \quad m \neq 0$$

When $m = n$, $\sqrt{t^2+a^2}$ is nearly zero over the midrange of integration. In this case we can employ the two term expansion

$$e^{-jk_oR} \cong 1 - jk_oR$$

allowing us to approximate $\Psi_n(z_n)$ as

$$\Psi_n(z_n) \approx \int_{\frac{-\Delta z}{2}}^{\frac{\Delta z}{2}} \left[\frac{1}{\sqrt{t^2+a^2}} - jk_o\right] dt = \ln\left(\frac{\sqrt{\left(\frac{\Delta z}{2}\right)^2 + a^2} + \frac{\Delta z}{2}}{\sqrt{\left(\frac{\Delta z}{2}\right)^2 + a^2} - \frac{\Delta z}{2}}\right) - jk_o\Delta z$$

and for $\Delta z \gg a$ this can be further simplified to give

$$\Psi_n(z_n) \approx 2\ln\left(\frac{\Delta z}{a}\right) - jk_o\Delta z; \quad \Delta z \gg a.$$

An alternative way in computing the integral $\Psi_n(z_m)$ is to *regularize* its near singular integrand with the addition and subtraction of the term $\frac{1}{\sqrt{t^2+a^2}}$ which can be integrated analytically. This gives

$$\begin{aligned}\Psi_n(z_m) &= \int_{(z_m-z_n)-\frac{\Delta z}{2}}^{(z_m-z_n)+\frac{\Delta z}{2}} \left[\frac{e^{-jk_o\sqrt{t^2+a^2}}}{\sqrt{t^2+a^2}} - \frac{1}{\sqrt{t^2+a^2}}\right] dt \\ &\quad + \ln\left(\frac{\sqrt{\left(z_m - z_n + \frac{\Delta z}{2}\right)^2 + a^2} + z_m - z_n + \frac{\Delta z}{2}}{\sqrt{\left(z_m - z_n - \frac{\Delta z}{2}\right)^2 + a^2} + z_m - z_n - \frac{\Delta z}{2}}\right)\end{aligned}$$

The new integrand is now slowly varying and can thus be evaluated numerically without difficulty.

To compute the current coefficients we must solve the system (4.33) and there are a number of commercially available routines which can perform this operation in a manner transparent to the user. Commonly used software libraries such as IMSL, LINPACK, and NAG include a variety of subroutines for a solution of (4.33). These are based on solution methods such as Gauss-Jordan elimination, Gaussian elimination, Crout or LU decomposition, most of which are discussed in numerical analysis textbooks.

If we choose to solve $\{I_m\}$ by inverting the matrix $[Z_{mn}]$, the required CPU time will be approximately

$$t \approx AN^2 + BN^3 + CN^2N_i \tag{4.37}$$

where N, of course, denotes the number of unknowns or the length of the column $\{I_n\}$ and N_i is the number of different excitations for which $\{I_n\}$ must

be computed. In addition,

A = time required to compute each value of Z_{mn}
BN^3 = time required to invert $[Z_{mn}]$

and

CN^2 = time required to perform the matrix multiplication $[Z_{mn}]^{-1}\{V_m\}$.

The actual values of the constants A, B and C are machine dependent. Expression (4.37) holds regardless of the procedure used to obtain the inverse, but clearly, for large N the second term of (4.37) dominates. However, a solution for $\{I_n\}$ can be obtained without a need to complete the inverse. In this case the Gauss-Jordan elimination requires N^3 operations to complete the solution whereas the Gaussian elimination needs $5N^3/6$ operations. In contrast, the LU (Lower-Upper) decomposition approach requires $N^3/3$ operations and is thus much faster. The LU decomposition scheme is also preferred because it results in better accuracy and stability as compared to other methods, particularly when N is large. Nevertheless, when N becomes very large, a direct solution of the linear system (4.33) may yield an inaccurate result due to machine round-off errors. An alternative in this case is to use an iterative solution scheme allowing some control of the solution error, and such a scheme is discussed at the end of this chapter.

Often, as is the case with the linear wire discussed here, the impedance matrix will posses certain symmetries which can be exploited in the solution of (4.33). It is easy to observe from (4.28), (4.31), (4.32) and (4.36) that $Z_{nm} = Z_{mn} = Z_{m-n} = Z_{|m-n|}$. Matricies of this type are referred to as symmetric Toeplitz and require order N^2 operations to complete the solution. Also, since the elements of $[Z_{mn}]$ can be generated from those in one row or a column, the fill time of the matrix can be reduced to only order N operations. Note, that if we were to consider a solution of the currents on a curved wire, then $Z_{mn} \neq Z_{|m-n|}$ but $Z_{nm} = Z_{mn}$ as a consequence of reciprocity (i.e. the matrix is still symmetric).

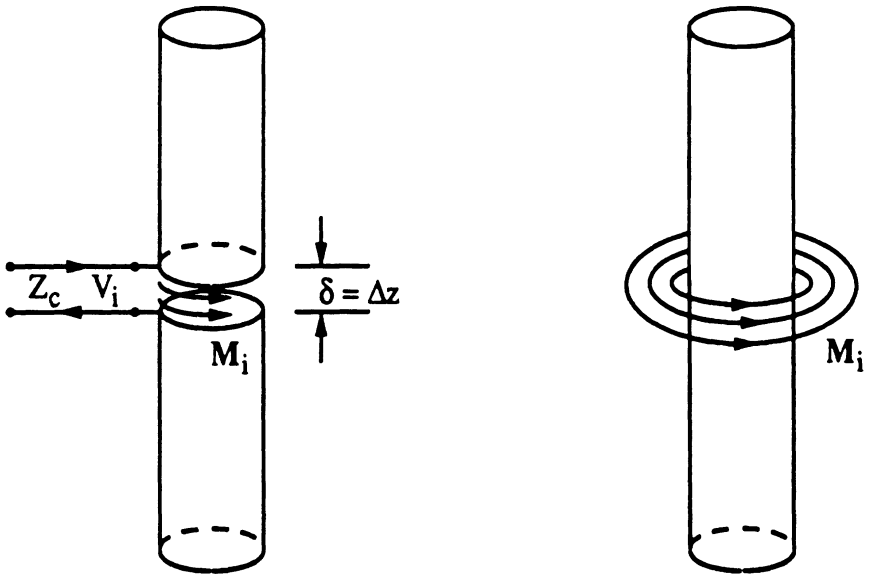

Figure 4.5: Source modeling for the center fed cylindrical dipole.

4.4 Source Modeling

4.4.1 Delta gap excitation

The wire antenna is usually center fed by a transmission line whose voltage can be measured at the terminals of the antenna. Assuming, the transmission line voltage at the wire terminals is V_i (see Figure 4.5), we may then write

$$V_i = -\int_{-\delta/2}^{\delta/2} \mathbf{E}^r \cdot \hat{z} dz = +\int_{-\delta/2}^{\delta/2} E_z^i dz = +E_z^i \delta \tag{4.38}$$

from small δ. Consequently

$$E_z^i = \begin{cases} \frac{+V_i}{\delta} & z = 0 \\ 0 & \text{elsewhere} \end{cases} \tag{4.39}$$

and this is referred to as the delta gap excitation model for the source field E_z^i. Note that (4.39) is equivalent to having a magnetic current loop

$$\mathbf{M}^i = -\hat{\rho} \times \mathbf{E}^i = \hat{\phi} \frac{V_i}{\delta} \tag{4.40}$$

of radius a as the excitation. In fact, the derivation of (4.38) requires that the delta gap is first closed making the conductor continuous. The excitation field E_z^i which is confined over the original gap length can then be replaced by the equivalent magnetic current loop $\mathbf{M}^i$. This, in turn generates a scattered field E_z^r at the conductor's surface so that the total field $E_z^i + E_z^r$ vanishes as required, a condition which was imposed in deriving (4.38). Inherently, the presence of the magnetic current generates discontinuous electric fields across its surface and for this particular case the electric field is zero in the interior side of $\mathbf{M}_i$ and equal to $\hat{z}E_z^i$ at its exterior side.

Wire current distributions obtained by solving the system (4.33) in conjunction with a delta gap modeling of the source are illustrated in figures 4.6 and 4.7. The curves in each figure correspond to $\lambda_o/2$ and λ_o long dipoles, respectively, of radius $a = 0.005\lambda_o$. It is seen that a rather large number of pulse basis are required for the current to converge to its final value. Generally, (i.e. provided the system has acceptable condition number), the correct distribution is obtained if the computed values of $I(z)$ do not change appreciably as N is increased. Having the correct value of $I(z)$ is extremely important for input impedance computations but the radiation pattern can be predicted with sufficient accuracy once $I(z)$ is known approximately. As expected, the computed current is sinusoidal in form except near the feed point and, thus, it is not surprising that the often assumed sinusoidal behavior of the wire current is sufficient for pattern prediction but much less so for input impedance computations. This is more apparent for the λ_o long dipole in which case the sinusoidal distribution will predict zero current at the feed.

Perhaps one of the reasons for the large number of expansion pulses required to reach convergence is the difficulty of the point matching procedure in satisfying the boundary condition at all z. As seen, from fig. 4.8, the wire surface fields obtained by integrating the numerically computed current given in fig. 4.6 do not vanish except at the match points z_m. Nevertheless, on the average, the surface field is zero as can be atested from the oscillatory behavior of the computed surface field given in fig. 4.8. Later, it will be discussed that higher order expansion functions and more robust testing procedures yield more satisfactory results with less unknowns.

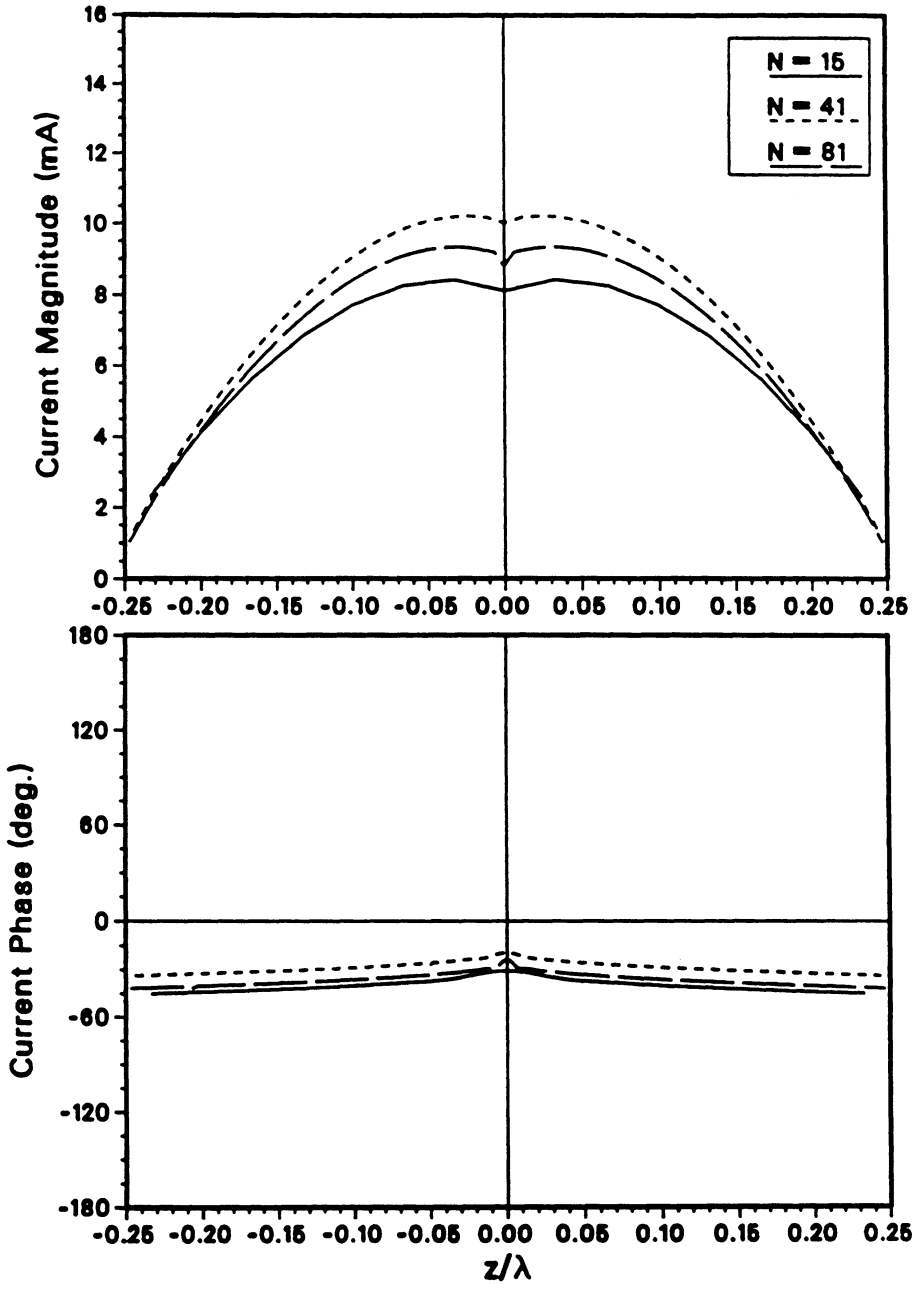

Figure 4.6: Computed current on a center-fed $\lambda_o/2$ dipole of radius $a = .005\lambda_o$ via the pulse basis-point matching solution method as a function of the sampling density. The source/excitation is a delta gap as given in (4.39).

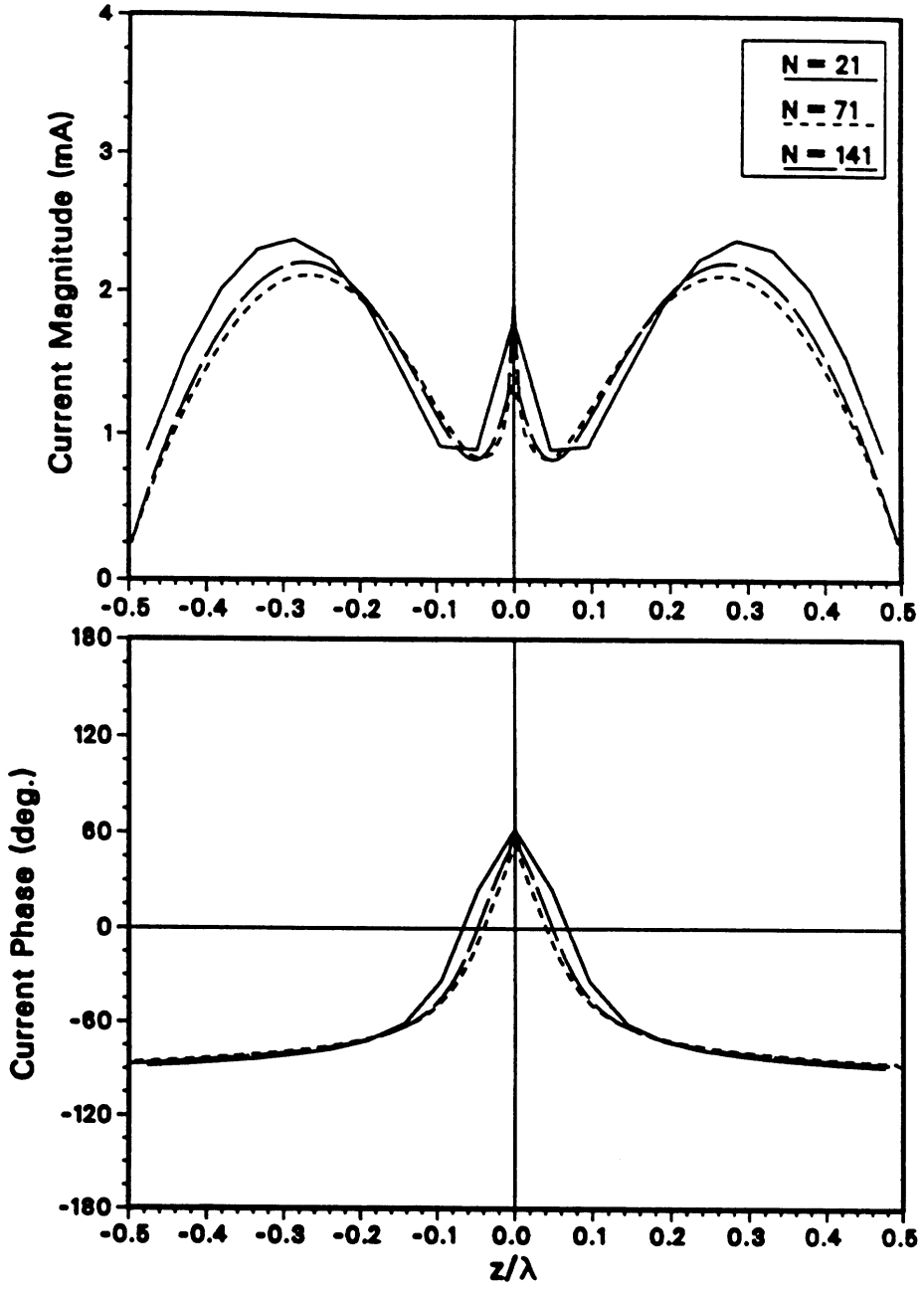

Figure 4.7: Computed current on a center-fed λ_o dipole of radius $a = .005\lambda_o$ via the pulse basis-point matching solution method as a function of the sampling density. The source/excitation is a delta gap as given in (4.39).

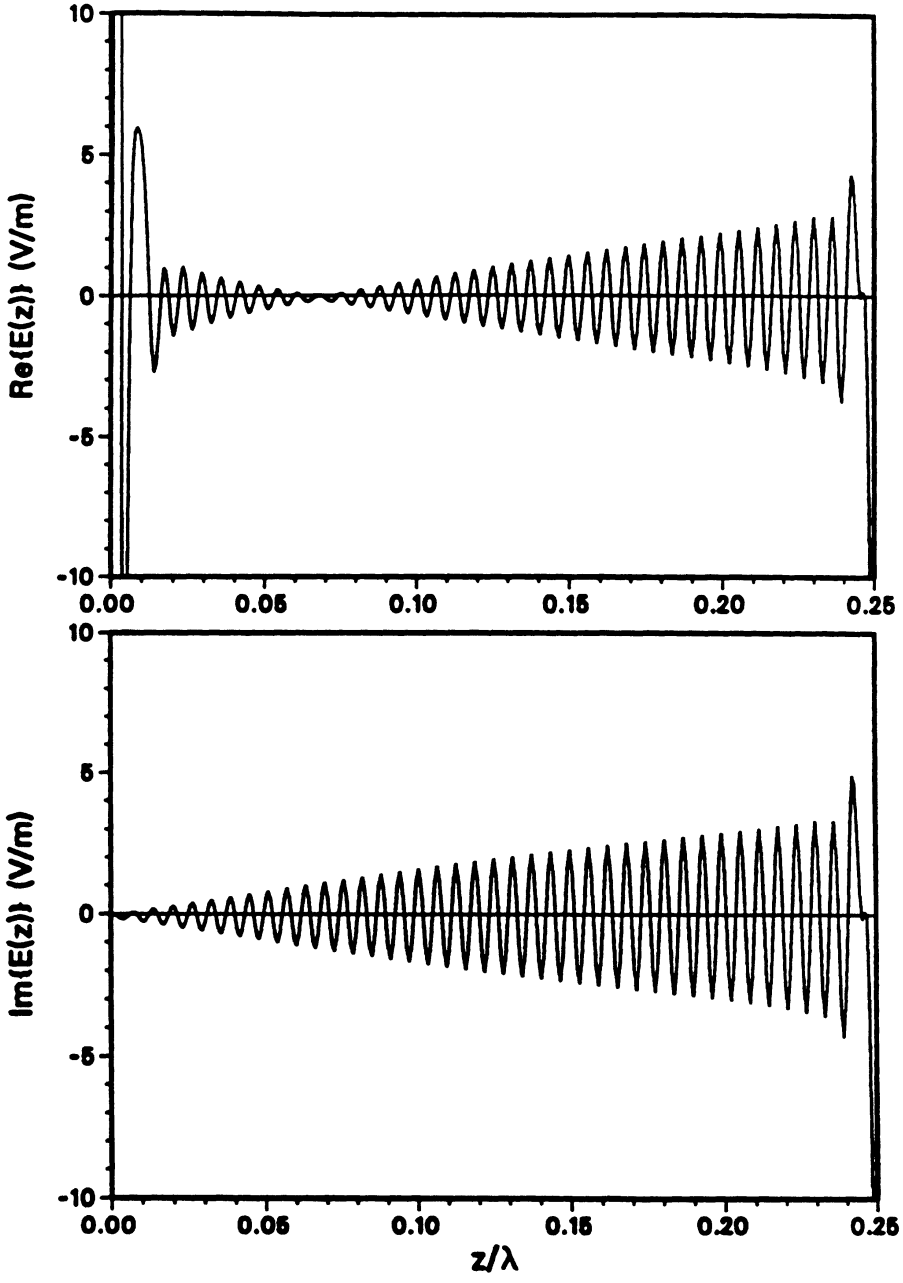

Figure 4.8: Value of the total field on the surface of the dipole computed by integrating the current obtained from a pulse basis-point matching solution ($2\ell = 0.5\lambda$, $a = 0.005\lambda$ and $N = 81$). A value of 5V/m corresponds to a 3.1% error.

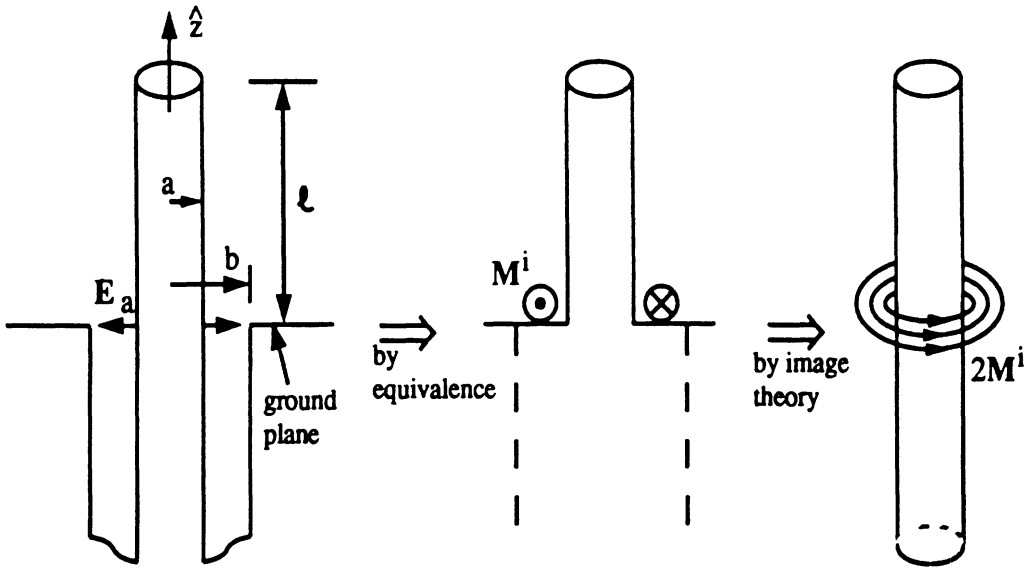

Figure 4.9: Magnetic frill model for a coaxially fed monopole/dipole.

4.4.2 Magnetic frill generator

As can be expected, (4.39) is not as accurate since the field is unlikely to be concentrated only within the gap. An alternative source model giving a smoothly varying excitation field around the gap is the magnetic frill generator. In this case the gap is equivalently replaced by a circumferentially directed surface magnetiuc current density existing in the region between $\rho = a$ and $\rho = b$, as shown. The value of the outer radius b is computed from a knowledge of the transmission lines characteristic impedance Z_c. When the wire antenna is fed by a coaxial cable it is shown below that the equivalent magnetic frill current can be computed in terms of the aperture fields in the usual manner.

Using the equivalence principle, the aperture is closed and replaced by the surface magnetic current

$$\mathbf{M}^i = \mathbf{E}^a \times \hat{z} \tag{4.41}$$

where

$$\mathbf{E}^a(\rho) = \hat{\rho}\frac{V_i}{2\rho \ln b/a} \qquad (V_i \text{ is a constant}) \tag{4.42}$$

as dictated by the lowest order mode supported in the coaxial transmission line. The radiated field by $\mathbf{M}^i$ may now be evaluated after invoking image

theory to double its strength and the length of the monopole to that of a dipole. From (2.63)

$$\mathbf{E}^i(\rho,z) = -\int_a^b \int_0^{2\pi} \left[\mathbf{M}^i(\rho') \times \hat{R}\right] \left(jk_o + \frac{1}{R}\right) \frac{e^{-jkR}}{4\pi R} \rho' d\phi' d\rho' \tag{4.43}$$

where

$$\mathbf{R} = |\mathbf{r} - \mathbf{r}'|$$

$$\mathbf{r} = \rho\hat{\rho} + z\hat{z}, \qquad \mathbf{r} = \rho'\hat{\rho} = \rho'(\hat{x}\cos\phi' + \hat{y}\sin\phi')$$

For $\rho = 0$ (observation at the center of the wire)

$$R = \sqrt{(\rho')^2 + z^2}$$

$$\hat{R} = \frac{\mathbf{r} - \mathbf{r}'}{R} = [-\hat{\rho}'\rho' + z\hat{z}]/R$$

$$\mathbf{M}^i(\rho') = -\hat{\phi}' \frac{V_i}{\rho' \ln b/a} = (\hat{x}\sin\phi' - \hat{y}\cos\phi') \frac{V_i}{\rho' \ln b/a}$$

$$\mathbf{M}^i(\rho') \times \hat{R} = [-\hat{z}\rho' - \hat{\rho}'z] \frac{V_i}{R\rho' \ln b/a}$$

Substituting the above expressions into (4.43) yields

$$\begin{aligned} E_z^i(\rho = 0, z) &= \frac{V_i}{\ln b/a} \int_a^b \int_o^{2\pi} \left(jk_o + \frac{1}{R}\right) \frac{e^{-jk_oR}}{4\pi R^2} \rho' d\phi' d\rho' \\ &= \frac{V_i}{2\ln b/a} \int_a^b \left(jk_o + \frac{1}{R}\right) \frac{e^{-jk_oR}}{R^2} \rho' d\rho' \end{aligned} \tag{4.44}$$

Noting that

$$-\frac{d}{d\rho'}\left\{\frac{e^{-jk_oR}}{R}\right\} = \left(jk_o + \frac{1}{R}\right) \frac{e^{-jk_oR}}{R} \frac{\rho'}{R}$$

(4.44) may be written as

$$E_z^i(\rho = 0, z) = -\frac{V_i}{2 \ln b/a} \int_a^b \frac{d}{d\rho'} \left\{ \frac{e^{-jk_o R}}{R} \right\} d\rho'$$

to yield

$$E_z^i(\rho = 0, z) = +\frac{V_i}{2 \ln b/a} \left[\frac{e^{-jk_o\sqrt{z^2+b^2}}}{\sqrt{z^2+b^2}} - \frac{e^{-jk_o\sqrt{z^2+a^2}}}{\sqrt{z^2+a^2}} \right] \tag{4.45}$$

For simplicity, we may assume

$$E_z^i(\rho = a, z) \approx E_z^i(\rho = 0, z)$$

to be substituted into (4.30) and (4.33) for the solution of the wire currents. Alternatively, we may pursue a direct evaluation of (4.43) to find [Tsai, IEEE Trans. Antenna & Propagat., Vol. AP-20, pp. 569-576, Sept. 1972]

$$E_z^i(\rho = a, z) = +V_i \frac{k_o(b^2 - a^2)e^{-jk_o R_o}}{8 \ln b/a R_o^2} \left\{ 2 \left[\frac{1}{k_o R_o} + j \left(1 - \frac{b^2 + a^2}{2R_o^2} \right) \right] \right. \tag{4.46}$$
$$\left. + \frac{a^2}{R_o} \left[\left(\frac{1}{k_o R_o} + j - j \frac{b^2 + a^2}{2R_o^2} \right) \left(-jk_o - \frac{2}{R_o} \right) + \left(-\frac{1}{k_o R_o^2} + j \frac{b^2 + a^2}{R_o^3} \right) \right] \right\}$$

where now

$$R_o = \sqrt{z^2 + a^2}$$

with

$$-\ell < z < \ell \, .$$

Figure 4.10 illustrates the current on a $1\lambda_o$ dipole computed with a magnetic frill model excitation. The current near the feed is now smoother than that obtained with the delta gap model. However, more samples are required to reach convergence and this is owed to the near singular behavior of the excitation field in (4.45).

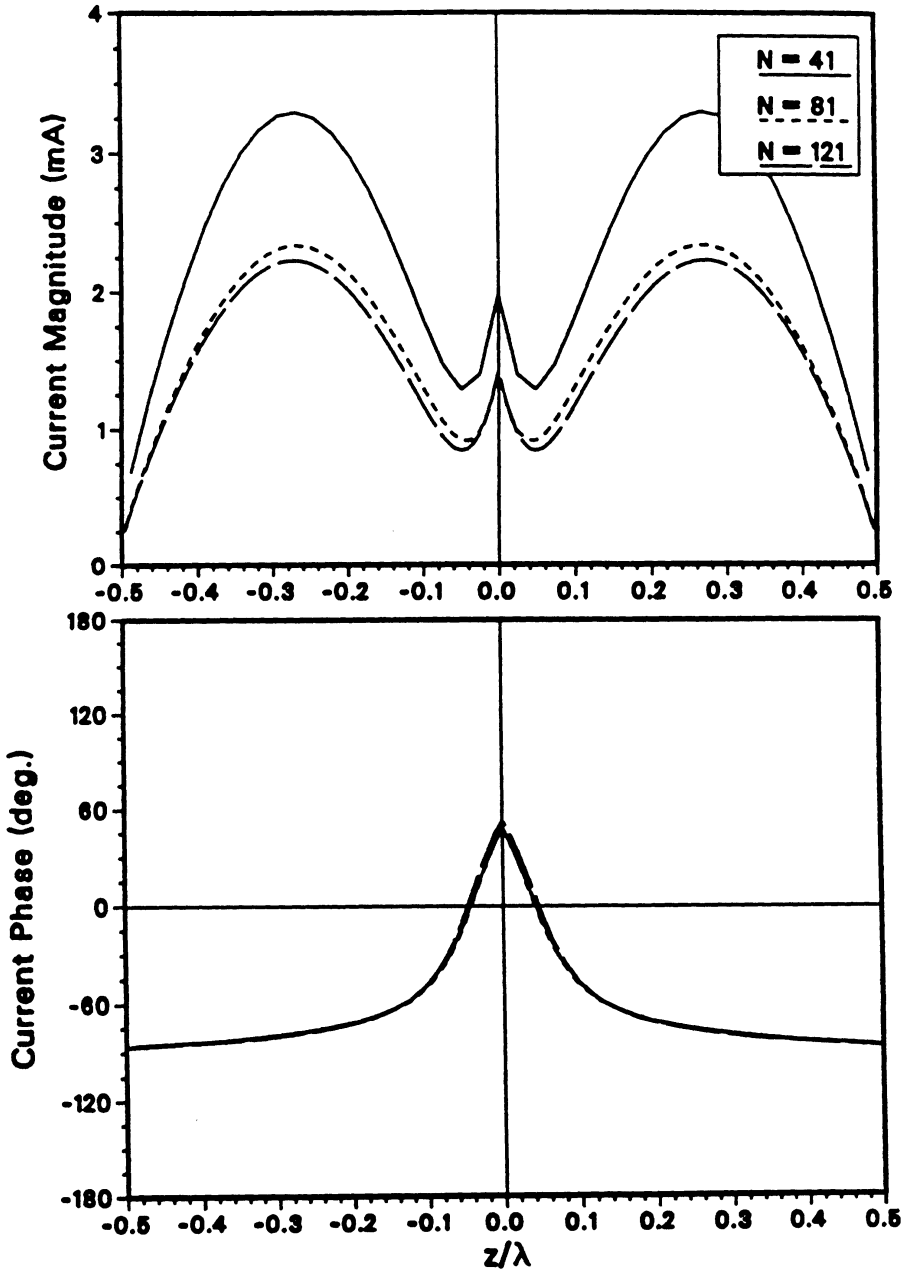

Figure 4.10: Computed current on a center-fed λ_o dipole of radius $a = .005\lambda_o$ via the pulse basis-point matching technique as a function of the sampling density. The source/excitation is the magnetic frill equivalent current as given in (4.45).

4.4.3 Plane Wave Incidence

If the cylindrical wire is considered as a scatterer, then $\mathbf{E}^i$ represents the incident field. The simplest form of this is a plane wave given by

$$\mathbf{E}^i = e^{jk_o \mathbf{r}_s \cdot \hat{r}_i} \tag{4.47}$$

where

$$\mathbf{r}_s = a\hat{\rho} + z\hat{z} = a\hat{x} + z\hat{z}|_{\phi=0}$$

if measured on the surface of the wire and

$$\hat{r}_i = \hat{x}\cos\phi_i \sin\theta_i + \hat{y}\sin\phi_i \sin\theta_i + \hat{z}\cos\theta_i \tag{4.48}$$

with (θ_i, ϕ_i) being the usual spherical angles denoting the direction of incidence.

Figures 4.11 and 4.12 show the current on the $\lambda_o/2$ and $1\lambda_o$ wire dipoles due to a plane wave incidence excitation. In contrast to the current on a center-fed dipole, this current has no discontinuous derivatives throughout the length of the dipole. Its form on the $\lambda_o/2$ dipole is clearly sinusoidal with its amplitude depending on the incidence angle. The same holds for longer wires with the exception of having a more complex lobing structure which can be explained by invoking the traveling wave theory.

4.5 Calculation of the Far Zone Field and Antenna Characteristics

Upon a solution of the system (4.33), one can proceed with the evaluation of the radiation or the scattering patterns if $\mathbf{E}$ is given by (4.48). From (2.77) we have

$$\begin{aligned} E_\theta^r &\approx jk_o Z_o \sin\theta \int_{-\ell}^{\ell} I(z') \frac{e^{-jk_o|\mathbf{r}-\mathbf{r}'|}}{4\pi|\mathbf{r}-\mathbf{r}'|} dz' \\ &\approx jk_o Z_o \sin\theta \frac{e^{jk_o r}}{4\pi r} \int_{-\ell}^{\ell} I(z') e^{jk_o z' \cos\theta} dz' \end{aligned} \tag{4.49}$$

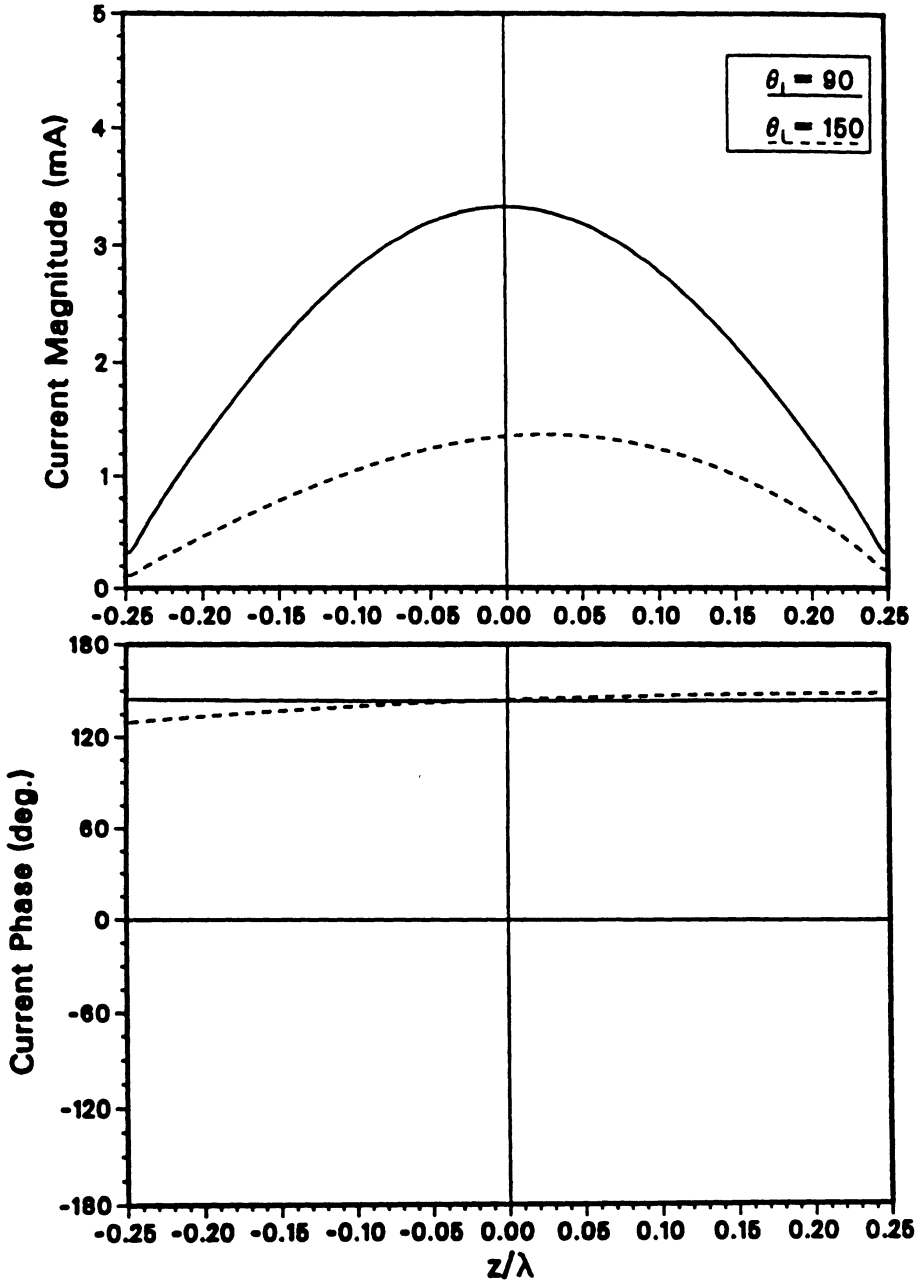

Figure 4.11: Current on a $\lambda_o/2$ wire of radius $a = .005\lambda$ generated by an incident plane wave at $\theta_i = 90°$ and $\theta_i = 150°$ as computed by the pulse basis-point matching technique ($a = 0.005\lambda_o, N = 101$).

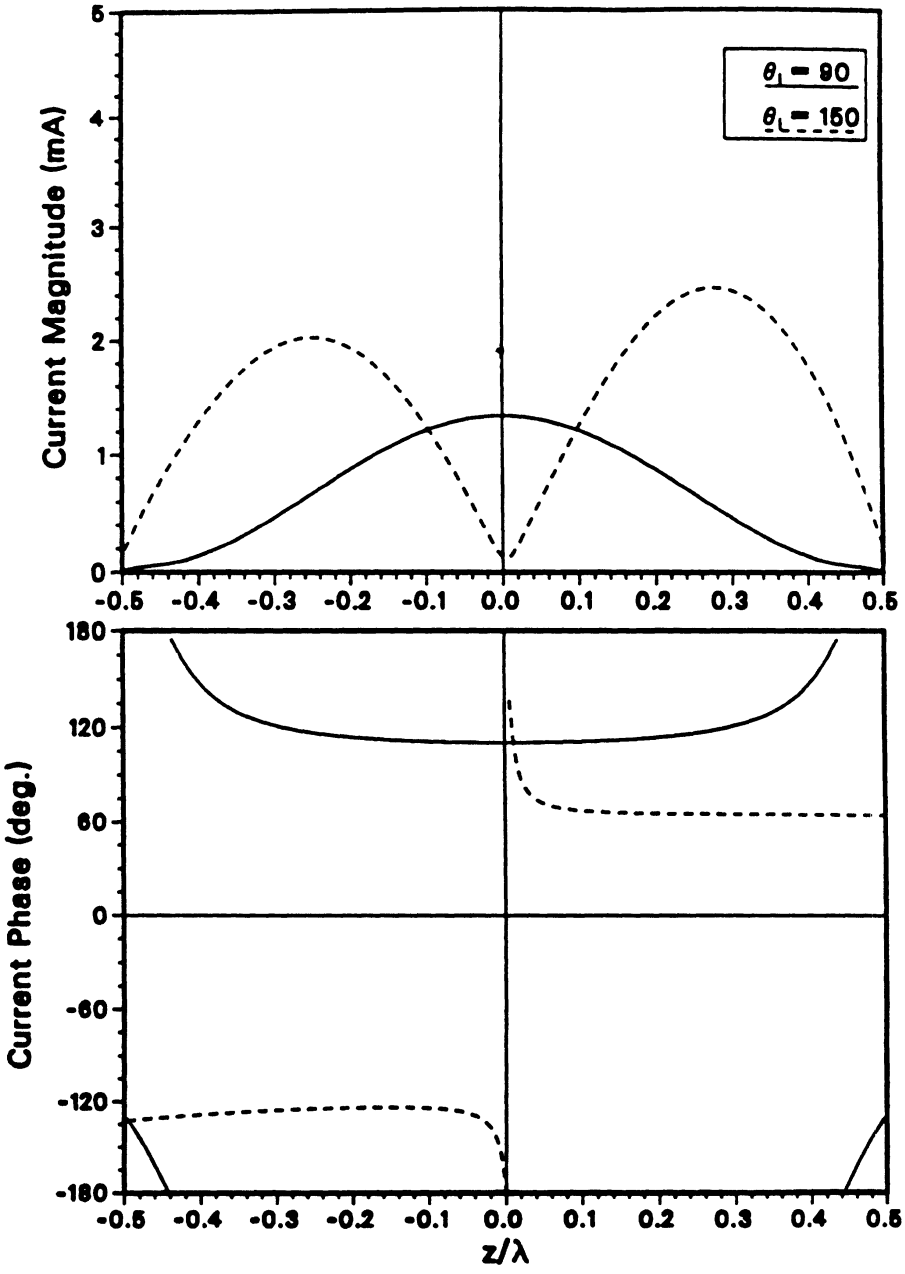

Figure 4.12: Current on a λ_o wire of radius $a = .005\lambda$ generated by an incident plane wave at $\theta_i = 90°$ and $\theta_i = 150°$ as computed by the pulse basis-point matching technique ($a = 0.005\lambda_o, N = 151$).

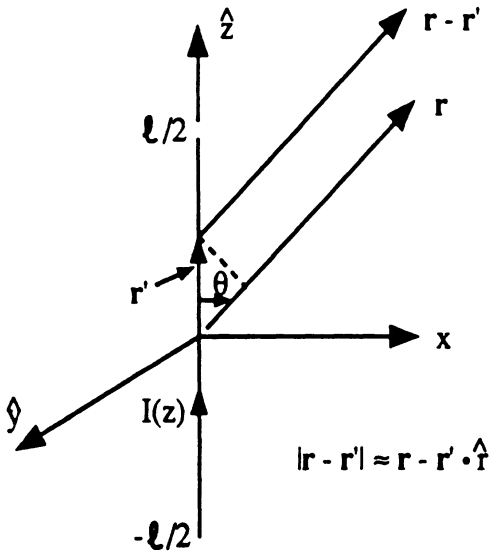

Figure 4.13: Geometry for computing the linear antenna's radiated field.

Using (14), we get

$$E_\theta^r(r,\theta) \approx jk_oZ_o \sin\theta \frac{e^{-jk_or}}{4\pi r} \sum_{n=0}^{N-1} I_n \int_{z_n-\frac{\Delta z}{2}}^{z_n+\frac{\Delta z}{2}} e^{jk_oz'\cos\theta} dz' \tag{4.50}$$

and upon performing the trivial integration we have

$$\begin{aligned} \mathbf{E}^r(r,\theta) &= jk_oZ_o\frac{e^{-jk_or}}{4\pi r}\Delta z \sin\theta \frac{\sin\left(\frac{k_o\Delta z\cos\theta}{2}\right)}{\left(\frac{k_o\Delta z\cos\theta}{2}\right)} \sum_{n=0}^{N-1} I_n e^{jk_oz_n\cos\theta} \\ &= jk_oZ_o\frac{e^{-jk_or}}{4\pi r}\Delta z \sin\theta \,\mathrm{sinc}\left(k_o\frac{\Delta z}{2}\cos\theta\right) \sum_{n=0}^{N-1} I_n e^{jk_oz_n\cos\theta} \end{aligned} \tag{4.51}$$

The radiation intensity of the antenna is given by

$$\begin{aligned} U(\theta,\phi) &= U(\theta) = \frac{r^2}{2Z_o}|E_\theta^r(\theta)|^2 \\ &= \frac{Z_o}{2}\left(\frac{k_o\Delta z\sin\theta}{4\pi}\right)^2 \mathrm{sinc}^2\left(k_o\frac{\Delta z}{2}\cos\theta\right)\left(\sum_{n=1}^{N} I_n e^{jk_oz_n\cos\theta}\right)^2 \end{aligned} \tag{4.52}$$

and the radiated power can be computed from

$$P_{\text{rad}} = \int_0^{2\pi} \int_0^{\pi} U(\theta, \phi) \sin\theta \, d\theta \, d\phi = 2\pi \int_0^{\pi} U(\theta) \sin\theta \, d\theta \tag{4.53}$$

with the integral to be evaluated numerically.

Given the radiated power, the directivity is found from

$$D = \frac{4\pi U_{\text{max}}}{P_{\text{rad}}} = \frac{4\pi U(\theta = \pi/2)}{P_{\text{rad}}} \tag{4.54}$$

Finally, the gain of the antenna can be easily computed from

$$G(\theta, \phi) = \frac{4\pi U(\theta, \phi)}{P_{\text{in}}}\bigg|_{\theta=\pi/2} = \frac{Z_o}{2P_{\text{in}}} \frac{(k_o \Delta z)^2}{4\pi} \left(\sum_{n=1}^{N} I_n \right)^2 \tag{4.55}$$

where P_{in} denotes the input power from the generator.

A parameter of crucial importance in controlling the efficiency of the antenna is its input impedance. This is given as

$$Z_{\text{in}} = \frac{V_i}{I_{\text{in}}} = \frac{E_z^i \Delta z}{I_{\text{in}}} \tag{4.56}$$

where $I_{\text{in}} = I_{\frac{N-1}{2}+1}$ is the value of the current element at the terminal under the obvious assumption that N is odd. However, the accuracy of (4.56) depends on the accuracy of I_{in} as computed from the solution of the system (4.33). Since we discretized the actual current distribution, I_{in} is only an approximation to the input current and is often not of acceptable accuracy unless N is very large. To avoid this difficulty when employing (4.56) we may instead use a stationary expression for the input impedance based on power relations. From Poynting's theorem we have

$$\begin{aligned} \frac{1}{2} I_{in} I_{in}^* Z_{in} &= \frac{1}{2} \oiint \mathbf{E}^r \times \mathbf{H}^{r*} \cdot d\mathbf{s} = -\int_{-\ell}^{\ell} \int_0^{2\pi} E_z^r H_\phi^{r*} a \, d\phi \, dz' \\ &= -\frac{1}{2} \int_{-\ell}^{\ell} E_z^r(a, z') I^*(z') dz' \end{aligned} \tag{4.57}$$

Since $\mathbf{J} = \hat{\rho} \times \hat{\phi} H_\phi$ giving $H_\phi = J_z = \frac{I(z)}{2\pi a}$. Thus,

$$Z_{in} = +\frac{1}{|I_{\text{in}}|^2} \int_{-\ell}^{\ell} E_z^i(a, z') I^*(z') dz \tag{4.58}$$

where we have set $E_z^r(a,z) = -E_z^i(a,z)$ as required by the boundary condition on the surface of the wire. Substituting (4.24) into (4.58) we obtain

$$Z_{in} = \frac{\Delta z}{|I_{in}|^2} \sum_{n=0}^{N-1} E_z^i(a,z_n) I_n^* \tag{4.59}$$

It is observed, that for a delta gap excitation (s (4.39)) (4.59) again reduces to (4.56). Note also that

$$Re(Z_{in}) = R_{in} = \frac{2P_{rad}}{I_{in}} . \tag{4.60}$$

The input impedance as computed from (4.56) is shown in figure 4.14 as a function of the wire's length and for various wire radii. As can be concluded from the presented current computations using the pulse basis-point matching solutions, up to 120 segments per wavelength may be required to accurately sample the current near the feed. When $Im(Z_{in}) = 0$, the dipole is said to be at resonance and its first resonance occurs when 2ℓ is just less than $0.5\lambda_o$, depending on the value of its radius. The bandwidth of an antenna is related to the slope of Z_{in} as a function of frequency and it is seen from figure 4.14 that thicker dipoles have a larger bandwidth. Radiation patterns for the $\lambda_o/2$, λ_o and $3\lambda_o/2$ dipoles are given in figure 4.15. We note, however, that these are identical to those predicted with the assumed sinusoidal distribution which follows from the transmission line model.

When the excitation is a plane wave, we are generally interested in the echo area or radar cross section (RCS) of the wire structure. The RCS is measured in units of square length and is given by

$$\sigma = \lim_{r\to\infty} 4\pi r^2 \frac{|\mathbf{E}^r|}{|\mathbf{E}^i|^2} \tag{4.61}$$

If the wire length is measured in wavelengths then the units of σ are square wavelengths (λ_o^2) and if the wire length is measured in meters then σ will be given in squared meters. The RCS of the $\lambda/2$, λ and 3λ long wires are shown in figures 4.16 and 4.17. The effect of wire thickness on the wire's RCS is pedicted in figure 4.18 where the value of broadside ($\theta_1 = 90°$) σ is plotted as a function of the wire's length for three different radii. This is a characteristic curve for the wire scatterer and displays its resonant behavior when $2\ell \approx (n+1)\lambda_o/2$

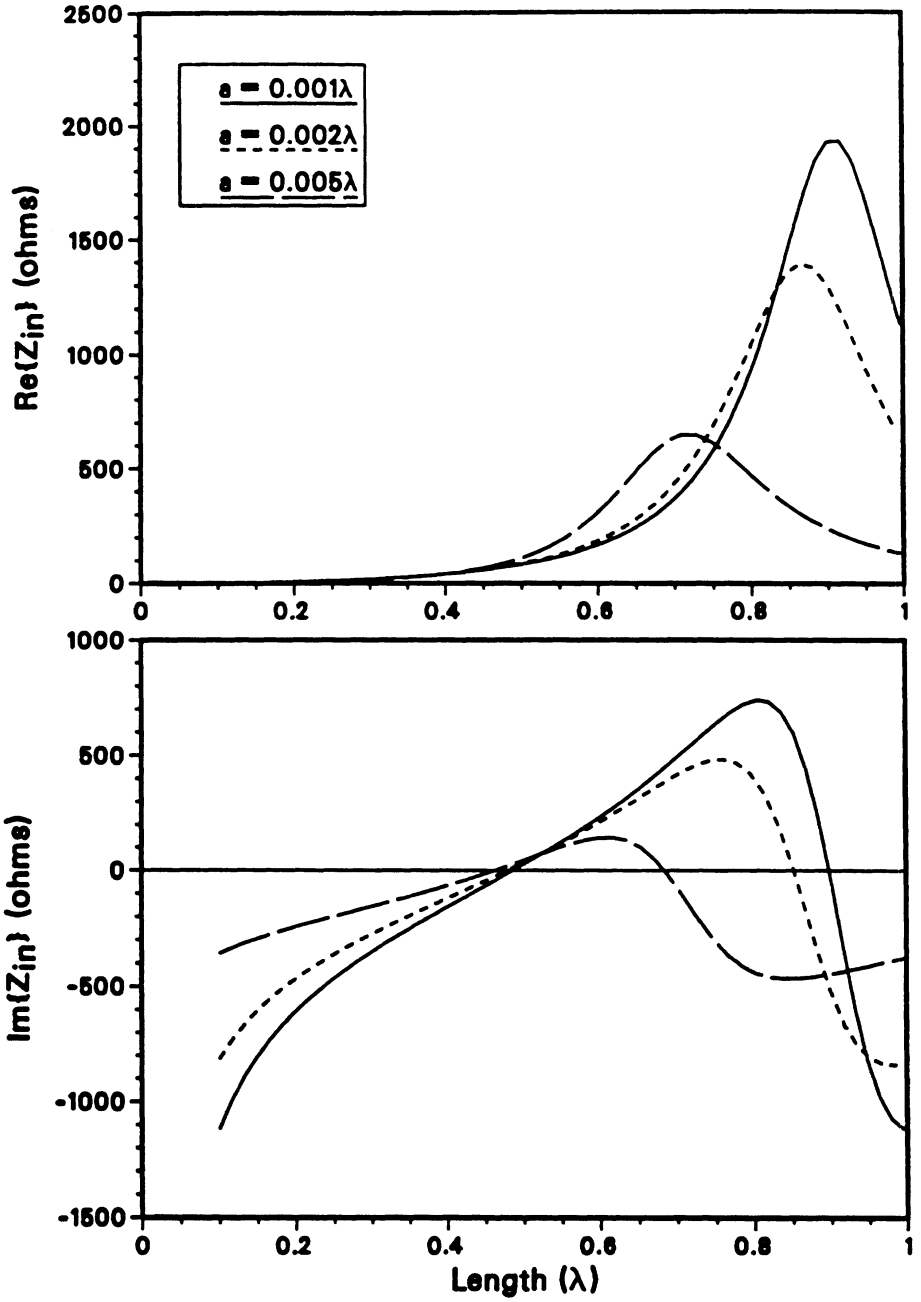

Figure 4.14: Input impedance of a dipole as a function of its length 2ℓ for three different wire radii. (a) resistive (b) reactance; The dipole is resonant when the reactance is zero.

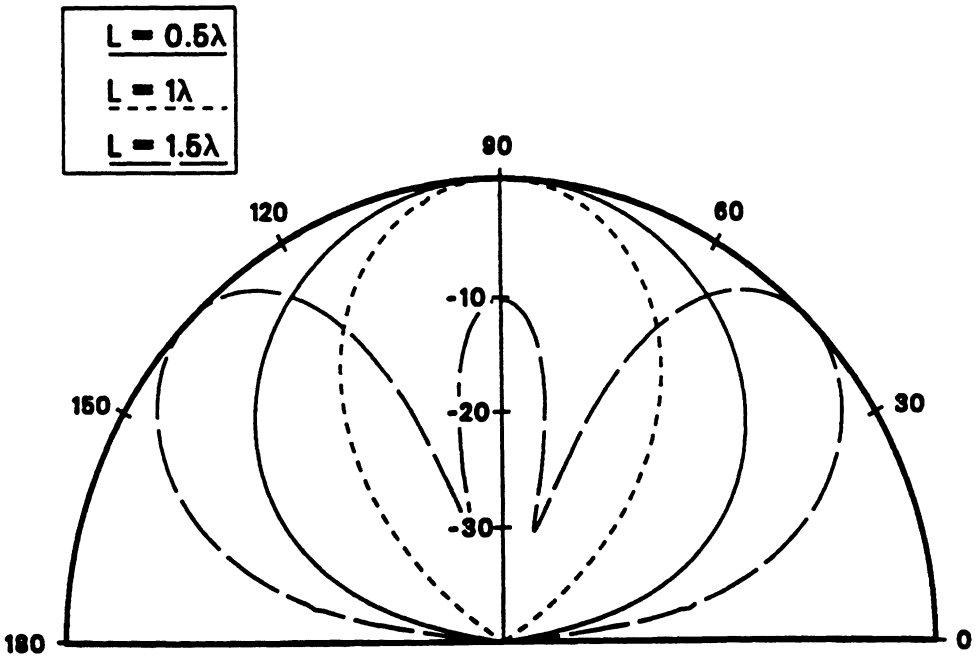

Figure 4.15: Radiation power patterns for the $\lambda_o/2$, $1\lambda_o$ and $1.5\lambda_o$ dipoles computed from the numerical solution of the dipole currents ($a = 0.005\lambda_o$).

for odd n. Basically, the RCS of the wire at those lengths reaches a local peak with each successive peak becoming larger as 2ℓ is increased. This property of the wire has been explored in many practical situations and we remark that the location of the RCS peak should correspond to the wire length at which $Im(Z_{in}) = 0$.

We observe that the echo area pattern of the longer wire as given in fig. 4.17 has a very strong lobe near $\theta = \pi$ (near grazing). This is a lobe characteristic to all thin wire scattering patterns and is always the one closest to $\theta = 0°$ or $\theta = \pi$. It is often referred to as the traveling wave lobe and to explain its presence let us assume that the wire is infinite in length. The incident plane wave (4.47) will then generate a current of the form $I_1 e^{jk_o z\cos\theta_i}$ where I_1 is a complex constant proportional to the incident wave's strength and can be computed analytically. This is, of course, a traveling current (whose propagation constant matches that of the incident wave) and if the wire is of finite extent, when it reaches the wire ends, it generates additional reflected currents of the form $I_2 e^{jk_o z}$ and $I_3 e^{-jk_o z}$, where I_2 and I_3 are again complex constants. Thus the current on the wire due to a plane wave excitation can be approximately represented as

$$I(z) = \sum_{n=1}^{3} I_n e^{jk_n z} \tag{4.62}$$

with $k_1 = k_o \cos\theta_o$, $k_2 = +k_o$ and $k_3 = -k_o$. From this representation it is not difficult to observe from the radiation integral (4.49) that the scattered field would peak at $\theta = \pi - \theta_i$ and at $\theta = 0$ or π if the coefficients I_n were comparably weighted. However, this is not the case and it turns out that the traveling wave lobe peak occurs when $I_{2,3}$ are at maximum.

The expansion (4.62) is, of course, a linear sum of three full wave basis functions, similar to those given by (4.22) - (4.23). It was constructed on the basis of the physical phenomena that take place on the straight wire and is thus most efficient for computational purposes. However, as noted earlier, this expansion is specific to the straight wire scatterer and cannot be employed for other wire shapes or arbitrary multiple wire structures.

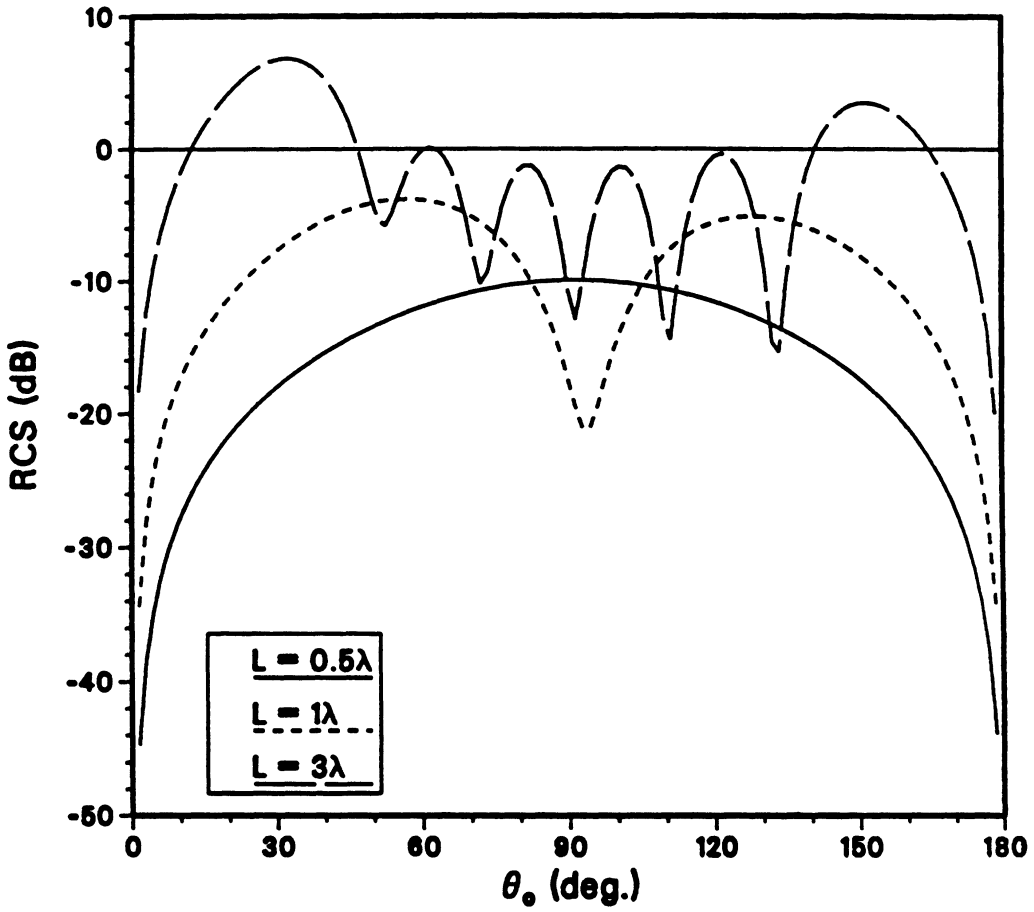

Figure 4.16: Bistatic radar cross section of three straight wires of length $2\ell = \lambda_o/2$, λ_o and $3\lambda_o$. The wires have a radius of $a = 0.005\lambda_o$ and the incident plane wave is illuminating the wire at an angle of $\theta_i = 150°$ (PWS-basis solution).

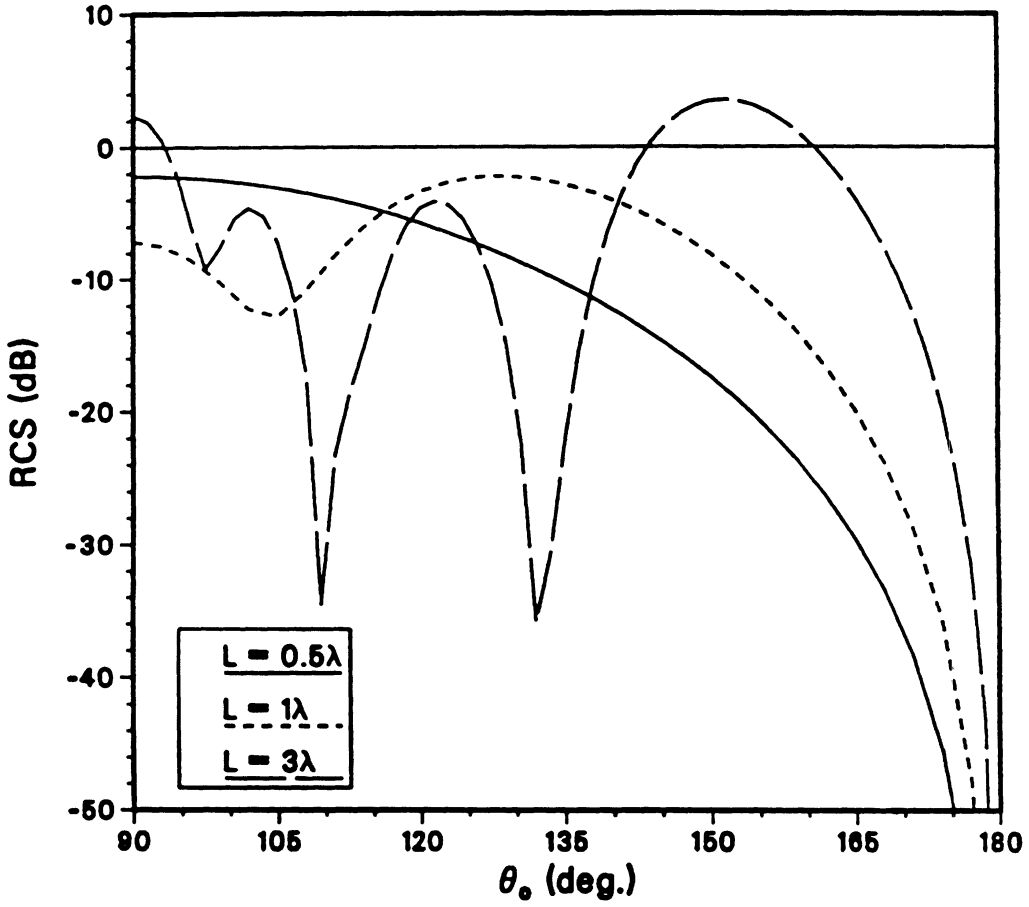

Figure 4.17: Backscatter radar cross section ($\theta = \theta_i$) for the three straight wires whose bistatic patterns are given in fig. 4.16.

4.6 Piecewise Sinusoidal Basis-Point Matching Solution

The piecewise sinusoidal (PWS) basis expansion renders a continuous current distribution and is thus more representative of the actual solutic This usually translates in less subsections/zones to reach convergence.

Substituting (4.21) into (4.18) yields

$$I(z) = \sum_{n=0}^{N} I_n \frac{\sin k_o(\Delta z - |z - z_n|)}{\sin k_o \Delta z} \tag{4.63}$$

where $z_n = -\ell + (n+1)\Delta z$. When this is substituted into (4.13), we obtain (see Appendix)

$$E_z^i(\rho = a, z) = \frac{j30}{\sin k_o \Delta z} \sum_{n=0}^{N-1} I_n \left[\frac{e^{-jk_o R_{1n}}}{R_{1n}} \right.$$
$$\left. -2\cos(k_o \Delta z) \frac{e^{-jk_o R_{2n}}}{R_{2n}} + \frac{e^{-jk_o R_{3n}}}{R_{3n}} \right] \tag{4.64}$$

in which

$$R_{1n} = \sqrt{(z - z_{n-1})^2 + a^2}$$

$$R_{2n} = \sqrt{(z - z_n)^2 + a^2}$$

and

$$R_{3n} = \sqrt{(z - z_{n+1})^2 + a^2}\,.$$

The fact that the radiated field by a sinusoidal source can be evaluated in a closed form is the principal advantage of $S_n(z)$ over $T_n(z)$.

A point matching solution of (4.64) follows the same procedure as discussed previously in connection with the pulse basis expansion. Upon evaluation of the coefficients I_n, the radiation pattern is again given by (4.49). From (4.63) we obtain

$$E_\theta(r, \theta) \approx \frac{jk_o Z_o}{\sin \vartheta} \frac{e^{-jk_o r}}{4\pi r} \sum_{n=0}^{N-1} I_n \int_{z_n - \Delta z}^{z_n + \Delta z} \frac{\sin k_o(\Delta z - |z' - z_n|)}{\sin(k_o \Delta z)} e^{jk_o z' \cos\theta} dz' \tag{4.65}$$

and on carrying out the integration we find

$$E_\theta(r,\theta) \approx j60\frac{e^{-jkr}}{r}\underbrace{\frac{\cos(k_o\Delta z\cos\theta)-\cos(k_o\Delta z)}{\sin\theta\sin(k_o\Delta z)}}_{\text{element pattern}}\sum_{n=0}^{N-1} I_n e^{jk_o z_n\cos\theta} \quad (4.66)$$

The evaluation of other parameters such as radiated power, gain, directivity and input impedance can be performed in a straightforward manner. Not surprisingly, the PWS representation can be shown to yield more accurate results for input impedance computations. This can be attested by examining the wire surface fields generated by the PWS-point matching solution. In contrast to the results in fig. 4.8, it is found that the surface field of this solution is now practically zero without even resorting to the more robust weighted residual method discussed next.

4.7 Method of Weighted Residuals/Moment Method

The point matching technique described above for solving integral equations ensures that the boundary condition is satisfied only at the match points z_m. In general, however, the boundary condition is not necessarily satisfied elsewhere, unless the sampling or testing interval Δz is extremely small and this fact was illustrated in figure 4.8. This is, of course, not cost effective since the CPU time is proportional to N^3 as given by (4.37).

An alternative testing procedure is to satisfy the boundary condition on an average sense over the length of the segment from z_n to z_{n+1}. To express this mathematically, let us first define the interproduct

$$\langle R(z), W_m(z)\rangle = \int_{-\ell}^{\ell} R(z)W_m^*(z)dz \quad (4.67)$$

and we will hereon refer to $R(z)$ as the residual and $W_m(z)$ as the weighting/test basis functions. Setting

$$R(z) = E_z^i(\rho=a,z) + E_z^r(\rho=a,z)\,, \quad (4.68)$$

choosing

$$W_m(z) = \begin{cases} 1 & z_m - \frac{\Delta z}{2} < z < z_m + \frac{\Delta z}{2} \\ 0 & \text{elsewhere} \end{cases} \tag{4.69}$$

and demanding that

$$\langle R(z), W_m(z) \rangle = 0 \tag{4.70}$$

leads to the integral equation

$$-\int_{z_m-\frac{\Delta z}{2}}^{z_m+\frac{\Delta z}{2}} E_z^i(\rho = a, z)dz = \int_{z_m-\frac{\Delta z}{2}}^{z_m+\frac{\Delta z}{2}} E_z^r(\rho = a, z)dz \tag{4.71}$$

Upon substitution of the expression for E_z^r as extracted from (4.30) yields,

$$-\int_{z_m-\frac{\Delta z}{2}}^{z_m+\frac{\Delta z}{2}} E_z^i(\rho = a, z) = -\frac{jZ_o}{2\lambda_o} \sum_{n=0}^{N-1} I_n \int_{z_m-\frac{\Delta z}{2}}^{z_m+\frac{\Delta z}{2}} [\Psi_n(z) + \Phi_n(z)]\, dz \tag{4.72}$$

from which we obtain the system

$$[Z_{mn}]\,[I_n] = [V_m] \tag{4.73}$$

where now

$$V_m = -\int_{z_m-\frac{\Delta z}{2}}^{z_m+\frac{\Delta z}{2}} E_z^i(\rho = a, z)dx \tag{4.74}$$

$$Z_{mn} = \frac{-jZ_o}{2\lambda_o} \int_{z_m-\frac{\Delta z}{2}}^{z_m+\frac{\Delta z}{2}} [\Psi_n(z) + \Phi_n(z)]\, dz \tag{4.75}$$

These can be evaluated numerically using, for example, Simpson's, midpoint or Gaussian rules of integration. Clearly, (4.70) along with (4.68) and (4.69) demand that the boundary conditions be satisfied on an average sense over the wire subintervals. When the weighting functions are piecewise constant (PWC), each current value over the subinterval is given equal weighting in this averaging process. A variety of other choices for $W_m(z)$ have, though, been employed successfully in the past. When $W_m(z)$ are chosen to be the same as

the current expansion basis function, the procedure for deriving the resulting system of equations is referred to as Galerkin's method. We also note that when

$$W_m(z) = \delta(z - z_m) \tag{4.76}$$

(4.70) reduces to the system (4.30) derived by the point-matching technique. The above procedure for discretizing the integral equation is formally referred to as the *weighted residual method* but is most often called the *method of moments* (MoM). Also, the pulse basis-point matching proceedure is more formally referred to as the *collocation method.*

The application of Galerkin's technique in conjunction with the piecewise sinusoidal basis functions to solve the linear antenna currents has been studied extensively and there are several general purpose programs based on this procedure. It is, therefore, instructive to describe the formulation and derive the resulting system of equation.

From (4.70), with

$$W_m(z) = \begin{cases} \frac{\sin(k_o(\Delta z - |z - z_m|))}{\sin k_o \Delta z} & z_{m-1} < z < z_{m+1} \\ 0 & \text{elsewhere} \end{cases} \tag{4.77}$$

and (see (4.64))

$$R(z) = E_z^i(\rho = a, z) - \frac{j30}{\sin(k_o \Delta z)} \sum_{n=0}^{N-1} I_n \left[\frac{e^{-jk_o R_{1n}}}{R_{1n}} - 2\cos(k_o \Delta z) \frac{e^{-jk_o R_{2n}}}{R_{2n}} + \frac{e^{-jk_o R_{3n}}}{R_{3n}} \right] \tag{4.78}$$

we obtain the usual system (4.62) with

$$V_m = -\int_{z_m - \Delta z}^{z_m + \Delta z} E^i(\rho = a, z) \frac{\sin[k_o(\Delta z - |z - z_m|)]}{\sin(k_o \Delta z)} dz \tag{4.79}$$

$$Z_{mn} = -\frac{-j30}{\sin k_o \Delta z} \int_{z_m - \Delta z}^{z_m + \Delta z} \frac{\sin[k_o(\Delta z - |z - z_m|]}{\sin(k_o \Delta z)} \left[\frac{e^{-jk_o R_{1n}}}{R_{1n}} - 2\cos(k_o \Delta z) \frac{e^{-jk_o R_{2n}}}{R_{2n}} + \frac{e^{-jk_o R_{3n}}}{R_{3n}} \right] dz \tag{4.80}$$

The impedance matrix elements may be easily evaluated numerically as given in (4.80) since the integrand is non singular. However, after some manipulation, the integral expression can be simplified and written in terms of the exponential integral which is tabulated. A compact expression for Z_{mn} is [Pozar, Artech House, 1985] [Richmond and Geary,]

$$Z_{mn} = \frac{+15}{\sin^2(k_o\Delta z)} \sum_{p=-2}^{2} \sum_{q=-1,2} A(p+3) e^{-jk_oq[|z_m - z_n| + p\Delta z]} E(k_o\beta_{pq}) \quad (4.81)$$

where

$$\begin{aligned} A(1) &= A(5) = 1 \\ A(2) &= A(4) = -4\cos(k_o\Delta z) \\ A(3) &= 2 + 4\cos^2(k_o\Delta z) \\ \beta_{pq} &= \sqrt{a^2 + [|z_m - z_n| + p\Delta z]^2} - q[|z_m - z_n| + p\Delta z] \end{aligned}$$

and $E(\alpha)$ is the exponential integral [Ambramowitz and Stegan, p. 228]. It can be defined in terms of the cosine and sine integrals as

$$E(\alpha) = Ci(\alpha) - jSi(\alpha) \quad (4.82)$$

where

$$Ci(\alpha) = -\int_{\alpha}^{\infty} \frac{\cos x}{x} dx \quad (4.83)$$

and

$$Si(x) = \int_{0}^{\alpha} \frac{\sin x}{x} dx \, . \quad (4.84)$$

For $x < 1$

$$\begin{aligned} Si(x) &\simeq x - \frac{x^3}{18} + \frac{x^5}{600} - \frac{x^7}{35,280} \\ Ci(x) &\simeq 0.577216 + \ln x - \frac{x^2}{4} + \frac{x^4}{96} - \frac{x^6}{4320} \end{aligned}$$

and for $x > 1$

$$Si(x) \approx \frac{\pi}{2} - f(x)\cos x - g(x)\sin x$$

$$Ci(x) \approx f(x)\sin x - g(x)\cos x\,,$$

with

$$f(x) \approx \frac{1}{x}\left[\frac{x^4 + 7.24116x^2 + 2.46394}{x^4 + 9.06858x^2 + 7.15743}\right]\,,$$

and

$$g(x) \approx \frac{1}{x^2}\left[\frac{x^4 + 7.54748x^2 + 1.56407}{x^4 + 12.72368x^2 + 15.72361}\right]\,.$$

As shown in figure 4.19 a smaller number of PWS basis are required to reach solution convergence.

4.8 Some Generalizations

The moment method application described above has been restricted to a linear wire antenna or scatterer. It can be easily though generalized to the case when several parallel wires are present describing, for example, a Yagi-Uda or a dipole log-periodic antenna. The discretization must now be extended to all parallel segments and some minor modifications should be introduced in the expressions for the impedance elements. In particular, the parameter 'a' defining the radius of the linear antenna should be replaced by ρ where (ρ, z) is the observation or testing point on the surface of one of the linear elements.

4.9 Moment Method for Non-Linear Wires

Typically, the antenna or scatterer will be composed of curved wire elements. Also, it is possible to model continuous metallic surfaces with a wire grid of sufficient density as shown in the figure. Acceptable grid densities are often 10 or more wires per linear wavelength on the surface.

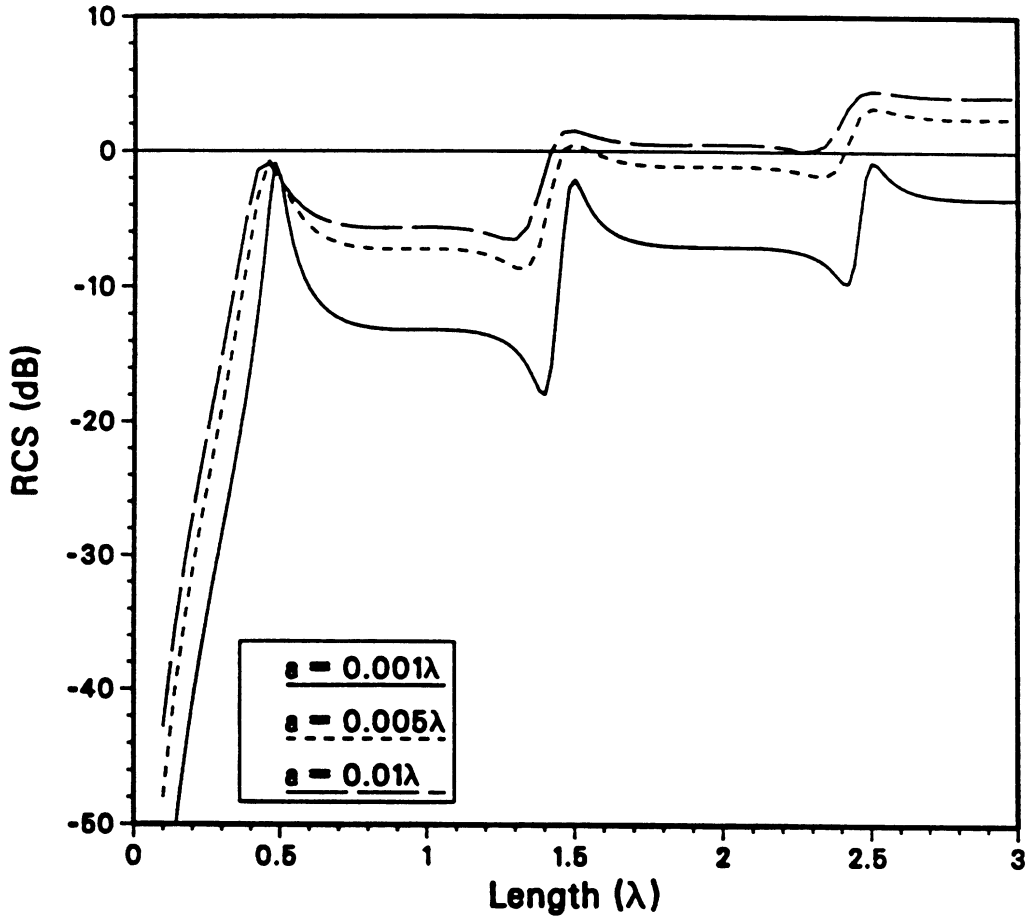

Figure 4.18: Backscatter RCS of three thin wires as a function of length (2ℓ) illuminated by a plane wave at normal incidence ($\theta_i = 90°$). (PWS-point matching solution with $\Delta Z = 0.01\lambda_o$)

Figure 4.19: Current distribution on a center-fed $3\lambda_o$ dipole of radius $a = 0.005\lambda_o$. The source is a delta gap.

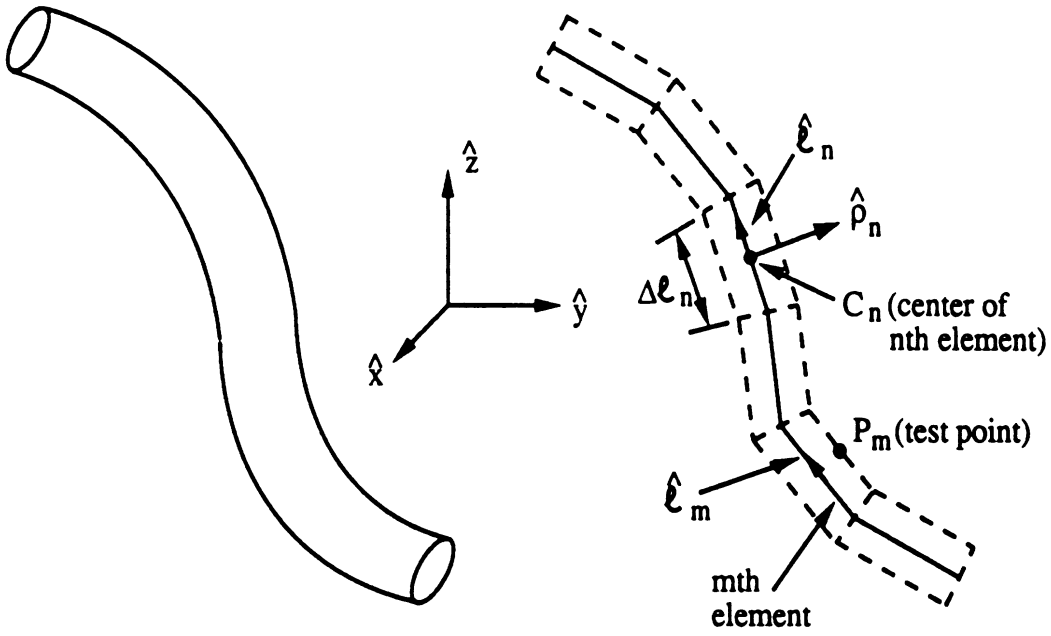

Figure 4.20: Segmentation of a curved wire for numerical modeling.

To develop a Moment Method formulation applicable to curved wires let us consider the curved wire geometry shown below and we may assume for simplicity a constant wire thickness equal to $2a \gg \lambda$. As usual, we are interested in determining the wire surface currents or more specifically the equivalent line current through the center of the wire.

In proceeding with a numerical solution, it is first necessary to discretize the wire as shown. This amounts to generating a model of the curved wire that is composed of a set of linear segments. Denoting the unit vector along the direction of the mth element as $\hat{\ell}_m$, the boundary condition to be satisfied on its surface is

$$\left(\mathbf{E}^i + \mathbf{E}^r\right) \cdot \hat{\ell}_m = 0 \tag{4.85}$$

If the curved wire is divided into N straight segments then $\mathbf{E}^r$ can be expressed as

$$\mathbf{E}^r = \sum_{n=1}^{N} \mathbf{E}_n^r = \sum_{n=1}^{N} \hat{\ell}_n \mathbf{E}_{\ell n}^r \tag{4.86}$$

where $\mathbf{E}_n^r$ is the field radiated by each linear segment. When employing PWC basis to expand the current on each element, $\mathbf{E}_n^r$ can be found from (2.52) or (3.13) upon performing the necessary coordinate transformations. Alternatively, if PWS basis are used the applicable expression for the radiated fields are given in the Appendix, after again incorporating the required coordinate transformations.

Following the usual moment method procedure, a system of N equations can be constructed from

$$\left\langle \left(\mathbf{E}^r + \mathbf{E}^i\right) \cdot \hat{\ell}_m \ , \quad W_m(\ell) \right\rangle = 0 \tag{4.87}$$

or

$$+ \sum_{n=1}^{N} \int_{\Delta\ell_m} \left(\mathbf{E}_n^r \cdot \hat{\ell}_m\right) W_m(\ell) d\ell = - \int_{\Delta\ell_m} \mathbf{E}^i \cdot \hat{\ell}_m W_m(\ell) d\ell \tag{4.88}$$

where $W_m(\ell)$ is the weighting or testing function for the mth element.

In the above we have consistently assumed a very small wire radius with respect to its length. This assumption allowed us to replace the wire surface current with an equivalent filamentary current at its center. From experience, this approximation which is highly desirable for simplifying calculations is generally valid for $\frac{a}{\ell} \leq 0.01\lambda$. For thicker wires a more exact formulation must be followed [see for example Miller and Deadrick, Ch. 4 in *Numerical and Asymptotic Techniques in Electromagnetics*, Springer-Verlag, NY, 1975].

4.10 Wires of Finite Conductivity

When the wire (or a portion of it) is of finite conductivity, the boundary condition to be satisfied is

$$\mathbf{J}_v = \sigma \mathbf{E}^{tot} \tag{4.89}$$

where $\mathbf{E}^{tot}$ is the total field within the wire, $\mathbf{J}_v$ is the volume current in A/m^2 and σ denotes the wire conductivity. For $a \ll \ell$ we can again replace $\mathbf{J}_v$ by an equivalent filamentary current at the center of the wire given by

$$I = \pi a^2 J_v \tag{4.90}$$

Incorporating this into (4.89) yields the condition

$$\mathbf{E}^{tot} = \hat{\ell} R_w I(\ell) \quad \text{or} \quad E_\ell^i + E_\ell^r = R_w I(\ell) \tag{4.91}$$

where

$$R_w = \frac{1}{\pi a^2 \sigma} \tag{4.92}$$

can be referred to as the resistivity of the wire.

The boundary condition (4.91) must now replace the one given in (4.1). This amounts to a modification of the impedance elements from Z_{mn} to Z'_{mn}, where

$$Z'_{mn} = \begin{cases} Z_{mn} & n \neq m \\ -R_w(\ell_m) \int_{\Delta \ell_m} f_m(\ell) W_m(\ell) d\ell + Z_{mm} & n = m \end{cases} \tag{4.93}$$

in which $R_w(\ell_m)$ denotes the resistivity of the wire at the mth element and $\mathbf{E}_n^r$ is the field radiated by the nth element. The wire current is expanded in the usual manner to yield the system

$$[Z'_{mn}]\{I_n\} = \{V_m\} \tag{4.94}$$

for a solution of the element amplitude coefficients I_n.

Often the wire antenna or scatterer with distributed loads is characterized with a surface impedance Z_s. The boundary condition satisfied on the surface of the wire then is

$$\mathbf{E}^{tot} = Z_s \mathbf{J}_s \tag{4.95}$$

where $\mathbf{J}_s$ denotes the surface current. Since

$$\mathbf{J}_s = \hat{\ell} \frac{I(\ell)}{2\pi a} \tag{4.96}$$

(4.95) may be rewritten as

$$\mathbf{E}^{tot} = \hat{\ell} \frac{Z_s}{2\pi a} I(\ell) \tag{4.97}$$

This is similar to (4.91) and thus a solution for the wire currents is found by setting the impedance elements equal to

$$Z'_{mn} = -\frac{Z_s}{2\pi a}\int_{\Delta\ell_m} f_n(\ell)W_m(\ell)d\ell + Z_{mn} \tag{4.98}$$

where Z_{mn} are the corresponding elements for the perfectly conducting wire. The integral in (4.98) is only over the common domain of the weighting and expansion functions. Thus, if $W_m(\ell)$ and $f_n(\ell)$ are among those in (4.19) - (4.21) Z'_{mn} will be equal to Z_{mn} except for the matrix elements $Z_{m(m\pm1)}$ and $Z_{(m\pm1)m}$.

4.11 Construction of Integral Equations via the Reaction/Reciprocity Theorem

The integral equations derived earlier via the application of the Moment Method procedure can also be derived by invoking the reaction or reciprocity theorem discussed in chapter 1. The reaction theorem is a mathematical relationship between two sets of sources and their generated fields. Assuming $(\mathbf{J},\mathbf{M})$ generate the fields $(\mathbf{E},\mathbf{H})$ and that $(\mathbf{J}_t,\mathbf{M}_t)$ generate the fields $(\mathbf{E}_t,\mathbf{H}_t)$, the reaction theorem states

$$\int\int\int (\mathbf{E}\cdot\mathbf{J}_t - \mathbf{H}\cdot\mathbf{M}_t)\,dv = \int\int\int (\mathbf{E}_t\cdot\mathbf{J} - \mathbf{H}_t\cdot\mathbf{M})\,dv\,. \tag{4.99}$$

Let us now set

$$(\mathbf{E},\mathbf{H}) = \left(\mathbf{E}^r + \mathbf{E}^i, \mathbf{H}^r + \mathbf{H}^i\right)$$

where $(\mathbf{E}^r,\mathbf{H}^r)$ are the fields radiated by the wire current J_s in the presence of the incident field $(\mathbf{E}^i,\mathbf{H}^i)$ having their source at infinity. Expression (4.99) then becomes

$$\begin{aligned}\int\int\int (\mathbf{E}^r\cdot\mathbf{J}_t - \mathbf{H}^r\cdot\mathbf{M}_t)\,dv + \int\int\int \left(\mathbf{E}^i\cdot\mathbf{J}_t - \mathbf{H}^i\cdot\mathbf{M}_t\right)dv \\ = \oiint (\mathbf{E}_t\cdot\mathbf{J}_s - \mathbf{H}_t\cdot\mathbf{M}_s)\,ds\end{aligned} \tag{4.100}$$

We now choose $\mathbf{M}_t = 0$ and set

$$\mathbf{J}_t = \hat{\ell}_m W_m(\ell) = \mathbf{J}_m(\ell) \tag{4.101}$$

concentrated at the center of the nth element of the perfectly conductive wire, where $W_m(\ell)$ is usually chosen to be equal (Galerkin's method) to the equivalent line current of the wire's mth element. The field generated by t source is now zero (essentially $\mathbf{J}_t$ radiates inside a closed hollow conductor) and (4.100) further reduces to

$$\oiint_{\substack{\text{wire}\\\text{surface}}} \mathbf{E}^r \cdot \mathbf{J}_m ds = -\oiint_{\substack{\text{wire}\\\text{surface}}} \mathbf{E}^i \cdot \mathbf{J}_m ds \tag{4.102}$$

when $\mathbf{J}_m$ is replaced by its equivalent line current at the center of the wire we have

$$\int\int \mathbf{E}^r \cdot \hat{\ell}_m W_m(\ell) d\ell = -\int\int \mathbf{E}^i \cdot \hat{\ell}_m W_m(\ell) d\ell \tag{4.103}$$

which is the same as (4.77) derived by the method of weighted residuals.

4.12 Iterative Solution Methods: The Conjugate Gradient Method

Instead of inverting the impedance matrix $[Z_{mn}]$ for a solution of the system (4.33) or (4.73), one could employ an iterative solution sheme. Among the numerous iterative solution schemes for such a system, the conjugate gradient (CG) method is most attractive because it guarantees convergence in a maximum of N iterations for an N-dimensional system (ignoring round-off errors). The CG method is a non-linear, semi-direct iterative scheme and was introduced by Hesteness and Steifel [ ] independently more than 40 years ago. Beginning with a random initial guess of the solution (including the zero vector) vector $\{I_n\}$, convergence is accomplished via a systematic orthogonalization of the solution vector with respect to the residual vector defined as the difference between the left and right hand sides of the system. The residual vector is computed at the end of each iteration and is used to find the next correction to the solution vector. The correction vectors are chosen to be orthogonal to the residual vectors which are linearly independent. This is

an essential condition for guaranteeing the convergence of the algorithm since at the Nth iteration the solution vector would have been constructed by N independent vectors (conjugate directions) which form a basis set of the N-dimensional space. Moreover, the algorithm will first proceed with corrections which will most greatly impact the minimization of the next residual vector. Consequently, convergence to within a reasonable degree of accuracy can be achieved after only a few (normally less than $N/3$) iterations.

The CG algorithm is derived in the Appendix and for the pertinent system it proceeds as follows:

Initialize the residual vector and conjugate direction:

$$\{r_1\} = \{V\} - [Z]\{I^1\}$$

$$\beta_o = \frac{1}{|[Z]^a\{r_1\}|^2}$$

$$p_1 = \beta_o[Z]^a\{r_1\}$$

For $k = 1, \ldots, n$ DO

$$\alpha_k = \frac{1}{|[Z]\{p_k\}|^2}$$

$$\{I^{k+1}\} = \{I^k\} + \alpha_k\{p_k\}$$

$$\{r_{k+1}\} = \{r_k\} - \alpha_k[Z]\{p_k\}$$

$$\beta_k = \frac{1}{|[Z]^a\{r_{k+1}\}|^2}$$

$$\{p_{k+1}\} = \{p_k\} + \beta_k[Z]^a\{r_{k+1}\}$$

terminate loop when normalized residual error

$$\frac{|r_{k+1}|}{|[Z]^a\{V\}|} < \text{tolerance}$$

or when $k = N$.

In the above algorithm, the columns or vectors $\{I^k\}$ represent the current expansion coefficients after the $(k-1)$th iteration, $\{r_k\}$ are the residual vectors and $\{p_k\}$ are the conjugate directions discussed above. Also, $[Z]^a$ denotes the adjoint of the impedance matrix which is equal to the complex conjugate transpose of $[Z_{mn}]$ and

$$|I^k|^2 = \sum_{n-1}^{N} I_n^k (I_n^k)^* \tag{4.104}$$

is the square norm of the vector $\{I^k\}$. Typical values for the tolerance range from .01 to 10^{-4}.

Excluding initialization, the above CG algorithm requires $2N^2 + 5N + 2$ multiplications and divisions (i.e. operations) per iteration. Thus, the CPU time required to reach convergence is of order $N^2 N_I$, if N_I is the number of iterations required to satisfy the tolerance condition. Thus, if N_I is not a small faction of N, the required CPU time to solve the system will again be of order N^3. However, the major advantage of the CG method is realized when the $[Z]$ matrix is Toeplitz as is the case for the straight wire. In this case, the fast Fourier transform (FFT) can be combined with the CG method to reduce the storage requirements and speed-up the solution. To see how this is accomplished let us first return to the original integral equation (4.11). By invoking the one-dimensional Fourier transform pair defined in (2.171) and the convolution theorem we can rewrite (4.11) as

$$\left\{E_z^i(\rho = a, z)\right\} = \frac{jZ_o}{k_o} \mathcal{F}^{-1}\left\{\tilde{I}(k_z)(k_o^2 - k_z^2)\tilde{G}_{wr}(k_z)\right\} \tag{4.105}$$

where

$$\tilde{I}(k_z) = \mathcal{F}\{I(z)\} = \int_{-\infty}^{\infty} I(z) P_{2\ell}(z) e^{-jk_z z} dz = \int_{-\ell}^{\ell} I(z) e^{-jk_z z} dz \tag{4.106}$$

and $\tilde{G}_{wr}(k_z)$ is correspondingly the Fourier transform of $G_{wr}(z)$ defined in (4.10). It is given by

$$\tilde{G}_{wr}(k_z) = \int_{-\infty}^{\infty} \frac{e^{-jk_o\sqrt{z^2+a^2}}}{4\pi\sqrt{z^2+a^2}} dz = \frac{1}{2\pi} K_o(a\sqrt{k_z^2 - k_o^2}) \tag{4.107}$$

where K_o is the modified Bessel function of the second kind and from (2.170) $\sqrt{k_o^2 - k_z^2} = -j\sqrt{k_z^2 - k_o^2}$. If we were to use the integral equation (4.7) which

involves the unreduced wire kernel then $\tilde{G}_{wr}(k_z)$ need be replaced by the transform of $G_{wu}(z)$ given by

$$\tilde{G}_{wu}(k_z) = \frac{1}{2\pi} I_o(a\sqrt{k_z^2 - k_o^2}) K_o(a\sqrt{k_z^2 - k_o^2}) \tag{4.108}$$

in which I_o is the modified Bessel function of the first kind. Note that although K_o in (4.107) and (4.108) becomes infinite when $k_o = k_z$, the argument of the inverse transform operator in (4.105) vanishes at that point because of the multiplying factor $(k_o^2 - k_z^2)$.

The importance of the algebraic expression (4.105) is apparent when it is realized that its right hand side gives the value of the entire column (i.e. for all z_m) resulting from the operation $[Z]\{I\}$ without having to actually generate and store the square matrix $[Z]$ or perform the matrix multiplication. However, before we can make practical use of this advantage, it is necessary to rewrite (4.105) in terms of the discrete Fourier transform (DFT) to permit its implementation on a computer. As a first step toward this, we define the discrete transform pair

$$\hat{I}_p = \hat{I}(p\Delta k_z) = \sum_{n=0}^{N-1} I(n\Delta z) W^{np} \tag{4.109a}$$

$$I_n = I(n\Delta z) = \frac{1}{N} \sum_{p=0}^{N-1} \hat{I}^*(p\Delta k_z)(W^{np})^* \tag{4.109b}$$

where $W = e^{-2\pi/N}$, Δk_z is the subinterval in the spectral domain given by $\Delta k_z = 1/N\Delta z$ and $\hat{I}_p = \hat{I}(p\Delta f)$ is the discrete transform of the sequence I_n.

Upon rewriting the expansion (4.18) as

$$I(z) = \sum_{n=0}^{N-1} I_n f_n(z - z_n) = f(z) * \sum_{n=0}^{N-1} I_n \delta(z - z_n) \tag{4.110}$$

where the * indicates convolution and taking its Fourier transform it is seen that the discrete form of $\tilde{I}(k_z)$ is given by

$$\tilde{I}(k_z) = \tilde{f}(k_z)\hat{I}_n \tag{4.111}$$

provided we set $k_z = n\Delta k_z$ for calculating $\tilde{f}(k_z)$. If pulse (PWC) basis are employed as expansion functions then

$$\tilde{f}(k_z) = \tilde{P}_{\Delta z}(k_z) = \Delta z \frac{\sin(k_z\Delta z/2)}{k_z\Delta z/2} = \Delta z \text{ sinc } (k_z\Delta z/2) \tag{4.112}$$

and for PWS basis,

$$\tilde{f}(k_z) = \tilde{S}(k_z) = \frac{2k_o[\cos(k_z\Delta z) - \cos(k_o\Delta z)]}{(k_o^2 - k_z^2)\sin(k_o\Delta z)} \tag{4.113}$$

We note that as $\Delta z \to 0$ then (4.112) and (4.113) reduce to a value equal to Δz and thus

$$\tilde{I}(k_z) \approx \Delta z \hat{I}_n$$

which is an expected result implying the basis $f(z) = \Delta z \delta(z)$.

The result (4.111) can now be substituted into (4.105) and perform the required DFT by setting $k_z = n\Delta k_z = n/N\Delta z$. However before doing so, it is instructive to also replace the transform of the derivative $\frac{\partial}{\partial z}$ by its discrete counterpart. To obtain it, we observe that

$$\mathcal{F}\left\{\frac{\Delta G(z)}{\Delta z}\right\} = \mathcal{F}\left\{\frac{G\left(z+\frac{\Delta z}{2}\right) - G\left(z-\frac{\Delta z}{2}\right)}{\Delta z}\right\} = j\frac{2\sin\left(k_z\frac{\Delta z}{2}\right)}{\Delta z}\tilde{G}(k_z) \tag{4.114}$$

which is the transform of the discrete derivative based on the two point formula. It simply implies that in (4.105) we must make the replacement

$$k_z \to \frac{2\sin\left(k_z\frac{\Delta z}{2}\right)}{\Delta z} = k_z \text{ sinc } \left(k_z\frac{\Delta z}{2}\right)$$

where sinc $\left(k_z\frac{\Delta z}{2}\right) \to 1$ as $\Delta z \to 0$, an expected result. Finally, to obtain the discrete counterpart of $\tilde{G}_{wr}(k_z)$ the simplest approach is to replace it by the sample train $\tilde{G}_{wr}(p\Delta k_z)$ with $p = -(N-1), \ldots, 0, 1, \ldots, N$ since the DFT must be of finite length equal to $2N$ in order to satisfy the convolution requirements. However, unless $\tilde{G}_{wr}(k_z)$ is of negligible value for $|k_z| > N\Delta k_z = 1/\Delta z$, this truncation will cause aliasing errors which will affect the convergence of the CG algorithm and the accuracy of the solution. To avoid aliasing, one approach is to increase the size of the DFT. Generally, though, the DFT must be an integer power of 2 to take advantage of the available FFT algorithms. If we then set $M = 2^\gamma$ where $M > 2N - 1$, in accordance with the above discussion we must have

$$\gamma = \text{Integer } \{\log_2(2N-1) + \rho\} \tag{4.115}$$

where $\rho \geq 1$ is an integer and determines the order of the FFT's dimension or pad. The minimum value of ρ is unity and can be increased as required to reduce aliasing. In this case all arrays must be increased accordingly, and except for $\tilde{G}_{wr}(n\Delta k_z)$ the rest must be padded with zeros. In particular, the first N points of the array $\{I_n\}$ are filled with the initial guess and the array is then transformed using a length of $M = 2^\gamma$ to obtain $\{\hat{I}_n\}$. To recover the next $\{I_n\}$ after inverse transformation only the first N points are again kept and the others are zeroed.

In accordance with the above discussion, the discrete counterpart of (4.105) is

$$\{V_n\}=\frac{jZ_o}{k_o}DFT^{-1}\left\{\left[k_o^2-n^2(\Delta k_z)^2\,\mathrm{sinc}\left(\frac{n\Delta k_z}{2}\Delta z\right)\right]\hat{I}_n\tilde{f}(n\Delta k_z)\tilde{G}_{wr}(n\Delta k_z)\right\} \tag{4.116}$$

The left and right hand sides of this equality should be interpreted as columns or vectors of length N with the one from the right side obtained after truncating the padded array. More specifically $V_n = E_z^i(\rho = a, z_n)$ whereas the right side should be equal to the column generated from the operation $[Z]\{I_n\}$. Thus, in the CG algorithm we should set

$$[Z]\{I_m\} = \frac{jZ_o}{k_o}DFT^{-1}\left\{\left[k_o^2 - n^2(\Delta k_z)^2\ \mathrm{sinc}\ \left(\frac{n\Delta k_z\Delta z}{2}\right)\right]\right.$$
$$\left.\cdot\,\hat{I}_n\tilde{f}(n\Delta k_z)\tilde{G}_{wr}(n\Delta k_z)\right\} \tag{4.117}$$

This eliminates a need to generate the matrix thus reducing the storage to $O(N)$ instead of $O(M^2)$ required with the direct solution. Moreover, because the DFT can be computed by performing only $M\log_2 M$ operations (provided $M = 2^\gamma$), the required CPU time per iteration is reduced to $4M(1+\log_2 M)$. Thus, the total solution CPU time becomes $4MN_1(1+\log_2 M)$ and as before N_I denotes the number of iterations to reach convergence. Actual CPU times for computing the current of a $1\lambda_o$ dipole are given in fig. 4.21. As seen, the CPU time in conjunction with the FFT (usually referred to as the CGFFT method) is nearly a linear function of the number of unknowns whereas the CPU time associated with the direct (matrix inversion) solution is a quadratic function of the unknowns. Also, we observe from figure 4.21 that the use of higher order basis leads to better convergence rates.

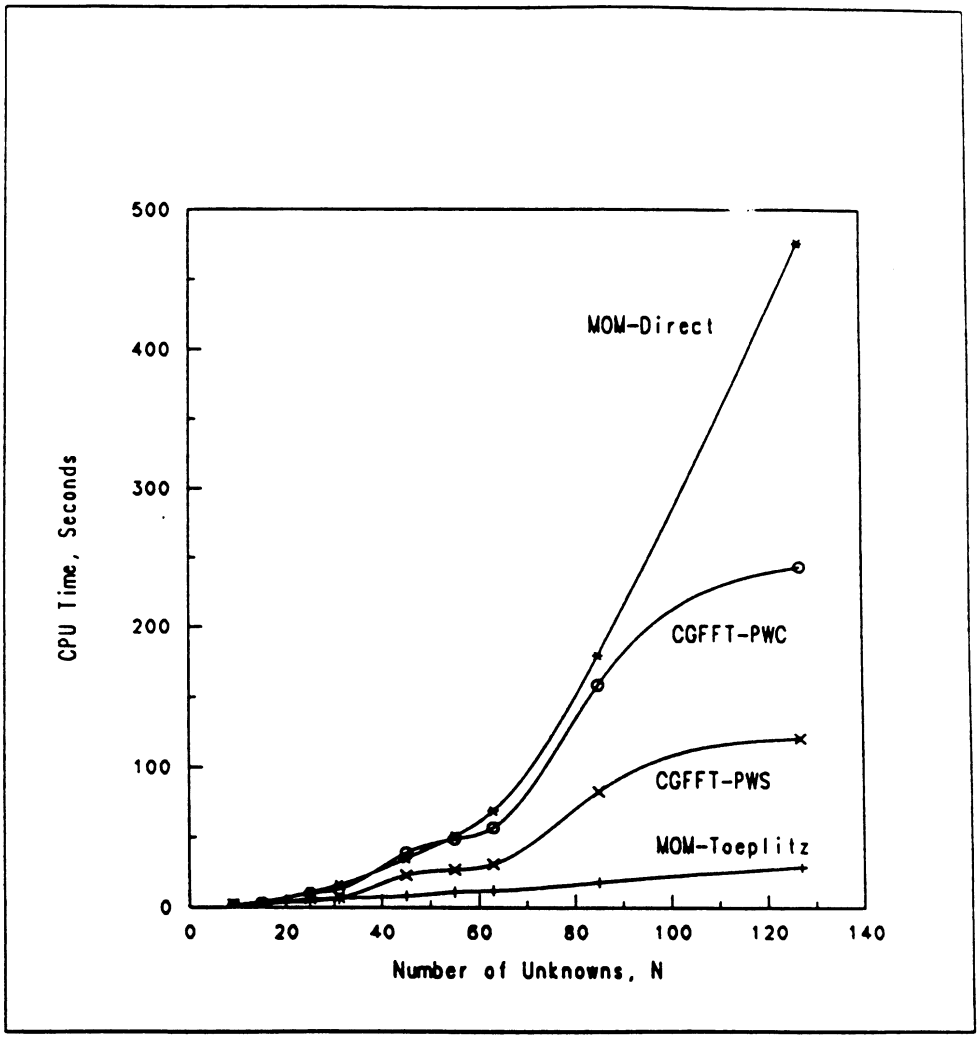

Figure 4.21: A comparison of the CPU time required by the MOM and the CGFFT formulations for the solution of the $1\lambda_o$ wire dipole problem.

We close this section by noting that an alternative and more appropriate way to compute the column $[Z]\{I_n\}$ is to consider the discretized equation

$$V_m = \sum_{n=0}^{N-1} I_n Z_{mn} = \sum_{n=0}^{N-1} I_n Z(m-n) = \sum_{n=0}^{N-1} I_n Z_{m-n}$$

Then by application of the discrete convolution theorem it follows that

$$\{V_m\} = DFT^{-1}\{\hat{Z}\hat{I}_n\}$$

where $\hat{Z}$ denotes the discrete transform of the sequence Z_{0n} or the sequence $Z_{m-n} = Z_p$ with $p = -(N-1), \ldots, 0, 1, 2, \ldots, N-1$. Because of the periodicity of the discrete FFT aliasing is eliminated once the FFT length is set equal to $2N-1$ to accomodate spreading due to the convolution. The sequence Z_{0n} can be obtained from the expressions given earlier by (4.36), (4.75) or (4.80). If $2N-1$ is not a power of 2 then the values of the Z_p sequence should be arranged as shown in figure 4.22.

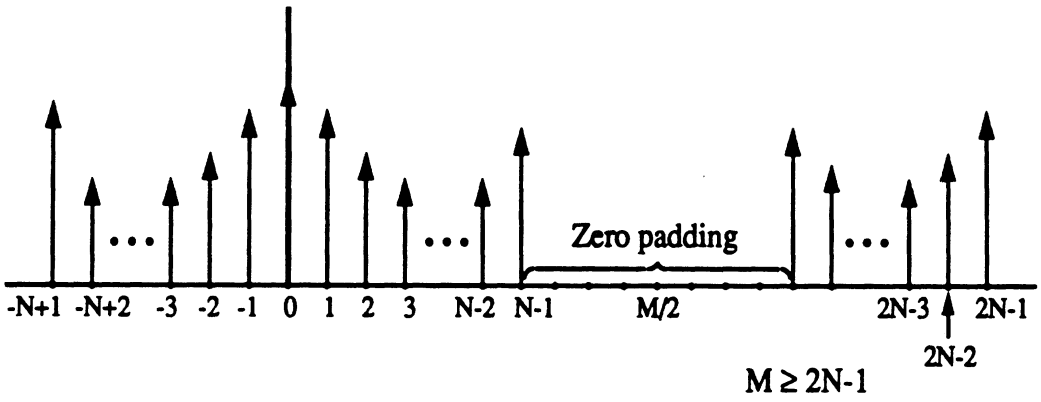

Figure 4.22: Arrangement of the $Z_{m-n} = Z_p$ sequence before inverse fourier transformation.

In general the computation of the Z_{mn} elements may be difficult due to kernel singularities and the requirement to perform rather involved integrations. In this case, a third alternative would be to return to (4.117) and replace $\tilde{G}_{wr}(k_z)$ by the discrete transform of the sequence

$$G_{wr}(z_n) = \frac{e^{-jk_o\sqrt{(n\Delta z)^2+a^2}}}{4\pi\sqrt{(n\Delta z)^2+a^2}}$$

with $n = -N-1, \ldots, 0, 1, \ldots, N-1$. This procedure should substantially reduce aliasing errors and is equivalent to setting

$$\hat{Z}_n = \frac{jZ_o}{k_o}\left\{\left[k^2 - n^2(\Delta k_z)^2 \text{ sinc } \left(\frac{n\Delta k_z \Delta z}{2}\right)\right]\tilde{f}(n\Delta k_z)\hat{G}_{wr}\right\}. \quad (4.118)$$

where $\hat{G}_{wr}$ corresponds to the transform of the discrete sequence $G_{wr}(z_n)$. By taking the inverse DFT of the above $\hat{Z}_n$ we will then (approximately) recover the original sequence Z_n. Any aliasing errors will be due to the truncation of $\tilde{f}(k_z)$ but these should be negligible.

Sample FORTRAN Moment Method Computer Program for Computing the Input Impedance, Radiation and Scattering by a Straight Wire

Compliments of

John R. Natzke

Program employs pulse or PWS basis
Magnetic frill or delta gap excitations for radiation
Wire Surface Fields can be computed
Many of the results in Chapter 4 were generated using this program.

```
C
C     DIP.FTN                          John R. Natzke
C                                      10/6/91
C
C       This program gives the solution for a dipole with
C       a gap or frill source or under plane wave illumination,
C       of length L and radius a.  The moment method
C       procedure is employed using point matching.  The
C       user is prompted for all parameters.
C
C       Link with subroutine package containing CGECO and CGESL.
C
      parameter(ip=500)
      integer PorD,SorM,GorF,pwsb,BorB
      real k,L,Llod,U(ip)
      complex ci,ctemp,Zin,ccIn,E,Er,Ei,LZ,S
      complex Z(ip,ip),In(ip),Vm(ip)

      integer ipvt(ip),iretrn
      real rc,krho
      complex wk(ip)

      open(1,file='dimdat')
      open(2,file='dimpdat')
      open(3,file='dampdat')
      open(4,file='draddat')
      open(7,file='drsrdat')
      open(8,file='disrdat')
      open(9,file='dcurdat')
      open(10,file='dcurpdat')

c...Declaring constant values
 10   ci=cmplx(0.0,1.)
      pi=3.141593
      k=2*pi
      Zo=sqrt(4.e-07*pi/8.854e-12)
      thetp=90
      SorM=1
      BorB=1
      noIter2=1
c...Prompting user for input data
        print *,'1) Plane wave or 2) Dipole source?'
        read *,PorD
        if(PorD .eq. 1)then
          print *,'1) Shorted or 2) Matched dipole?'
          read *,SorM
          pwsb=2
        else
          print *,'1) Gap or 2) Frill model?'
          read *,GorF
        endif
        print *,'Enter length (wavelengths):'
        read *,L
        print *,'Wire radius (wavelengths):'
        read *,a
        print *,'Number of elements:'
        if(PorD .eq. 2)
     &   print *,'  Even for PWS, Odd for pulse basis--'
        read *,Ne
        dz=L/Ne
12      print *,'Resistive loading (pulse basis assumed) (1=yes)?'
        read *,ires
        if(ires .eq. 1)then
          print *,'The dipole is loaded on each side,',
     &      ' symmetrically about the center.'
          print *,'Resistivity (ohm/m):'
          read *,R
          print *,'Length of load (wavelengths):'
          read *,Llod
          Nlod=int(Llod/dz)
```

```
      print *,'  Actual length of load =',Nlod*dz,Nlod
      print *,'Tapered load (1=yes)?'
      read *,itap
      if(itap .eq. 1)then
        print *,'Order of taper (1 = linear):'
        read *,it
        slp=1
        jstart=1
      else
        slp=0
        it=1
        print *,'Start of load (# of elements from end):'
        read *,jstart
      endif
      pwsb=2
    else if(SorM .ne. 2)then
      print *,'1) piece-wise sinusoidal or 2) pulse bases?'
      read *,pwsb
    endif
    if(PorD .eq. 1)then
      print *,'1) Backscatter or 2) Bistatic?'
      read *,BorB
    endif
    print *,'Number of iterations:'
    read *,noIter
    if(noIter .eq. 1)then
      niter=0
      if(PorD .eq. 1)then
        print *,'Angle of incidence:'
        read *,thetp
      endif
      print *,'Surface field calculation (1=yes)?'
      read *,isur
      if(isur .eq. 1)then
        print *,'Number of surface field points:'
        read *,M
        dzm=L/M
      endif
    else
      print *,'Iterating with respect to'
      print *,'  1) angle 2) length 3) resistivity:'
      read *,niter
      if(niter .eq. 2 .and. ires .eq. 1) GOTO 12
      if(niter .eq. 2) print *,'  (Assuming dz=increment/m)'
      print *,'Initial, final, and increment:'
      read *,star,fina,step
      noIter=int((fina-star)/step)+1
      if(niter .eq. 1)then
        if(BorB .eq. 1 .and. PorD .eq. 1)then
          thetp=star
          ibac=1
        else
          noIter=1
          noIter2=int((fina-star)/step)+1
          thet=star
        endif
      else if(niter .eq. 2)then
        print *,'Enter m (even integer > 0):'
        read *,im
        L=star
        Ne=2*int(L/step/2*im)+(pwsb-1)
        step=im*L/Ne
        noIter=int((fina-star)/step)+1
        dz=step/im
        ibac=2
      else
        R=star
        ibac=2
      endif
      if(PorD .eq. 1 .and. (BorB.ne.1.or.niter.ne.1))then
```

```
            print *,'Angle of incidence:'
            read *,thetp
          endif
        endif
        if(BorB .eq. 2 .and. niter .ne. 1)then
          print *,'Angle of observation:'
          read *,thet
        endif
        b=exp(2*pi*75/Zo)*a
c---End of input data

      DO 700 iter=1,noIter
        if(pwsb .eq. 1)then
          N=Ne-1
          dzstart=dz
        else
          N=Ne
          dzstart=dz/2
        endif
        thep=thetp*pi/180.0
        print *,' '
        print *, ' L = ',L,' N = ',N,' dz =',dz
        if(ires .eq. 1) print *,' R =',R
        if(SorM .eq. 2)then
          PorD=2
          GorF=1
        endif
        do 340 isorm=1,SorM
        print *,' Generating impedance and source matrices . . .'
c**********************************************************************
c******************   Impedance, Source,   ************************
c******************   and Current Matrices   **********************
c**********************************************************************
        do 220 j=1,N
          zm=-L/2+dzstart+(j-1)*dz
          if(iter .eq. 1 .or. ibac .eq. 2)then
          if(j .eq. 1)then
            do 210 i=1,N
              zn=-L/2+dzstart+(i-1)*dz
              R1=sqrt((zm-zn+dzstart)**2+a**2)
              R2=sqrt((zm-zn)**2+a**2)
              R3=sqrt((zm-zn-dzstart)**2+a**2)
              if(pwsb .eq. 1)then
                Z(j,i)=-ci*30/sin(k*dz)
     &              *(cexp(-ci*k*R1)/R1
     &              -2*cos(k*dz)*cexp(-ci*k*R2)/R2
     &              +cexp(-ci*k*R3)/R3)
              else
                if(i .eq. j)then
                  Z(j,i)=-ci*k*Zo/4/pi
     &              *(alog((sqrt((dz/2)**2+a**2)+dz/2)
     &               /(sqrt((dz/2)**2+a**2)-dz/2))-ci*k*dz
     &              -k*((zm-zn+dz/2)*(1+ci*k*R1)/(k*R1)**3
     &              *cexp(-ci*k*R1)-(zm-zn-dz/2)*(1+ci*k*R3)
     &              /(k*R3)**3*cexp(-ci*k*R3)))
                else
                  Z(j,i)=-ci*k*Zo/4/pi
     &              *(dz/6*(cexp(-ci*k*R1)/R1+4*cexp(-ci*k*R2)/R2
     &               +cexp(-ci*k*R3)/R3)
     &              -k*((zm-zn+dz/2)*(1+ci*k*R1)/(k*R1)**3
     &               *cexp(-ci*k*R1)-(zm-zn-dz/2)*(1+ci*k*R3)
     &               /(k*R3)**3*cexp(-ci*k*R3)))
                endif
              endif
210         continue
          else
            do 246 i=1,N
              if(i .lt. j)then
                Z(j,i)=Z(i,j)
              else if(i .ge. j)then
```

```
                Z(j,i)=Z(j-1,i-1)
              endif
246         continue
          endif
          endif
c...Incident Field (Source) matrix elements
          if(PorD .eq. 1)then
c   E-POL incident field
            Vm(j)=sin(thep)*cexp(ci*k*zm*cos(thep))
          else if(GorF .eq. 1)then
c   Gap source
            if(j .eq. (N+1)/2)then
              Vm(j)=-1./dz
            else
              Vm(j)=0
            endif
          else
c   Frill model
            Vm(j)=0.5/alog(b/a)
     &         *(cexp(-ci*k*sqrt(zm**2+b**2))/sqrt(zm**2+b**2)
     &         -cexp(-ci*k*sqrt(zm**2+a**2))/sqrt(zm**2+a**2))
          endif
          In(j)=Vm(j)
220     continue
c...Resistive loading
        if(ires .eq. 1)then
          do 222 j=1,N
            if((j.ge.jstart.and.j.le.(jstart+Nlod-1)))then
              Z(j,j)=Z(j,j)-R*(1+slp*(1-j)/Nlod)**it
            else if((j.ge.(N-jstart-Nlod+2)
     &                .and.j.le.(N-jstart+1)))then
              Z(j,j)=Z(j,j)-R*(1+slp*(j-N)/Nlod)**it
            endif
222       continue
        endif
c...Matched dipole
        if(PorD .eq. 1 .and. SorM .eq. 2)then
          Z((N+1)/2,(N+1)/2)=Z((N+1)/2,(N+1)/2)-conjg(Zin)/dz
        endif
        print *,' Solving [Zmn][In] = [Vm] . . .'
c...Calling subroutines to calculate the current matrix
        if(iter.eq.1.or.ibac.eq.2) call CGECO(Z,ip,N,ipvt,rc,wk)
        call CGESL(Z,ip,N,ipvt,In,0)
        print *,'     The condition number is ',rc
c*********************************************************************
c*******************   Aperture Impedance   **********************
c*********************************************************************
        if(PorD .ne. 1)then
          if(GorF .eq. 1)then
            Zin=1/In((N+1)/2)
          else
            Zin=0.0
            do 300 i=1,N
              ccIn=conjg(In(i))
              if(pwsb .eq. 1)then
                Zin=1./cabs(In((N+1)/2))**2*(-Vm(i)*ccIn)
     &               *4/k*sin(k*dz/2)**2/sin(k*dz)+Zin
              else
                Zin=dz/cabs(In((N+1)/2))**2*(-Vm(i)*ccIn)+Zin
              endif
300         continue
          endif
          print *,' Input impedance: ',Zin
cr          if(R .eq. 0) rnorm4=real(Zin)
          write(1,*) L,Real(Zin)
          write(2,*) L,aImag(Zin)
        endif
        if(SorM .eq. 2)then
          PorD=1
        endif
```

```
340     continue
c*********************************************************************
c************************   Current   ****************************
c*********************************************************************
        if(noIter .eq. 1)then
          write(9,*) '"N =',Ne,'"'
          write(10,*) '"N =',Ne,'"'
          if(pwsb .eq. 1)then
            write(9,*) -L/2,0
            write(10,*) -L/2,pha(In(1))
          endif
          do 480 i=1,N
            zm=-L/2+dzstart+(i-1)*dz
            write(9,*) zm,cabs(In(i))*1000
            write(10,*) zm,pha(In(i))
480       continue
          if(pwsb .eq. 1)then
            write(9,*) L/2,0
            write(10,*) L/2,pha(In(N))
          endif
        endif
c*********************************************************************
c**********************   Surface Field   ************************
c*********************************************************************
        if(isur .eq. 1)then
          print *,' Calculating surface electric field . . .'
          write(7,*) '"N =',Ne,'"'
          write(8,*) '"N =',Ne,'"'
          do 520 j=M/2,M+1
            zm=-L/2+(j-1)*dzm
            Er=0
c   Radiatied Field
            do 510 i=1,N
              zn=-L/2+dzstart+(i-1)*dz
              R1=sqrt((zm-zn+dzstart)**2+a**2)
              R2=sqrt((zm-zn)**2+a**2)
              R3=sqrt((zm-zn-dzstart)**2+a**2)
              if(pwsb .eq. 1)then
                LZ=-ci*30/sin(k*dz)
     &              *(cexp(-ci*k*R1)/R1
     &              -2*cos(k*dz)*cexp(-ci*k*R2)/R2
     &              +cexp(-ci*k*R3)/R3)
              else
                if(zm .eq. zn)then
                  LZ=-ci*k*Zo/4/pi
     &              *(alog((sqrt((dz/2)**2+a**2)+dz/2)
     &               /(sqrt((dz/2)**2+a**2)-dz/2))-ci*k*dz
     &              -k*((zm-zn+dz/2)*(1+ci*k*R1)/(k*R1)**3
     &              *cexp(-ci*k*R1)-(zm-zn-dz/2)*(1+ci*k*R3)
     &              /(k*R3)**3*cexp(-ci*k*R3)))
                else
                  LZ=-ci*k*Zo/4/pi
     &              *(dz/6*(cexp(-ci*k*R1)/R1+4*cexp(-ci*k*R2)/R2
     &               +cexp(-ci*k*R3)/R3)
     &              -k*((zm-zn+dz/2)*(1+ci*k*R1)/(k*R1)**3
     &               *cexp(-ci*k*R1)-(zm-zn-dz/2)*(1+ci*k*R3)
     &               /(k*R3)**3*cexp(-ci*k*R3)))
                endif
              endif
              Er=In(i)*LZ+Er
510         continue
c   Incident Field
            if(PorD .eq. 1)then
              Ei=-sin(thep)*cexp(ci*k*zm*cos(thep))
            else if(GorF .eq. 1)then
              if(zm .ge. -dz/2 .and. zm .le. dz/2)then
                Ei=1./dz
              else
                Ei=0
              endif
```

```
            else
              Ei=-0.5/alog(b/a)
     &           *(cexp(-ci*k*sqrt(zm**2+b**2))/sqrt(zm**2+b**2)
     &           -cexp(-ci*k*sqrt(zm**2+a**2))/sqrt(zm**2+a**2))
            endif
c   Total Field
            E=Er+Ei
            write(7,*) zm,Real(E)
            write(8,*) zm,aImag(E)
520       continue
        endif
c*****************************************************************
c******************   Far Field Parameters   *********************
c*****************************************************************
        if(BorB .eq. 1)then
          thet=thetp
        endif
        rnorm3=0
        do 650 iter2=1,noIter2
          the=pi/180*thet
          S=0
c...Far field amplitude
          do 600 i=1,N
            zm=-L/2+dzstart+(i-1)*dz
            S=In(i)*cexp(ci*k*zm*cos(the))+S
600       continue
          if(pwsb .eq. 1)then
            S=ci*60*(cos(k*dz*cos(the))-cos(k*dz))
     &         /sin(the)/sin(k*dz)*S
          else
            S=-ci*k*Zo/4/pi*dz*sin(the)
     &         *sinc(k*dz/2*cos(the))*S
          endif
          print *,' S: ',cabs(S),thet
c   RCS
          if(PorD .eq. 1)then
            RCS=4*pi*cabs(S)**2
            print *,' RCS: ',RCS,', ',10*alog10(RCS),' dB'
            if(R .eq. 0) rnorm=10*alog10(RCS)
            write(3,*) thet,10*alog10(RCS)
c   Power received
            if(SorM .ne. 1)then
              Prec=cabs(In((N+1)/2))**2*Real(Zin)/2
              print *,' Prec: ',Prec*1000,', ',
     &              10*alog10(Prec*1000),' dBm'
              if(R .eq. 0) rnorm2=10*alog10(Prec)
              write(4,*) R,10*alog10(Prec)-rnorm2
            endif
          else
c   Radiation intensity
            U(iter2)=cabs(S)**2/2/Zo
            if(U(iter2) .gt. rnorm3) rnorm3=U(iter2)
c   Gain
            if(the .eq. pi/2)then
              G=4*pi*U(iter2)
     &          /(Real(In((N+1)/2))/2)
              print *,' Gain: ',G,', ',10*alog10(G),' dB'
              if(R .eq. 0) rnorm=10*alog10(G)
              write(3,*) R,10*alog10(G)-rnorm
            endif
          endif
          thet=thet+step
650     continue

        if(niter .eq. 1)then
          thetp=thetp+step
        else if(niter .eq. 2)then
          L=L+step
          Ne=Ne+im
        else
```

```
          R=R+step
        endif
700   continue
        if(niter .eq. 1 .and. PorD .eq. 2)then
          thet=star
          do 710 iter2=1,noIter2
            write(4,*) thet,10*alog10(U(iter2)/rnorm)
            thet=thet+step
710       continue
        endif
        print *,'Again (1=yes)?'
        read *,ians
        if(ians .eq. 1) GOTO 10
        print *,' '
        print *,'OUTPUT FILES:'
        print *,'  Current (mag,phase):          dcurdat,dcurpdat'
        print *,'  Input Impedance (real,imag): dimdat,dimpdat'
        if(isur.eq.1)
     &  print *,'  Surface field (real,imag):   drsrdat,disrdat'
        print *,'  RCS or Gain (dB):            dampdat'
800   call exit
      END
```

Integral Equation Formulation for Microstrip Antennas and Scatterers

Spectral Green's Functions For Substrate Geometry

This chapter describes the derivation of the Green's function associated with a grounded dielectric slab. Though there are such Green's functions available in the literature, these are usually presented in an incomplete form and often contain typographical errors. It is therefore instructive to derive them here since their use is crucial in this study.

Geometry

The geometry we consider here is illustrated in Figure 1 where a unit infinite- simal electric current source oriented in the $\hat{x}$ direction is located on the surface of a dielectric substrate backed by a perfectly conducting plane. The coordinate system is chosen so that the x-y plane is coincident with the grounded plane. The substrate is assumed to have a thickness of d, a permittivity of $\epsilon_r\epsilon_0$, and a permeability of the free-space. The current source is then located at (x', y', d). In the following, we begin with Maxwell's equations to find the resulting E_x, E_y, and E_z fields.

Maxwell's Equations in Spatial Form

The source-free Maxwell's equations are

$$\nabla \times \overline{E} = -j\omega\mu_0\overline{H} \tag{1}$$

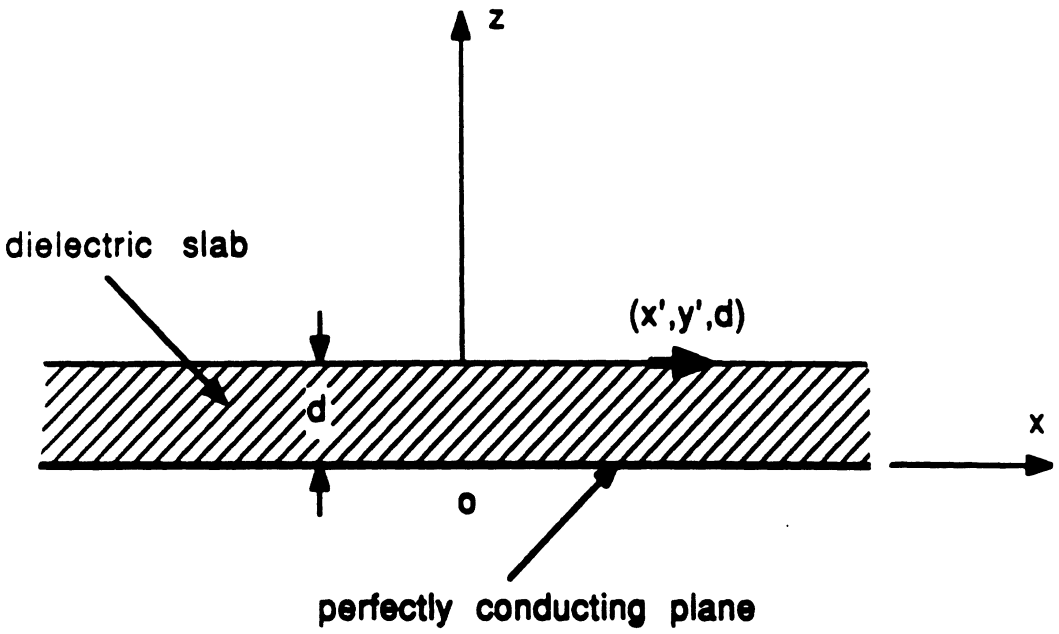

Figure 1: Geometry of a grounded dielectric slab.

$$\nabla \times \overline{H} = j\omega\epsilon_i\epsilon_0\overline{E} \tag{2}$$

where an $e^{j\omega t}$ time convention is employed and ω is the angular frequency. In the above, $\epsilon_i = \epsilon_1 = \epsilon_r$ inside the dielectric substrate and $\epsilon_i = \epsilon_2 = 1$ in air. Equations (1) and (2) can be easily transformed to the two vector wave equations

$$\nabla \times \nabla \times \overline{E} - k_0^2\epsilon_i\overline{E} = 0 \tag{3}$$
$$\nabla \times \nabla \times \overline{H} - k_0^2\epsilon_i\overline{H} = 0 \tag{4}$$

and since $\nabla \cdot (\epsilon_i\overline{E}) = 0$ and $\nabla \cdot \overline{H} = 0$, they can be further reduced into six scalar wave equations. They are

$$\nabla^2 E_z + k_0^2\epsilon_i E_z = 0 \tag{5}$$
$$\nabla^2 H_z + k_0^2\epsilon_i H_z = 0 \tag{6}$$

for the z components and

$$\left(\epsilon_i k_0^2 + \frac{\partial^2}{\partial z^2}\right) E_x = \frac{\partial^2}{\partial x \partial z} E_z - j\omega\mu_0 \frac{\partial}{\partial y} H_z \tag{7}$$
$$\left(\epsilon_i k_0^2 + \frac{\partial^2}{\partial z^2}\right) E_y = \frac{\partial^2}{\partial y \partial z} E_z + j\omega\mu_0 \frac{\partial}{\partial x} H_z \tag{8}$$
$$\left(\epsilon_i k_0^2 + \frac{\partial^2}{\partial z^2}\right) H_x = \frac{\partial^2}{\partial x \partial z} H_z + j\omega\epsilon_i\epsilon_0 \frac{\partial}{\partial y} E_z \tag{9}$$
$$\left(\epsilon_i k_0^2 + \frac{\partial^2}{\partial z^2}\right) H_y = \frac{\partial^2}{\partial y \partial z} H_z - j\omega\epsilon_i\epsilon_0 \frac{\partial}{\partial x} E_z \tag{10}$$

for the other components.

Maxwell's Equations in Spectral Form

To solve (5) and (6), we introduce the Fourier transform pair

$$\tilde{F}(k_x, k_y, z) = \int_{-\infty}^{\infty}\int_{-\infty}^{\infty} F(x, y, z) e^{-jk_x x} e^{-jk_y y} dk_x dk_y \tag{11}$$
$$F(x, y, z) = \frac{1}{4\pi^2}\int_{-\infty}^{\infty}\int_{-\infty}^{\infty} \tilde{F}(k_x, k_y, z) e^{jk_x x} e^{jk_y y} dx dy \tag{12}$$

where F represents any component of electric and magnetic fields. In the transform domain, equations (5) and (6) can be written as

$$\frac{\partial^2 \tilde{E}_z}{\partial z^2} + k_i^2 \tilde{E}_z = 0 \tag{13}$$

$$\frac{\partial^2 \widetilde{H}_z}{\partial z^2} + k_i^2 \widetilde{H}_z = 0 \tag{14}$$

where $k_i^2 = k_1^2 = \epsilon_r k_0^2 - \beta^2$ within the substrate, $k_i^2 = k_2^2 = k_0^2 - \beta^2$ in air and $\beta^2 = k_x^2 + k_y^2$. Similarly (7)-(10) become

$$\tilde{E}_x = \frac{jk_x}{\beta^2}\frac{\partial}{\partial z}\tilde{E}_z + \frac{\omega\mu_0 k_y}{\beta^2}\widetilde{H}_z \tag{15}$$

$$\tilde{E}_y = \frac{jk_y}{\beta^2}\frac{\partial}{\partial z}\tilde{E}_z - \frac{\omega\mu_0 k_x}{\beta^2}\widetilde{H}_z \tag{16}$$

$$\widetilde{H}_x = \frac{jk_x}{\beta^2}\frac{\partial}{\partial z}\widetilde{H}_z - \frac{\omega\epsilon_i\epsilon_0 k_y}{\beta^2}\tilde{E}_z \tag{17}$$

$$\widetilde{H}_y = \frac{jk_y}{\beta^2}\frac{\partial}{\partial z}\widetilde{H}_z + \frac{\omega\epsilon_i\epsilon_0 k_x}{\beta^2}\tilde{E}_z \tag{18}$$

Solutions in Spectral Form

The solution of (13) and (14) must satisfy the radiation condition and as a result the spectral field components take the form

$$\tilde{E}_z = Ae^{-jk_2 z}, \quad \mathrm{Im}k_2 < 0, \quad \text{for } z > d \tag{19}$$

$$\widetilde{H}_z = Be^{-jk_2 z}, \quad \mathrm{Im}k_2 < 0, \quad \text{for } z > d \tag{20}$$

$$\tilde{E}_z = C\cos k_1 z + D\sin k_1 z, \quad \text{for } d > z > 0 \tag{21}$$

$$\widetilde{H}_z = E\sin k_1 z + F\cos k_1 z, \quad \text{for } d > z > 0 \tag{22}$$

where A, B, C, D, E, and F are the unknown constants to be determined by applying the boundary conditions.

Since the boundary conditions at $z = 0$ require that $E_x = E_y = 0$, from (15)-(16) and (21)-(22) we find that $D = F = 0$. To determine the remaining four constants, we use the boundary conditions at the air-dielectric interface ($z = d$) which are

$$E_x^+ - E_x^- = 0 \tag{23}$$

$$E_y^+ - E_y^- = 0 \tag{24}$$

$$H_x^+ - H_x^- = 0 \tag{25}$$

$$H_y^+ - H_y^- = -\delta(x - x')\delta(y - y') \tag{26}$$

where the superscript "+" denotes the associated quantity in the plane of $z = d + 0$ and "−" denotes the associated quantity in the plane of $z = d - 0$. In addition, (x', y') denotes the location of a possible x-directed current impulse excitation. Upon application of (23)-(26) we find

$$A = \frac{k_x k_1 \sin k_1 d}{j\omega\epsilon_0 T_m} e^{-jk_x x'} e^{-jk_y y'} e^{jk_2 d} \tag{27}$$

$$B = \frac{k_y \sin k_1 d}{j T_e} e^{-jk_x x'} e^{-jk_y y'} e^{jk_2 d} \tag{28}$$

$$C = j\frac{k_2 e^{-jk_2 d}}{k_1 \sin k_1 d} A \tag{29}$$

$$E = \frac{e^{-jk_2 d}}{\sin k_1 d} B \tag{30}$$

where

$$T_e = k_1 \cos k_1 d + j k_2 \sin k_1 d \tag{31}$$

$$T_m = \epsilon_r k_2 \cos k_1 d + j k_1 \sin k_1 d \tag{32}$$

Substituting now the constants into (19)-(20) we find that for $z > d$

$$\tilde{E}_x = \frac{Z_0}{j k_0} \frac{(\epsilon_r k_0^2 - k_x^2) k_2 \cos k_1 d + j k_1 (k_0^2 - k_x^2) \sin k_1 d}{T_e T_m} \cdot \sin k_1 d \, e^{-jk_x x'} e^{-jk_y y'} e^{-jk_2 (z-d)} \tag{33}$$

$$\tilde{E}_y = \frac{j Z_0}{k_0} \frac{k_x k_y (k_2 \cos k_1 d + j k_1 \sin k_1 d)}{T_e T_m} \cdot \sin k_1 d \, e^{-jk_x x'} e^{-jk_y y'} e^{-jk_2 (z-d)} \tag{34}$$

The fields E_x and E_y for $z > d$ can then be found via inverse Fourier transformation as described in (11).

Dyadic Green's Function

The total radiated field transverse to z can be written as

$$\overline{E}_T(x,y,z) = \int\int_S \bar{\bar{G}}(x,y,z|x',y') \cdot \overline{J}_s(x',y')dx'dy' \tag{35}$$

where $\bar{\bar{G}} = \hat{x}\hat{x}G_{xx} + \hat{y}\hat{x}G_{yx} + \hat{y}\hat{y}G_{yy} + \hat{x}\hat{y}G_{xy}$ is the pertinent dyadic Green's function and $\overline{J}_s = J_x\hat{x} + J_y\hat{y}$ is a two-dimensional radiating surface current residing at the interface $z = d$. In accordance with the development in the previous section (see (33)-(34)),

$$G_{xx} = \frac{-jZ_0}{4\pi^2 k_0}\int_{-\infty}^{\infty}\int_{-\infty}^{\infty} \frac{(\epsilon_r k_0^2 - k_x^2)k_2 \cos k_1 d + jk_1(k_0^2 - k_x^2)\sin k_1 d}{T_e T_m}$$

$$\cdot \sin k_1 d\, e^{-jk_2(z-d)} e^{jk_x(x-x')} e^{jk_y(y-y')} dk_x dk_y \tag{36}$$

$$G_{yx} = \frac{jZ_0}{4\pi^2 k_0}\int_{-\infty}^{\infty}\int_{-\infty}^{\infty} \frac{k_x k_y(k_2 \cos k_1 d + jk_1 \sin k_1 d)}{T_e T_m}$$

$$\cdot \sin k_1 d\, e^{-jk_2(z-d)} e^{jk_x(x-x')} e^{jk_y(y-y')} dk_x dk_y \tag{37}$$

valid for $z > d$. Denoting

$$\tilde{G}_{xx} = \frac{-jZ_0}{4\pi^2 k_0}\frac{(\epsilon_r k_0^2 - k_x^2)k_2 \cos k_1 d + jk_1(k_0^2 - k_x^2)\sin k_1 d}{T_e T_m}\sin k_1 d \tag{38}$$

$$\tilde{G}_{yx} = \frac{jZ_0}{4\pi^2 k_0}\frac{k_x k_y(k_2 \cos k_1 d + jk_1 \sin k_1 d)}{T_e T_m}\sin k_1 d \tag{39}$$

we may rewrite (36)-(37) as

$$G_{xx} = \int_{-\infty}^{\infty}\int_{-\infty}^{\infty} \tilde{G}_{xx} e^{-jk_2(z-d)} e^{jk_x(x-x')} e^{jk_y(y-y')} dk_x dk_y \tag{40}$$

$$G_{yx} = \int_{-\infty}^{\infty}\int_{-\infty}^{\infty} \tilde{G}_{yx} e^{-jk_2(z-d)} e^{jk_x(x-x')} e^{jk_y(y-y')} dk_x dk_y \tag{41}$$

where we observe that $\tilde{G}_{xx}$ and $\tilde{G}_{yx}$ are not transforms of G_{xx} and G_{yx} but simply functionals introduced for convenience. The other two components of $\bar{\bar{G}}$, namely G_{yy} and G_{xy}, can be found by a simple interchange in

coordinates. They are

$$G_{yy} = \int_{-\infty}^{\infty}\int_{-\infty}^{\infty} \tilde{G}_{yy} e^{-jk_2(z-d)} e^{jk_x(x-x')} e^{jk_y(y-y')} dk_x dk_y \qquad (42)$$

$$G_{xy} = \int_{-\infty}^{\infty}\int_{-\infty}^{\infty} \tilde{G}_{xy} e^{-jk_2(z-d)} e^{jk_x(x-x')} e^{jk_y(y-y')} dk_x dk_y \qquad (43)$$

where

$$\tilde{G}_{yy} = \frac{-jZ_0}{4\pi^2 k_0} \frac{(\epsilon_r k_0^2 - k_y^2)k_2 \cos k_1 d + jk_1(k_0^2 - k_y^2)\sin k_1 d}{T_e T_m} \sin k_1 d \qquad (44)$$

$$\tilde{G}_{xy} = \tilde{G}_{yx} \qquad (45)$$

The E_z component of the field inside the dielectric can be found from (21), (27) and (29). We have

$$E_z = \int\int_S (G'_{zx}\hat{z}\hat{x} + G'_{zy}\hat{z}\hat{y}) \cdot \overline{J}_s(x', y') dx' dy' \quad 0 < z < d \qquad (46)$$

where

$$G'_{zx} = \int_{-\infty}^{\infty}\int_{-\infty}^{\infty} \tilde{G}'_{zx} e^{+jk_x(x-x')} e^{+jk_y(y-y')} dk_x dk_y \qquad (47)$$

$$\tilde{G}'_{zx} = \frac{jk_x k_2 \cos k_1 z}{T_m}\left(\frac{-jZ_o}{4\pi^2 k_o}\right); \qquad 0 < z < d \qquad (48)$$

$$G'_{zy} = \int_{-\infty}^{\infty}\int_{-\infty}^{\infty} \tilde{G}'_{zy} e^{+jk_x(x-x')} e^{+jk_y(y-y')} dk_x dk_y \qquad (49)$$

$$\tilde{G}'_{zy} = \frac{jk_y k_2 \cos k_1 z}{T_m}\left(\frac{-jZ_o}{4\pi^2 k_o}\right); \qquad 0 < z < d \qquad (50)$$

In general, we may then write

$$\overline{E}(x, y, z) = \int_{\substack{\text{domain of} \\ \overline{J}_i = \hat{x}J_{ix} + \hat{y}J_{iy}}} \int \bar{\bar{G}}(x, y, z/x', y') \cdot \overline{J}_i(x', y') dx' dy' \quad z > 0 \qquad (51)$$

with

$$\bar{\bar{G}} = G_{xx}\hat{x}\hat{x} + G_{xy}\hat{x}\hat{y} + G_{yy}\hat{y}\hat{y} + G_{yx}\hat{y}\hat{x} + G_{zx}\hat{z}\hat{x} + G_{zy}\hat{z}\hat{y} \qquad (52)$$

By invoking reciprocity the x and y components of the field due to a z directed dipole at $z = d$ is given by

$$\begin{aligned} \overline{E}(z,y,z) &= (G_{xz}\hat{x}\hat{z} + G_{yz}\hat{y}\hat{z}) \cdot \hat{z} J_{iz} \\ &= (G_{zx}\hat{x}\hat{z} + G_{zy}\hat{y}\hat{z}) \cdot \hat{z} J_{iz} \end{aligned} \qquad (53)$$

Patch Geometry and Current Fomulation

Let us consider a rectangular patch on a substrate as illustrated below

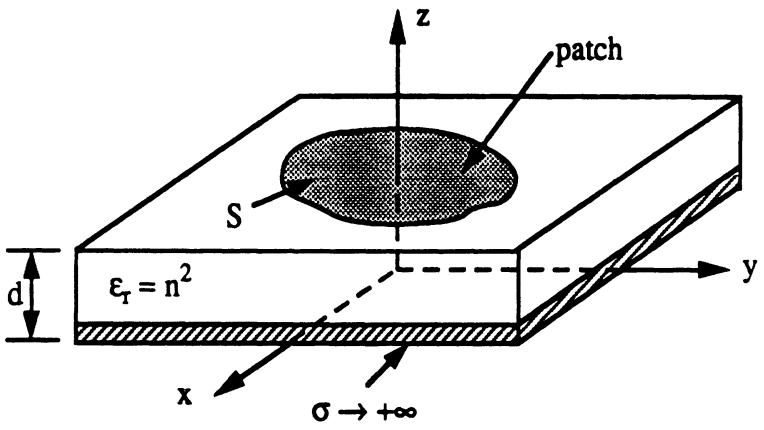

As discussed earlier, the excitation of the patch may be modeled by a delta source at $(x_o, y_o, 0)$ as

$$\overline{J}_i = \hat{z} J_{zo} \delta(x - x_o)\delta(y - y_o) \qquad 0 < z < d \qquad (54)$$

This is expected to generate currents on the patch's surface that in turn produce the radiated field. These will be of the form

$$\overline{J}_s(x,y) = \hat{x} J_x(x,y) + \hat{y} J_y(x,y) \qquad (55)$$

and thier corresponding radiated field can be found from (35) and (46).

To evaluate the patch currents (54), we may impose the boundary condition

$$E_x = 0, \qquad E_y = 0 \qquad \text{at } z = d, (x, y) \in S \tag{56}$$

on the surface of the patch S. Enforcing these via the method of weighted residuals yields the integral equation(s)

$$\int\int_S \overline{E}^r \cdot \overline{J}_t ds = -\int\int \overline{E}^i \cdot \overline{J}_t ds \tag{57}$$

where $\overline{J}_t$ represents the weighting functions of the form (55).

Before proceeding further with the numerical solution of (57), we must first employ appropriate expansion basis for the patch current. Since the x directed currents must vanish on the patch edges at $x = 0$ and $x = a$, we may expand them as

$$J_x(x, y) = \sum_{n=1}^{N} I_n^x J_n^x \tag{58}$$

where

$$J_n^x = \frac{\sin k_o(\Delta x - |x - x_n|)}{\sin k_o \Delta x} P_{2\Delta y}(y - y_n); \tag{59}$$

$$x_n - \Delta x < x < x_n + \Delta x \qquad y_n - \Delta y < y < y_n + \Delta y$$

are the basis functions and I_n^x are the constant coefficients. An illustration of the expansion functions is shown below and we observe that each of these resembles a roof-top.

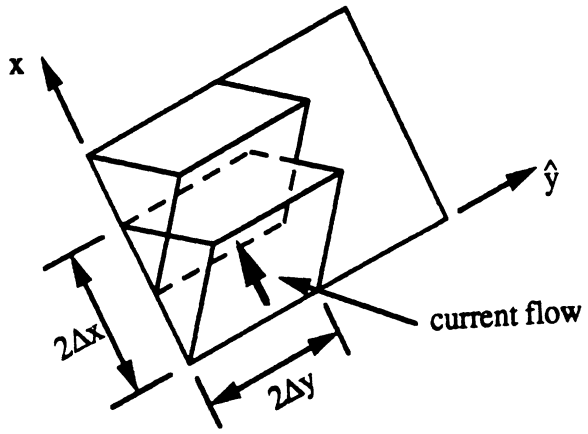

The y-directed currents may be similarly expanded as

$$J_y(x,y) = \sum_{n=1}^{N} I_n^y J_n^y \tag{60}$$

where

$$J_n^y = \frac{\sin k_o(\Delta y - |y - y_n|)}{\sin k_o \Delta y} P_{2\Delta x}(x - x_n)$$

$$x_n - \Delta x < x < x_n + \Delta x \qquad y_n - \Delta y < y < y_n + \Delta y \tag{61}$$

and I_n^y are the corresponding constant coefficients.

The radiated field due to each of the expansion basis or modes can be evaluated from (35). We have,

$$E_n^x(x,y,z) = \int_{x_n - \frac{\Delta x}{2}}^{x_n + \frac{\Delta x}{2}} \int_{y_n - \frac{\Delta y}{2}}^{y_n + \frac{\Delta y}{2}} [G_{xx} J_n^x(x',y') + G_{xy} J_n^y(x',y')]\, dx'dy' \tag{62}$$

$$E_n^y(x,y,z) = \int_{x_n - \frac{\Delta x}{2}}^{x_n + \frac{\Delta x}{2}} \int_{y_n - \frac{\Delta y}{2}}^{y_n + \frac{\Delta y}{2}} [G_{yy} J_n^y(x',y') + G_{yx} J_n^x(x',y')]\, dx'dy' \tag{63}$$

where E_n^x denotes the x component of the field attributed to the nth mode and likewise E_n^y denotes the y component of the field attributed to the same mode. Setting

$$\overline{J}_t(x,y) = \overline{J}_m(x,y) = \begin{cases} \hat{x} J_m^x(x,y) \\ \quad or \\ \hat{y} J_m^y(x,y) \end{cases} \qquad m = 1,2,\cdots,N \tag{64}$$

implying a Galerkin's formulation, and substituting into (57) yields the following coupled pair of equations

$$\sum_{n=1}^{N} \int\int_{S_m} E_n^x(x,y,d) J_m^x(x,y) dxdy = -\int\int_{S_m} E_x^i(x,y,d) J_m^x(x,y) dxdy$$

$$\sum_{n=1}^{N} \int\int_{S_m} E_n^y(x,y,d) J_m^y(x,y) dxdy = -\int\int_{S_m} E_y^i(x,y,d) J_m^y(x,y) dxdy \tag{65}$$

In (65), S_m denotes the area occupied by the weighting functions or test mode $J_m(x,y)$. In particular, S_m is defined by the area included in the region $x_m - \Delta x < x < x_m + \Delta x$, $y_m - \Delta y < y < y_m + \Delta y$. The system of equations may be written more compactly as

$$\begin{aligned} -\sum_{n=1}^{N} (I_n^x Z_{mn}^{xx} + I_n^y Z_{mn}^{xy}) &= V_m^x \\ -\sum_{n=1}^{N} (I_n^x Z_{mn}^{yx} + I_n^y Z_{mn}^{yy}) &= V_m^y \end{aligned} \tag{66}$$

in which

$$\begin{aligned} Z_{nm}^{xx} = &\int_{-\infty}^{\infty}\int_{-\infty}^{\infty}\int\int_{S_n}\int\int_{S_m} \tilde{G}_{xx} e^{jk_x(x-x')} e^{jk_y(y-y')} \cdot \frac{\sin[k_o(\Delta x - |x' - x_n|)]}{\sin k_o \Delta x} \\ &\cdot \frac{\sin[k_o(\Delta x - |x - x_m|)]}{\sin k_o \Delta x} dx dy dx' dy' dk_x dk_y \end{aligned} \tag{67}$$

$$\begin{aligned} Z_{nm}^{xy} = Z_{nm}^{yx} = &\int_{-\infty}^{\infty}\int_{-\infty}^{\infty}\int\int_{S_n}\int\int_{S_m} \tilde{G}_{xy} e^{jk_x(x-x')} e^{jk_y(y-y')} \\ &\cdot \frac{\sin[k_o(\Delta y - |y' - y_n|)]}{\sin k_o \Delta y} \cdot \frac{\sin[k_o(\Delta x - |x - x_m|)]}{\sin k_o \Delta x} dx dy dx' dy' dk_x dk_y \end{aligned} \tag{68}$$

$$\begin{aligned} Z_{nm}^{yy} = &\int_{-\infty}^{\infty}\int_{-\infty}^{\infty}\int\int_{S_n}\int\int_{S_m} \tilde{G}_{yy} e^{jk_x(x-x')} e^{jk_y(y-y')} \cdot \frac{\sin[k_o(\Delta y - |y' - y_n|)]}{\sin k_o \Delta y} \\ &\cdot \frac{\sin[k_o(\Delta y - |y - y_m|)]}{\sin k_o \Delta y} dx dy dx' dy' dk_x dk_y \end{aligned} \tag{69}$$

$$V_m^x = \int\int_{S_m} E_x^i(x,y,d) J_m^x(x,y) dx dy \tag{70}$$

and

$$V_m^y = \int\int_{S_m} E_y^i(x,y,d) J_m^y(x,y) dx dy. \tag{71}$$

The computation of $V_m^{x,y}$ requires knowledge of the excitation field $E_{x,y}^i$ due to the source $\overline{J}_i(x,y)$ as given in (54). However, by invoking reciprocity $V_m^{x,y}$ can be rewritten as

$$V_m^x = \int\int\int_{V_i} E_m^{zx}(x,y,z) J_z^i(x,y) dx dy dz \tag{72}$$

$$V_m^y = \int\int\int_{V_i} E_m^{zy}(x,y,z) J_z^i(x,y) dx dy dz \tag{73}$$

where V_i denotes the volume of the source current J_i, E_m^{zx} denotes the z components of the field due to the mode J_m^x and likewise E_m^{zy} denotes the field due to the J_m^y mode. From (46) they are given by

$$E_m^{zx} = \int_{-\infty}^{\infty}\int_{-\infty}^{\infty}\int\int_{S_m} \tilde{G}_{zx}' e^{jk_x(x-x')} e^{jk_y(y-y')} J_m^x(x',y') dx' dy' \qquad 0 < z < d \tag{74}$$

$$E_m^{zy} = \int_{-\infty}^{\infty}\int_{-\infty}^{\infty}\int\int_{S_m} \tilde{G}_{zy}' e^{jk_x(x-x')} e^{jk_y(y-y')} J_m^y(x',y') dx' dy' \qquad 0 < z < d \tag{75}$$

Except for the infinite integrals, the integrations over S_n and S_m can be evaluated analytically. In particular, these integrations can be eliminated by introducing the Fourier transforms of the modes given by

$$\mathcal{F}(J_n^x) = \int\int_{S_n} J_n^x(x,y) e^{jk_x x} e^{jk_y y} dx dy \tag{76}$$

$$\mathcal{F}(J_n^y) = \int\int_{S_n} J_n^y(x,y) e^{jk_x x} e^{jk_y y} dx dy \tag{77}$$

Using (76) and (77), the impedance elements may be rewritten as

$$Z_{nm}^{xx} = \int_{-\infty}^{\infty}\int_{-\infty}^{\infty} \tilde{G}_{xx} \mathcal{F}(J_n^x) \mathcal{F}^*(J_m^x) dk_x dk_y \tag{78}$$

$$Z_{nm}^{xy} = \int_{-\infty}^{\infty}\int_{-\infty}^{\infty} \tilde{G}_{xy} \mathcal{F}(J_n^y) \mathcal{F}^*(J_m^x) dk_x dk_y \tag{79}$$

$$Z_{nm}^{yy} = \int_{-\infty}^{\infty}\int_{-\infty}^{\infty} \tilde{G}_{yy}\mathcal{F}(J_n^y)\mathcal{F}^*(J_m^y)dk_x dk_y \tag{80}$$

where "*" indicates complex conjugation. Similarly, from (72) - (75),

$$V_m^x = \int_{-\infty}^{\infty}\int_{-\infty}^{\infty} \tilde{G}'_{zx} e^{jk_x x_o} e^{jk_y y_o}\mathcal{F}(J_m^x)dk_x dk_y \tag{81}$$

$$V_m^y = \int_{-\infty}^{\infty}\int_{-\infty}^{\infty} \tilde{G}'_{zy} e^{jk_x x_o} e^{jk_y y_o}\mathcal{F}(J_m^y)dk_x dk_y \tag{82}$$

$$G'_{zx} = \left(\frac{jZ_o}{4\pi^2 k_o}\right)\frac{jk_x k_2 \sin(k_1 d)}{k_1 T_m}; \qquad G'_{zy} = G'_{zx}(k_x \to k_y)$$

For a solution of the system (66), it remains to evaluate the integrals (78) - (82). These are all of the same form and in particular their integrands have the same demoninator which becomes singular at the zeros of T_e and T_m, given in (31) and (32). These zeros correspond to the TE and TM surface wave poles and complicate a numerical evaluation of the integrals. For convenience, the infinite integral may be written in polar coordinates via the transformation

$$\begin{aligned} k_x &= \beta\cos\alpha \\ k_y &= \beta\sin\alpha. \end{aligned} \tag{83}$$

Thus, the integrals in (78) - (82) may be written in the form

$$\int\int_{-\infty}^{\infty}(\quad)dk_x dk_y = \int_0^{2\pi}\int_0^{\infty}(\quad)d\beta d\alpha \tag{84}$$

There will be at least one propagating TM mode (unless $\epsilon_r = 1$) and perhaps a few more depending on the thickness of the substrate and the value of ϵ_r. For real ϵ_r, the zeros of T_e and T_m occur at real values of $\beta = \beta_p$ and can be shown to be within the range

$$k_o < \beta_o < \sqrt{\epsilon_r}k_o$$

If loss is present (complex ϵ_r) then β_o moves off the real axis to $\beta_o - j\gamma$. To avoid numerical difficulties in the evaluation of (84), a standard procedure is to isolate the section near the pole location as follows:

$$\int_o^{2\pi}\int_o^{\infty}(\quad)d\beta d\alpha = \int_o^{2\pi}\left\{\int_o^{\beta_o-\delta}(\quad)d\beta + \int_{\beta_o-\delta}^{\beta_o+\delta}(\quad)d\beta + \int_{\beta_o+\delta}^{\infty}(\quad)d\beta\right\}d\alpha \qquad (85)$$

where

$$I_\delta = \int_{\beta_o-\delta}^{\beta_o+\delta}(\quad)d\beta = \int_{\beta_o-\delta}^{\beta_o+\delta}\frac{f(\beta)}{g(\beta)}d\beta \qquad (86)$$

can be evaluated analytically for small δ. Suppose $g(\beta)$ has a zero at $\beta = \beta_o - j\gamma$ then by using a Taylor series expansion

$$g(\beta) \cong (\beta - \beta_o + j\gamma)g'(\beta_o - j\gamma) \qquad (87)$$

Substituting (87) into (86) and setting $f(\beta) \approx f(\beta_o - j\gamma)$ yields

$$I_\delta = \frac{jf(\beta_o - j\gamma)}{g'(\beta_o - j\gamma)}\tan^{-1}\left\{\frac{-2\delta\gamma}{\gamma^2 - \delta^2}\right\}. \qquad (88)$$

Input Impedance Computation

$$Z_{in} = -\frac{1}{I_{probe}}\int_0^d \hat{z}\cdot\overline{E}(x_o, y_o, z)dz$$

$$I_{probe} = J_{z_o}(2\pi r_o); \qquad r_o = \text{radius of the probe}$$

Far Zone Fields From Microstrip Patch

To find the far zone radiated field by a single patch, one can proceed by evaluating the Fourier integrals in (40) - (43) using the stationary-phase formula [10]. Another much easier approach is to employ the reciprocity theorem [11]. Here we discuss both approaches.

Consider the integral

$$I(\Omega) = \int_{-\infty}^{\infty}\int_{-\infty}^{\infty} f(x,y)e^{j\Omega q(x,y)}dxdy, \qquad \Omega > 0 \tag{89}$$

where $q(x,y)$ is a real function and it has a simple, real stationary point (x_s, y_s) defined by

$$\frac{\partial q}{\partial x} = 0 \quad \text{and} \quad \frac{\partial q}{\partial y} = 0 \quad \text{at } (x_s, y_s). \tag{90}$$

Provided f is regular near (x_s, y_s), then an asymptotic approximation of $I(\Omega)$ for large Ω is given by

$$I(\Omega) \approx f(x_s, y_s)e^{j\Omega q(x_s,y_s)}\left(\frac{2\pi}{\Omega}\right)\frac{e^{j(\pi/4)\sigma}}{|det(\partial^2 q/\partial x_s \partial y_s)|^{1/2}} \tag{91}$$

where

$$\sigma = sgnd_1 + sgnd_2 \tag{92}$$

in which (d_1, d_2) are the eigenvalues of the matrix comprising the elements $\partial^2 q/\partial x_s \partial y_s$.

The above stationary-phase formula can be applied for the evaluation of (40) - (43) which can be written as

$$\begin{aligned}\overline{\overline{G}} &= \frac{1}{4\pi^2}\int_{-\infty}^{\infty}\int_{-\infty}^{\infty}\tilde{\tilde{G}}(k_x,k_y)e^{j(k_2 d - k_x x' - k_y y')} \\ &\quad \cdot\ e^{jr(k_x \sin\theta\cos\phi + k_y \sin\theta\sin\phi - k_2\cos\theta)}dk_x dk_y\end{aligned} \tag{93}$$

where (r, θ, ϕ) are the usual spherical coordinates describing the observation point. Comparing (93) to (89), the following identifications are possible:

$$\begin{aligned} f &= \frac{1}{4\pi^2}\tilde{\tilde{G}}(k_x,k_y)e^{j(k_2 d - k_x x' - k_y y')} \\ \Omega &= r \\ q &= k_x \sin\theta\cos\phi + k_y \sin\theta\sin\phi - k_2\cos\theta. \end{aligned}$$

The stationary point is found in accordance with (90) and is given by

$$k_{xs} = -k_o \sin\theta\cos\phi, \qquad k_{ys} = -k_o \sin\theta\sin\phi \tag{94}$$

and together with

$$\left|\det(\partial^2 q/\partial k_{xs}\partial k_{ys})\right|^{1/2} = \frac{1}{k_o\cos\theta}, \qquad \sigma = 2 \tag{95}$$

we obtain

$$\overline{\overline{G}} \approx \frac{jk_o\cos\theta}{2\pi r} e^{jk_o r}\tilde{\tilde{\overline{G}}}(k_{xs}, k_{ys}) e^{jk_o(\cos\theta d + \sin\theta\cos\phi x' + \sin\theta\sin\phi y')} \tag{96}$$

for large r. The transverse component of the far field radiated by a single patch with current $\overline{J}_s(x,y)$ is then given by

$$\begin{aligned}\overline{E}_{ff} &= \frac{jk_o\cos\theta}{2\pi r} e^{-jk_o r}\tilde{\tilde{\overline{G}}}(k_{xs}, k_{ys}) e^{jk_o d\cos\theta} \\ &\cdot \int\int_{S_p} \overline{J}_s(x',y') e^{jk_o(\sin\theta\cos\phi x' + \sin\theta\sin\phi y')} dx'dy'.\end{aligned} \tag{97}$$

Note that f is not regular at $\theta = \pi/2$ and therefore the above asymptotic expression is not valid there.

We now consider the second approach. In accordance with the reciprocity theorem, if $\overline{E}_1$ is the field due to $\overline{J}_1$ and $\overline{E}_2$ is the field due to $\overline{J}_2$, then

$$\int\int\int \overline{E}_1 \cdot \overline{J}_2 dV = \int\int\int \overline{E}_2 \cdot \overline{J}_1 dV \tag{98}$$

holds. Assume now that a current element Il is situated at point (r,θ,ϕ) and oriented in the $\hat{\theta}$ direction. This current element, if away from the dielectric surface, produces a spherical wave of the form

$$\overline{E}^i = -j\frac{k_o Z_o Il}{4\pi r} e^{-jk_o(|\bar{r}-\bar{r}'|)}\hat{\theta} \tag{99}$$

where $\hat{r}'$ is a point near the origin. We observe that (99) can be approximated as a plane wave with TM polarization and, therefore, the plane wave reflection coefficient R^{TM} can be employed to find the reflected field near

the origin. The total field at the dielectric surface near the origin is then given by

$$\overline{E}_1 = -j\frac{k_o Z_o Il}{4\pi r}e^{jk_o r}(1 - R^{TM})e^{jk_o(\cos\theta d + \sin\theta\cos\phi x' + \sin\theta\sin\phi y')}\hat{\theta}. \quad (100)$$

Let now $\bar{e} = \overline{E}_2$ denote the electric field at (r, θ, ϕ) produced by the patch current $\overline{J}_s = \overline{J}_2$. From the reciprocity theorem (98), we then have

$$\int\int\int \overline{E}_2 \cdot \overline{J}_1 dv = \bar{e} \cdot Il\hat{\theta} = -j\frac{k_o Z_o Il}{4\pi r}e^{-jk_o r}(1 - R^{TM})e^{jk_o d\cos\theta}$$

$$\cdot \int\int_{S_p} e^{jk_o(\sin\theta\cos\phi x' + \sin\theta\sin\phi y')}\hat{\theta} \cdot \overline{J}_s(x', y')dx', dy' \quad (101)$$

which yields

$$e_\theta = -j\frac{k_o Z_o}{4\pi r}e^{-jk_o r}(1 - R^{TM})e^{jk_o d\cos\theta}$$

$$\cdot \int\int_{S_p} e^{jk_o(\sin\theta\cos\phi x' + \sin\theta\sin\phi y')}\hat{\theta} \cdot \overline{J}_s(x', y')dx'dy'. \quad (102)$$

Similarly, by orienting the element current in the $\hat{\phi}$ direction, we find that

$$e_\phi = -j\frac{k_o Z_o}{4\pi r}e^{-jk_o r}(1 + R^{TE})e^{jk_o d\cos\theta}$$

$$\cdot \int\int_{S_p} e^{jk_o(sin\theta\cos\phi x' + \sin\theta\sin\phi y')}\hat{\phi} \cdot \overline{J}_s(x', y')dx'dy'. \quad (103)$$

It can be shown that the field given by (102) - (103) is the same as that in (97). They all exhibit a feature of geometrical optics and are, thus, accurate provided the observation point is not near the dielectric surface where the surface wave contribution may become appreciable. Therefore, in the region $0 \leq \theta < \pi/2$ we have

$$e_\theta = -j\frac{k_o Z_o}{4\pi}\frac{e^{-jk_o r}}{r}(1 - R^{TM})e^{jk_o d\cos\theta}(\cos\theta\cos\phi I_x + \cos\theta\sin\phi I_y)$$

$$e_\phi = -j\frac{k_o Z_o}{4\pi}\frac{e^{-jk_o r}}{r}(1 + R^{TE})e^{jk_o d\cos\theta}(-\sin\phi I_x + \cos\phi I_y) \quad (104)$$

where the components $I_{x,y}$ are integrals given by

$$I_{x,y} = \int\int_{S_p} J_{x,y}e^{jk_o(x\sin\theta\cos\phi + y\sin\theta\sin\phi)}dxdy. \quad (105)$$

References

[1] K. Carver and J. Mink, "Microstrip Antenna Technology," *IEEE Trans. Antennas & Propagat.*, 1981.

[2] N. K. Uzunoglu, N. G. Alexopoulos and J. G. Fikioris, "Radiation Properties of Microstrip Dipoles," *IEEE Trans. Antennas & Propagat.*, Vol. AP-27, pp. 853–858, Nov. 1979.

[3] D. Pozar, "Input Impedance and Mutual Coupling of Rectangular Microstrip Antennas," *IEEE Trans. Antennas & Propagat.*, Vol. AP-30, 1982.

[4] J. R. Mosig, F. E. Gandial, "General Integral Equation Formulation for Microstrip Antennas and Scatterers," *IEE Proceedings*, part H, 1985.

[5] D. Pozar, "Radiation and Scattering from a Microstrip Patch on a Uniaxial Substrate," *IEEE Trans. Antennas & Propagat.*, Vol. AP-35, pp. 613–621, June 1987.

[6] P. B. Katehi and N. G. Alexopoulos, "On the Modeling of Electromagnetically Coupled Microstrip Antennas — the Printed Stripe Dipole," *IEEE Trans. Antennas & Propagat.*, Vol. AP-32, No. 11, Nov. 1984.

[7] P. B. Katehi and N. G. Alexopoulos, "Real Axis Integration of Sommerfeld Type Integrals with Application to Printed Circuit Antennas," *J. Math Physics*, Vol. 24, No. 3, March 1983.

[8] D. M. Pozar and D. H. Schaubert, "Analysis of an Infinite Array of Rectangular Microstrip Patches with Idealized Probe Feeds," *IEEE Trans. Antennas & Propagat.*, Vol. AP-32, pp. 1101–1107, Oct. 1984.

[9] J. J. Jin and J. L. Volakis, "Electromagnetic Scattering by a Perfectly Conducting Patch Array on a Dielectric Slab," in *IEEE Trans. Antennas & Propagat.*, Vol. AP-38, May 1990.

[10] L. B. Felsen and N. Marcuvitz, *Radiation and Scattering of Waves*, Chapt. 4, Englewood Cliffs, N. J.: Prentice Hall, 1973.

[11] R. F. Harrington, *Time-Harmonic Electromagnetic Fields*, Chapt. 3, New York: McGraw-Hill, 1961.

Computation of Surface Wave Poles

The surface wave poles correspond to the values of $\beta = \beta_o = \beta_{sw}$ at which

$$T_m = \varepsilon_r \underbrace{\sqrt{k_o^2 - \beta^2}}_{k_2} \cos\left(\sqrt{\varepsilon_r k_o^2 - \beta^2}\, d\right) + j\sqrt{\varepsilon_r k_o^2 - \beta^2} \sin\left(\underbrace{\sqrt{\varepsilon_r k_o^2 - \beta^2}}_{k_1} d\right) = 0 \tag{1}$$

or

$$T_e = \sqrt{\varepsilon_r k_o^2 - \beta^2} \cos\left(\sqrt{\varepsilon_r k_o^2 - \beta^2}\, d\right) + j\sqrt{k_o^2 - \beta^2} \sin\left(\sqrt{\varepsilon_r k_o^2 - \beta^2}\, d\right) = 0 \tag{2}$$

setting

$$u = \sqrt{\varepsilon_r k_o^2 - \beta^2} \tag{3}$$

and substituting into (1) and (2) gives

$$j\varepsilon_r \sqrt{k_o^2 - \beta^2} = u \tan(ud) \tag{4}$$

and

$$-j\sqrt{k_o^2 - \beta^2} = u \cot(ud) \tag{5}$$

respectively. From (3), we further have

$$\beta^2 = -u^2 + \varepsilon_r k_o^2$$

and when this is introduced into (4) - (5) gives

$$j\varepsilon_r\left(-j\sqrt{(\varepsilon_r - 1) k_o^2 - u^2}\right) = u \tan(ud)$$

$$-j\left(-j\sqrt{(\varepsilon_r - 1) k_o^2 - u^2}\right) = u \cot(ud)$$

or

$$(ud)\tan(ud) = \varepsilon_r d\sqrt{(\varepsilon_r - 1)\,k_o^2 - u^2}$$

$$(ud)\tan(ud) = \varepsilon_r d\sqrt{(\varepsilon_r - 1)\,k_o^2 - u^2}$$

$$(ud)\cot(ud) = d\sqrt{(\varepsilon_r - 1)\,k_o^2 - u^2}$$

The above can be solved graphically as illustrated below.

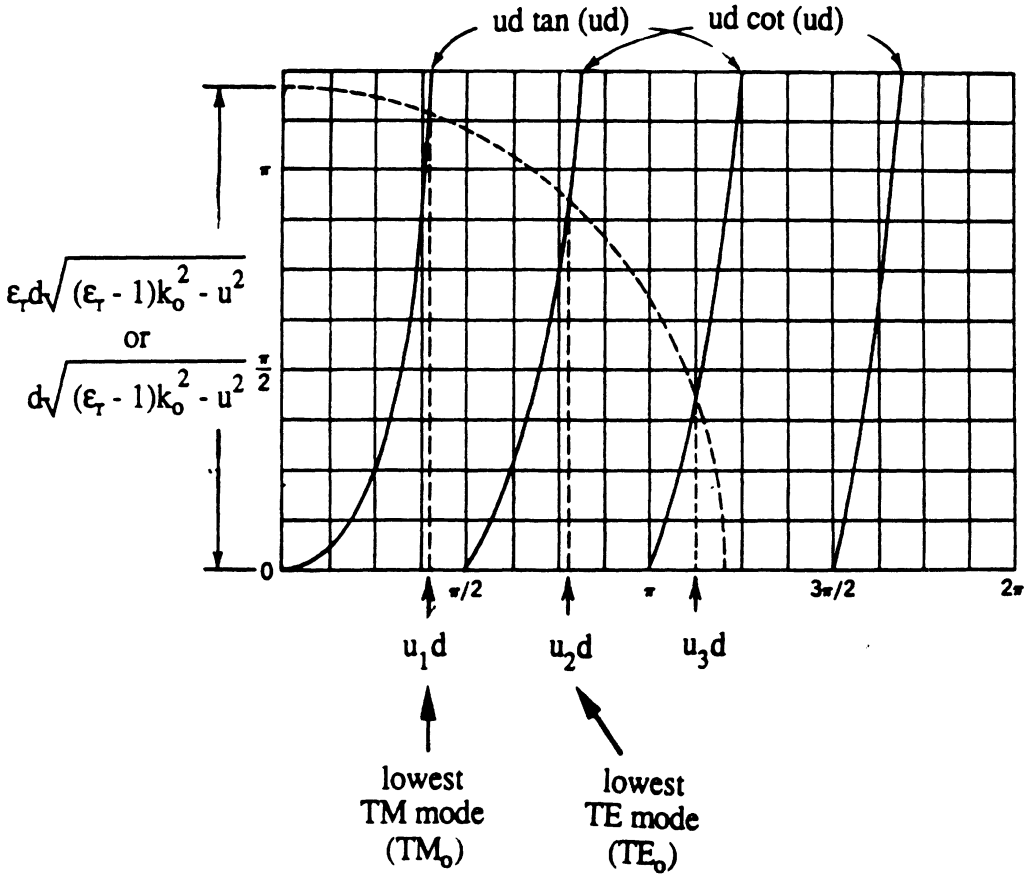

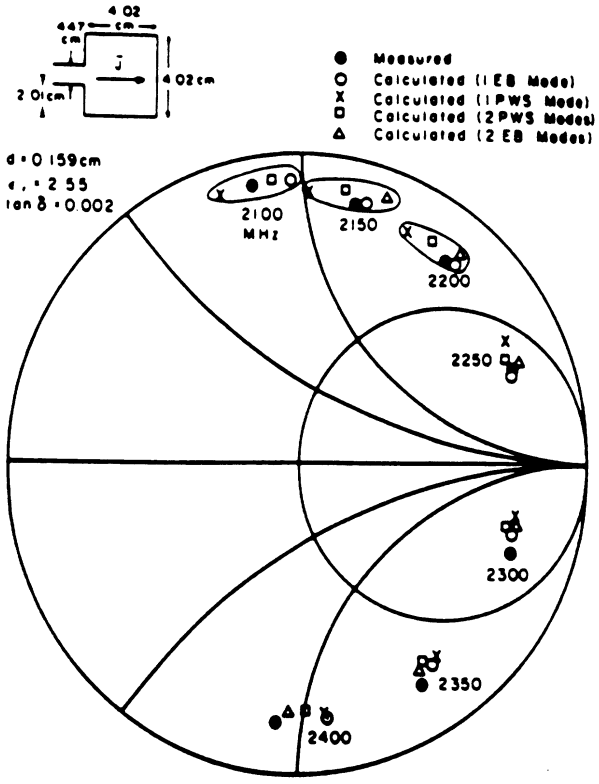

Fig. Measured and calculated input impedance of an edge-fed microstrip antenna. Calculations made using one and two EB and PWS modes.

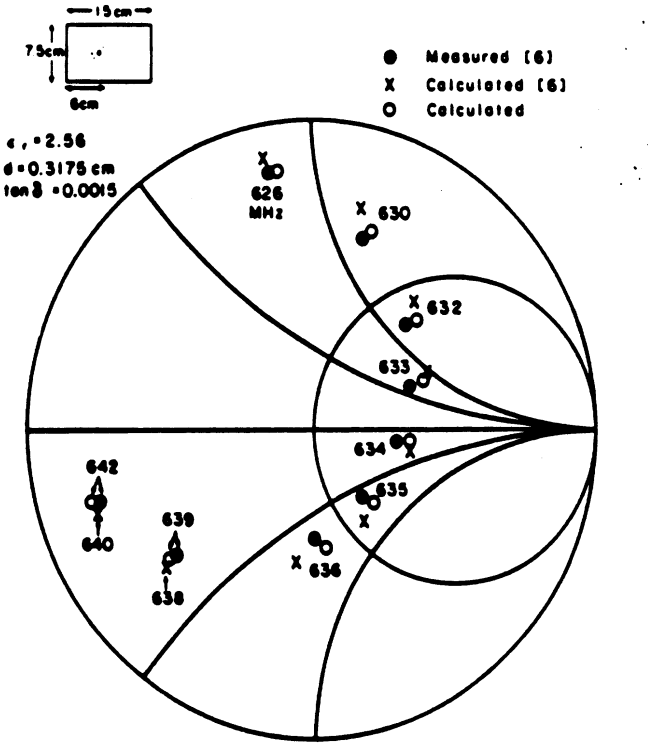

Fig. Measured and calculated input impedance of a coax-fed microstrip antenna compared with calculations from

From Pozar [33], 1982

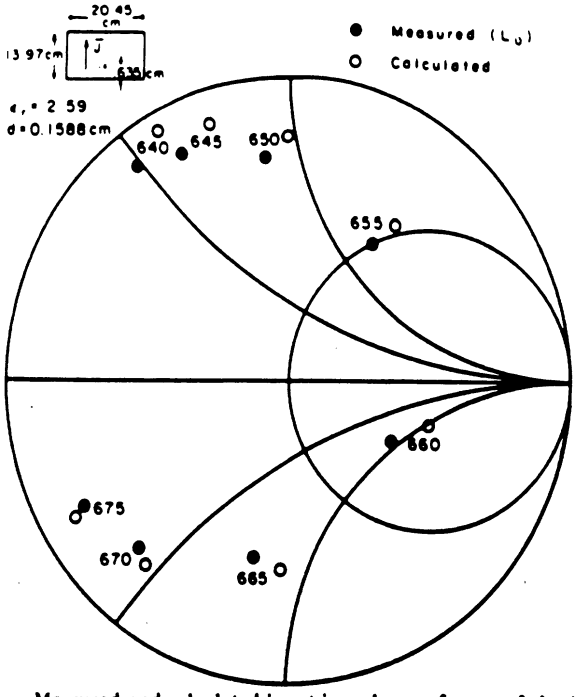

Fig. Measured and calculated input impedance of a coax-fed microstrip antenna.

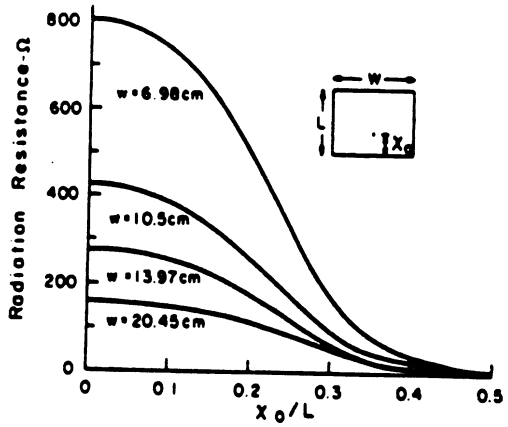

Fig. Radiation resistance for a coax-fed microstrip antenna versus feed position and width. L = 13.97 cm, ϵ_r = 2.60, d = 0.1588 cm, tan δ = .002.

from Pozar [3], 1982.

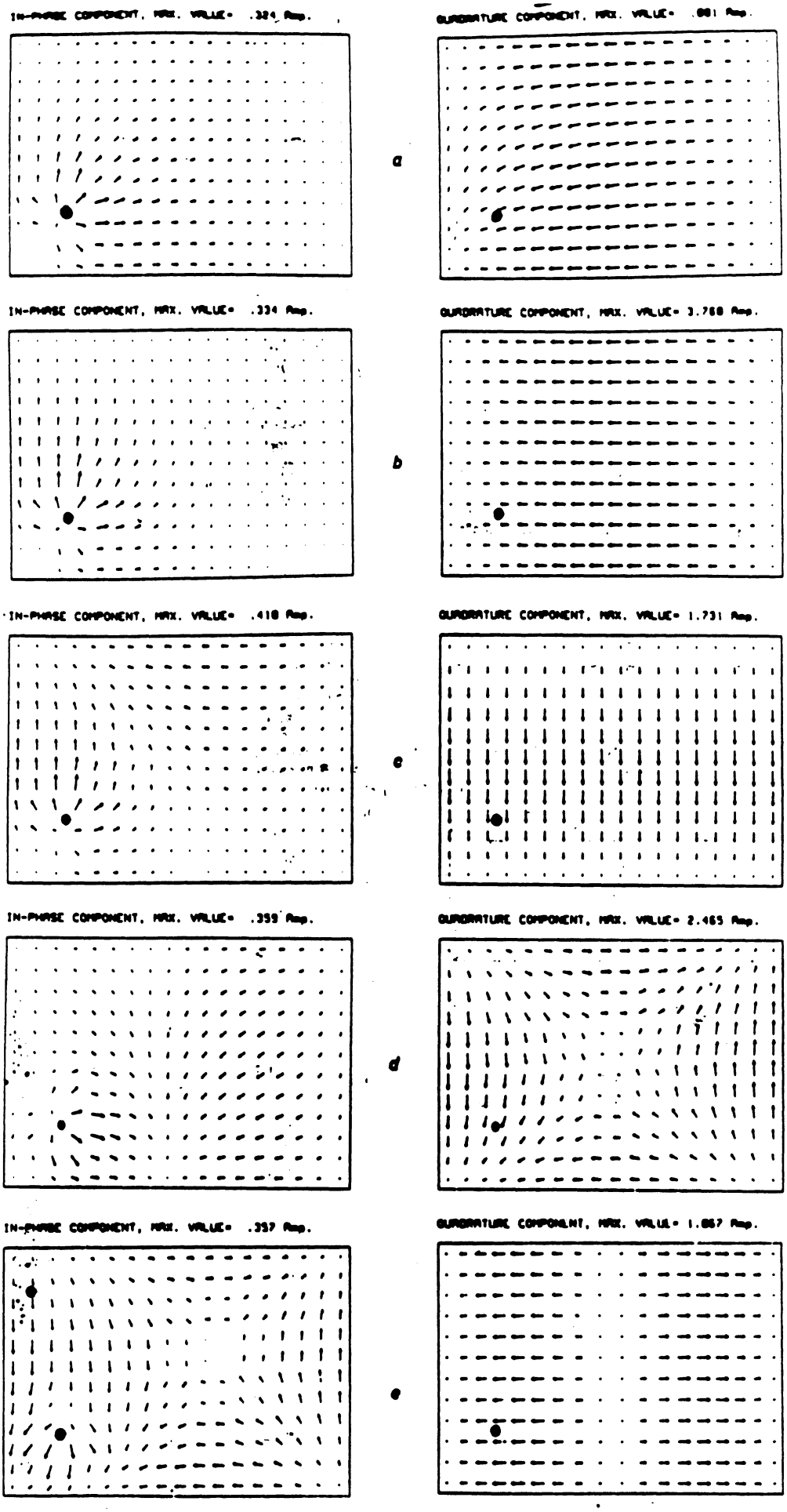

atch size
50x40 mm
$= d = 0.8mm$
$= 4.34$
$m\delta = .002$
atch
onductivity
$\Gamma = \sigma_{cu}/4.$

y
x

Real and imaginary parts of the surface current for a rectangular coaxial-fed microstrip antenna

a Below resonance $f = f_{10}/2 = 0.603$ GHz
b TM_{10} resonance $f = f_{10} = 1.206$ GHz
c TM_{01} resonance $f = f_{01} = 1.783$ GHz
d TM_{11} resonance $f = f_{11} = 2.177$ GHz
e TM_{20} resonance $f = f_{20} = 2.405$ GHz

1985.

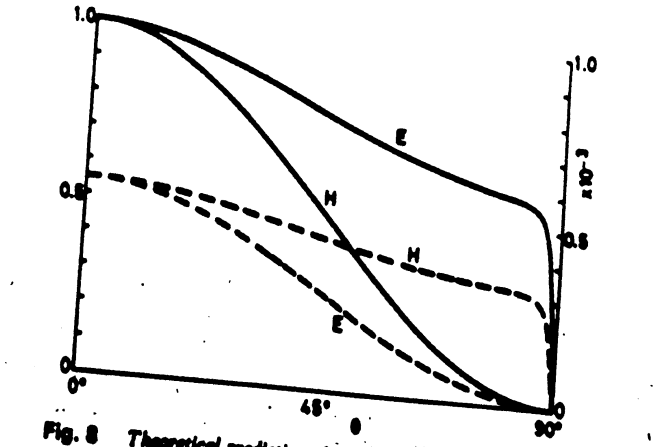

Fig. 8 Theoretical predictions for the radiation pattern of a rectangular microstrip antenna
E: E-plane ($\phi = 0°$)
H: H-plane ($\phi = 90°$)
——— copolar radiation (left vertical scale)
- - - - crosspolar radiation (right vertical scale)

John Mosig and Gardiol [43], 1985

patch size: 60×40mm

height: $h = d = 0.8$mm

$\varepsilon_r = 4.34$, $\tan\delta = 0.002$

patch conductivity $\sigma = \sigma_{Cu}/4$.

Radiation Pattern at first resonance.

From U-M report 389604-7-T by Jin & Volakis

PATCH ARRAYS

320

- This write-up is for a patch array on a dielectric slab simulating a bandpass Radome structure. To apply to the case of a microstrip patch array simply change the reflection coefficients R_{TE} and R_{TM} and set $T_{EE} = T_{TM} = 0$ (no transmission).

please see handwritten notes in text

Formulation for Patch Currents

In this chapter, Floquet's theorem is employed in conjuction with the Green's functions derived earlier to develop an equation for the electric currents generated on an infinite periodic patch array due to a plane wave excitation.

3.1 Geometry of an Infinite Array

The geometry of an infinite periodic patch array is shown in Figure 3.1, where a periodic array of conducting patches with periodicities T_x and T_y in the x and y directions, respectively, is residing on the surface of a dielectric slab. To be consistent with the notation used in the last chapter, the thickness of the slab is assumed to be d and the chosen coordinate system is shown in Figure 3.1.

The excitation field to be considered is a plane wave, but other excitation can be employed if expressed as a superposition of plane waves through the use of the Fourier integral. Further, although the formulation to be presented is in general valid for arbitrary polarizations, particular attention is concentrated in the case of transverse electric (TE) and transverse magnetic (TM) incidences. For the TE

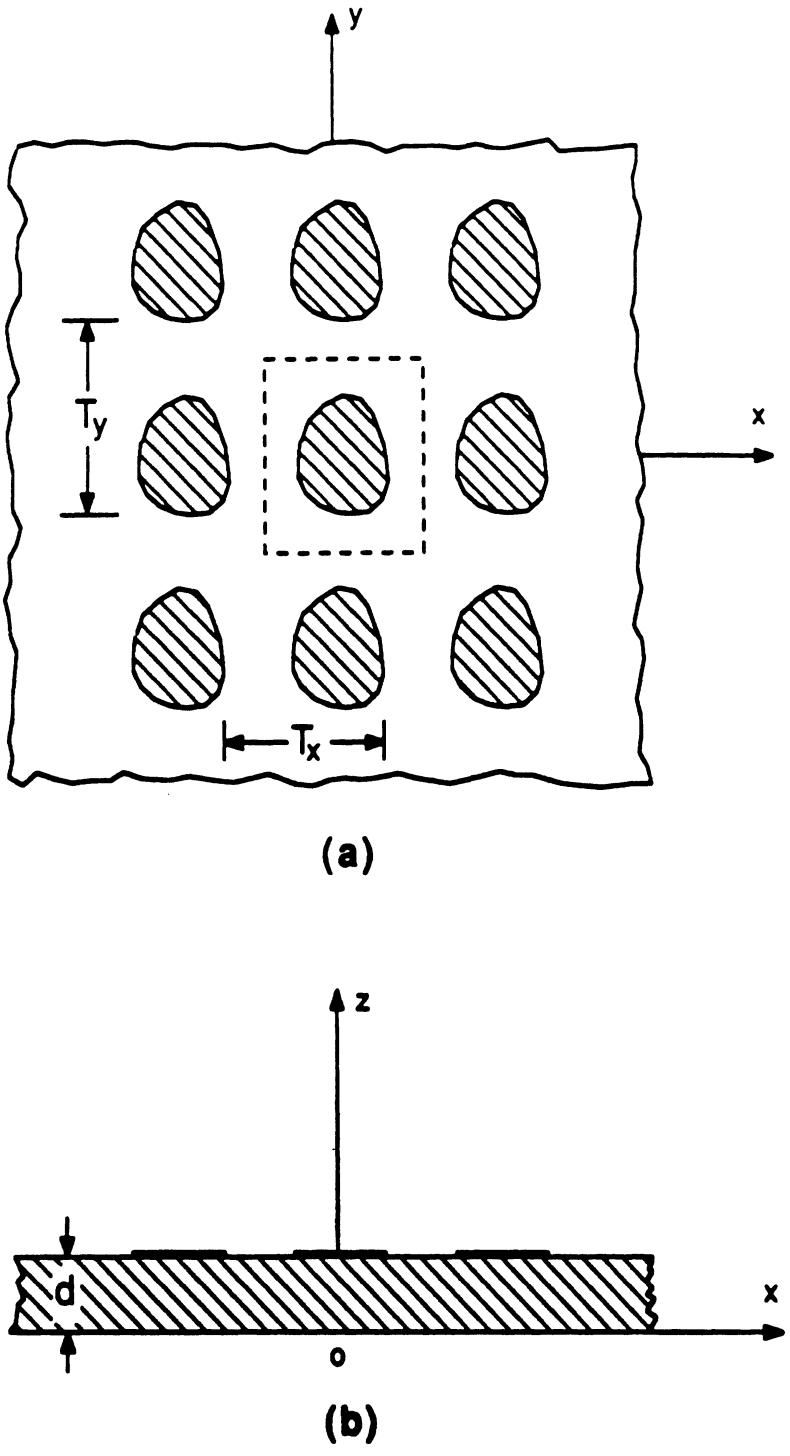

Figure 3.1: Geometry of a periodic patch array on a dielectric slab. (a) Top view. (b) Side view.

case, the incident electric field can be written as

$$\overline{E}^i(\bar{\rho}, z) = (-\hat{x}\sin\phi^i + \hat{y}\cos\phi^i)E_0 e^{j\bar{k}_T^i\cdot\bar{\rho}} e^{jk_0 z\cos\theta^i} \tag{3.1}$$

while for the TM case, it is given by

$$\overline{E}^i(\bar{\rho}, z) = (\hat{x}\cos\theta^i\cos\phi^i + \hat{y}\cos\theta^i\sin\phi^i - \hat{z}\sin\theta^i)E_0 e^{j\bar{k}_T^i\cdot\bar{\rho}} e^{jk_0 z\cos\theta^i} \tag{3.2}$$

where $\bar{\rho} = \hat{x}x + \hat{y}y$ and $\bar{k}_T^i = \hat{x}k_x^i + \hat{y}k_y^i$ in which $k_x^i = k_0\sin\theta^i\cos\phi^i$ and $k_y^i = k_0\sin\theta^i\sin\phi^i$. *

If the conducting patches are absent, a reflected and transmitted plane wave will result. Since these fields are required later in the formulation, we proceed to derive them for the TE and TM cases.

For the TE case, the reflected field can be expressed as

$$\overline{E}^r(\bar{\rho}, z) = (-\hat{x}\sin\phi^i + \hat{y}\cos\phi^i)E_0 R^{TE} e^{j2k_0 d\cos\theta^i} e^{j\bar{k}_T^i\cdot\bar{\rho}} e^{-jk_0 z\cos\theta^i} \tag{3.3}$$

in which R^{TE} is the corresponding reflection coefficient given by

$$R^{TE} = \frac{\cos\theta^i - j\sqrt{\epsilon_r - \sin^2\theta^i}C_0}{\cos\theta^i + j\sqrt{\epsilon_r - \sin^2\theta^i}C_0} \quad \text{for slab} \tag{3.4}$$

where

$$C_0 = \frac{j\sqrt{\epsilon_r - \sin^2\theta^i}\sin(k_0 d\sqrt{\epsilon_r - \sin^2\theta^i}) + \cos\theta^i\cos(k_0 d\sqrt{\epsilon_r - \sin^2\theta^i})}{j\sqrt{\epsilon_r - \sin^2\theta^i}\cos(k_0 d\sqrt{\epsilon_r - \sin^2\theta^i}) - \cos\theta^i\sin(k_0 d\sqrt{\epsilon_r - \sin^2\theta^i})}.$$

for slab

The transmitted field is found as

$C_0 = -\cot\left(k_0 d\sqrt{\varepsilon_r - \sin^2\theta^i}\right)$ for Substrate of thickness d

$$\overline{E}^t(\bar{\rho}, z) = (-\hat{x}\sin\phi^i + \hat{y}\cos\phi^i)E_0 T^{TE} e^{jk_0 d\cos\theta^i} e^{j\bar{k}_T^i\cdot\bar{\rho}} e^{jk_0 z\cos\theta^i} \tag{3.5}$$

* In the case of antenna arrays
$k_x^i = k_0\sin\theta_s\cos\phi_s$ $k_y^i = k_0\sin\theta_s\sin\phi_s$

in which T^{TE} is the corresponding transmission coefficient given by

$$T^{TE} = \frac{j\sqrt{\epsilon_r - \sin^2\theta^i}(1 + R^{TE})}{j\sqrt{\epsilon_r - \sin^2\theta^i}\cos(k_0 d\sqrt{\epsilon_r - \sin^2\theta^i}) - \cos\theta^i \sin(k_0 d\sqrt{\epsilon_r - \sin^2\theta^i})}. \quad (3.6)$$

Similarly, for the TM case the reflected field is

$$\overline{E}^r(\bar{\rho}, z) = -(\hat{x}\cos\theta^i\cos\phi^i + \hat{y}\cos\theta^i\sin\phi^i + \hat{z}\sin\theta^i)$$
$$\cdot E_0 R^{TM} e^{j2k_0 d\cos\theta^i} e^{j\bar{k}_T^i\cdot\bar{\rho}} e^{-jk_0 z\cos\theta^i} \quad (3.7)$$

where again R^{TM} is the reflection coefficient given by

$$R^{TM} = \frac{\epsilon_r\cos\theta^i - j\sqrt{\epsilon_r - \sin^2\theta^i}C_1}{\epsilon_r\cos\theta^i + j\sqrt{\epsilon_r - \sin^2\theta^i}C_1} \quad (3.8)$$

with

$$C_1 = \frac{j\sqrt{\epsilon_r - \sin^2\theta^i}\sin(k_0 d\sqrt{\epsilon_r - \sin^2\theta^i}) + \epsilon_r\cos\theta^i\cos(k_0 d\sqrt{\epsilon_r - \sin^2\theta^i})}{j\sqrt{\epsilon_r - \sin^2\theta^i}\cos(k_0 d\sqrt{\epsilon_r - \sin^2\theta^i}) - \epsilon_r\cos\theta^i\sin(k_0 d\sqrt{\epsilon_r - \sin^2\theta^i})}.$$

The transmitted field is found as

$$\overline{E}^t(\bar{\rho}, z) = (\hat{x}\cos\theta^i\cos\phi^i + \hat{y}\cos\theta^i\sin\phi^i - \hat{z}\sin\theta^i)$$
$$\cdot E_0 T^{TM} e^{jk_0 d\cos\theta^i} e^{j\bar{k}_T^i\cdot\bar{\rho}} e^{jk_0 z\cos\theta^i} \quad (3.9)$$

in which T^{TM} is the corresponding transmission coefficient given by

$$T^{TM} = \frac{j\sqrt{\epsilon_r - \sin^2\theta^i}(1 + R^{TM})}{j\sqrt{\epsilon_r - \sin^2\theta^i}\cos(k_0 d\sqrt{\epsilon_r - \sin^2\theta^i}) - \epsilon_r\cos\theta^i\sin(k_0 d\sqrt{\epsilon_r - \sin^2\theta^i})} \quad (3.10)$$

3.2 Floquet's Theorem

In accordance with Floquet's theorem, the electric current supported by the array residing on the plane $z = d$ may be deduced by that on a single patch.

Namely, the array current distribution can be written as

$$\overline{J}_s(x,y) = \bar{j}(x,y)e^{j(k_x'x+k_y'y)} \tag{3.11}$$

where $\bar{j}(x,y)$ is a two-dimensional periodic function. It can, therefore, be expanded in a Fourier series

$$\bar{j}(x,y) = \sum_{p=-\infty}^{\infty}\sum_{q=-\infty}^{\infty} \hat{\bar{j}}_{pq}\psi_{pq}(x,y) \tag{3.12}$$

where

$$\hat{\bar{j}}_{pq} = \frac{1}{T_xT_y}\int\int_{S_p} \bar{j}(x',y')\psi_{pq}^*(x',y')dx'dy' \tag{3.13}$$

$$\psi_{pq}(x,y) = e^{j(k_{xp}x+k_{yq}y)} \tag{3.14}$$

in which S_p denotes the area of a single patch, $k_{xp} = 2\pi p/T_x$, $k_{yq} = 2\pi q/T_y$, and p and q are integers representing the Floquet modes.

3.3 Scattered Field

From Section 2.5, the transverse part of the scattered field for $z > d$ as produced by the current $\overline{J}_s$ is

$$\overline{E}_T^s(x,y,z) = \int_{-\infty}^{\infty}\int_{-\infty}^{\infty} \overline{\overline{G}}\cdot\overline{J}_s(x',y')dx'dy' \tag{3.15}$$

and by employing (2.53) in conjuction with (3.11), it becomes

$$\begin{aligned}\overline{E}_T^s(x,y,z) &= \frac{1}{4\pi^2}\int_{-\infty}^{\infty}\int_{-\infty}^{\infty}\left[\int_{-\infty}^{\infty}\int_{-\infty}^{\infty}\tilde{\overline{\overline{G}}}e^{-jk_z(z-d)}e^{jk_x(x-x')}e^{jk_y(y-y')}dk_xdk_y\right] \\ &\quad\cdot\sum_{p=-\infty}^{\infty}\sum_{q=-\infty}^{\infty}\hat{\bar{j}}_{pq}e^{j(k_{xp}'x+k_{yq}'y)}dx'dy'\end{aligned} \tag{3.16}$$

where $k'_{xp} = k_{xp} + k^i_x$ and $k'_{yq} = k_{yq} + k^i_y$. Interchanging the order of integration, we now obtain

$$\begin{aligned}\overline{E}^s_T(x,y,z) &= \frac{1}{4\pi^2}\int_{-\infty}^{\infty}\int_{-\infty}^{\infty}\int_{-\infty}^{\infty}\int_{-\infty}^{\infty}\tilde{\overline{\overline{G}}}\cdot\sum_{p=-\infty}^{\infty}\sum_{q=-\infty}^{\infty}\hat{\overline{j}}_{pq}e^{-jk_2(z-d)} \\ &\quad \cdot e^{jk_x x}e^{jk_y y}e^{j(k'_{xp}-k_x)x'}e^{j(k'_{yq}-k_y)y'}dx'dy'dk_x dk_y \qquad (3.17)\\ &= \int_{-\infty}^{\infty}\int_{-\infty}^{\infty}\tilde{\overline{\overline{G}}}\cdot\sum_{p=-\infty}^{\infty}\sum_{q=-\infty}^{\infty}\hat{\overline{j}}_{pq}e^{-jk_2(z-d)}e^{jk_x x}e^{jk_y y} \\ &\quad \cdot\delta(k'_{xp}-k_x)\delta(k'_{yq}-k_y)dk_x dk_y. \qquad (3.18)\end{aligned}$$

Further, by interchanging the orders of summation and integration we obtain

$$\overline{E}^s_T(x,y,z) = \sum_{p=-\infty}^{\infty}\sum_{q=-\infty}^{\infty}\tilde{\overline{\overline{G}}}(k'_{xp},k'_{yq})\cdot\hat{\overline{j}}_{pq}e^{j[k'_{xp}x+k'_{yq}y-k'_{2pq}(z-d)]} \qquad (3.19)$$

upon evaluation of the integrals, where $\tilde{\overline{\overline{G}}}(k'_{xp},k'_{yq})$ is obtained by replacing k_x and k_y with k'_{xp} and k'_{yq}, respectively, in (2.45)-(2.46) and (2.51)-(2.52).

3.4 Equation for Patch Currents

The equation for the electric currents can be obtained by applying the boundary condition on the patch. This demands a vanishing tangential electric field on the patch, that is

Not present in antenna Mode operation

$$\overline{E}^i_T + \overline{E}^r_T + \overline{E}^s_T = 0 \quad \text{on the patch.} \qquad (3.20)$$

Upon substitution of (3.19) into (3.20) we then obtain

$$\sum_{p=-\infty}^{\infty}\sum_{q=-\infty}^{\infty}\tilde{\overline{\overline{G}}}(k'_{xp},k'_{yq})\cdot\hat{\overline{j}}_{pq}e^{j(k'_{xp}x+k'_{yq}y)} = -\overline{E}^i_T(x,y,d) - \overline{E}^r_T(x,y,d) \qquad (3.21)$$

Not present in antenna Mode operation

for $0 \leq \theta^i < \pi/2$. [In the case when $\pi/2 < \theta^i \leq \pi$, $\overline{E}_T^i + \overline{E}_T^r$ in (3.21) should be replaced by the transverse component of the transmitted field.] — only for antenna mode operation

We note that an alternative expression for (3.21) is

$$\sum_{p=-\infty}^{\infty} \sum_{q=-\infty}^{\infty} \overline{\overline{\tilde{G}}}(k'_{xp}, k'_{yq}) \cdot \hat{\tilde{j}}_{pq} \psi_{pq}(x,y) = \overline{B} \tag{3.22}$$

where $\overline{B}$ is given by

Not present in antenna mode operation.

$$\overline{B} = -\left[\overline{E}_T^i(x,y,d) + \overline{E}_T^r(x,y,d)\right] e^{-j(k_x^i x + k_y^i y)} \tag{3.23}$$

and can be shown to be invariant to (x,y). Specifically, for the TE case

$$\overline{B} = (-\hat{x}\sin\phi^i + \hat{y}\cos\phi^i) E_0 (1 + R^{TE}) e^{jk_0 d\cos\theta^i} \tag{3.24}$$

and for the TM case

$$\overline{B} = (\hat{x}\cos\theta^i\cos\phi^i + \hat{y}\cos\theta^i\sin\phi^i) E_0 (1 - R^{TM}) e^{jk_0 d\cos\theta^i}. \tag{3.25}$$

Solving (3.22), one obtains the current distribution on the patches.

Chapter 4

Numerical Implementation

In this chapter, we describe a numerical procedure for solving (3.22). The procedure employs the Conjugate Gradient-Fast Fourier Transform (CG-FFT) technique which appears to be the natural and best choice for the solution.

4.1 Discretization of Geometry

The first step of the CG-FFT solution is to discretize the geometry. For this, we first divide the region of one period into small rectangular cells of dimension $\Delta x \times \Delta y$. The surface of the patch is then generated based on the premise that any planar area may be approximated by a collection of the rectangular cells. Figure 4.1 shows three examples of such a discretization as applied to square, circular and triangular patches.

4.2 Discretization of Currents

Roof-top functions are used below to expand the patch currents. These allow a better representation of the currents and can provide a faster converging series

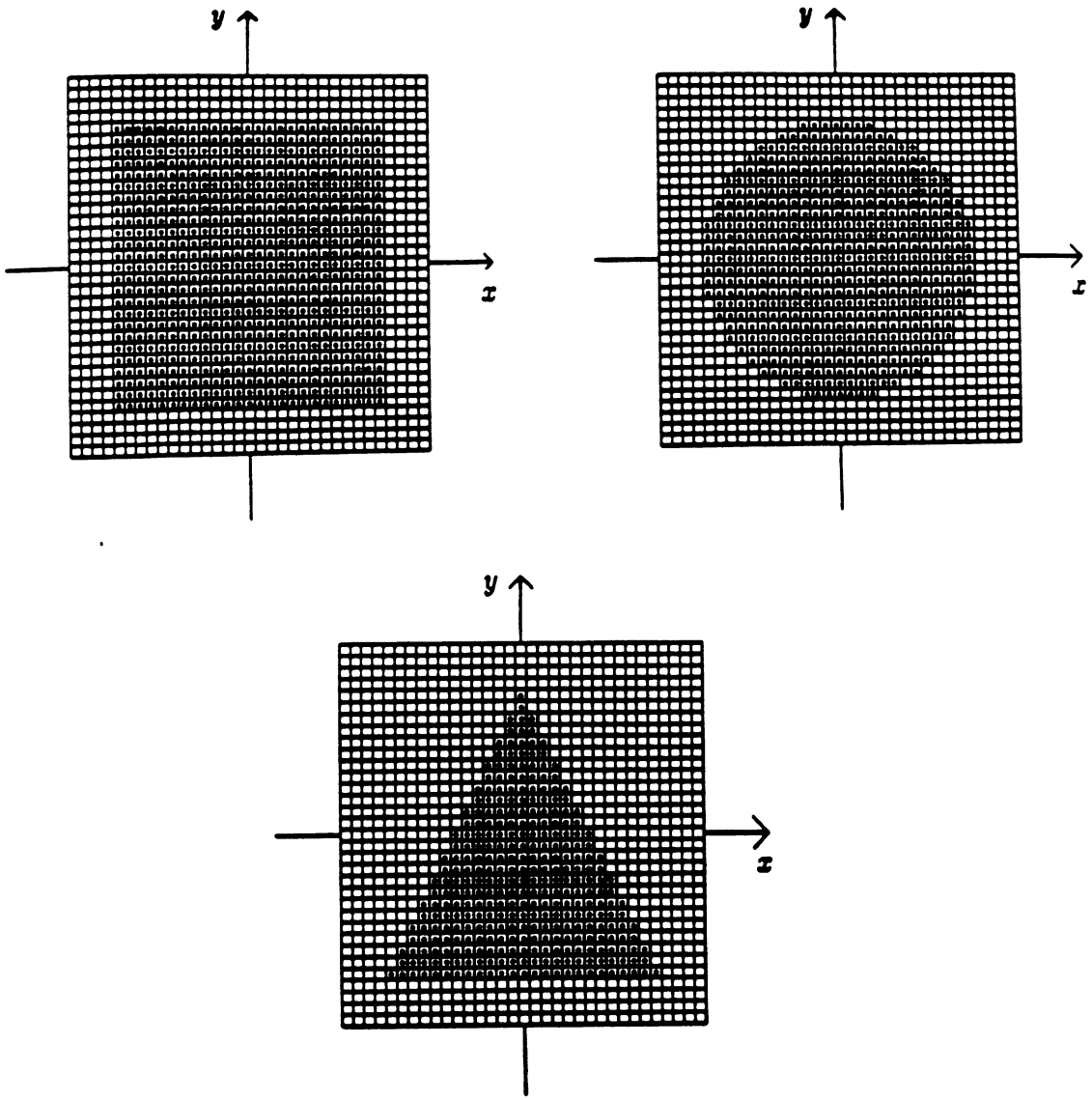

Figure 4.1: Discretization of a square, circular, and triangular patch.

than pulse basis. The current distribution can then be written as

$$j_x(x,y) = \sum_{m=-M/2}^{M/2-1} \sum_{n=-N/2}^{N/2-1} j_{xmn} \Lambda_{m+1/2}(x) \Pi_n(y) \tag{4.1}$$

$$j_y(x,y) = \sum_{m=-M/2}^{M/2-1} \sum_{n=-N/2}^{N/2-1} j_{ymn} \Pi_m(x) \Lambda_{n+1/2}(y) \tag{4.2}$$

where

$$\Lambda_m(x) = \begin{cases} 1 - |x - m\Delta x|/\Delta x, & |x - m\Delta x| < \Delta x \\ 0, & |x - m\Delta x| > \Delta x \end{cases} \tag{4.3}$$

$$\Pi_m(x) = \begin{cases} 1, & |x - m\Delta x| < \Delta x/2 \\ 0, & |x - m\Delta x| > \Delta x/2 \end{cases} \tag{4.4}$$

M and N denote the number of cells along the x and y directions, respectively, and $\bar{j}_{mn} = \hat{x} j_{xmn} + \hat{y} j_{ymn}$ are the unknown constant coefficients of the expansion.

Substituting now (4.1)-(4.2) into (3.13) leads to

$$\begin{aligned} \hat{j}_{xpq} &= \frac{1}{T_x T_y} \sum_{m=-M/2}^{M/2-1} \sum_{n=-N/2}^{N/2-1} j_{xmn} \\ &\quad \cdot \int \Lambda_{m+1/2}(x) e^{-jk_{xp}x} dx \int \Pi_n(y) e^{-jk_{yq}y} dy \qquad (4.5) \\ &= \frac{1}{MN} \mathrm{sinc}^2\left(\frac{p\pi}{M}\right) \mathrm{sinc}\left(\frac{q\pi}{N}\right) e^{-jp\pi/M} \\ &\quad \cdot \sum_{m=-M/2}^{M/2-1} \sum_{n=-N/2}^{N/2-1} j_{xmn} e^{-j(2\pi pm/M + 2\pi qn/N)} \qquad (4.6) \end{aligned}$$

where we note that $\Delta x/T_x = 1/M$ and $\Delta y/T_y = 1/N$. Similarly,

$$\begin{aligned} \hat{j}_{ypq} &= \frac{1}{MN} \mathrm{sinc}\left(\frac{p\pi}{M}\right) \mathrm{sinc}^2\left(\frac{q\pi}{N}\right) e^{-jq\pi/N} \\ &\quad \cdot \sum_{m=-M/2}^{M/2-1} \sum_{n=-N/2}^{N/2-1} j_{ymn} e^{-j(2\pi pm/M + 2\pi qn/N)}. \qquad (4.7) \end{aligned}$$

The left hand side of (3.22) then becomes

$$\begin{aligned}
&\sum_{p=-\infty}^{\infty}\sum_{q=-\infty}^{\infty}\bar{\bar{\tilde{G}}}(k'_{xp},k'_{yq})\cdot\bar{\hat{j}}_{pq}\psi_{pq}(x,y)\\
&\quad=\frac{1}{MN}\sum_{p=-\infty}^{\infty}\sum_{q=-\infty}^{\infty}\operatorname{sinc}\left(\frac{p\pi}{M}\right)\operatorname{sinc}\left(\frac{q\pi}{N}\right)\\
&\qquad\cdot\left\{\left[\hat{x}\hat{x}\tilde{G}_{xx}(k'_{xp},k'_{yq})+\hat{y}\hat{x}\tilde{G}_{yx}(k'_{xp},k'_{yq})\right]\operatorname{sinc}\left(\frac{p\pi}{M}\right)e^{-jp\pi/M}\right.\\
&\qquad\left.+\left[\hat{x}\hat{y}\tilde{G}_{xy}(k'_{xp},k'_{yq})+\hat{y}\hat{y}\tilde{G}_{yy}(k'_{xp},k'_{yq})\right]\operatorname{sinc}\left(\frac{q\pi}{N}\right)e^{-jq\pi/N}\right\}\\
&\qquad\cdot\left[\sum_{m=-M/2}^{M/2-1}\sum_{n=-N/2}^{N/2-1}\bar{j}_{mn}e^{-j(2\pi pm/M+2\pi qn/N)}\right]e^{j(k_{xp}x+k_{yq}y)}. \qquad (4.8)
\end{aligned}$$

4.3 Application of Galerkin's Technique

From (3.22) the equations for determining the constants are

$$\begin{aligned}
&\frac{1}{MN}\sum_{p=-\infty}^{\infty}\sum_{q=-\infty}^{\infty}\left[\hat{x}\hat{x}\tilde{G}_{xx}(k'_{xp},k'_{yq})\operatorname{sinc}^2\left(\frac{p\pi}{M}\right)\operatorname{sinc}\left(\frac{q\pi}{N}\right)e^{-jp\pi/M}\right.\\
&\left.+\hat{x}\hat{y}\tilde{G}_{xy}(k'_{xp},k'_{yq})\operatorname{sinc}\left(\frac{p\pi}{M}\right)\operatorname{sinc}^2\left(\frac{q\pi}{N}\right)e^{-jq\pi/N}\right]\\
&\cdot\left[\sum_{m=-M/2}^{M/2-1}\sum_{n=-N/2}^{N/2-1}\bar{j}_{mn}e^{-j(2\pi pm/M+2\pi qn/N)}\right]e^{j(k_{xp}x+k_{yq}y)}\\
&=B_x \qquad (4.9)
\end{aligned}$$

for x component and

$$\begin{aligned}
&\frac{1}{MN}\sum_{p=-\infty}^{\infty}\sum_{q=-\infty}^{\infty}\left[\hat{y}\hat{x}\tilde{G}_{yx}(k'_{xp},k'_{yq})\operatorname{sinc}^2\left(\frac{p\pi}{M}\right)\operatorname{sinc}\left(\frac{q\pi}{N}\right)e^{-jp\pi/M}\right.\\
&\left.+\hat{y}\hat{y}\tilde{G}_{yy}(k'_{xp},k'_{yq})\operatorname{sinc}\left(\frac{p\pi}{M}\right)\operatorname{sinc}^2\left(\frac{q\pi}{N}\right)e^{-jq\pi/N}\right]\\
&\left[\sum_{m=-M/2}^{M/2-1}\sum_{n=-N/2}^{N/2-1}\bar{j}_{mn}e^{-j(2\pi pm/M+2\pi qn/N)}\right]e^{j(k_{xp}x+k_{yq}y)}\\
&B_y \qquad (4.10)
\end{aligned}$$

for y component. To solve for $\bar{j}_{mn}$, (4.9)-(4.10) must now be converted to a system of equations by employing Galerkin's technique. Accordingly, the weighting functions are chosen the same as the current density expansion functions. In so doing, we multiply (4.9) by $\Lambda_{s+1/2}(x)\Pi_t(y)$ and (4.10) by $\Pi_s(x)\Lambda_{t+1/2}(y)$ ($s = -M/2, ..., M/2-1$; $t = -N/2, ..., N/2-1$) and by integrating over the patch, we obtain

$$\begin{aligned}
&\frac{1}{MN}\sum_{p=-\infty}^{\infty}\sum_{q=-\infty}^{\infty}\left[\hat{x}\hat{x}\tilde{G}_{xx}(k'_{xp},k'_{yq})\mathrm{sinc}^4\left(\frac{p\pi}{M}\right)\mathrm{sinc}^2\left(\frac{q\pi}{N}\right)\right.\\
&\left.+\hat{x}\hat{y}\tilde{G}_{xy}(k'_{xp},k'_{yq})\mathrm{sinc}^3\left(\frac{p\pi}{M}\right)\mathrm{sinc}^3\left(\frac{q\pi}{N}\right)e^{j(p\pi/M-q\pi/N)}\right]\\
&\cdot\left[\sum_{m=-M/2}^{M/2-1}\sum_{n=-N/2}^{N/2-1}\bar{j}_{mn}e^{-j(2\pi pm/M+2\pi qn/N)}\right]e^{j(2\pi ps/M+2\pi qt/N)}\\
&=B_x
\end{aligned}\tag{4.11}$$

and

$$\begin{aligned}
&\frac{1}{MN}\sum_{p=-\infty}^{\infty}\sum_{q=-\infty}^{\infty}\left[\hat{y}\hat{x}\tilde{G}_{yx}(k'_{xp},k'_{yq})\mathrm{sinc}^3\left(\frac{p\pi}{M}\right)\mathrm{sinc}^3\left(\frac{q\pi}{N}\right)\right.\\
&\left.\cdot e^{-j(p\pi/M-q\pi/N)}+\hat{y}\hat{y}\tilde{G}_{yy}(k'_{xp},k'_{yq})\mathrm{sinc}^2\left(\frac{p\pi}{M}\right)\mathrm{sinc}^4\left(\frac{q\pi}{N}\right)\right]\\
&\cdot\left[\sum_{m=-M/2}^{M/2-1}\sum_{n=-N/2}^{N/2-1}\bar{j}_{mn}e^{-j(2\pi pm/M+2\pi qn/N)}\right]e^{j(2\pi ps/M+2\pi qt/N)}\\
&=B_y.
\end{aligned}\tag{4.12}$$

Equations (4.11) and (4.12) now form a system of equations for the unknown coefficients $\bar{j}_{mn}$.

4.4 CG-FFT Technique

It can be shown that (4.11)-(4.12) can be written as

$$\frac{1}{MN}\sum_{p'=-M/2}^{M/2-1}\sum_{q'=-N/2}^{N/2-1}\tilde{\tilde{A}}(k'_{xp'},k'_{yq'})\cdot\left[\sum_{m=-M/2}^{M/2-1}\sum_{n=-N/2}^{N/2-1}\bar{j}_{mn}e^{-j(2\pi p'm/M+2\pi q'n/N)}\right]$$

$$\cdot e^{j(2\pi p's/M+2\pi q't/N)}=\overline{B} \tag{4.13}$$

where

$$\tilde{A}_{xx}(k'_{xp'},k'_{yq'})=\sum_{u=-\infty}^{\infty}\sum_{v=-\infty}^{\infty}\tilde{G}_{xx}(k'_{xp''},k'_{yq''})\text{sinc}^4\left(\frac{p''\pi}{M}\right)\text{sinc}^2\left(\frac{q''\pi}{N}\right) \tag{4.14}$$

$$\tilde{A}_{xy}(k'_{xp'},k'_{yq'})=\sum_{u=-\infty}^{\infty}\sum_{v=-\infty}^{\infty}\tilde{G}_{xy}(k'_{xp''},k'_{yq''})\text{sinc}^3\left(\frac{p''\pi}{M}\right)\text{sinc}^3\left(\frac{q''\pi}{N}\right)\cdot e^{j(p''\pi/M-q''\pi/N)} \tag{4.15}$$

$$\tilde{A}_{yx}(k'_{xp'},k'_{yq'})=\sum_{u=-\infty}^{\infty}\sum_{v=-\infty}^{\infty}\tilde{G}_{yx}(k'_{xp''},k'_{yq''})\text{sinc}^3\left(\frac{p''\pi}{M}\right)\text{sinc}^3\left(\frac{q''\pi}{N}\right)\cdot e^{-j(p''\pi/M-q''\pi/N)} \tag{4.16}$$

$$\tilde{A}_{yy}(k'_{xp'},k'_{yq'})=\sum_{u=-\infty}^{\infty}\sum_{v=-\infty}^{\infty}\tilde{G}_{yy}(k'_{xp''},k'_{yq''})\text{sinc}^2\left(\frac{p''\pi}{M}\right)\text{sinc}^4\left(\frac{q''\pi}{N}\right) \tag{4.17}$$

with $p''=p'+uM$, $q''=q'+vN$. Here, we note that for large (u,v) the terms of the summations in (4.14)-(4.17) are of the order

$$\frac{1}{(uv)^2(u^2+v^2)^{1/2}} \tag{4.18}$$

resulting in a rapid series convergence.

In accordance with the definition of the discrete Fourier transform and its inverse [9], (4.13) can be symbolically written as

$$\text{FFT}^{-1}\left\{\tilde{\tilde{A}}(k'_{xp'},k'_{yq'})\cdot[\text{FFT}\,\{\bar{j}_{mn}\}]\right\}=\overline{B} \tag{4.19}$$

and it is then clear that (4.19) is suited for a conjugate gradient iterative solution eliminating a need for an explicit generation of a square impedance matrix.

The CG-FFT algorithm for solving (4.19) is described as follows:

Initialize the residual and search vectors:

$$\overline{R}_1 = \overline{B} - \mathrm{FFT}^{-1}\left\{\tilde{\tilde{\tilde{A}}}(k'_{xp'}, k'_{yq'}) \cdot \left[\mathrm{FFT}\left\{\bar{J}^{(1)}_{mn}\right\}\right]\right\} \tag{4.20}$$

$$\overline{X}_1 = \mathrm{FFT}^{-1}\left\{\left[\tilde{\tilde{\tilde{A}}}^{*}(k'_{xp'}, k'_{yq'})\right]^{T} \cdot \left[\mathrm{FFT}\left\{\overline{R}_1\right\}\right]\right\} \tag{4.21}$$

$$\beta_0 = \frac{1}{\langle \overline{X}_1, \overline{X}_1 \rangle} \tag{4.22}$$

$$\overline{P}_1 = \beta_0 \overline{X}_1. \tag{4.23}$$

Iterate for $k = 1, 2, ..., NM$:

$$\overline{Y}_k = \mathrm{FFT}^{-1}\left\{\tilde{\tilde{\tilde{A}}}(k'_{xp'}, k'_{yq'}) \cdot \left[\mathrm{FFT}\left\{\overline{P}_k\right\}\right]\right\} \tag{4.24}$$

$$\alpha_k = \frac{1}{\langle \overline{Y}_k, \overline{Y}_k \rangle} \tag{4.25}$$

$$\bar{J}^{(k+1)}_{mn} = \bar{J}^{(k)}_{mn} + \alpha_k \overline{P}_k \tag{4.26}$$

$$\overline{R}_{k+1} = \overline{R}_k - \alpha_k \overline{Y}_k \tag{4.27}$$

$$\overline{X}_{k+1} = \mathrm{FFT}^{-1}\left\{\left[\tilde{\tilde{\tilde{A}}}^{*}(k'_{xp'}, ' k_{yq'})\right]^{T} \cdot \left[\mathrm{FFT}\left\{\overline{R}_{k+1}\right\}\right]\right\} \tag{4.28}$$

$$\beta_k = \frac{1}{\langle \overline{X}_{k+1}, \overline{X}_{k+1} \rangle} \tag{4.29}$$

$$\overline{P}_{k+1} = \overline{P}_k + \beta_k \overline{X}_{k+1}. \tag{4.30}$$

Terminate at $k = MN$ or when

$$\frac{||\overline{R}_{k+1}||_2}{||\overline{B}||_2} < \text{tolerance}. \tag{4.31}$$

Note that the quantity $\left[\tilde{\tilde{\tilde{A}}}^{*}(k'_{xp'}, k'_{yq'})\right]^{T}$ is the adjoint expression for $\tilde{\tilde{\tilde{A}}}(k'_{xp'}, k'_{yq'})$.

Chapter 5

Reflection, Transmission and Diffraction of a Periodic Array

The usual parameters characterizing an infinite periodic patch array are the reflection and transmission coefficients. In high frequency applications, high order Bragg diffractions could also be of interest. In this chapter, we describe the procedure for computing these reflected, transmitted and diffracted fields and present some numerical results.

5.1 Reflection and Transmission Coefficients

Once the currents $\bar{j}_{mn}$ are found from a solution of (4.19), the reflection and transmission coefficients can be evaluated in a straightforward manner. To show this, we refer to (3.19) which is repeated below

$$\bar{E}_T^s(x,y,z) = \sum_{p=-\infty}^{\infty} \sum_{q=-\infty}^{\infty} \bar{\bar{G}}(k'_{xp}, k'_{yq}) \cdot \hat{j}_{pq} e^{j[k'_{xp}x + k'_{yq}y - k'_{zpq}(z-d)]}. \tag{5.1}$$

It is seen that only the Floquet mode corresponding to $(p,q) = (0,0)$ contributes the scattered field in the direction of reflection. Thus, the transverse component

of this scattered field is

$$\overline{E}_T^s(x,y,z) = \overline{\overline{G}}(k_x^i, k_y^i) \cdot \hat{\bar{j}}_{00} e^{j[k_x^i x + k_y^i y - k_z^i (z-d)]} \tag{5.2}$$

where

$$\hat{\bar{j}}_{00} = \frac{1}{MN} \sum_{m,n} \bar{j}_{mn}. \tag{5.3}$$

The same Floquet mode $(0,0)$ contributes the scattered field in the direction of transmission and this can again be found in a similar way by employing the dyadic Green's function applicable in the region $z \leq 0$. The transverse component of this scattered field is found as

$$\overline{E}_T^s(x,y,z) = \overline{\overline{G}}'(k_x^i, k_y^i) \cdot \hat{\bar{j}}_{00} e^{j(k_x^i x + k_y^i y + k_z^i z)} \tag{5.4}$$

where $\hat{\bar{j}}_{00}$ is again given by (5.3).

The total reflected and transmitted fields of the array are then obtained by adding the scattered fields to the reflected field, (3.3) or (3.7), and transmitted field, (3.5) or (3.9), associated with the dielectric slab in isolation.

5.2 Bragg Diffractions

Under certain circumstance, it is possible to obtain higher order Bragg diffractions than the zeroth order (reflection and transmission) considered above. Such diffractions occur when

$$k_{2pq}' > 0 \quad \text{or} \quad k_{xp}'^2 + k_{yq}'^2 < k_0^2 \tag{5.5}$$

which may be satisfied by certain nonzero (p, q). The direction (θ_{pq}, ϕ_{pq}) of a possible (p, q) diffraction is determined from the relations

$$\sin\theta_{pq}\cos\phi_{pq} = \sin\theta^i\cos\phi^i + \frac{p\lambda}{T_x} \tag{5.6}$$

$$\sin\theta_{pq}\sin\phi_{pq} = \sin\theta^i\sin\phi^i + \frac{q\lambda}{T_y} \tag{5.7}$$

in which λ is the free-space wavelength, and the magnitude of the corresponding diffracted field in the half space $z > d$ can be obtained from its transverse component given by

$$\overline{E}_T(p, q) = \tilde{\tilde{G}}(k'_{xp}, k'_{yq}) \cdot \hat{\hat{j}}_{pq}. \tag{5.8}$$

From (5.6)-(5.7) it is seen that the diffractions appear in pairs and are symmetric with respect to the x-y plane. The diffracted field in the half space $z < 0$ can be found in a similar way.

5.3 Numerical Results

In the following, we present some numerical results for the reflection by and transmission through an infinite periodic array associated with three types of element patch geometries illustrated in Figure 5.1.

Figure 5.2 shows the reflection and transmission coefficients of a square patch array on a dielectric slab having $d = 0$, 0.1 and 0.2 cm for normal incidence. For the free-standing ($d = 0$) case the result agrees with that obtained by Cwik and Mittra [8]. The general effect of the dielectric layer is seen to shift the resonant frequency of the array. Also, note that at frequencies greater than 15 GHz higher order Bragg

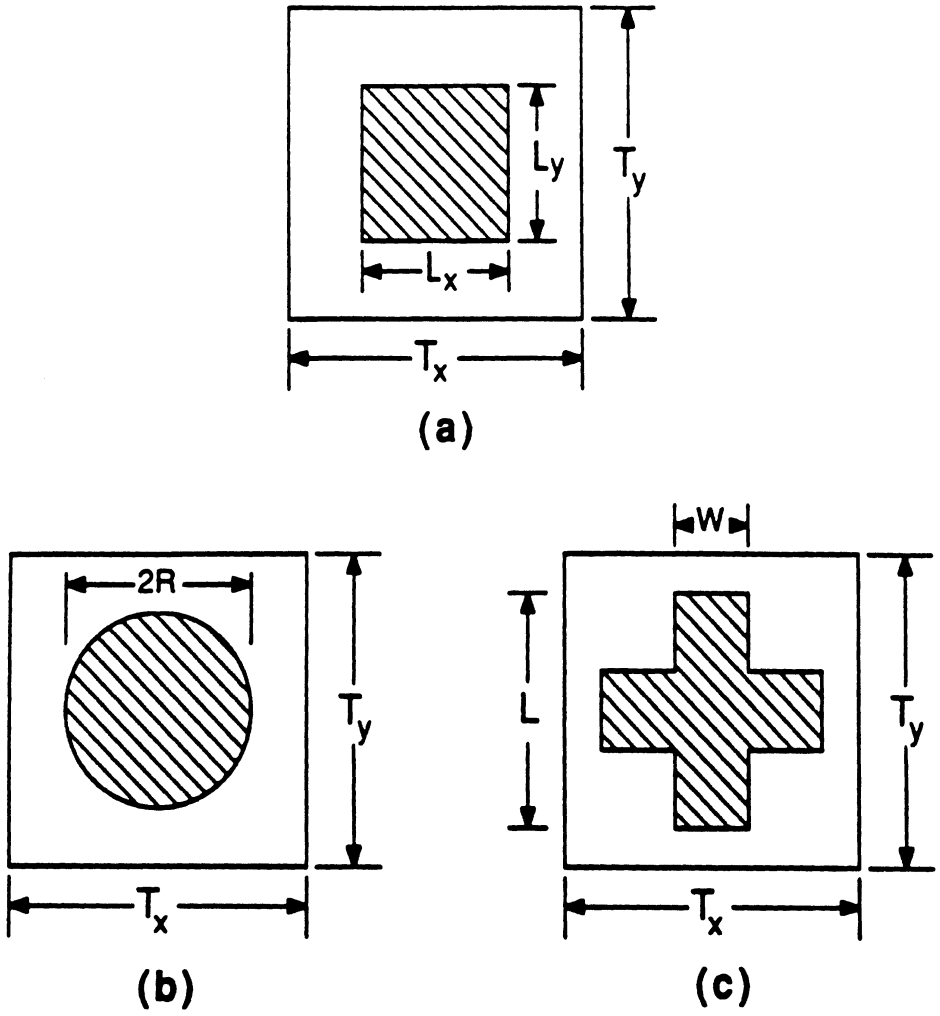

Figure 5.1: Three types of cell geometries. (a) A square patch cell. (b) A circular patch cell. (c) A cross-shaped patch cell.

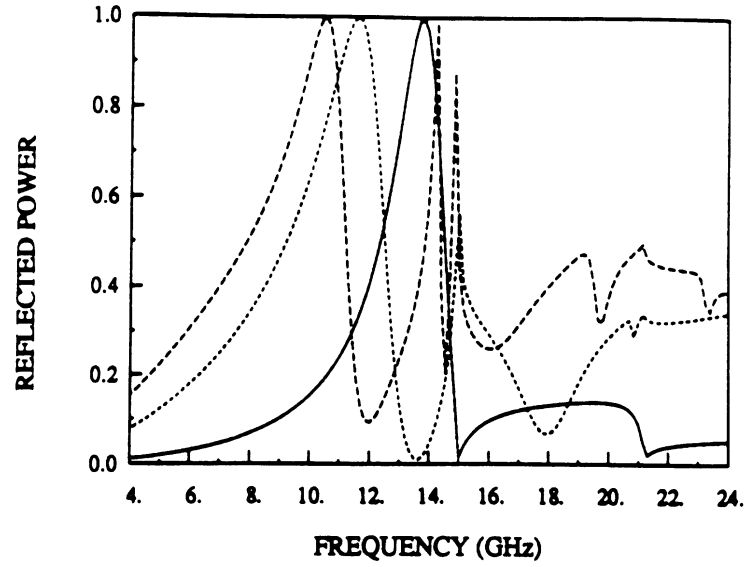

(a)

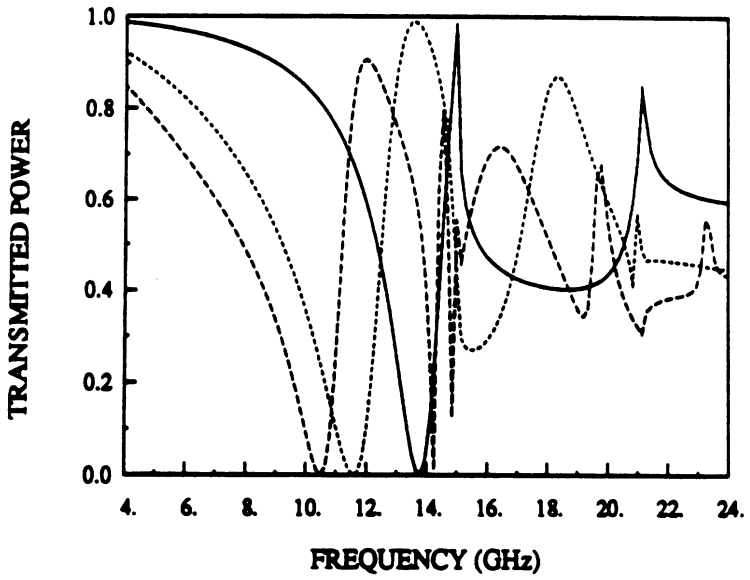

(b)

Figure 5.2: (a) Reflection and (b) transmission coefficients vs frequency for an array of square patches with various dielectric slab thicknesses; $T_x = T_y = 2.0$ cm, $L_x = L_y = 1.0$ cm, $\epsilon_r = 3.5$, $\theta^i = 0$, $\phi^i = 0$; (——) $d = 0.0$ cm; (- - - -) $d = 0.1$ cm; (- - -) $d = 0.2$ cm.

diffractions occur and as a result the reflection and transmission coefficients are no longer complementary.

Figures 5.3-5.4 show the reflection and transmission coefficients of the same patch array for three different angles of incidence. As the angle of incidence changes the frequency where the higher order Bragg diffraction occurs also changes.

Figure 5.5 shows the reflection and transmission coefficients of a circular patch array as a function of the angle of incidence. The circular patch is approximately modelled as a collection of square cells. It is seen that higher order Bragg diffractions occur when $\theta^i > 26°$.

The effect of loss in the dielectric slab is shown in Figure 5.6 where the reflected, transmitted and dissipated power are plotted versus frequency for a cross-shaped patch array. Results are shown for various lossy slabs and the dissipated power is computed in accordance with the relation

$$\begin{aligned} \text{Dissipated Power} &= \text{Incident Power} - \text{Reflected Power} \\ &\quad - \text{Transmitted Power} \end{aligned} \tag{5.9}$$

which is valid up to the frequency where the first order Bragg mode beyond the zeroth order appears.

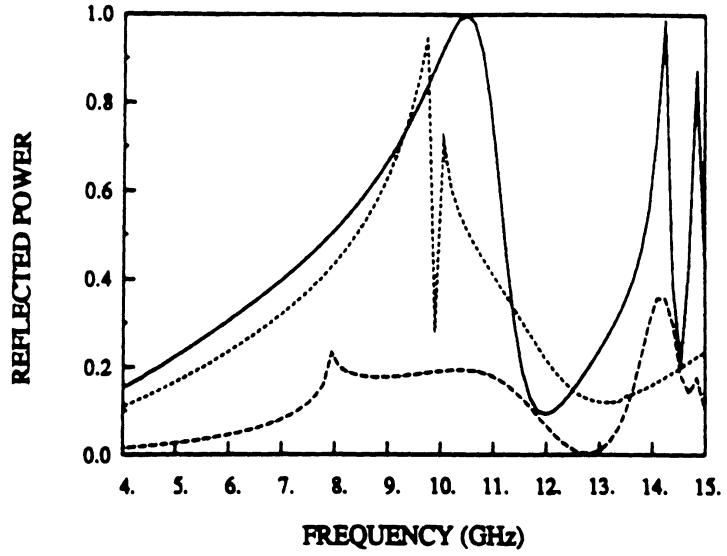

(a)

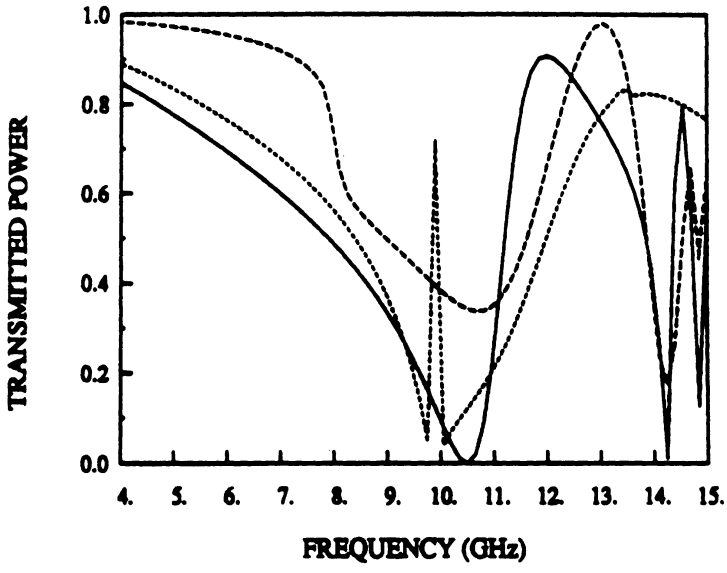

(b)

Figure 5.3: (a) Reflection and (b) transmission coefficients vs frequency for an array of square patches for three incident angles for TM incidence; $T_x = T_y = 2.0$ cm, $L_x = L_y = 1.0$ cm, $\epsilon_r = 3.5$, $d = 0.2$ cm, $\phi^i = 0$; (——) $\theta^i = 0$ degree; (- - - -) $\theta^i = 30$ degrees; (- - -) $\theta^i = 60$ degrees.32

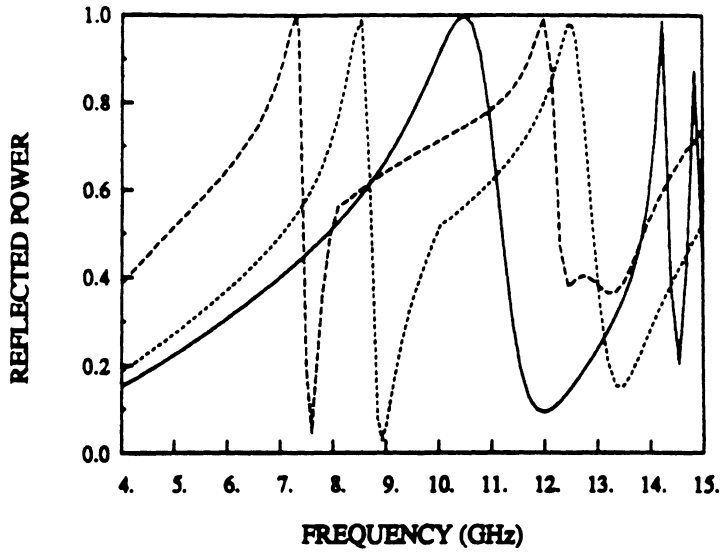

(a)

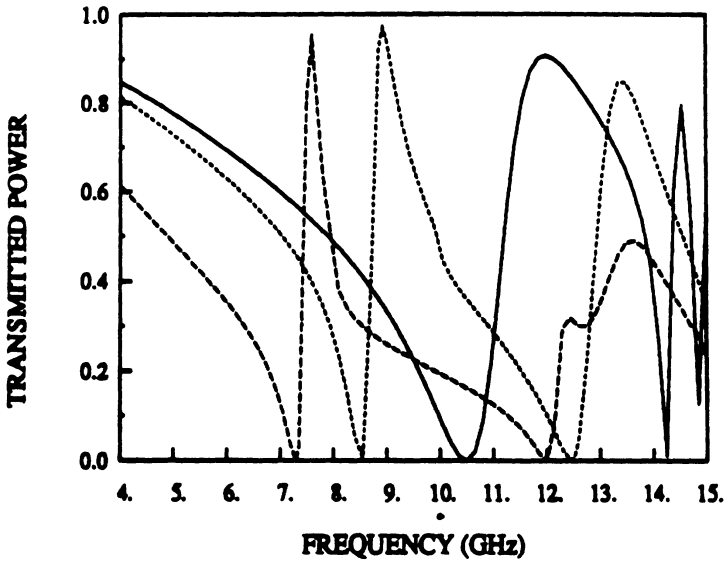

(b)

Figure 5.4: (a) Reflection and (b) transmission coefficients vs frequency for an array of square patches for three incident angles for TE incidence; $T_x = T_y = 2.0$ cm, $L_x = L_y = 1.0$ cm, $\epsilon_r = 3.5$, $d = 0.2$ cm, $\phi^i = 0$; (——) $\theta^i = 0$ degree; (- - - -) $\theta^i = 30$ degrees; (- - -) $\theta^i = 60$ degrees.33

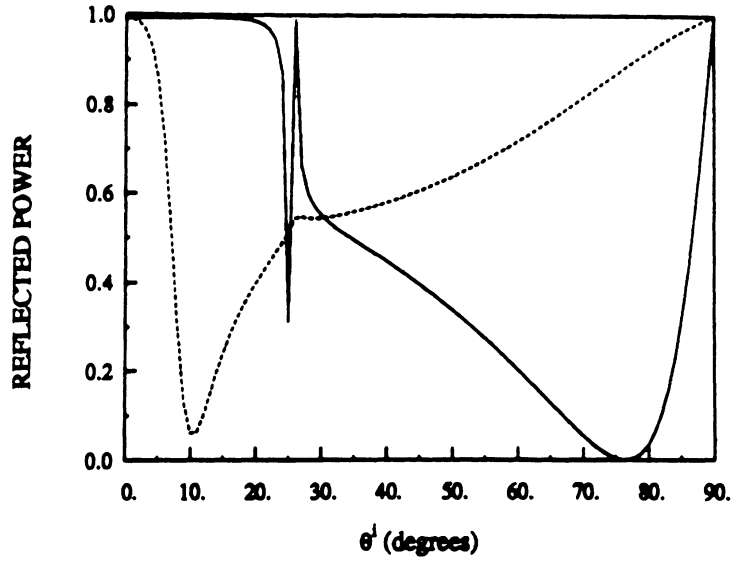

(a)

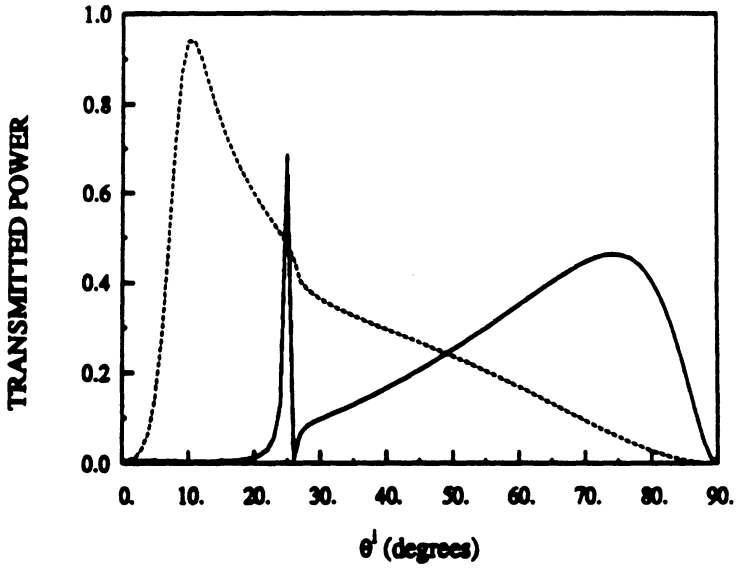

(b)

Figure 5.5: (a) Reflection and (b) transmission coefficients vs angle of incidence for an array of circular patches; $T_x = T_y = 2.0$ cm, $R = 0.625$ cm, $\epsilon_r = 3.5$, $d = 0.2$ cm, $\phi^i = 0$, $f = 10.4$ GHz; (——) TM incidence; (- - - -) TE incidence.

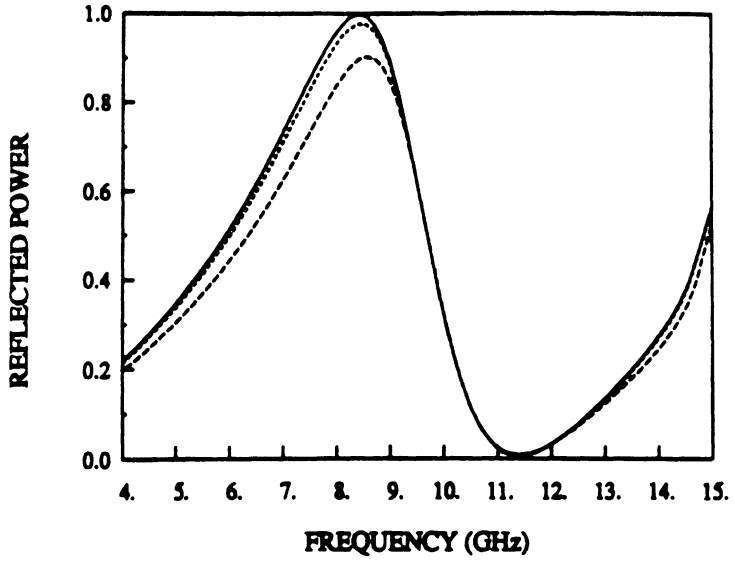
REFLECTED POWER
1.0
0.8
0.6
0.4
0.2
0.0
4. 5. 6. 7. 8. 9. 10. 11. 12. 13. 14. 15.
FREQUENCY (GHz)

(a)

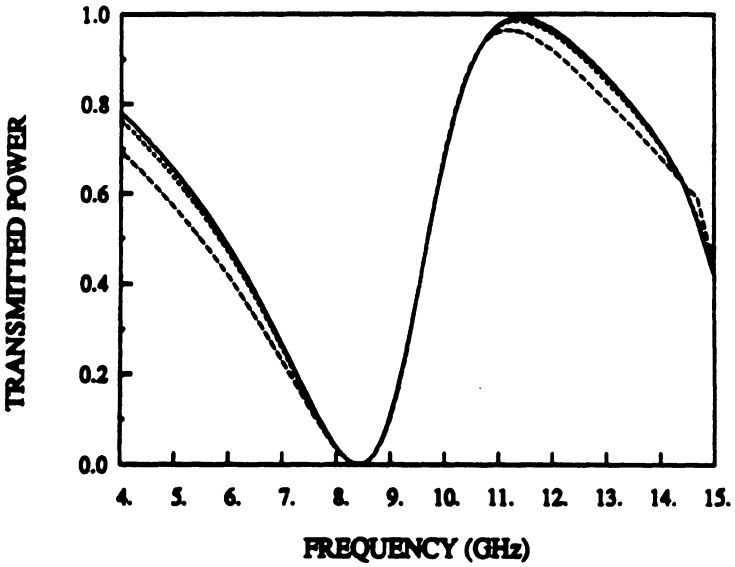
TRANSMITTED POWER
1.0
0.8
0.6
0.4
0.2
0.0
4. 5. 6. 7. 8. 9. 10. 11. 12. 13. 14. 15.
FREQUENCY (GHz)

(b)

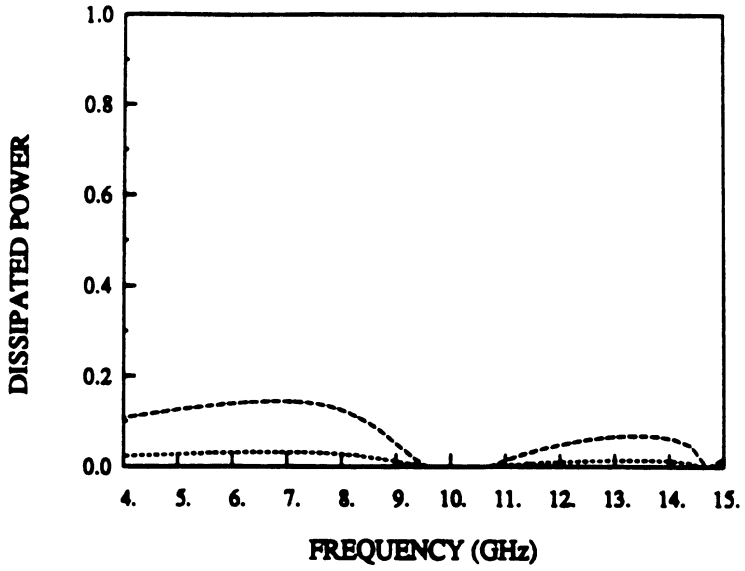

(c)

Figure 5.6: (a) Reflected, (b) transmitted and (c) dissipated power vs frequency for an array of cross-shaped patches with various lossy dielectric slabs; $T_x = T_y = 2.0$ cm, $L = 1.5$ cm, $W = 0.5$ cm, $d = 0.1$ cm, $\theta^i = 0$, $\phi^i = 0$; (——) $\epsilon_r = 4.0$; (- - - -) $\epsilon_r = 4.0 - j0.1$; (- - -) $\epsilon_r = 4.0 - j0.5$.

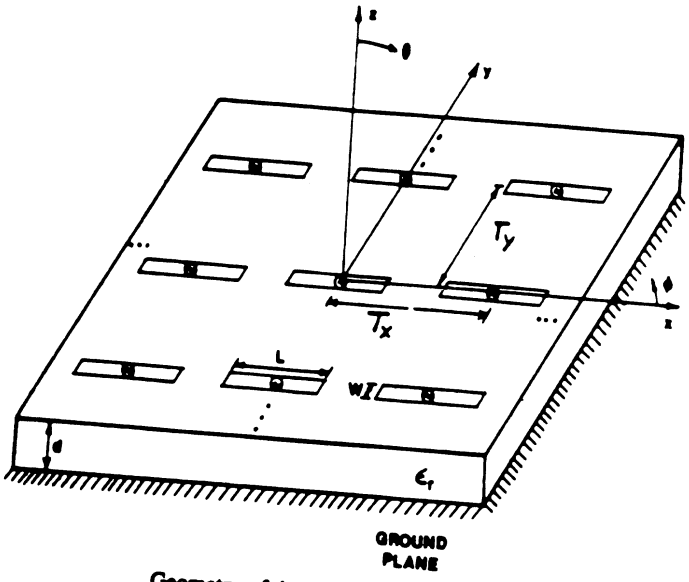

Geometry of the infinite array of printed dipoles.

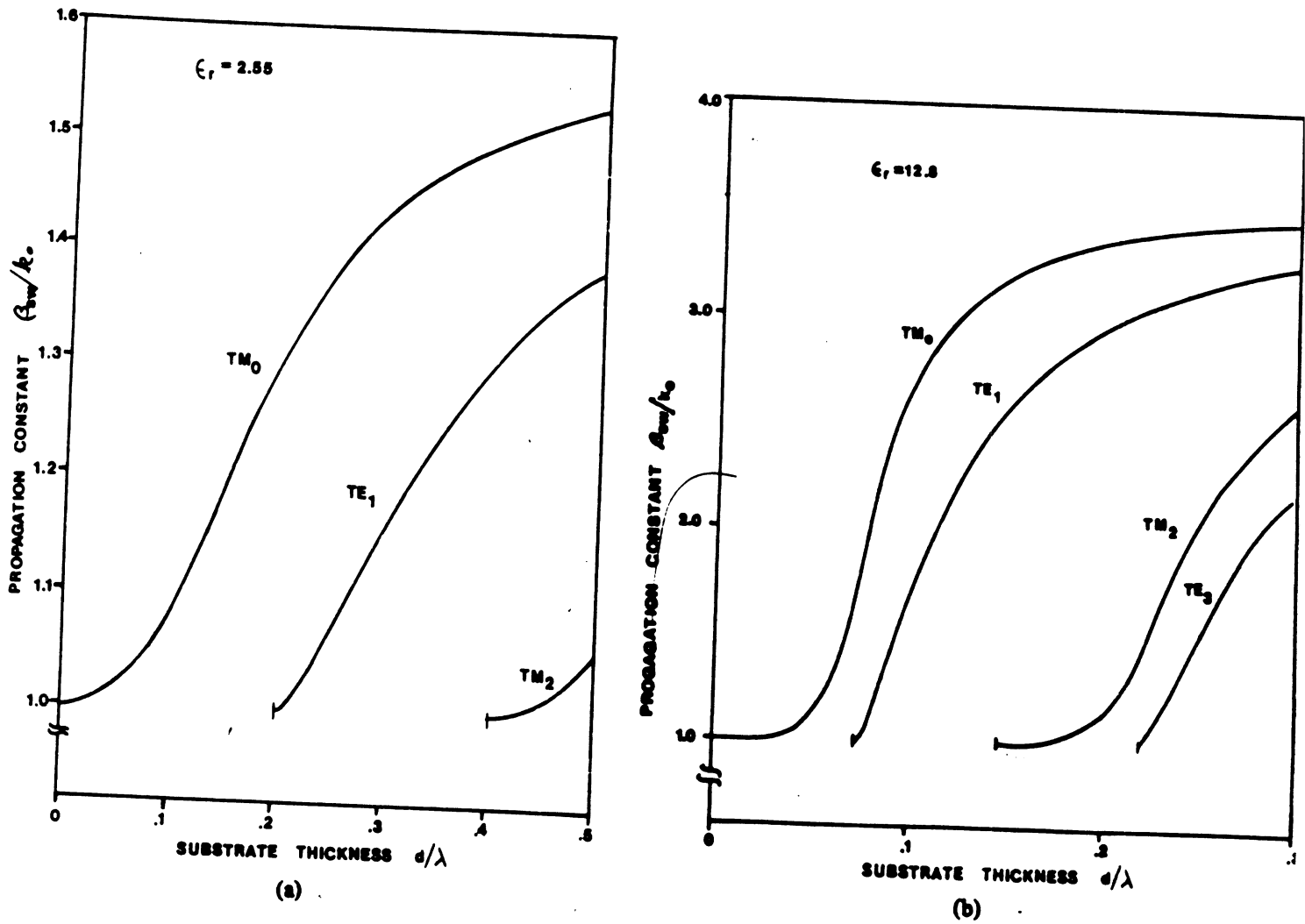

Normalized surface wave propagation constants for a grounded dielec-

β_{sw} : surface propagation constant

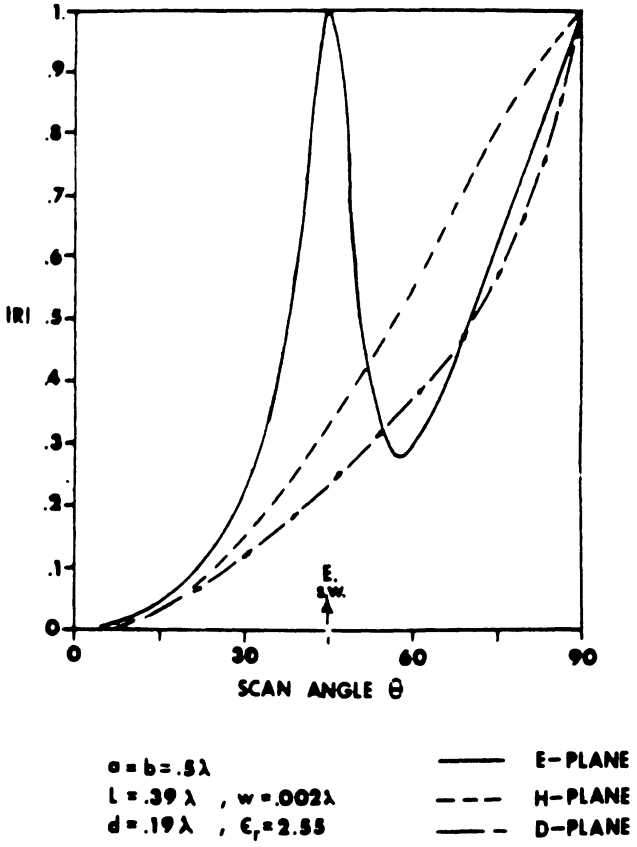

(a)

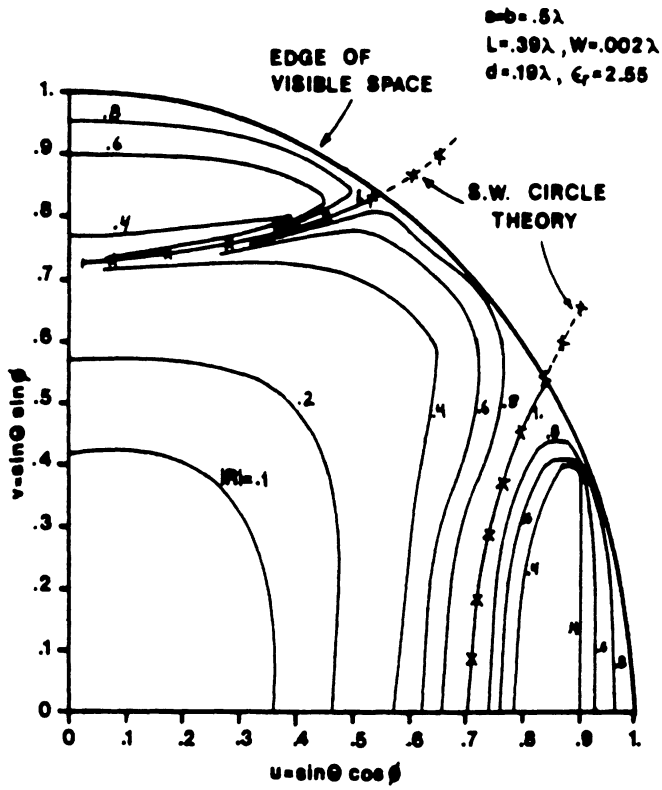

(b)

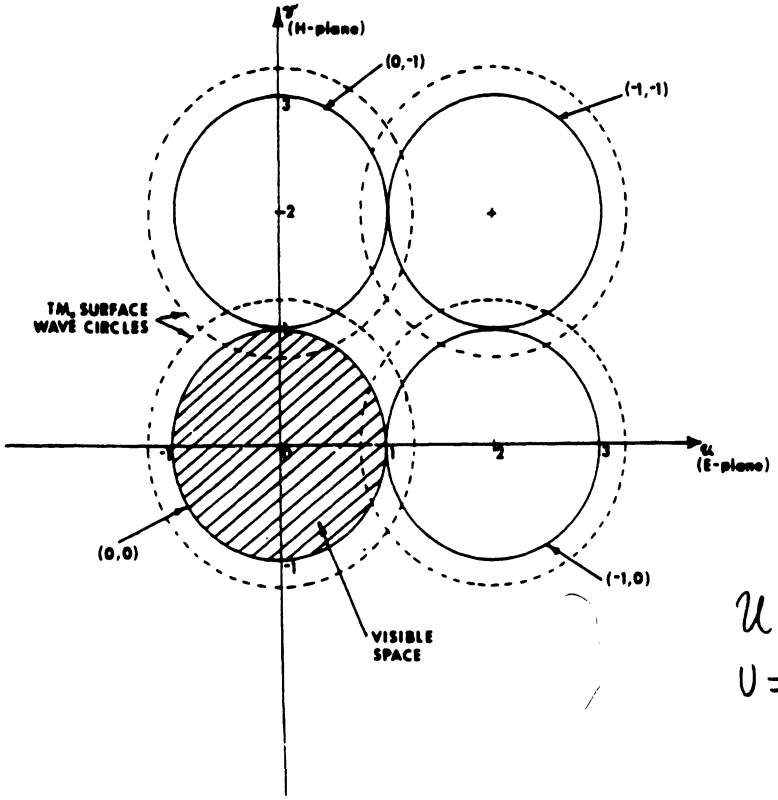

$$R = \frac{Z_{in} - Z_b}{Z_{in} + Z_b}$$

Z_b = line characteristic Impedance

$$u = \sin\theta_s \cos\phi_s$$

$$v = \sin\theta_s \sin\phi_s$$

(c)

Scan characteristics of infinite printed dipole array. (a) Reflection coefficient magnitude for *E*-, *H*-, and *D*-planes, (b) Contour plot in *u*-*v* plane of reflection coefficient magnitude. $Z_b = 75 + j0\Omega$. (c) Surface wave circle diagram.

D. M. Pozar and D. H. Schaubert "Scan Blindness in Infinite Phase Arrays of

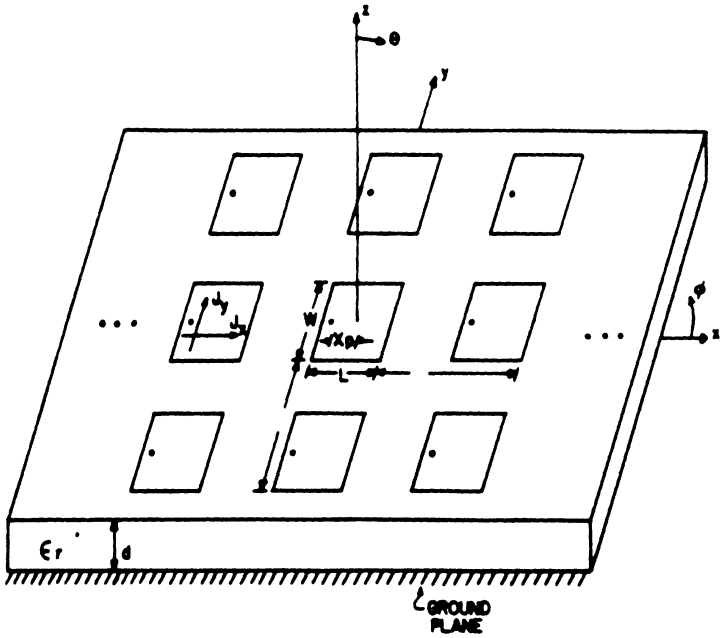

Geometry of an infinite array of microstrip patches. The ground plane is in the $z = 0$ plane and the top of the substrate is in the $z = d$ plane.

D. M. Pozar and D. H. Schaubert, "Analysis of an Infinite Array of Rectangular Microstrip Patches with Idealized Probe Feeds," IEEE Trans. Antennas & Propagation, pp. 1101-1107, Oct. 1984.

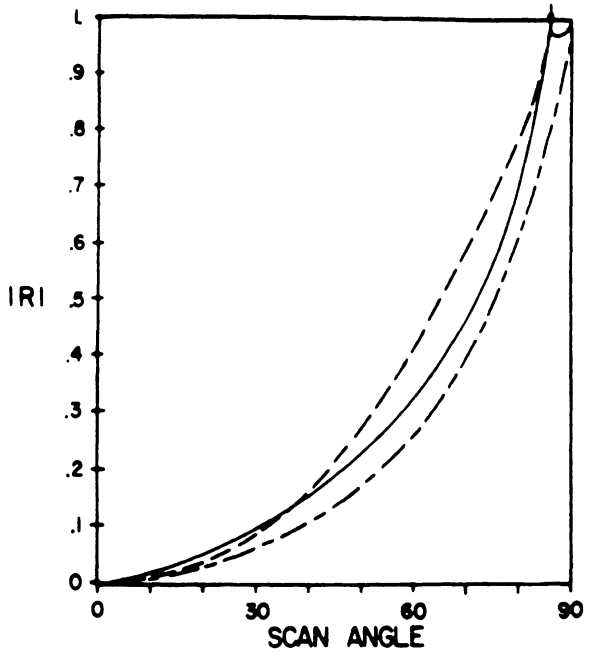

$\epsilon_r = 2.55$
$d = 0.02\ \lambda_0$
$a = b = 0.5\ \lambda_0$
$L = 0.3\ \lambda_0$
$W = 0.3\ \lambda_0$
$X_p = L/4$
$Z_b = 97.\Omega$

—— E-PLANE
– – – H-PLANE
—·— D-PLANE

Reflection coefficient magnitude of an infinite microstrip array.

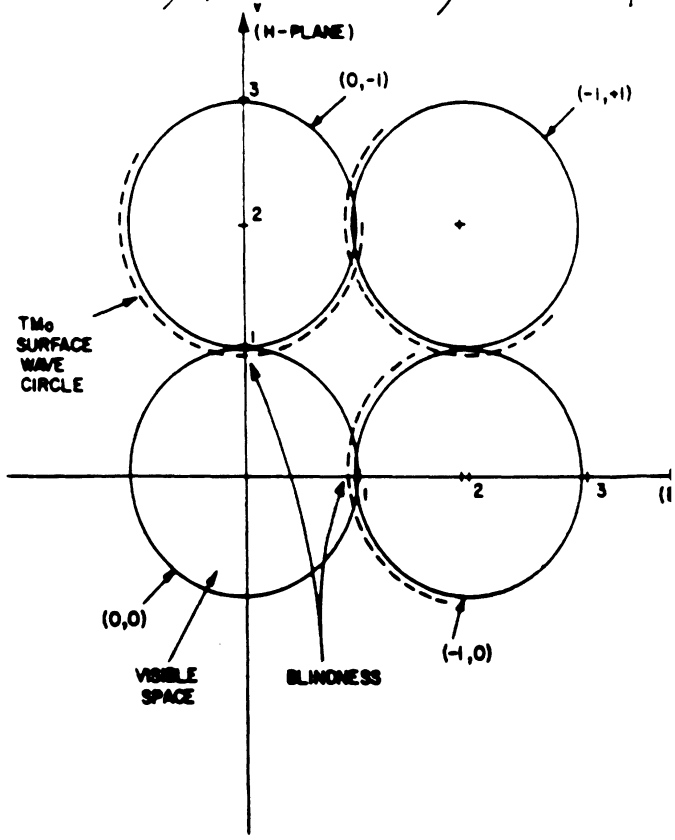

Surface wave circle diagram interpretation of scan blindness array of Fig. 4.

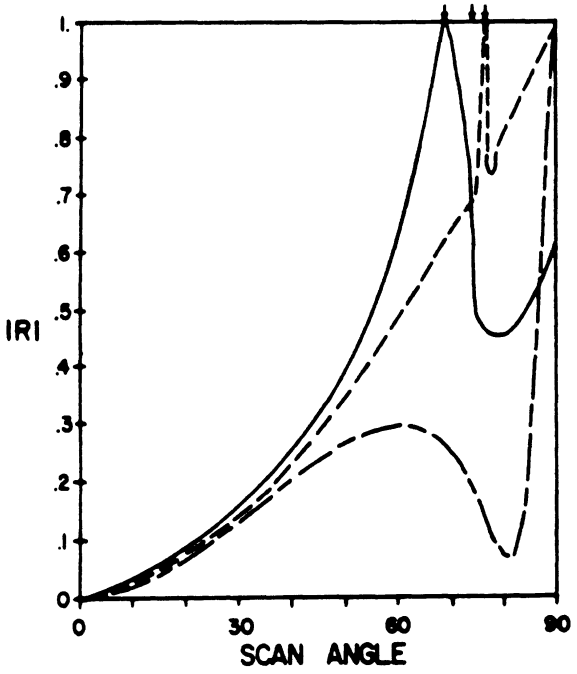

$\epsilon_r = 2.55$
$d = 0.06\ \lambda_0$
$a = 0.51\ \lambda_0$
$b = 0.50\ \lambda_0$
$L = 0.28\ \lambda_0$
$W = 0.3\ \lambda_0$
$X_p = L/2$
$Z_b = 86.\Omega$

—— E-PLANE
– – – H-PLANE
—·— D-PLANE

Reflection coefficient magnitude of an infinite microstrip array.

$$R = \frac{Z_{in} - Z_L}{Z_{in} + Z_L}$$

Z_L = line characteristic impedance

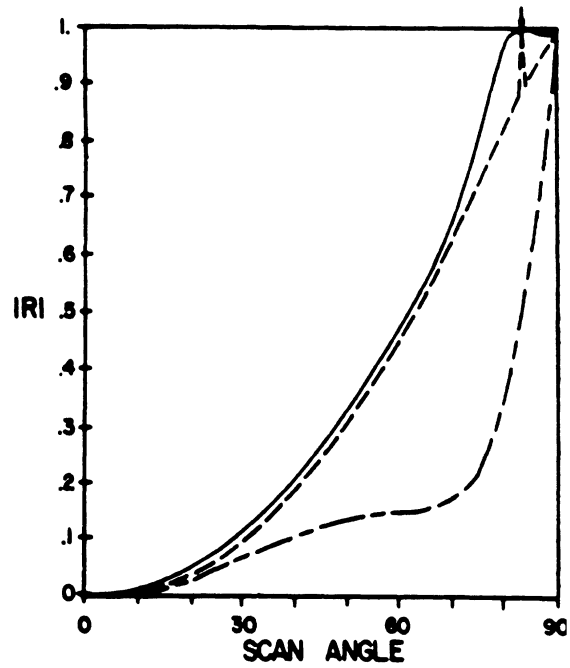

$\epsilon_r = 12.8$
$d = 0.02\ \lambda_0$
$a = b = 0.5\lambda_0$
$L = 0.131\ \lambda_0$
$W = 0.18\ \lambda_0$
$X_p = L/2$
$Z_b = 403\Omega$

—— E-PLANE
– – – H-PLANE
—·— D-PLANE

Reflection coefficient magnitude of an infinite micros